NBS

Technical Note No. 101

TRANSMISSION LOSS PREDICTIONS FOR TROPOSPHERIC COMMUNICATION CIRCUITS

VOLUME I

P. L. RICE, A. G. LONGLEY, K. A. NORTON, AND A. P. BARSIS

U. S. DEPARTMENT OF COMMERCE
NATIONAL BUREAU OF STANDARDS

THE NATIONAL BUREAU OF STANDARDS

The National Bureau of Standards is a principal focal point in the Federal Government for assuring maximum application of the physical and engineering sciences to the advancement of technology in industry and commerce. Its responsibilities include development and maintenance of the national standards of measurement, and the provisions of means for making measurements consistent with those standards; determination of physical constants and properties of materials; development of methods for testing materials, mechanisms, and structures, and making such tests as may be necessary, particularly for government agencies; cooperation in the establishment of standard practices for incorporation in codes and specifications; advisory service to government agencies on scientific and technical problems; invention and development of devices to serve special needs of the Government; assistance to industry, business, and consumers in the development and acceptance of commercial standards and simplified trade practice recommendations; administration of programs in cooperation with United States business groups and standards organizations for the development of international standards of practice; and maintenance of a clearinghouse for the collection and dissemination of scientific, technical, and engineering information. The scope of the Bureau's activities is suggested in the following listing of its four Institutes and their organizational units.

Institute for Basic Standards. Electricity. Metrology. Heat. Radiation Physics. Mechanics. Applied Mathematics. Atomic Physics. Physical Chemistry. Laboratory Astrophysics.* Radio Standards Laboratory: Radio Standards Physics; Radio Standards Engineering.** Office of Standard Reference Data.

Institute for Materials Research. Analytical Chemistry. Polymers. Metallurgy. Inorganic Materials. Reactor Radiations. Cryogenics.** Office of Standard Reference Materials.

Central Radio Propagation Laboratory. Ionosphere Research and Propagation. Troposphere and Space Telecommunications. Radio Systems. Upper Atmosphere and Space Physics.

Institute for Applied Technology. Textiles and Apparel Technology Center. Building Research. Industrial Equipment. Information Technology. Performance Test Development. Instrumentation. Transport Systems. Office of Technical Services. Office of Weights and Measures. Office of Engineering Standards. Office of Industrial Services.

---

* NBS Group, Joint Institute for Laboratory Astrophysics at the University of Colorado.
** Located at Boulder, Colorado.

NATIONAL BUREAU OF STANDARDS

Technical Note 101

Issued May 7, 1965

TRANSMISSION LOSS PREDICTIONS FOR TROPOSPHERIC COMMUNICATION CIRCUITS

VOLUME 1

P. L. Rice, A. G. Longley, K. A. Norton, and A. P. Borsis
Central Radio Propogation Loborotory
Notionol Bureou of Stondords
Boulder, Colorodo

FOREWORD

A short history of the development of the prediction methods in this Technical Note will permit the reader to compare them with earlier procedures. Some of these methods were first reported by Norton, Rice and Vogler [1955]. Further development of forward scatter predictions and a better understanding of the refractive index structure of the atmosphere led to changes reported in an early unpublished NBS report and in NBS Technical Note 15 [Rice, Longley and Norton, 1959]. The methods of Technical Note 15 served as a basis for part of another unpublished NBS report which was incorporated in Air Force Technical Order T.O. 31Z-10-1 in 1961. A preliminary draft of the current technical note was submitted as a U.S. Study Group V contribution to the CCIR in 1962.

Technical Note 101 uses the metric system throughout. For most computations both a graphical method and formulas suitable for a digital computer are presented. These include simple and comprehensive formulas for computing diffraction over smooth earth and over irregular terrain, as well as methods for estimating diffraction over an isolated rounded obstacle. New empirical graphs are included for estimating long-term variability for several climatic regions, based on data that have been made available to NBS.

For paths in a continental temperate climate, these predictions are practically the same as those published in 1961. The reader will find that a number of graphs have been simplified and that many of the calculations are more readily adaptable to computer programming. The new material on time availability and service probability in several climatic regions should prove valuable for areas other than the U.S.A.

Note: This Technical Note consists of two volumes as indicated in the Table of Contents.

TABLE OF CONTENTS

Volume 1

TABLE OF CONTENTS

Volume 2

TRANSMISSION LOSS PREDICTIONS FOR
TROPOSPHERIC COMMUNICATION CIRCUITS

P. L. Rice, A. G. Longley, K. A. Norton, and A. P. Barsis

1. INTRODUCTION

This report presents comprehensive methods for predicting cumulative distributions of transmission loss for a wide range of radio frequencies over any type of terrain and in several climatic regions. Such quantitative estimates of propagation characteristics help to determine how well proposed radio systems will meet requirements for satisfactory service, free from harmful interference. Thus they should provide an important step toward more efficient use of the radio frequency spectrum.

The need for comprehensive and accurate prediction methods is clearly demonstrated when measured transmission loss data for a large number of radio paths are shown as a function of path length. In figures I.1 to I.4 of annex I, long-term median values of attenuation relative to free space for more than 750 radio paths are plotted versus distance. The extremely wide scatter of these data is due mainly to path-to-path differences in terrain profiles and effective antenna heights. Values recorded for a long period of time over a single path show comparable ranges, sometimes exceeding 100 decibels. Such tremendous path-to-path and time variations must be carefully considered, particularly in cases of possible interference between co-channel or adjacent-channel systems.

The detailed point-to-point prediction methods described here depend on propagation path geometry, atmospheric refractivity near the surface of the earth, and specified characteristics of antenna directivity. They have been tested against measurements in the radio frequency range 40 to 10,000 MHz (megacycles per second). Extension of the methods to higher frequencies requires estimates of attenuation due to absorption and scattering of radio energy by various constituents of the atmosphere.

Predictions of long-term median reference values of transmission loss are based on current radio propagation theory. A large sample of radio data was used to develop the empirical predictions of regional, seasonal, and diurnal changes in long-term medians. Estimates of long-term fading relative to observed medians are given for several climatic regions and periods of time, including some regions where few observations are available.

Predictions of transmission loss for paths within the radio horizon are based on geometric-optics ray theory. For paths with a common horizon, Fresnel-Kirchoff knife-edge diffraction theory is applied and extended to predict diffraction attenuation over isolated rounded obstacles. For double horizon paths that extend only slightly beyond the horizon, a modification of the Van der Pol-Bremmer method for computing field intensity in the far diffraction region is

used. For longer paths, extending well beyond the radio horizon, predictions are based on forward scatter theory. Radio data were used to estimate the efficiency of scattering at various heights in the atmosphere. Where some doubt exists as to which propagation mechanism predominates, transmission loss is calculated by two methods and the results are combined.

Annex I includes a set of "standard" curves of basic transmission loss and curves showing attenuation below free space for earth space communications, prepared using the methods described in the report. Such curves, and the medians of data shown on figures I.1 to I.4, may serve for general qualitative analysis, but clearly do not take account of particular terrain profiles or climatic effects that may be encountered over a given path.

Annex II supplements the discussion of transmission loss and directive antenna gains given in section 2. This annex contains a discussion of antenna beam orientation, polarization, and multipath coupling loss.

Annex III contains information required for unusual paths, including exact formulas for computing line-of-sight transmission loss with ground reflections, as well as modifications of the formulas for antenna beams which are elevated, or directed out of the great circle plane. Sample calculations and analytic expressions suitable for use on a digital computer are also included.

Annex IV reviews tropospheric propagation theory with particular attention to the mechanisms of forward scatter from atmospheric turbulence, from layers, or from small randomly oriented surfaces. References to some of the work in this field are included.

Annex V presents a discussion of "phase interference fading" as contrasted to "long-term power fading", provides a method for computing the probability of obtaining adequate service in the presence of noise and/or interfering signals, and includes a brief summary of ways to achieve optimum use of the radio frequency spectrum.

Figures are placed at the end of each section, and those which are not vertical should be turned counter-clockwise. (The ordinate labels would be upside down if the usual convention were followed.)

Previous Technical Notes in this series, numbered 95 to 103, describe tropospheric propagation phenomena and siting problems [Kirby, Rice, and Maloney, 1961], certain meteorological phenomena and their influence on tropospheric propagation [Dutton, 1961; Dutton and Thayer, 1961], synoptic radio meteorology [Bean, Horn, and Riggs, 1962], techniques for measuring the refractive index of the atmosphere [McGavin, 1962], determination of system parameters [Florman and Tary, 1962], performance predictions for communication links [Barsis, Norton, Rice, and Elder, 1961], and equipment characteristics [Barghausen, et al, 1963].

2. THE CONCEPTS OF SYSTEM LOSS, TRANSMISSION LOSS, PATH ANTENNA GAIN, AND PATH ANTENNA POWER GAIN

Definitions have been given in CCIR Recommendation 341 for system loss, L_s, transmission loss, L, propagation loss, L_p, basic transmission loss, L_b, path antenna gain, G_p, and path antenna power gain, G_{pp}. This section restates some of the definitions, introduces a definition of "path loss", L_o, illustrates the use of these terms and concepts, and describes methods of measurement [Norton, 1953, 1959, Wait 1959]. The notation used here differs slightly from that used in Recommendation 341 and in Report 112 [CCIR 1963a, b]. For the frequency range considered in this report system loss, transmission loss, and propagation loss can be considered equal with negligible error in almost all cases, because antenna gains and antenna circuit resistances are essentially those encountered in free space.

2.1 System Loss and Transmission Loss

The system loss of a radio circuit consisting of a transmitting antenna, receiving antenna, and the intervening propagation medium is defined as the dimensionless ratio, p_t'/p_a', where p_t' is the radio frequency power input to the terminals of the transmitting antenna and p_a' is the resultant radio frequency signal power available at the terminals of the receiving antenna. The system loss is usually expressed in decibels:

$$L_s = 10 \log (p_t'/p_a') = P_t' - P_a' \quad db \qquad (2.1)$$

Throughout this report logarithms are to the base 10 unless otherwise stated.

The inclusion of ground and dielectric losses and antenna circuit losses in L_s provides a quantity which can be directly and accurately measured. In propagation studies, however, it is convenient to deal with related quantities such as transmission loss and basic transmission loss which can be derived only from theoretical estimates of radiated power and available power for various hypothetical situations.

In this report, capital letters are often used to denote the ratios, expressed in db, dbu, or dbw, of the corresponding quantities designated with lower-case type. For instance, in (2.1), $P_t' = 10 \log p_t'$ in dbw corresponds to p_t' in watts.

Transmission loss is defined as the dimensionless ratio p_t/p_a, where p_t is the total power radiated from the transmitting antenna in a given band of radio frequencies, and p_a is the resultant radio frequency signal power which would be available from an equivalent loss-free antenna. The transmission loss is usually expressed in decibels:

$$L = 10 \log (p_t/p_a) = P_t - P_a \approx L_s - L_{et} - L_{er} \quad db \qquad (2.2)$$

$$L_{et} = 10 \log \ell_{et}, \quad L_{er} = 10 \log \ell_{er} \qquad (2.3)$$

where $1/\ell_{et}$ and $1/\ell_{er}$ as defined in the next subsection are power radiation and reception effeciencies for the transmitting and receiving antennas, respectively. With the frequencies and antenna heights usually considered for tropospheric communication circuits, these efficiencies are nearly unity and the difference between L_s and L is negligible. With antennas a fraction of a wavelength above ground, as they usually are at lower frequencies, and especially when horizontal polarization is used, L_{et} and L_{er} are not negligible, but are influenced substantially by the presence of the ground and other nearby portions of the antenna environment.

From transmitter output to receiver input, the following symbols are used:

Transmitter Output Power	Power Input to Antenna	Total Radiated Power	Available Power at Loss-Free Receiving Antenna	Available Power at Actual Receiving Antenna	Available Power at Receiver Input
$P_{\ell t}$ $\rightarrow$	P'_t $\rightarrow$	P_t $\rightarrow$	P_a $\rightarrow$	P'_a $\rightarrow$	$P_{\ell r}$
$L_{\ell t}$	L_{et}	L	L_{er}		$L_{\ell r}$

L_s
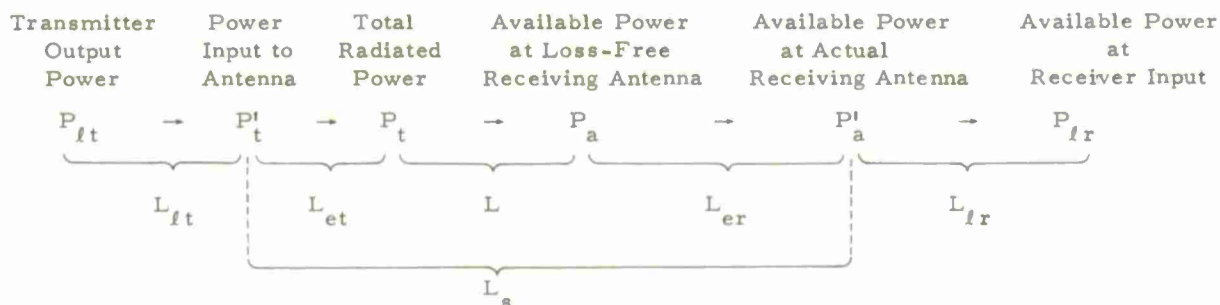
It should be noted that $L_{\ell t}$ and $L_{\ell r}$ are conceptually different. Since $P_{\ell t}$ and P'_t represent the power observed at the transmitter and at the transmitting antenna, respectively, $L_{\ell t}$ includes both transmission line and mismatch losses. Since P'_a and $P_{\ell r}$ represent available power at the receiving antenna and at the receiver, mismatch losses must be accounted for separately, since $L_{\ell r}$ includes only the transmission line loss between the antenna and the receiver.

2.2 Available Power from the Receiving Antenna

The above definitions of system loss and transmission loss depend upon the concept of available power, the power that would be delivered to the receiving antenna load if its impedance were conjugately matched to the receiving antenna impedance. For a given radio frequency ν in hertz, let $z_{\ell\nu}$, z'_ν, and z_ν represent the impedances of the load, the actual lossy antenna in its actual environment, and an equivalent loss-free antenna, respectively:

$$z_{\ell\nu} = r_{\ell\nu} + i x_{\ell\nu} \tag{2.4a}$$

$$z'_\nu = r'_\nu + i x'_\nu \tag{2.4b}$$

$$z_\nu = r_\nu + i x_\nu \tag{2.4c}$$

where r and x in (2.4) represent resistance and reactance, respectively. Let $p_{\ell\nu}$ represent the power delivered to the receiving antenna load and write $p'_{a\nu}$ and $p_{a\nu}$, respectively, for the available power at the terminals of the actual receiving antenna and at the terminals of the equivalent loss-free receiving antenna. If v'_ν is the actual open-circuit r.m.s. voltage at the antenna terminals, then

$$p_{\ell\nu} = \frac{v'^2_\nu r_{\ell\nu}}{\left| z'_\nu + z_{\ell\nu} \right|^2} \tag{2.5}$$

When the load impedance conjugately matches the antenna impedance, so that $z_{\ell\nu} = z'^*_\nu$ or $r_{\ell\nu} = r'_\nu$ and $x_{\ell\nu} = -x'_\nu$, (2.5) shows that the power $p_{\ell\nu}$ delivered to the load is equal to the power $p'_{a\nu}$ available from the _actual_ antenna:

$$p'_{a\nu} \equiv \frac{v'^2_\nu}{4 r'_\nu} \tag{2.6}$$

Note that the available power from an antenna depends only upon the characteristics of the antenna, its open-circuit voltage v'_ν, and the resistance r'_ν, and is independent of the load

impedance. Comparing (2.5) and (2.6), we define a mismatch loss factor

$$\ell_{m\nu} \equiv \frac{p'_{a\nu}}{p_{\ell\nu}} = \frac{\left(r'_\nu + r_{\ell\nu}\right)^2 + \left(x'_\nu + x_{\ell\nu}\right)^2}{4\ r'_\nu\ r_{\ell\nu}} \tag{2.7}$$

such that the power delivered to a load equals $p'_{a\nu}/\ell_{m\nu}$. When the load impedance conjugately matches the antenna impedance, $\ell_{m\nu}$ has its minimum value of unity, and $p_{\ell\nu} = p'_{a\nu}$. For any other load impedance, somewhat less than the available power is delivered to the load. The power available from the equivalent loss-free antenna is

$$P_{a\nu} = \frac{v_\nu^2}{4\ r_\nu} \tag{2.8}$$

where v_ν is the open circuit voltage for the equivalent loss-free antenna.

Comparing (2.6) and (2.8), it should be noted that the available power $p'_{a\nu}$ at the terminals of the actual lossy receiving antenna is less than the available power $P_{a\nu} \equiv \ell_{er\nu} p'_{a\nu}$ for a loss-free antenna at the same location as the actual antenna:

$$\ell_{er\nu} \equiv \frac{P_{a\nu}}{p'_{a\nu}} = \frac{r'_\nu v_\nu^2}{r_\nu v'^2_\nu} \geq 1 \tag{2.9}$$

The open circuit voltage v'_ν for the actual lossy antenna will often be the same as the open circuit voltage v_ν for the equivalent loss-free antenna, but each receiving antenna circuit must be considered individually.

Similarly, for the transmitting antenna, the ratio of the total power $p'_{t\nu}$ delivered to the antenna at a frequency ν is $\ell_{et\nu}$ times the total power $p_{t\nu}$ radiated at the frequency ν:

$$\ell_{et\nu} \equiv p'_{t\nu}/p_{t\nu} \tag{2.10}$$

The concept of available power from a transmitter is not a useful one, and $\ell_{et\nu}$ for the transmitting antenna is best defined as the above ratio. However, the magnitude of this ratio can be obtained by calculation or measurement by treating the transmitting antenna as a receiving antenna and then determining $\ell_{et\nu}$ to be the ratio of the available received powers from the equivalent loss-free and the actual antennas, respectively.

General discussions of $\ell_{er\nu}$ are given by Crichlow et al [1955] and in a report prepared under CCIR Resolution No. 1 [Geneva 1963c]. The loss factor $\ell_{er\nu}$ was successfully

determined in one case by measuring the power $p_{t\nu}$ radiated from a loss-free target transmitting antenna and calculating the transmission loss between the target transmitting antenna and the receiving antenna. There appears to be no way of directly measuring either $l_{er\nu}$ or $l_{et\nu}$ without calculating some quantity such as the radiation resistance or the transmission loss. In the case of reception with a unidirectional rhombic terminated in its characteristic impedance, $l_{er\nu}$ could theoretically be greater than 2 [Harper, 1941], since nearly half the received power is dissipated in the terminating impedance and some is dissipated in the ground. Measurements were made by Christiansen [1947] on single and multiple wire units and arrays of rhombics. The ratio of power lost in the termination to the input power varied with frequency and was typically less than 3 db.

For the frequency band ν_l to ν_m it is convenient to define the effective loss factors L_{er} and L_{et} as follows:

$$L_{er} = 10 \log \frac{\displaystyle\int_{\nu_l}^{\nu_m} (d\, p_{a\nu}/d\nu)\ d\nu}{\displaystyle\int_{\nu_l}^{\nu_m} (d\, p'_{a\nu}/d\nu)\ d\nu} \ db \qquad (2.11)$$

$$L_{et} = 10 \log \frac{\displaystyle\int_{\nu_l}^{\nu_m} (d\, p'_{t\nu}/d\nu)\ d\nu}{\displaystyle\int_{\nu_l}^{\nu_m} (d\, p_{t\nu}/d\nu)\ d\nu} \qquad (2.12)$$

The limits ν_l and ν_m on the integrals (2.11) and (2.12) are chosen to include essentially all of the wanted signal modulation side bands, but ν_l is chosen to be sufficiently large and ν_m sufficiently small to exclude any appreciable harmonic or other unwanted radiation emanating from the wanted signal transmitting antenna.

2.3 Antenna Directive Gain and Power Gain

A transmitting antenna has a directive gain $g_t(\hat{r})$ in the direction of a unit vector $\hat{r}$ if:

(1) it radiates a total of p_t watts through the surface of any large sphere with the antenna at its center, and

(2) it radiates $g_t p_t /(4\pi)$ watts per steradian in the direction $\hat{r}$.

The same antenna has a power gain $g_t'(\hat{r})$ in the direction $\hat{r}$ if:

(1) the power input to the antenna terminals is $p_t' = \ell_{et} p_t$, and

(2) it radiates $g_t' p_t'/(4\pi)$ watts per steradian in the direction $\hat{r}$.

The antenna power gain g_t' is smaller than the directive gain g_t simply as a result of the loss factor ℓ_{et}. It follows that

$$G_t(\hat{f}) = G_t'(\hat{f}) + L_{et} \qquad\qquad (2.13a)$$

expressed in decibels above the gain of an isotropic radiator. Note that the antenna power gain $G_t'(\hat{f})$ is less than the antenna directive gain $G_t(\hat{f})$ by the amount L_{et} db, where the power radiation efficiency $1/\ell_{et}$ is independent of the direction $\hat{f}$.

The gain of an antenna is the same whether it is used for transmitting or receiving. For a receiving antenna, the directive gain $G_r(\hat{f})$ and power gain $G_r'(\hat{f})$ are related by

$$G_r(\hat{f}) = G_r'(\hat{f}) + L_{er} . \qquad\qquad (2.13b)$$

The remainder of this report will deal with directive gains, since the power gains may be determined simply by subtracting L_{et} or L_{er}. The maximum value of a directive gain $G(\hat{f})$ is designated simply as G. As noted in Annex II, it is sometimes useful to divide the directive gain into principal and cross-polarization components.

An idealized antenna in free space with a half-power semi-beamwidth δ expressed in radians, and with a circular beam cross-section, may be assumed to radiate x percent of its power isotropically through an area equal to $\pi\delta^2$ on the surface of a large sphere of unit radius, and to radiate $(100-x)$ percent of its power isotropically through the remainder of the sphere. In this case the power radiated in the direction of the main beam is equal to $xp_t /(100\pi\delta^2)$ watts and the maximum gain g is, by definition, equal to $4\pi x/(100\pi\delta^2)$. One may assume a beam solid angle efficiency $x = 56$ percent for parabolic reflectors with 10db tapered illumination, and obtain $g = 2.24/\delta^2$. The maximum free space gain G in decibels relative to an isotropic radiator is then

$$G = 10 \log g = 3.50 - 20 \log \delta \quad \text{db} \qquad\qquad (2.14)$$

If azimuthal and vertical beamwidths $2\delta_w$ and $2\delta_z$ are different:

$$\delta = \sqrt{\delta_w \delta_z} \qquad (2.15)$$

The above analysis is useful in connection with measured antenna radiation patterns.

For antennas such as horns or parabolic reflectors which have a clearly definable physical aperture, the concept of antenna aperture efficiency is useful. For example, the free space maximum gain of a parabolic dish with a 56 percent aperture efficiency and a diameter D is the ratio of 56 percent of its area to the effective absorbing area of an isotropic radiator:

$$G = 10 \log \left[\frac{0.56 \pi D^2/4}{\lambda^2/4\pi} \right] = 20 \log D + 20 \log f - 42.10 \quad \text{db} \qquad (2.16)$$

where D and λ are in meters and f is the radio frequency in megahertz, MHz. Equations (2.14) and (2.16) are useful for determining the gains of actual antennas only when their beam solid angle efficiencies or aperture efficiencies are known, and these can be determined accurately only by measurement.

With a dipole feed, for instance, and $10 < D/\lambda < 25$, experiments have shown the following empirical formula to be superior to (2.16):

$$G = 23.3 \log D + 23.3 \log f - 55.1 \quad \text{db} \qquad (2.17)$$

where D is expressed in meters and f in MHz.

Cozzens [1962] has published a nomograph for determining paraboloidal maximum gain as a function of feed pattern and angular aperture. Discussions of a variety of commonly-used antennas are given in recent books [Jasik, 1961; Thourel, 1960].

Much more is known about the amplitude, phase, and polarization response of available antennas in the directions of maximum radiation or reception than in other directions. Most of the theoretical and developmental work has concentrated on minimizing the transmission loss between antennas and on studies of the response of an arbitrary antenna to a standard plane wave. An increasing amount of attention, however, is being devoted to maximizing the transmission loss between antennas in order to reject unwanted signals. For this purpose it is important to be able to specify, sometimes in statistical terms, the directivity, phase, and polarization response of an antenna in every direction from which multipath components of each unwanted signal may be expected. Appendix II is devoted to this subject.

For the frequencies of interest in this report, antenna radiation resistances r_ν at any radio frequency ν hertz are usually assumed independent of their environment, or else the immediate environment is considered part of the antenna, as in the case of an antenna mounted on an airplane or space vehicle.

2.4 Polarization Coupling Loss and Multipath Coupling Loss

It is sometimes necessary to minimize the response of a receiving antenna to unwanted signals coming from a single source by way of different paths. This requires attention to the amplitudes, polarizations, and relative phases of a number of waves arriving from different directions. In any theoretical model, the phases of principal and cross-polarization components of each wave, as well as the relative phase response of the receiving antenna to each component, must be considered. Complex voltages are added at the antenna terminals to make proper allowance for this amplitude and phase information.

In Annex II it is shown how complex vectors $\vec{\underline{e}}$ and $\vec{\underline{e}}_r$ may be used to represent transmitting and receiving antenna radiation and reception patterns which will contain amplitude, polarization, and phase information [Kales, 1951] for a given free-space wavelength, λ. A bar is used under the symbol for a complex vector $\vec{\underline{e}} = \vec{e}_p + i\,\vec{e}_c$, where $i = \sqrt{-1}$ and $\vec{e}_p$, $\vec{e}_c$ are real vectors which may be associated with principal and cross-polarized components of a uniform elliptically polarized plane wave.

Calculating the power transfer between two antennas in free space, complex polarization vectors $\hat{\underline{p}}(\hat{r})$ and $\hat{\underline{p}}_r(-\hat{r})$ are determined for each antenna as if it were the transmitter and the other were the receiver. Each antenna must be in the far field or radiation field of the other:

$$\hat{\underline{p}}(\hat{r}) = \vec{\underline{e}}/\left|\vec{\underline{e}}\right| \;,\; \hat{\underline{p}}_r(-\hat{r}) = \vec{\underline{e}}_r/\left|\vec{\underline{e}}_r\right| \tag{2.18}$$

$$\vec{\underline{e}} = \vec{e}_p + i\,\vec{e}_c \;,\; \vec{\underline{e}}_r = \vec{e}_{pr} + i\,\vec{e}_{cr} \tag{2.19}$$

$$\left|\vec{\underline{e}}\right|^2 = e_p^2 + e_c^2 \;,\; \left|\vec{\underline{e}}_r\right|^2 = e_{pr}^2 + e_{cr}^2 \tag{2.20}$$

The sense of polarization of the field $\vec{\underline{e}}$ is right-handed or left-handed depending on whether the axial ratio of the polarization ellipse, a_x, is positive or negative:

$$a_x = e_c/e_p \tag{2.21}$$

The polarization is circular if $\left|e_p\right| = \left|e_c\right|$ and linear if $e_c = 0$, where $\vec{e}_p = e_p\,\hat{e}_p$ is in the principal polarization direction defined by the unit vector $\hat{e}_p$.

The available power p_a may be written as

$$P_a = s(\vec{r})\; a_e(-\hat{r})\,\left|\hat{\underline{p}} \cdot \hat{\underline{p}}_r\right|^2 \text{ watts} \tag{2.22}$$

$$s(\vec{r}) = \left|\vec{e}\right|^2 / (2\,\eta_0) \ \text{watts}/\text{km}^2 \tag{2.23}$$

$$a_e(-\hat{f}) = g_r(-\hat{f}) \left[\lambda^2/(4\pi) \right] \ \text{km}^2 \tag{2.24}$$

where $s(\vec{r})$ is the total mean power flux density at the receiving antenna, $a_e(-\hat{f})$ is the effective absorbing area of the receiving antenna in the direction $-\hat{f}$, and $\left|\hat{p} \cdot \hat{p}_r\right|^2$ is the polarization efficiency for a transfer of energy in free space and at a single radio frequency. The corresponding polarization coupling loss is

$$L_{cp} = -10 \ \log \ \left|\vec{p} \cdot \vec{p}_r\right|^2 \ \text{db} \tag{2.25}$$

In terms of the axial ratios a_x and a_{xr} defined by (II.15) and (II.17) and the acute angle ψ_p between principal polarization vectors $\vec{e}_p$ and $\vec{e}_{pr}$, the polarization efficiency may be written as

$$\left|\hat{p} \cdot \hat{p}_r\right|^2 = \frac{\cos^2\psi_p\,(a_x a_{xr} + 1)^2 + \sin^2\psi_p\,(a_x + a_{xr})^2}{(a_x^2 + 1)\,(a_{xr}^2 + 1)} \tag{2.26}$$

This is the same as (II.29). Annex II explains how these definitions and relationships are extended to the general case where antennas are not in free space.

There is a maximum transfer of power between two antennas if the polarization ellipse of the receiving antenna has the same sense, eccentricity, and principal polarization direction as the polarization ellipse of the incident radio wave. The receiving antenna is completely "blind" to the incident wave if the sense of polarization is opposite, the eccentricity is the same, and the principal polarization direction is orthogonal to that of the incident wave. In theory this situation would result in the complete rejection of an unwanted signal propagating in a direction $-\hat{f}$. Small values of $g_r(-\hat{f})$ could at the same time discriminate against unwanted signals coming from other directions.

When more than one plane wave is incident upon a receiving antenna from a single source, there may be a "multipath coupling loss" which includes beam orientation, polarization coupling, and phase mismatch losses. A statistical average of phase incoherence effects, such as that described in subsection 9.4, is called "antenna-to-medium coupling loss." Multipath coupling loss is the same as the "loss in path antenna gain," L_{gp}, defined in the next subsection. Precise expressions for L_{gp} may also be derived from the relationships in annex II.

2.5 Path Loss, Basic Transmission Loss, Path Antenna Gain, and Attenuation Relative to Free Space

Observations of transmission loss are often normalized to values of "path loss" by subtracting the sum of the maximum free space gains of the antennas, $G_t + G_r$, from the transmission loss, L. Path loss is defined as

$$L_o = L - G_t - G_r \text{ db.} \qquad (2.27)$$

Path loss should not be confused with basic transmission loss. Basic transmission loss, L_b, is the system loss for a situation where the actual antennas are replaced at the same locations by hypothetical antennas which are:

(1) Isotropic, so that $G_t(\hat{f}) = 0$ db and $G_r(-\hat{f}) = 0$ db for all important propagation directions, $\hat{f}$.

(2) Loss-free, so that $L_{et} = 0$ db and $L_{er} = 0$ db.

(3) Free of polarization and multipath coupling loss, so that $L_{cp} = 0$ db.

Corresponding to this same situation, the path antenna gain, G_p, is defined as the change in the transmission loss if hypothetical loss-free isotropic antennas with no multipath coupling loss were used at the same locations as the actual antennas.

The transmission loss between any two antennas is defined by (2.2):

$$L = P_t - P_a \text{ db}$$

where P_t dbw is the total power radiated from the transmitting antenna and P_a dbw is the corresponding available power from a loss-free receiving antenna which is otherwise equivalent to the actual receiving antenna.

Replace both antennas by loss-free isotropic antennas at the same locations, with no coupling loss between them and having the same radiation resistances as the actual antennas, and let P_{ab} represent the resulting available power at the terminals of the hypothetical isotropic receiving antenna. Then the basic transmission loss L_b, the path antenna gain G_p, and the path antenna power gain G_{pp}, are given by

$$L_b = P_t - P_{ab} = L + G_p \text{ db} \qquad (2.28)$$

$$G_p = P_a - P_{ab} = L_b - L \text{ db} \qquad (2.29a)$$

$$G_{pp} = P'_a - P_{ab} = L_b - L_s \text{ db} \qquad (2.29b)$$

In free space, for instance:

$$P_a = P_t + G_t(\hat{f}) + G_r(-\hat{f}) - L_{cp} + 20 \log \left(\frac{\lambda}{4\pi r} \right) \text{ dbw} \qquad (2.30a)$$

$$P_{ab} = P_t + 20 \log \left(\frac{\lambda}{4\pi r} \right) \text{ dbw} \qquad (2.30b)$$

A special symbol, L_{bf}, is used to denote the corresponding basic transmission loss in free space:

$$L_{bf} = 20 \log \left(\frac{4\pi r}{\lambda} \right) = 32.45 + 20 \log f + 20 \log r \quad \text{db} \qquad (2.31)$$

where the antenna separation r is expressed in kilometers and the free space wavelength λ equals $0.2997925/f$ kilometers for a radio frequency f in megahertz.

When low gain antennas are used, as on aircraft, the frequency dependence in (2.31) indicates that the service range for UHF equipment can be made equal to that in the VHF band only by using additional power in direct proportion to the square of the frequency. Fixed point-to-point communications links usually employ high-gain antennas at each terminal, and for a given antenna size more gain is realized at UHF than at VHF, thus more than compensating for the additional free space loss at UHF indicated in (2.31).

Comparing (2.28), (2.29), and (2.30), it is seen that the path antenna gain in free space, G_{pf}, is

$$G_{pf} = G_t(\hat{f}) + G_r(-\hat{f}) - L_{cp} \quad \text{db} \qquad (2.32)$$

For most wanted propagation paths, this is well approximated by $G_t + G_r$, the sum of the maximum antenna gains. For unwanted propagation paths it is often desirable to minimize G_{pf}. This can be achieved not only by making $G_t(\hat{f})$ and $G_r(-\hat{f})$ small, but also by using different polarizations for receiving and transmitting antennas so as to maximize L_{cp}.

In free space the transmission loss is

$$L = L_{bf} - G_{pf} \quad \text{db} \qquad (2.33)$$

The concepts of basic transmission loss and path antenna gain are also useful for normalizing the results of propagation studies for paths which are not in free space. Defining an "equivalent free-space transmission loss", L_f, as

$$L_f = L_{bf} - G_p, \qquad (2.34)$$

note that G_p in (2.34) is not equal to $G_t + G_r$ unless this is true for the actual propagation path. It is often convenient to investigate the "attenuation relative to free space", A, or the basic transmission loss relative to that in free space, defined here as

$$A = L_b - L_{bf} = L - L_f \quad db \tag{2.35}$$

This definition, with (2.34), makes A independent of the path antenna gain, G_p. Where terrain has little effect on line-of-sight propagation, it is sometimes desirable to study A rather than the transmission loss, L.

Although G_p varies with time, it is customary to suppress this variation [Hartman, 1963] and to estimate only the quantity

$$G_{pm} = L_{bm}(50) - L_m(50) \tag{2.36}$$

where $L_{bm}(50)$ and $L_m(50)$ are long-term median values of L_b and L.

Multipath coupling loss, or the "loss in path antenna gain", L_{gp}, is defined as the difference between basic transmission loss and path loss, which is equal to the sum of the maximum gains of the transmitting and receiving antennas minus the path antenna gain:

$$L_{gp} = L_b - L_o = G_t + G_r - G_p \quad db \tag{2.37}$$

The loss in path antenna gain will therefore, in general, include components of beam orientation loss and polarization coupling loss as well as any aperture-to-medium coupling loss that may result from scattering by the troposphere, by rough or irregular terrain, or by terrain clutter such as vegetation, buildings, bridges, or power lines.

2.6 Propagation Loss and Field Strength

This subsection defines terms that are most useful at radio frequencies lower than those where tropospheric propagation effects are dominant.

Repeating the definitions of r and r' used in subsection 2.2, and introducing the new parameter r_f:

$\quad$ $r_{t, r}$ = antenna radiation resistance,

$\quad$ $r'_{t, r}$ = resistance component of antenna input impedance,

$\quad$ $r_{ft, fr}$ = antenna radiation resistance in free space,

where subscripts t and r refer to the transmitting antenna and receiving antenna, respectively. Next define

$$L_{et} = 10 \log (r'_t/r_t), \quad L_{er} = 10 \log (r'_r/r_r) \tag{2.38}$$

$$L_{ft} = 10 \log (r'_t/r_{ft}), \quad L_{fr} = 10 \log (r'_r/r_{fr}) \tag{2.39}$$

$$L_{rt} = 10 \log (r_t/r_{ft}) = L_{ft} - L_{et} \tag{2.40a}$$

$$L_{rr} = 10 \log (r_r/r_{fr}) = L_{fr} - L_{er} \tag{2.40b}$$

[Actually, (2.11) and (2.12) define L_{et} and L_{er} while (2.38) defines r_t and r_r, given r'_t and r'_r].

Propagation loss first defined by Wait [1959] is defined by the CCIR [1963a] as

$$L_p = L_s - L_{ft} - L_{fr} = L - L_{rt} - L_{rr} \quad db \tag{2.41}$$

Basic propagation loss is

$$L_{pb} = L_p + G_p \tag{2.42}$$

Basic propagation loss in free space is the same as the basic transmission loss in free space, L_{bf}, defined by (2.31).

The system loss L_s defined by (2.1) is a measurable quantity, while transmission loss L, path loss L_o, basic transmission loss L_b, attenuation relative to free space A, propagation loss L_p, and the field strength E are derived quantities, which in general require a theoretical calculation of $L_{et, er}$ and/or $L_{ft, fr}$ as well as a theoretical estimate of the loss in path antenna gain L_{gp}.

The following paragraphs explain why the concepts of effective radiated power, E.R.P. and an equivalent plane wave field strength are not recommended for reporting propagation data.

A half-wave antenna radiating a total of p_t watts produces a free space field intensity equal to

$$s_o = 1.64\, p_t/(4\pi r^2) \quad \text{watts/km}^2 \tag{2.43}$$

at a distance r kilometers in its equatorial plane, where the directive gain is equal to its maximum value 1.64, or 2.15 db. The field is linearly polarized in the direction of the antenna. In general, the field intensity s_p at a point $\vec{r}$ in free space and associated with the principal polarization for an antenna is

$$s_p(\vec{r}) = p_t\, g_p(\hat{r})/(4\pi r^2) \quad \text{watts/km}^2 \tag{2.44}$$

as explained in annex II. In (2.44), $\vec{r} = r\hat{r}$ and $g_p(\hat{r})$ is the principal polarization directive gain in the direction $\hat{r}$. A similar relation holds for the field intensity $s_c(\vec{r})$ associated with the cross-polarized component of the field.

Effective radiated power is associated with a prescribed polarization for a test antenna and is determined by comparing s_o as calculated using a field intensity meter or standard signal source with s_p as measured using the test antenna:

$$\text{E.R.P.} = P_t + 10\log(s_p/s_o) = P_t + G_{pt}(\hat{r}_1) - 2.15 \quad \text{dbw} \tag{2.45}$$

where $\hat{r}_1$ in free space is the direction towards the receiving antenna and in general is the initial direction of the most important propagation path to the receiver.

This ambiguity in definition, with the difficulties which sometimes arise in attempting to separate characteristics of an antenna from those of its environment, make the effective radiated power E.R.P. an inferior parameter, compared with the total radiated power P_t, which can be more readily measured. The following equation, with P_t determined from (2.45), may be used to convert reported values of E.R.P. to estimates of the transmitter power output $P_{\ell t}$ when transmission line and mismatch losses $L_{\ell t}$ and the power radiation efficiency $1/\ell_{et}$ are known:

$$P_{\ell t} = P_t' + L_{\ell t} = P_t + L_{et} + L_{\ell t} \quad \text{dbw} \tag{2.46}$$

The electromagnetic field discussed in annex II is a complex vector function in space and time, and information about amplitude, polarization, and phase is required to describe it. A real antenna responds to the total field surrounding it, rather than to E, which corresponds to the r.m.s. amplitude of the usual "equivalent" electromagnetic field, defined at a single point and for a specified polarization.

For converting reported values of E in dbu to estimates of $P_{\ell t}$ or estimates of the available power $P_{\ell r}$ at the input to a receiver, the following relationships may be useful:

$$P_{\ell t} = E + L_{\ell t} + L_{ft} - G_t + L_{pb} - 20 \log f - 107.22 \quad \text{dbw} \tag{2.47}$$

$$P_{\ell r} = E - L_{\ell r} - L_{fr} + G_r - L_{gp} - 20 \log f - 107.22 \quad \text{dbw} \tag{2.48}$$

$$P_{\ell r} = P_a' - L_{\ell r} = P_a - L_{er} - L_{\ell r} \quad \text{dbw} \tag{2.49}$$

In terms of reported values of field strength E_{1kw} in dbu per kilowatt of effective radiated power, estimates of the system loss, L_s, basic propagation loss L_{pb}, or basic transmission loss L_b may be derived from the following equations,

$$L_s = 139.37 + L_{et} + L_{fr} - G_p + G_t - G_{pt}(\hat{r}_1) + 20 \log f - E_{1kw} \quad \text{db} \tag{2.50}$$

$$L_{pb} = 139.37 - L_{rt} + G_t - G_{pt}(\hat{r}_1) + 20 \log f - E_{1kw} \quad \text{db} \tag{2.51}$$

$$L_b = 139.37 + L_{rr} + G_t - G_{pt}(\hat{r}_1) + 20 \log f - E_{1kw} \quad \text{db} \tag{2.52}$$

provided that estimates are available for all of the terms in these equations.

For an antenna whose radiation resistance is unaffected by the proximity of its environment, $L_{rt} = L_{rr} = 0$ db, $L_{ft} = L_{et}$, and $L_{fr} = L_{er}$. In other cases, especially important for frequencies less than 30 MHz with antenna heights commonly used, it is often assumed that $L_{rt} = L_{rr} = 3.01$ db, $L_{ft} = L_{et} + 3.01$ db, and $L_{fr} = L_{er} + 3.01$ db, corresponding to the assumption of short vertical electric dipoles above a perfectly-conducting infinite plane. At low and very low frequencies, L_{et}, L_{er}, L_{ft}, and L_{fr} may be very large. Propagation curves at HF and lower frequencies may be given in terms of L_p or L_{pb} so that it is not necessary to specify L_{et} and L_{er}.

Naturally, it is better to measure L_s directly than to calculate it using (2.50). It may be seen that the careful definition of L_s, L_p, L, or L_o is simpler and more direct than the definition of L_b, L_{pb}, A, or E.

The equivalent free-space field strength E_o in dbu for one kilowatt of effective radiated power is obtained by substituting $P_{\ell t} = P_t = E.R.P. = 30$ dbw, $G_{pt}(\hat{r}_1) = G_t = 2.15$ db, $L_{\ell t} = L_{ft} = 0$ db, and $L_{pb} = L_{bf}$ in (2.45)-(2.47), where L_{bf} is given by (2.31):

$$E_o = 106.92 - 20 \log d \quad \text{dbu/kw} \tag{2.53}$$

where r in (2.31) has been replaced by d in (2.53). Thus e_o is 224.3 millivolts per meter at one kilometer or 139.4 millivolts per meter at one mile. In free space, the

"equivalent inverse distance field strength", E_I, is the same as E_o. If the antenna radiation resistances r_t and r_r are equal to the free space radiation resistances r_{ft} and r_{fr}, then (2.52) provides the following relationship between E_{1kw} and L_b with $G_{pt}(\hat{r}_1) = G_t$:

$$E_{1kw} = 139.37 + 20 \log f - L_b \quad \text{dbu/kw} \tag{2.54}$$

Consider a short vertical electric dipole above a perfectly-conducting infinite plane, with E.R.P. = 30 dbw, $G_t = 1.76$ db, and $L_{rr} = 3.01$ db. From (2.45) $P_t = 30.39$ dbw, since $G_{pt}(\hat{r}_1) = 1.76$ db. Then from (2.52) the equivalent inverse distance field is

$$E_I = E_o + L_{rt} + L_{rr} = 109.54 - 20 \log d \quad \text{dbu/kw} \tag{2.55}$$

corresponding to $e_I = 300$ mv/m at one kilometer, or $e_I = 186.4$ mv/m at one mile. In this situation, the relationship between E_{1kw} and L_b is given by (2.52) as

$$E_{1kw} = 142.38 + 20 \log f - L_b \quad \text{dbu/kw} \tag{2.56}$$

The foregoing suggests the following general expressions for the equivalent free space field strength E_o and the equivalent inverse distance field E_I:

$$E_o = (P_t - L_{rt} + G_t) - 20 \log d + 74.77 \quad \text{dbu} \tag{2.57}$$

$$E_I = E_o + L_{rt} + L_{rr} \quad \text{dbu} \tag{2.58}$$

Note that L_{rt} in (2.57) is not zero unless the radiation resistance of the transmitting antenna in its actual environment is equal to its free space radiation resistance. The definition of "attenuation relative to free space" given by (2.35) as the basic transmission loss relative to that in free space, may be restated as

$$A = L_b - L_{bf} = L - L_f = E_I - E \quad \text{db} \tag{2.59}$$

Alternatively, attenuation relative to free space, A_t, might have been defined (as it sometimes is) as basic propagation loss relative to that in free space:

$$A_t = L_{pb} - L_{bf} = A - L_{rt} - L_{rr} = E_o - E \quad \text{db} \tag{2.60}$$

For frequencies and antenna heights where these definitions differ by as much as 6 db, caution should be used in reporting data. For most paths using frequencies above

50 MHz, $L_{rt} + L_{rr}$ is negligible, but caution should again be used if the loss in path antenna gain L_{gp} is not negligible. It is then important not to confuse the "equivalent" free space loss L_f given by (2.34) with the loss in free space given by (2.33).

3. ATMOSPHERIC ABSORPTION

At frequencies above 2 GHz attenuation of radio waves due to absorption or scattering by constituents of the atmosphere, and by particles in the atmosphere, may seriously affect microwave relay links, communication via satellites, and radio and radar astronomy. At frequencies below 1 GHz the total radio wave absorption by oxygen and water vapor for propagation paths of 1000 kilometers or less will not exceed 2 decibels. Absorption by rainfall begins to be barely noticeable at frequencies from 2 to 3 GHz, but may be quite appreciable at higher frequencies.

For frequencies up to 100 GHz, and for both optical and transhorizon paths, this section provides estimates of the long-term median attenuation A_a of radio waves by oxygen and water vapor, the attenuation A_r due to rainfall, and the order of magnitude of absorption by clouds of a given water content. The estimates are based on work reported by Artman and Gordon [1954], Bean and Abbott [1957], Bussey [1950], Crawford and Hogg [1956], Gunn and East [1954], Hathaway and Evans [1959], Hogg and Mumford [1960], Hogg and Semplak [1961], Lane and Saxton [1952], Laws and Parsons [1943], Perlat and Voge [1953], Straiton and Tolbert [1960], Tolbert and Straiton [1957], and Van Vleck [1947a, b; 1951].

3.1 Absorption by Water Vapor and Oxygen

Water vapor absorption has a resonant peak at a frequency of 22.23 GHz, and oxygen absorption peaks at a number of frequencies from 53 to 66 GHz and at 120 GHz. Figure 3.1, derived from a critical appraisal of the above references, shows the differential absorption γ_{oo} and γ_{wo} in decibels per kilometer for both oxygen and water vapor, as determined for standard conditions of temperature and pressure and for a surface value of absolute humidity equal to 10 grams per cubic meter. These values are consistent with those prepared for the Xth Plenary Assembly of the CCIR by U.S. Study Group IV [1963d] except that the water vapor density is there taken to be 7.5 g/m^3. For the range of absolute humidity likely to occur in the atmosphere, the water vapor absorption in db/km is approximately proportional to the water vapor density.

The total atmospheric absorption A_a decibels for a path of length r_o kilometers is commonly expressed in one of two ways, either as the integral of the differential absorption $\gamma(r)$ dr:

$$A_a = \int_0^{r_o} \gamma(r) \ dr \quad db \tag{3.1}$$

or in terms of an absorption coefficient $\Gamma(r)$ expressed in reciprocal kilometers:

$$A_a = -10 \ \log \ \exp \left[-\int_0^{r_o} \Gamma(r) \ dr \right] = 4.343 \int_0^{r_o} \Gamma(r) \ dr \quad db \tag{3.2}$$

3-1

The argument of the logarithm in (3.2) is the amount of radiowave energy that is not absorbed in traversing the path.

The total gaseous absorption A_a over a line-of-sight path of length r_o kilometers is

$$A_a = \int_0^{r_o} dr \left[\gamma_o(h) + \gamma_w(h) \right] \quad db \tag{3.3}$$

where h is the height above sea level at a distance r from the lower terminal, measured along a ray path between terminals. For radar returns, the total absorption is $2A_a$ db.

Considering oxygen absorption and water vapor absorption separately, (3.3) may be written

$$A_a = \gamma_{oo} r_{eo} + \gamma_{wo} r_{ew} \quad db \tag{3.4}$$

where r_{eo} and r_{ew} are effective distances obtained by integrating γ_o/γ_{oo} and γ_w/γ_{wo} over the ray path.

The effective distances r_{eo} and r_{ew} are plotted versus r_o and frequency for elevation angles θ_o = 0, 0.01, 0.02, 0.05, 0.1, 0.2, 0.5, 1, and $\pi/2$ radians in figures 3.2-3.4. Figure 3.5 shows the relationship between r_o and the sea level arc distance, d, for these values of θ_o.

A_a may be estimated from figures I.21 to I.26 of annex I, where attenuation relative to free space, A, is plotted versus f, θ_o, and r_o, ignoring effects of diffraction by terrain.

For nonoptical paths, the ray from each antenna to its horizon makes an angle θ_{ot} or θ_{or} with the horizontal at the horizon, as illustrated in figure 6.1 of section 6. The horizon rays intersect at distances d_1 and d_2 from the transmitting and receiving terminals. The total absorption A_a is the sum of values A_{at} and A_{ar}

$$A_a = A_{at} + A_{ar}$$

(3.5)

where $\qquad A_{at} \equiv A_a (f, \theta_{ot}, d_1), \quad A_{ar} \equiv A_a (f, \theta_{or}, d_2)$

For propagation over a smooth earth, $\theta_{ot} = \theta_{or} = 0$, and $A_a \cong 2A_a (f, 0, d/2)$. For transhorizon paths and the frequency range 0.1 - 10 GHz, figure 3.6 shows A_a plotted versus distance over a smooth earth between 10 meter antenna heights.

3.2 Sky-Noise Temperature

The nonionized atmosphere is a source of radio noise, with the same properties as a reradiator that it has as an absorber. The effective sky-noise temperature T_s may be determined by integrating the gas temperature T multiplied by the differential fraction of reradiated power that is not absorbed in passing through the atmosphere to the antenna:

$$T_s(°K) = \int_0^\infty T(r)\Gamma(r) \exp\left[-\int_0^r \Gamma(r') \, dr'\right] dr \qquad (3.6)$$

where the absorption coefficient $\Gamma(r)$ in reciprocal kilometers is defined by (3.2) For instance, assuming

$$T(r) = (288 - 6.5h)°K \quad \text{for} \quad h \leq 12 \text{ km,}$$

and

$$T(r) = 210°K \qquad \text{for} \quad h \geq 12 \text{ km,}$$

figure 3.7 shows the sky-noise temperature due to oxygen and water vapor for various angles of elevation and for frequencies between 0.1 and 100 GHz.

In estimating antenna temperatures, the antenna pattern and radiation from the earth's surface must also be considered.

3.3 Attenuation by Rain

The attenuation of radio waves by suspended water droplets and rain often exceeds the combined oxygen and water vapor absorption. Water droplets in fog or rain will scatter radio waves in all directions whether the drops are small compared to the wavelength or comparable to the wavelength. In the latter case, raindrops trap and absorb some of the radio wave energy; accordingly, rain attenuation is much more serious at millimeter wavelengths than at centimeter wavelengths.

In practice it has been convenient to express rain attenuation as a function of the precipitation rate, R_r, which depends on both the liquid water content and the fall velocity of the drops, the latter in turn depending on the size of the drops. There is little evidence that rain with a known rate of fall has a unique drop-size distribution, and the problem of estimating the attenuation of radio waves by the various forms of precipitation is quite difficult.

Total absorption A_r due to rainfall over a path of length r_o can be estimated by integrating the differential rain absorption $\gamma_r(r)\,dr$ along the direct path between two intervisible antennas, or along horizon rays in the case of transhorizon propagation:

$$A_r = \int_0^{r_o} \gamma_r(r)\,dr \quad \text{decibels} \tag{3.7}$$

Fitting an arbitrary mathematical function empirically to theoretical results given by Hathaway and Evans [1959] and Ryde and Ryde [1945], the rate of absorption by rain γ_r may be expressed in terms of the rainfall rate R_r in millimeters per hour as

$$\gamma_r = K R_r^{\alpha} \quad \text{db/km} \tag{3.8}$$

for frequencies above 2 GHz. The functions $K(f_G)$ and $\alpha(f_G)$ are plotted in figures 3.8 and 3.9, where f_G is the radio frequency in GHz.

$$K = [\, 3(f_G - 2)^2 - 2(f_G - 2)\,] \times 10^{-4} \tag{3.9a}$$

$$\alpha = [\, 1.14 - 0.07(f_G - 2)^{\frac{1}{3}}\,] \, [\, 1 + 0.085(f_G - 3.5)\, \exp(-0.006\, f_G^2)\,] \tag{3.9b}$$

An examination of the variation of rainfall rate with height suggests a relation of the form

$$R_r / R_{rs} = \exp(-0.2\, h^2) \tag{3.10}$$

where R_{rs} is the surface rainfall rate. Then

$$A_r = \gamma_{rs} r_{er} \quad db, \tag{3.11}$$

$$\gamma_{rs} = K R_{rs}^{\alpha} \quad db/km, \qquad r_{er} = \int_0^{r_o} dr \exp(-0.2 \, \alpha \, h^2) \quad km \tag{3.12}$$

where γ_{rs} is the surface value of the rate of absorption by rain, and r_{er} is an "effective rainbearing distance". Figures 3.10-3.13 show r_{er} versus r_o for several values of θ_o and α. The curves shown were computed using (3.12).

A "standard" long-term cumulative distribution of rain absorption is estimated, using some statistics from Ohio analyzed by Bussey [1950], who relates the cumulative distribution of instantaneous path average rainfall rates for 25, 50, and 100-kilometer paths, respectively, with the cumulative distributions for a single rain gauge of half-hour, one-hour, and two-hour mean rainfall rates, recorded for a year. The total annual rainfall in Ohio is about 110 centimeters.

Rainfall statistics vary considerably from region to region, sometimes from year to year, and often with the direction of a path (with or across prevailing winds). For instance, in North America, east-west systems seem particularly vulnerable, as they lie along the path of frequent heavy showers.

For very long paths, the cumulative distribution of instantaneous path average rainfall rates, $\overline{R}_r$, depends on how R_r varies with elevation above the surface and upon the correlation of rainfall with distance along the path. Figure 3.14 provides estimates of the instantaneous path average rainfall rate $\overline{R}_r$ exceeded for 0.01, 0.1, 1, and 5 percent of the year as a function of r_{er} and normalized to a total annual rainfall of 100 cm. To obtain A_r from (3.11), replace R_{rs} in (3.12) with $\overline{R}_r$ from figure 3.14, multiplied by the ratio of the total annual rainfall and 100 cm. These estimates are an extrapolation of the results given by Bussey [1950] and are intended to allow for the average variation of R_r with height, as given by (3.10) and allowed for in the definition of r_{er}, and for the correlation of surface rainfall rate R_{rs} with distance along the surface, as analyzed by Bussey.

3.4 Attenuation in Clouds

Cloud droplets are regarded here as those water or ice particles having radii smaller than 100 microns or 0.01 cm. Although a rigorous approach to the problem of attenuation by clouds must consider drop-size distribution, it is more practical to speak of the water content of clouds rather than the drop-size distribution. Reliable measurements of both parameters are scarce, but it is possible to make reasonable estimates of the water content, M, of a cloud from a knowledge of the vertical extent of the cloud and the gradients of pressure, temperature, and mixing ratio, which is the ratio of the mass of water vapor to the mass of dry air in which it is mixed. The absorption within a cloud can be written as

$$A_c = K_1 M \quad db \tag{3.13}$$

where A_c is the total absorption attenuation within the cloud, K_1 is an attenuation coefficient, values for which are given in table 3.1, and M is the liquid water content of the cloud, measured in grams per cubic meter. The amount of precipitable water, M, in a given pressure layer can be obtained by evaluating the average mixing ratio in the layer, multiplying by the pressure difference, and dividing by the gravity. Using this method of obtaining M and the values of K_1 from table 3.1, it is possible to get a fairly reliable estimate of the absorption of radio energy by a cloud.

Several important facts are demonstrated by table 3.1. The increase in attenuation with increasing frequency is clearly shown. The values change by about an order of magnitude from 10 to 30 GHz. Cloud attenuation can be safely neglected below 6 GHz. The data presented here also show that attenuation increases with decreasing temperature. These relations are a reflection of the dependence of the refractive index on both wavelength and temperature. The different dielectric properties of water and ice are illustrated by the difference in attenuation. Ice clouds give attenuations about two orders of magnitude smaller than water clouds of the same water content.

TABLE 3.1

One-Way Attenuation Coefficient, K_1, in db/km/gm/m^3

Temperature (°C)		Frequency, GHz,			
		33	24	17	9.4
Water	20	0.647	0.311	0.128	0.0483
	10	0.681	0.406	0.179	0.0630
Cloud	0	0.99	0.532	0.267	0.0858
	-8	1.25	0.684	0.34 (extrapolated)	0.112 (extrapolated)
Ice	0	8.74×10^{-3}	6.35×10^{-3}	4.36×10^{-3}	2.46×10^{-3}
Cloud	-10	2.93×10^{-3}	2.11×10^{-3}	1.46×10^{-3}	8.19×10^{-4}
	-20	2.0×10^{-3}	1.45×10^{-3}	1.0×10^{-3}	5.63×10^{-4}

SURFACE VALUES γ_{oo} AND γ_{wo} OF ABSORPTION
BY OXYGEN AND WATER VAPOR
PRESSURE 760mm Hg
TEMPERATURE 20°C
WATER VAPOR DENSITY 10g/m³

DIFFERENTIAL ABSORPTION γ IN DECIBELS PER KILOMETER

FREQUENCY IN GHz

Figure 3.1

3 - 7
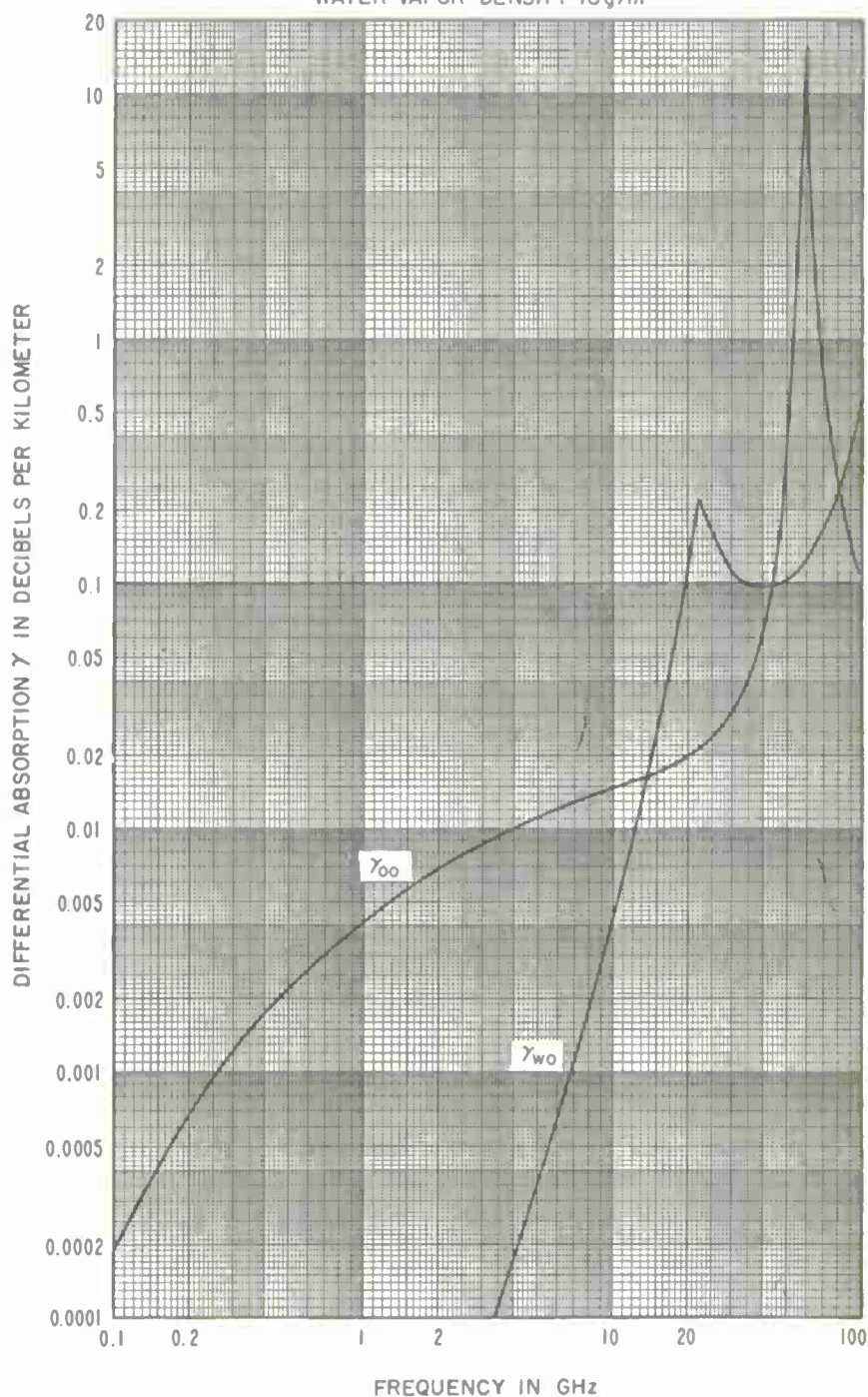
EFFECTIVE DISTANCES r_{eo} AND r_{ew} FOR ABSORPTION BY OXYGEN AND WATER VAPOR
$\theta_0 = 0, 0.01, 0.02$
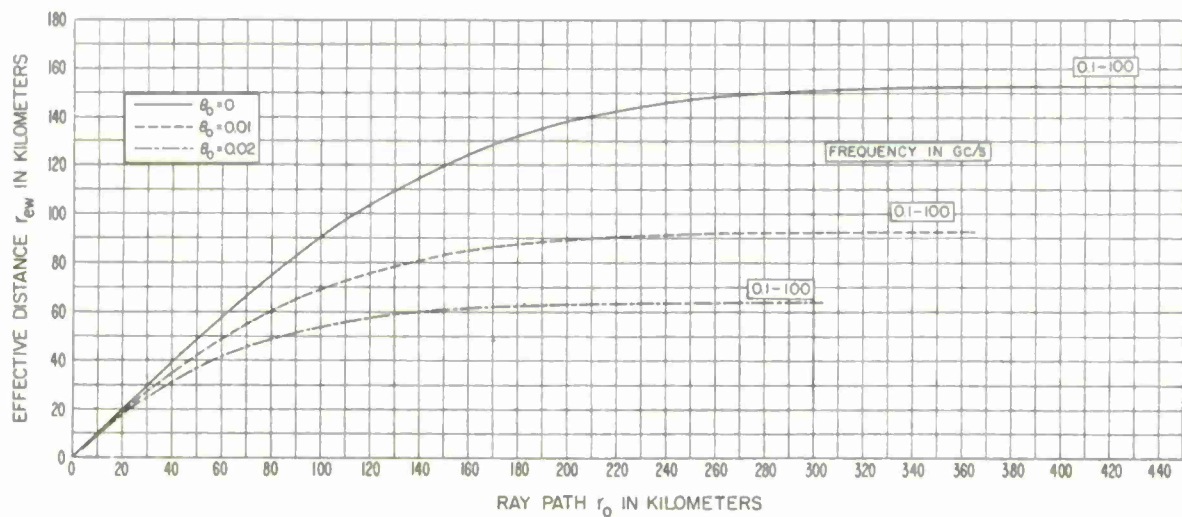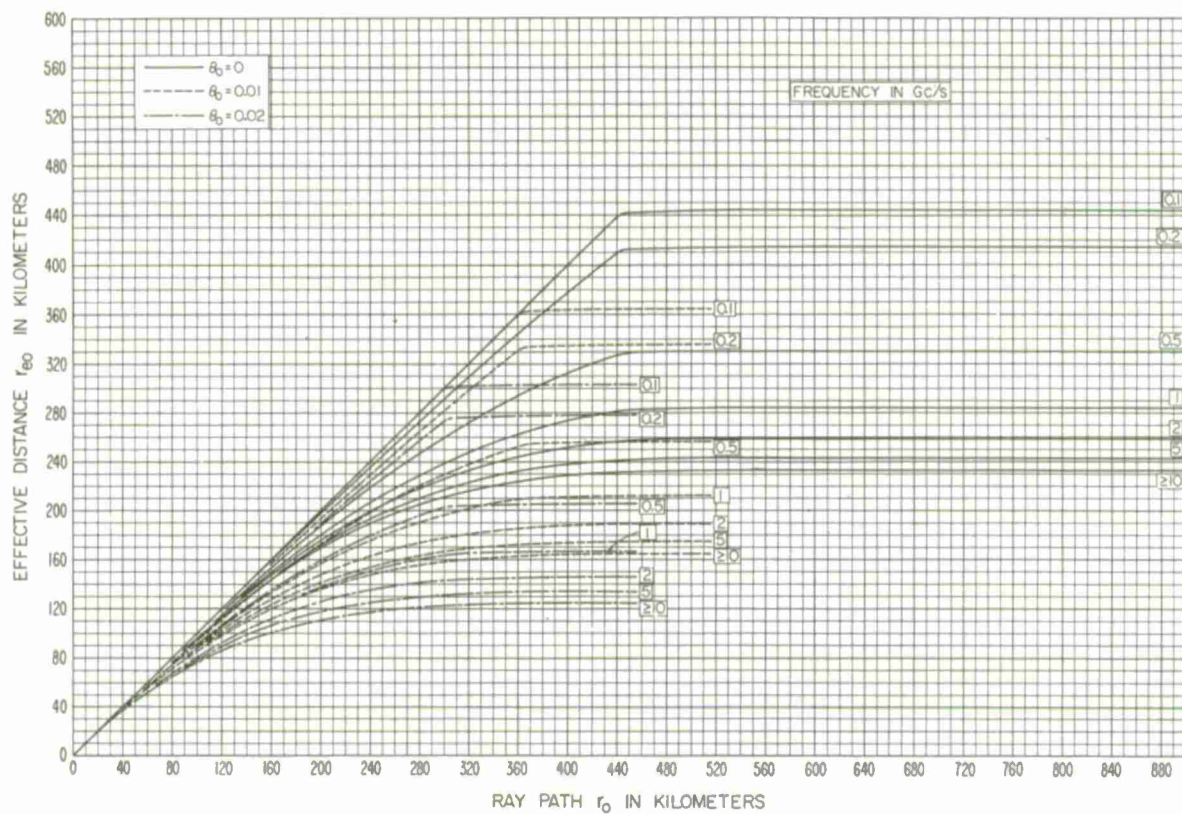
Figure 3.2

EFFECTIVE DISTANCES r_{eo} AND r_{ew} FOR ABSORPTION BY OXYGEN AND WATER VAPOR
$\theta_0 = 0.05,\ 0.1,\ 0.2$
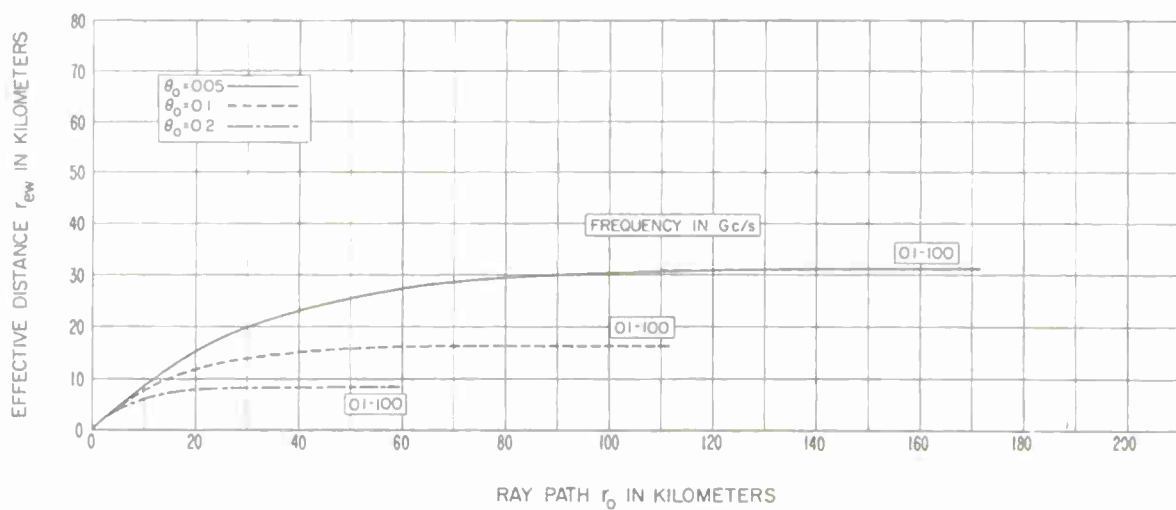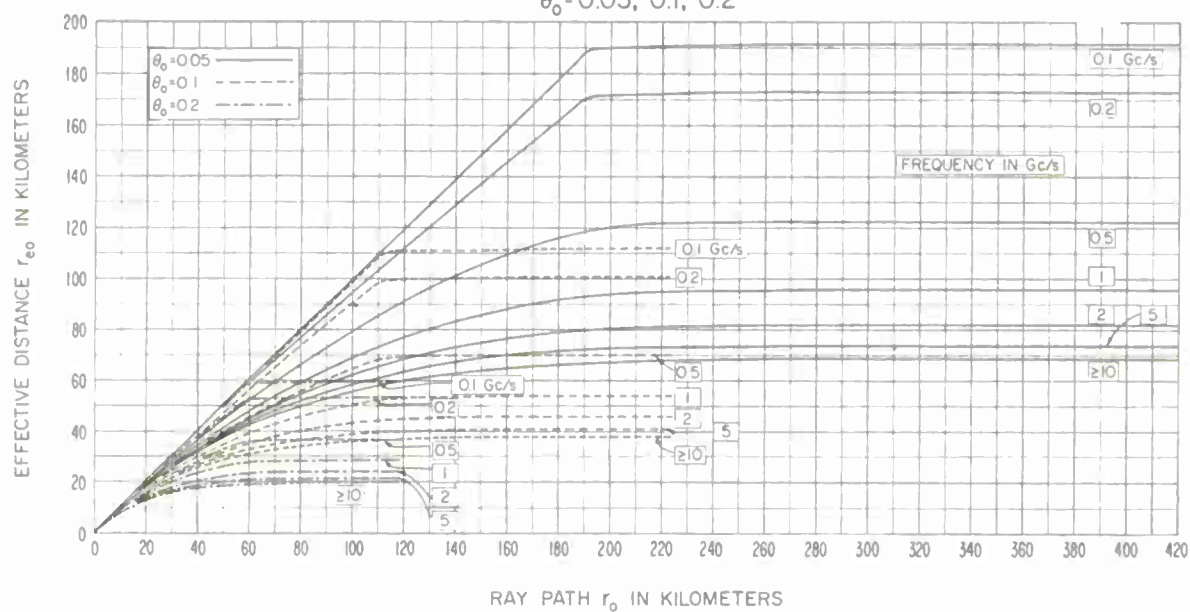
Figure 3.3

EFFECTIVE DISTANCES r_{eo} AND r_{ew} FOR ABSORPTION BY OXYGEN AND WATER VAPOR
$\theta_0 = 0.5, 1, \pi/2$
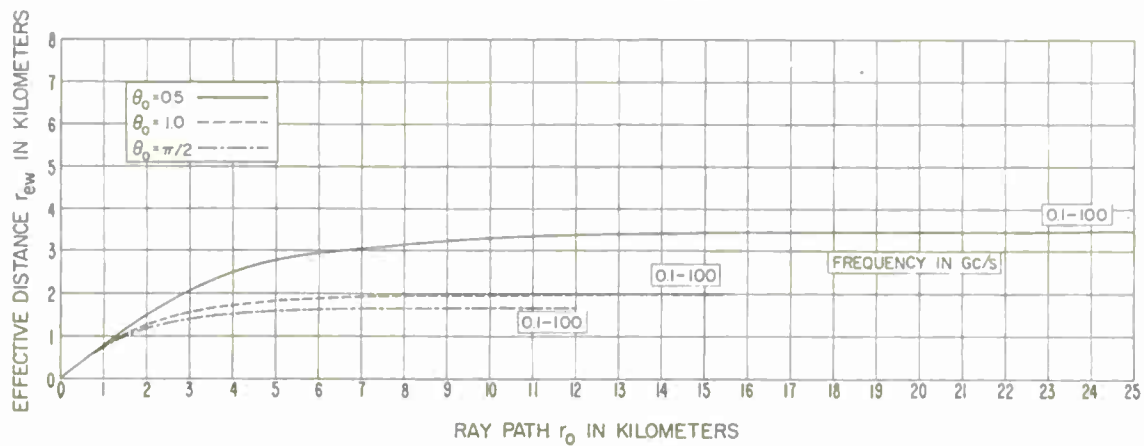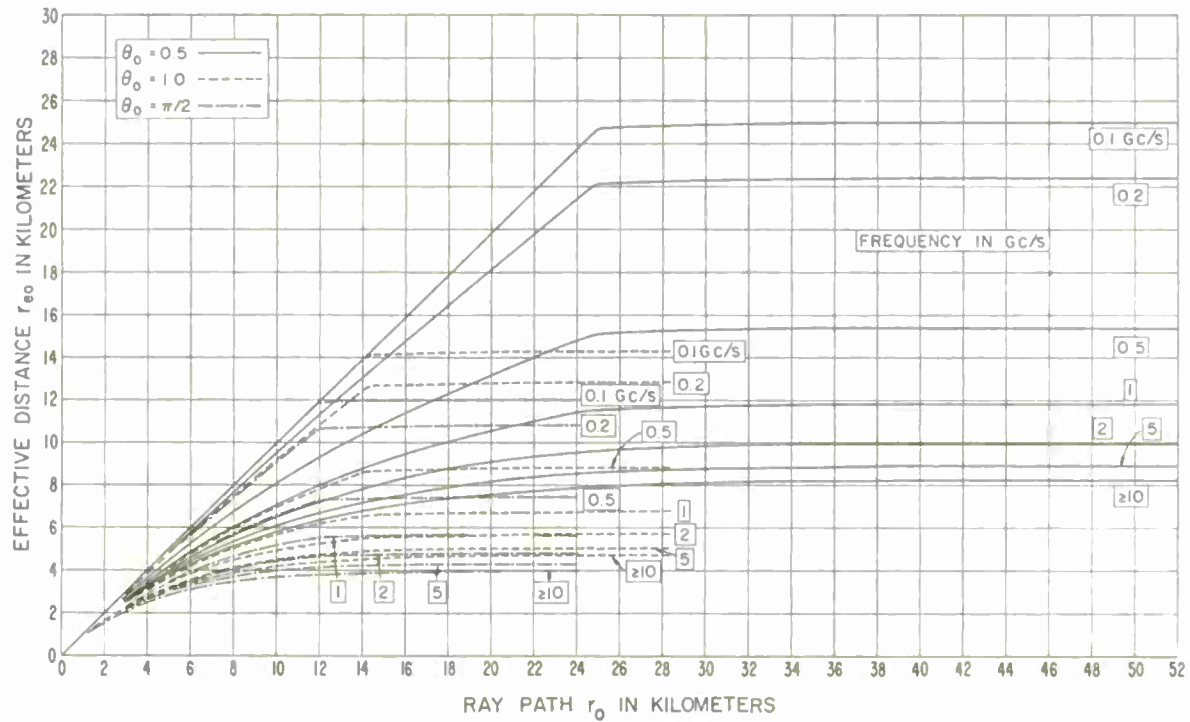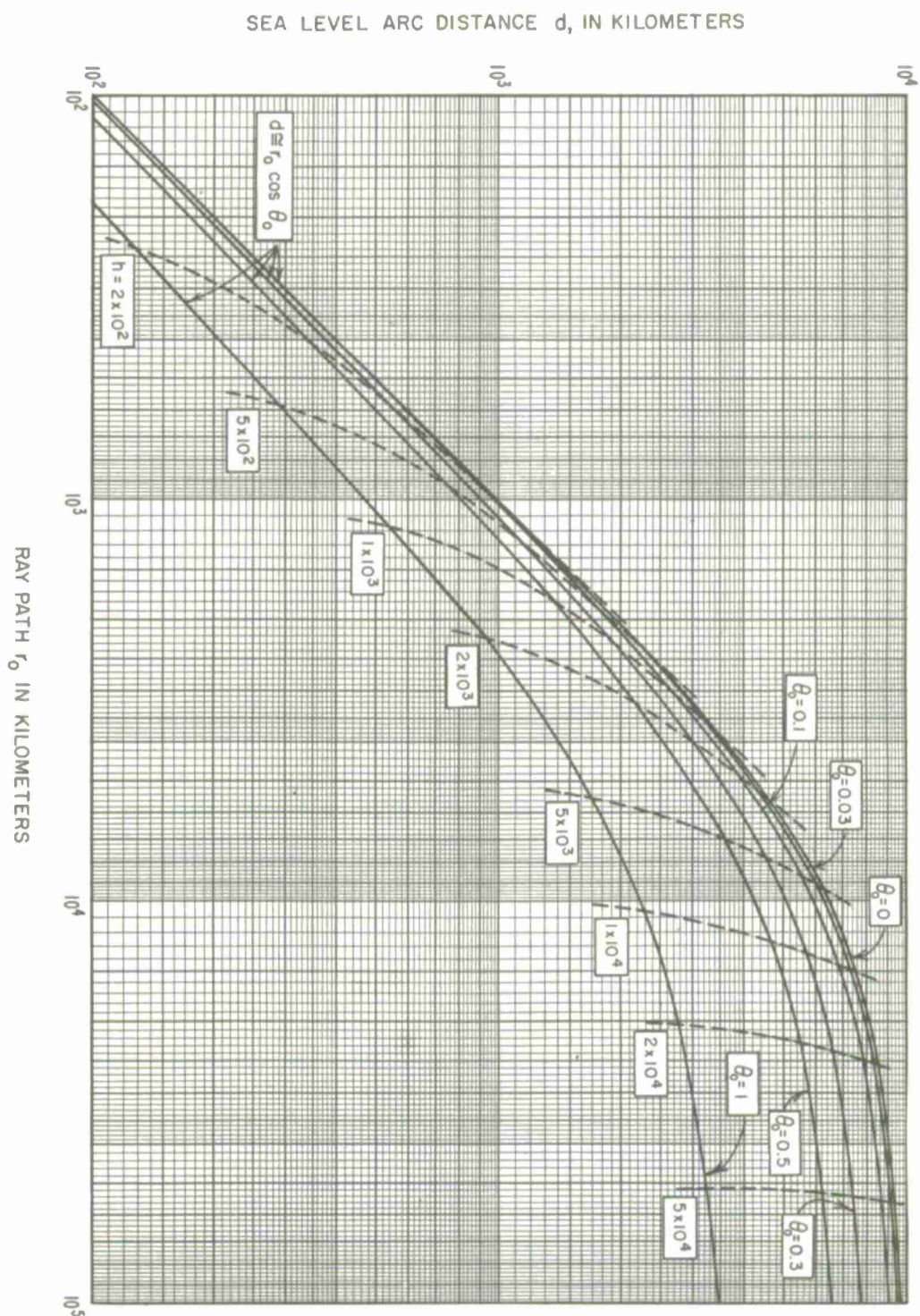
Figure 3.4

RAY PATH LENGTH, r_0, VERSUS SEA LEVEL ARC DISTANCE, d
$\theta_0 = 0, 0.03, 0.1, 0.3, 0.5, 1$

SEA LEVEL ARC DISTANCE d, IN KILOMETERS

RAY PATH r_0 IN KILOMETERS

Figure 3.5

3-11

OXYGEN AND WATER VAPOR ABSORPTION IN DECIBELS

ESTIMATE OF MEDIAN OXYGEN AND WATER VAPOR ABSORPTION
FROM AUGUST DATA, WASHINGTON, D. C.

FREQUENCY IN MHz

DISTANCE IN KILOMETERS

Figure 3.6

3-12
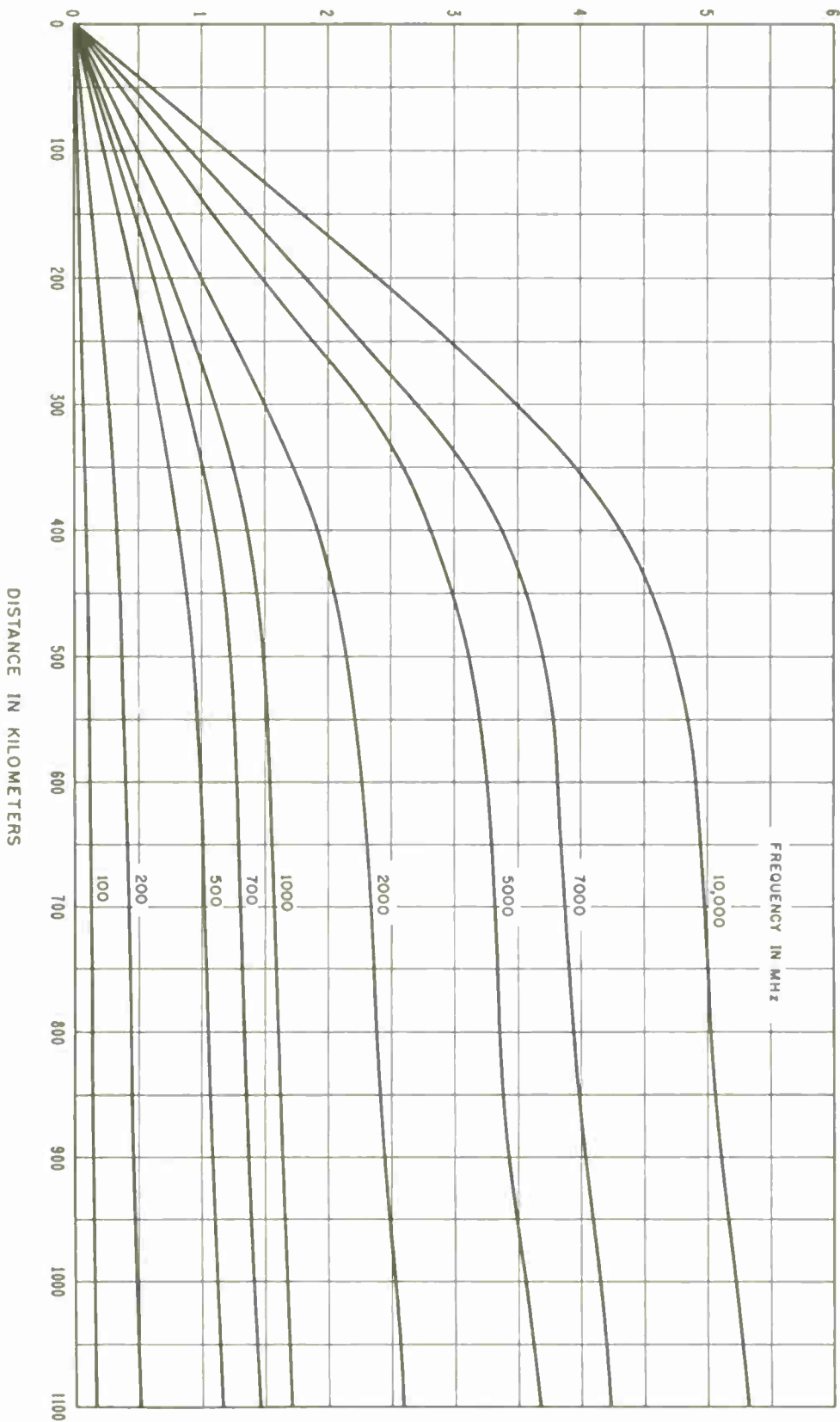
SKY NOISE TEMPERATURE DUE TO RERADIATION BY OXYGEN AND WATER VAPOR

Figure 3.7

3-13
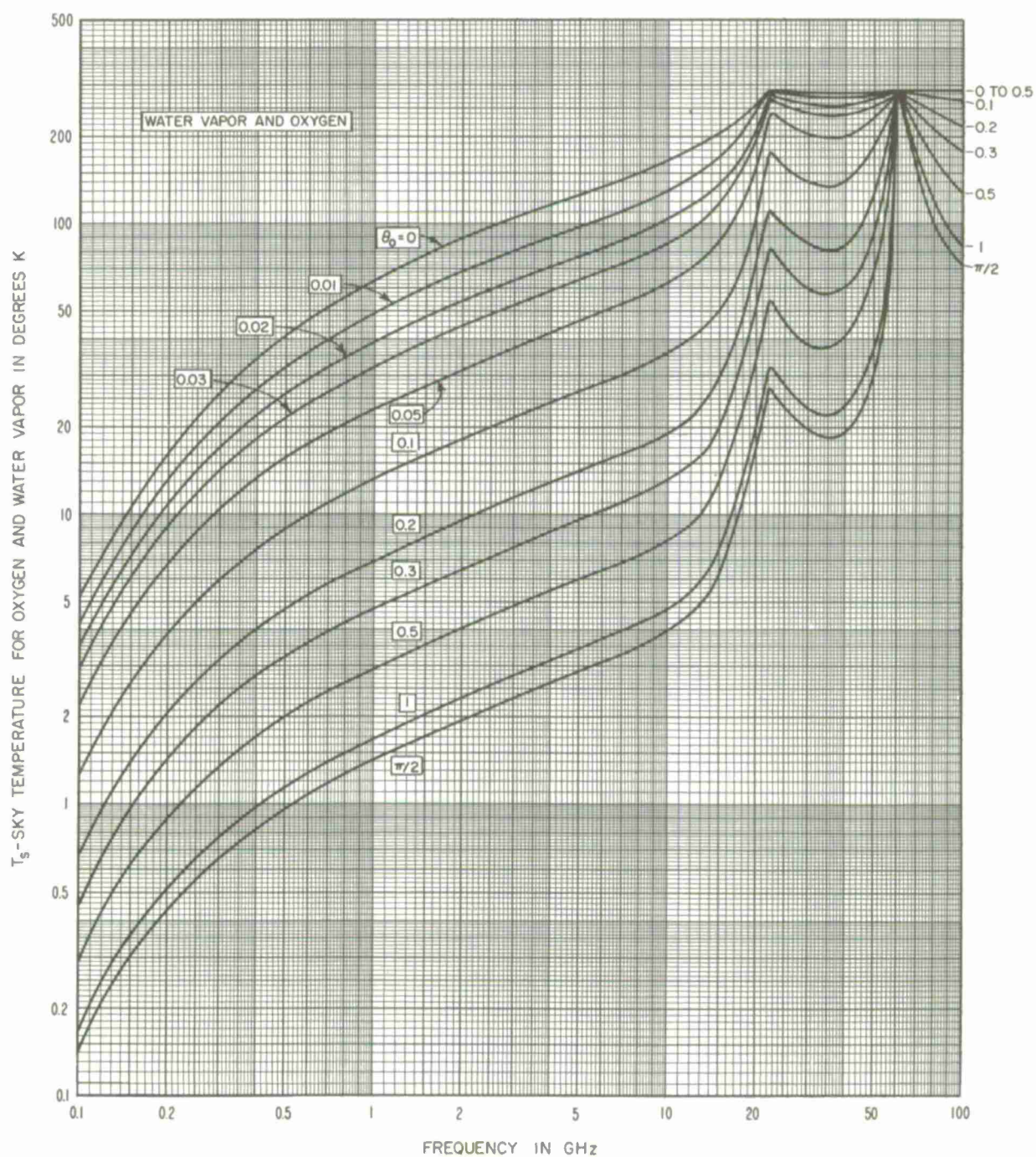
RAINFALL ABSORPTION COEFFICIENT K vs FREQUENCY

$$\gamma = KR_r^\alpha \text{ db/km, WHERE } R_r \text{ IS THE}$$
RAINFALL RATE IN MILLIMETERS/HOUR

$$K = \left[3(f_G-2)^2 - 2(f_G-2)\right] \times 10^{-4}$$

$$\alpha = \left[1.14 - 0.07(f_G-2)^{1/3}\right]\left[1 + 0.085(f_G-3.5)\exp(-0.006 f_G^2)\right]$$

FREQUENCY f_G IN GHz
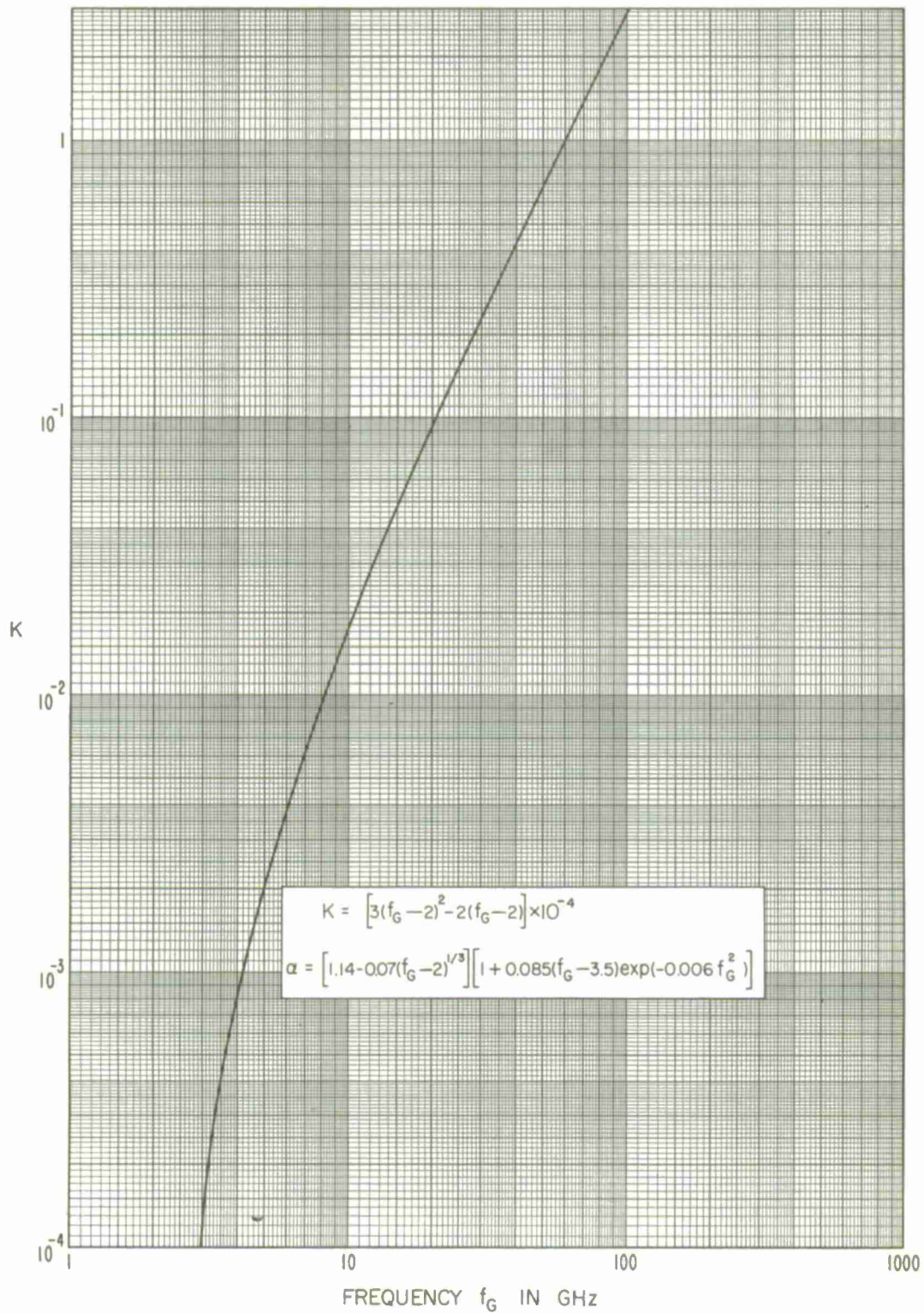
Figure 3.8

RAINFALL ABSORPTION EXPONENT α vs FREQUENCY
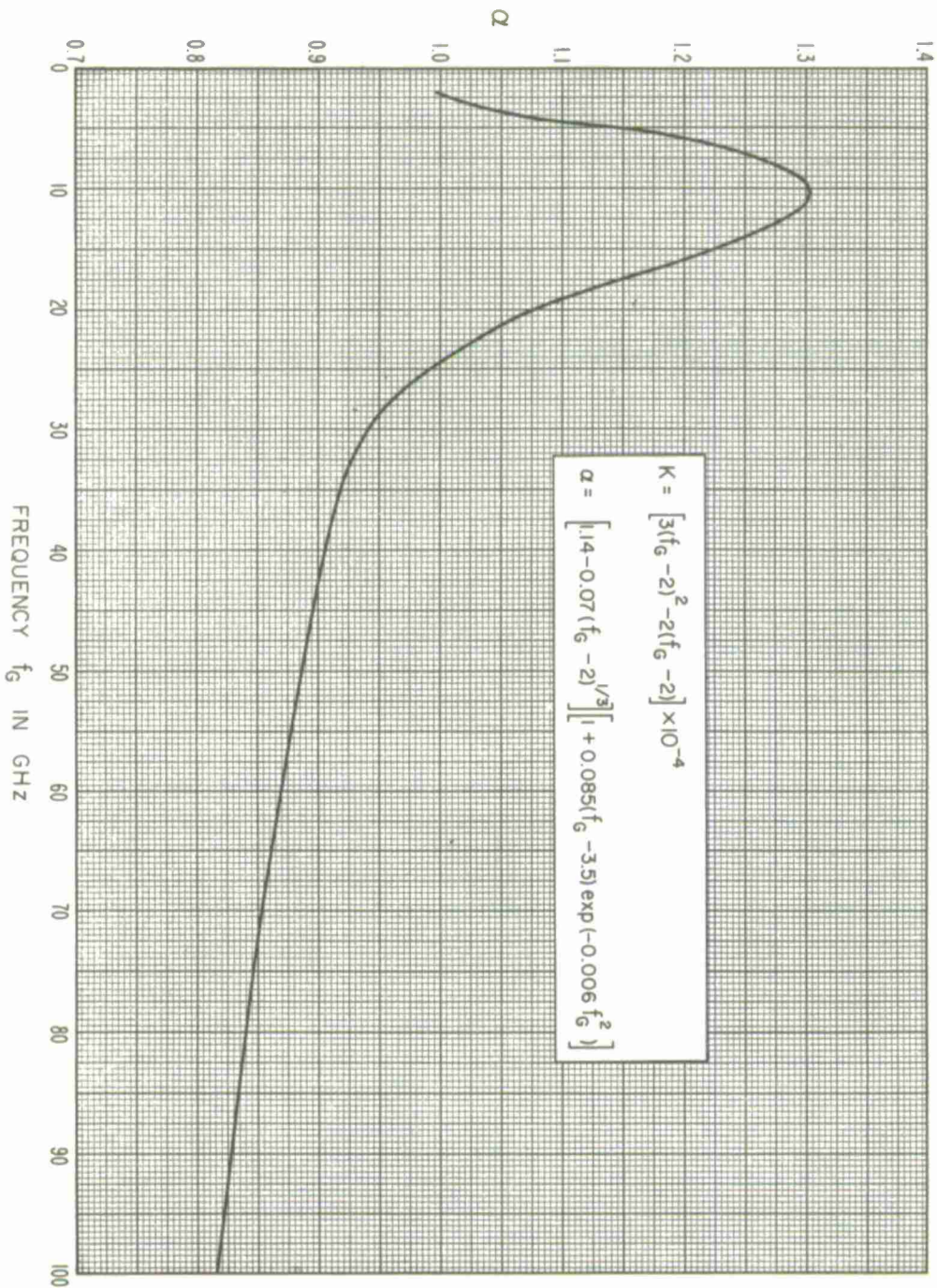
$\gamma = K R_r^\alpha$ db/km, WHERE R_r IS THE

RAINFALL RATE IN MILLIMETERS/HOUR

$$K = \left[3(f_G - 2)^2 - 2(f_G - 2) \right] \times 10^{-4}$$

$$\alpha = \left[1.14 - 0.07(f_G - 2) \right]^{1/3} \left[1 + 0.085(f_G - 3.5) \exp(-0.006\, f_G^2) \right]$$

Figure 3.9

FREQUENCY f_G IN GHz
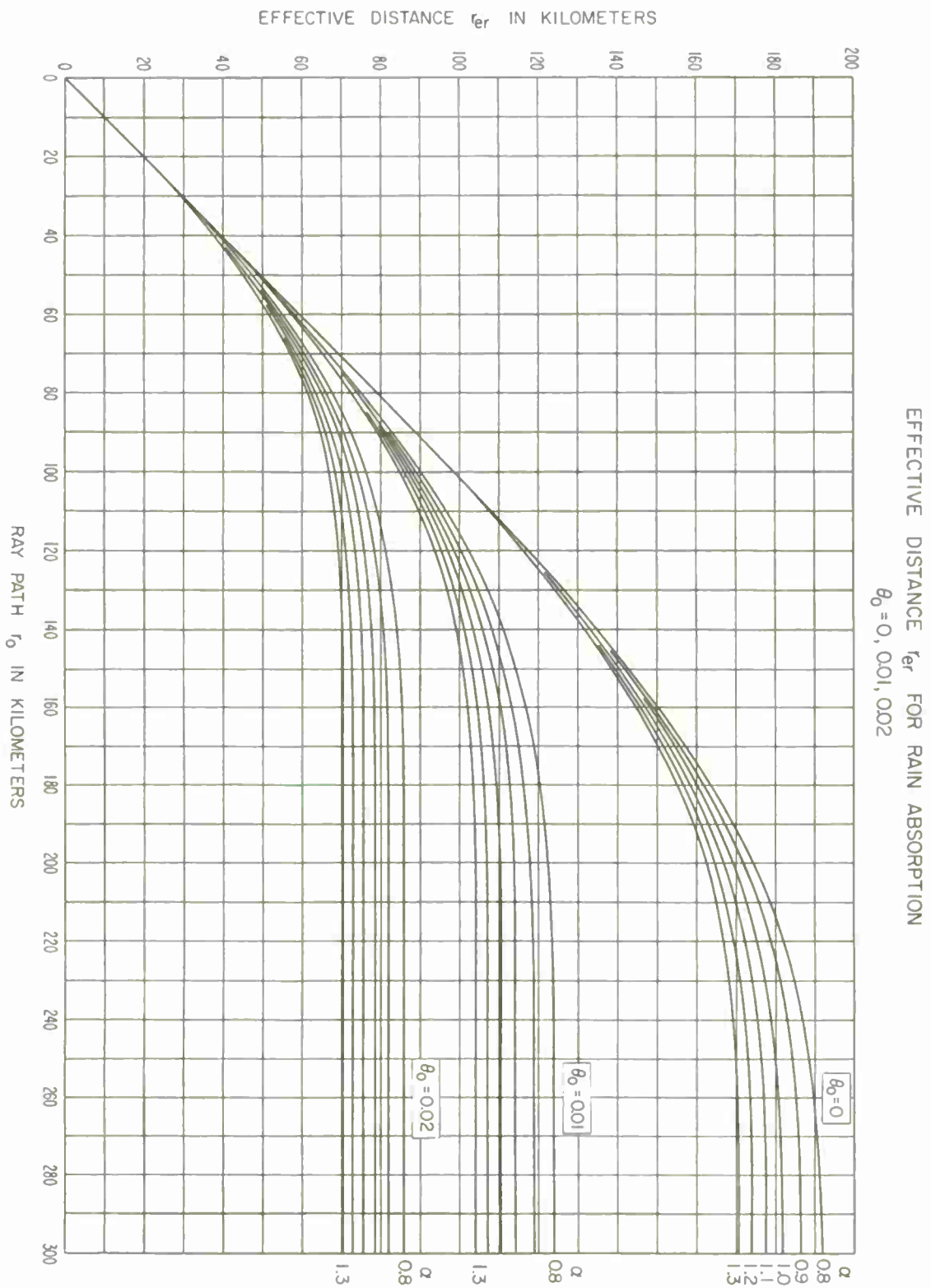
Figure 3.10

EFFECTIVE DISTANCE r_{er} FOR RAIN ABSORPTION
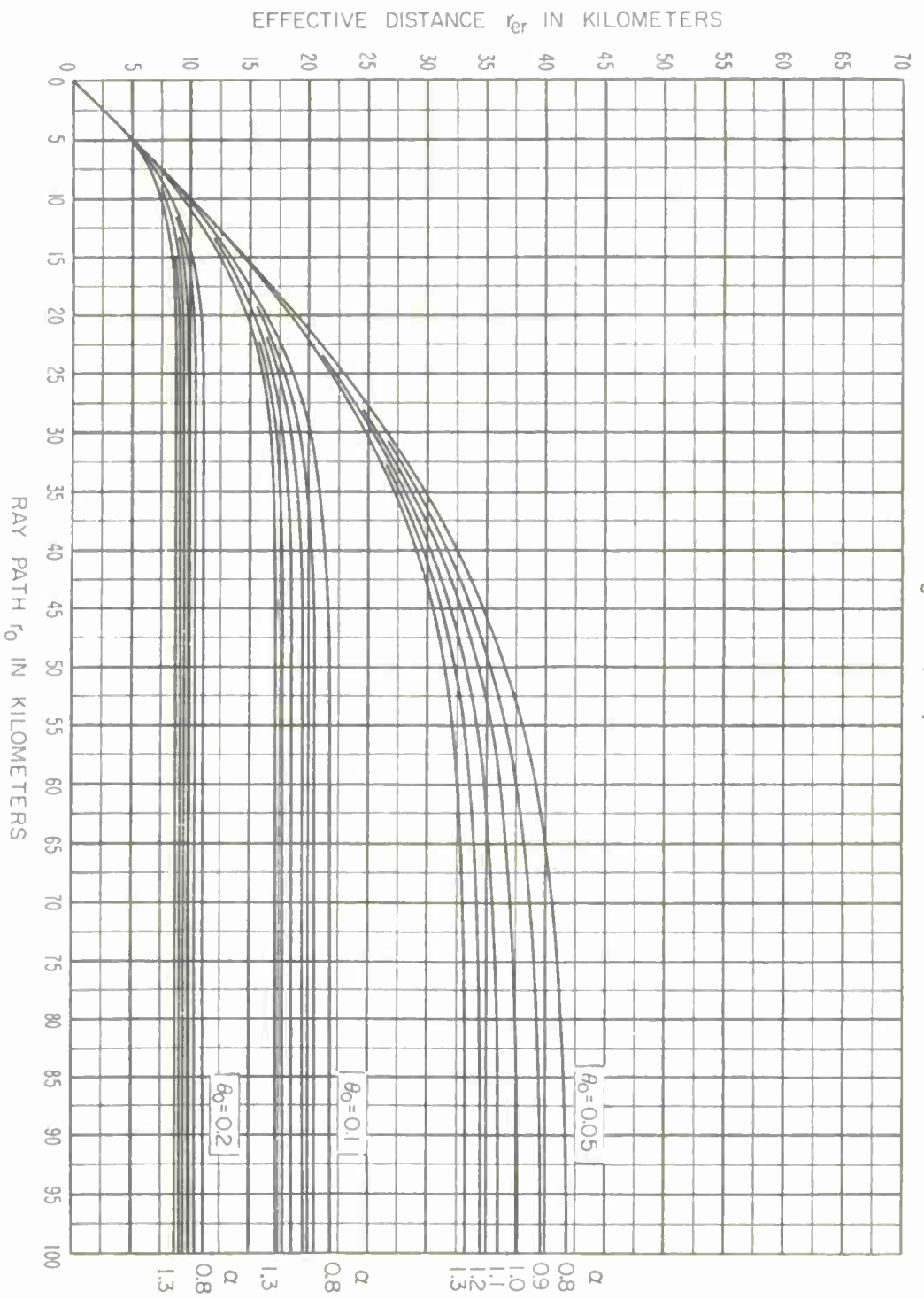
$\theta_0 = 0,\ 0.01,\ 0.02$

EFFECTIVE DISTANCE r_{er} IN KILOMETERS

RAY PATH r_0 IN KILOMETERS

Figure 3.11

EFFECTIVE DISTANCE r_{er} FOR RAIN ABSORPTION
$\theta_0 = 0.05, 0.1, 0.2$

EFFECTIVE DISTANCE r_{er} IN KILOMETERS

RAY PATH r_0 IN KILOMETERS

EFFECTIVE DISTANCE r_{er} FOR RAIN ABSORPTION
$\theta_0 = 0.5$ AND 1

Figure 3.12

Figure 3.13

EFFECTIVE DISTANCE r_{er} FOR RAIN ABSORPTION
$\theta_0 = \pi/2$

$r_{er}(\theta_0, r_0) = \int_0^6 \exp(-0.2\alpha h^2)\, dr$ km

$= \sqrt{\pi/(0.4\alpha)}\ \text{erf}\,(r_0\sqrt{0.2\alpha}\ )$ km

$A_r = KR_{rs}^\alpha\, r_{er}(\theta_0, r_0)$

	ASYMPTOTIC VALUES	
	FOR $r_0 \longrightarrow \infty$:	
α	$\sqrt{\pi/(0.4\alpha)}$	
0.8/km²	2.2156 km	
0.9/km²	2.1494 km	
1.0/km²	1.9817 km	
1.1/km²	1.8894 km	
1.2/km²	1.8090 km	
1.3/km²	1.7380 km	

EFFECTIVE DISTANCE r_{er} IN KILOMETERS

RAY PATH r_0 IN KILOMETERS

3-19
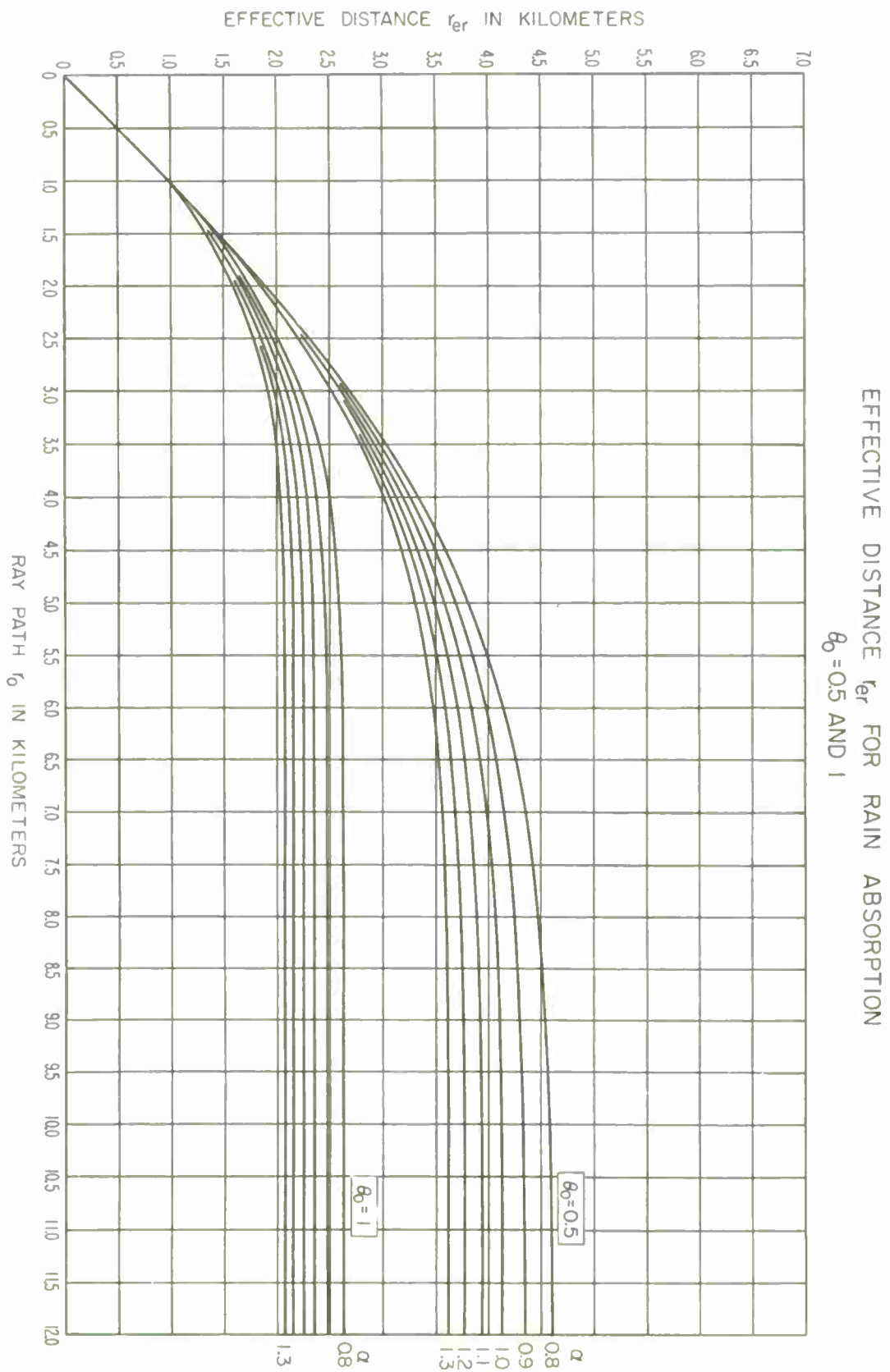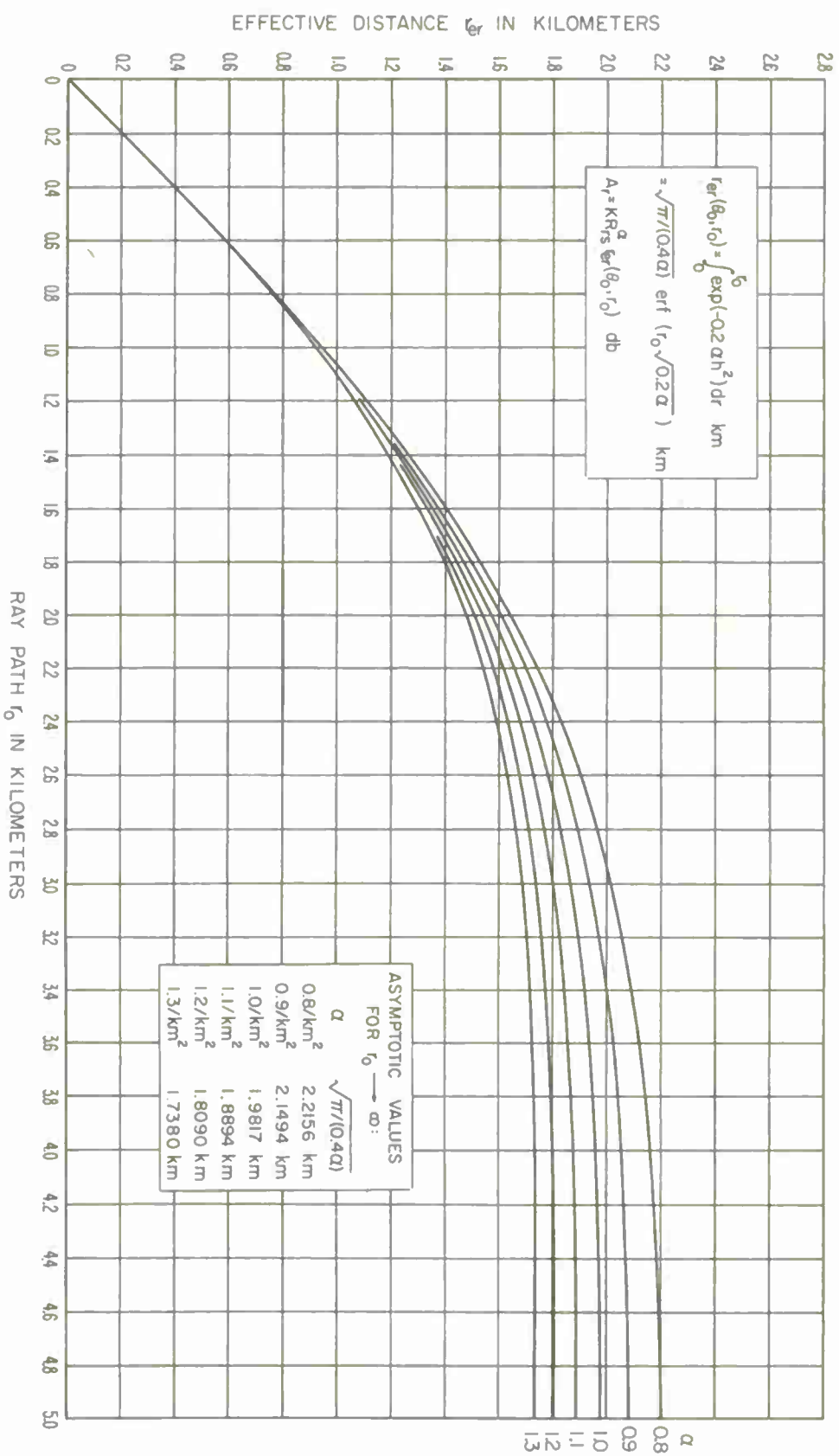
PATH AVERAGE RAINFALL RATE, $\overline{R}_r$, VS EFFECTIVE RAINBEARING DISTANCE, r_{er}
(TOTAL ANNUAL RAINFALL, 100 cm)

PERCENT OF THE YEAR
THAT $\overline{R}_r$ IS EXCEEDED

0.01%

0.1%

1%

5%

PATH AVERAGE RAINFALL RATE, $\overline{R}_r$, IN MILLIMETERS PER HOUR

EFFECTIVE RAINBEARING DISTANCE, r_{er}, IN KILOMETERS

Figure 3.14

3-20
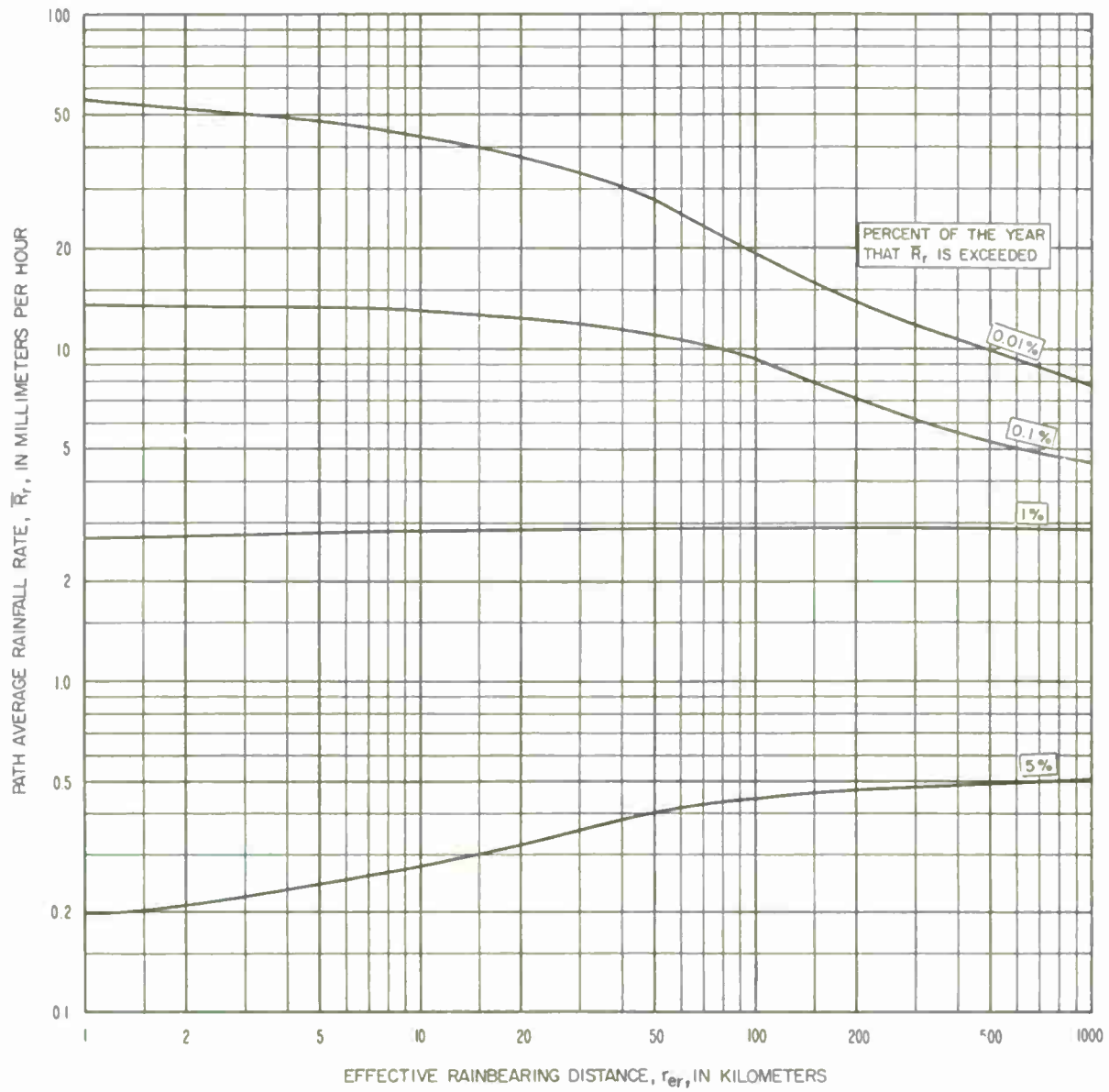
4. DETERMINATION OF AN EFFECTIVE EARTH'S RADIUS

The bending of a radio ray as it passes through the atmosphere is largely determined by the gradient of the refractive index near the earth's surface. In order to represent radio rays as straight lines, at least within the first kilometer above the surface, an "effective earth's radius" is defined as a function of the refractivity gradient, ΔN, or of the surface refractivity value N_s,

$$N_s = (n_s - 1) \times 10^6 \tag{4.1}$$

where n_s is the atmospheric refractive index at the surface of the earth.

In the United States the following empirical relationship has been established between the mean N_s and the mean refractivity gradient ΔN in the first kilometer above the surface:

$$\Delta N/km = -7.32 \exp(0.005577 \, N_s) \tag{4.2}$$

Similar values have been established in West Germany and in the United Kingdom, [CCIR 1963e].

In this paper values of N_s are used to characterize average atmospheric conditions during periods of minimum field strength. In the nortnern temperate zone, field strengths and values of N_s reach minimum values during winter afternoons. Throughout the world, regional changes in expected values of transmission loss depend on minimum monthly mean values of a related quantity, N_o, which represents surface refractivity reduced to sea level:

$$N_s = N_o \exp(-0.1057 \, h_s) \tag{4.3}$$

where h_s is the elevation of the surface above mean sea level, in kilometers, and the refractivity N_o is read from the map shown in figure 4.1 and taken from Bean, Horn, and Ozanich [1960].

Most of the refraction of a radio ray takes place at low elevations, so it is appropriate to determine N_o and h_s for locations corresponding to the lowest elevation of the radio rays most important to the geometry of a propagation path. As a practical matter for within-the-horizon paths, h_s is defined as the ground elevation immediately below the lower antenna terminal, and N_o is determined at the same location. For beyond-the-horizon paths, h_s and N_o are determined at the radio horizons along the great circle path between the antennas, and N_s is the average of the two values calculated from (4.3). An exception to this latter rule occurs if an antenna is more than 150 meters below its radio horizon; in such a case, h_s and N_o should be determined at the antenna location.

The effective earth's radius, a, is given by the following expression:

$$a = a_o [1 - 0.04665 \exp(0.005577 \, N_s)]^{-1} \tag{4.4}$$

where a_o is the actual radius of the earth, and is taken to be 6370 kilometers. Figure 4.2 shows the effective earth's radius, a, plotted versus N_s. The total bending of a radio ray which is elevated more than 0.785 radians (45°) above the horizon and which passes all the way through the earth's atmosphere is less than half a milliradian. For studies of earth-satellite communication ray bending is important at low angles. At higher angles it may often be neglected and the actual earth's radius is then used in geometrical calculations.

    Large values of ΔN and N_s are often associated with atmospheric ducting, which is usually important for part of the time over most paths, especially in maritime climates. The average occurrence of strong layer reflections, superrefraction, ducting, and other focusing and defocusing effects of the atmosphere is taken into account in the empirical time variability functions to be discussed in section 10. Additional material on ducting will be found in papers by Anderson and Gossard [1953a, b], Bean [1959], Booker [1946], Booker and Walkinshaw [1946], Clemow and Bruce-Clayton [1963], Dutton [1961], Fok, Vainshtein, and Belkina [1958], Friend [1945], Hay and Unwin [1952], Ikegami [1959], Kitchen, Joy, and Richards [1958], Nomura and Takaku [1955], Onoe and Nishikori [1957], Pekeris [1947], Schünemann [1957], and Unwin [1953].

MINIMUM MONTHLY SURFACE REFRACTIVITY VALUES REFERRED TO MEAN SEA LEVEL
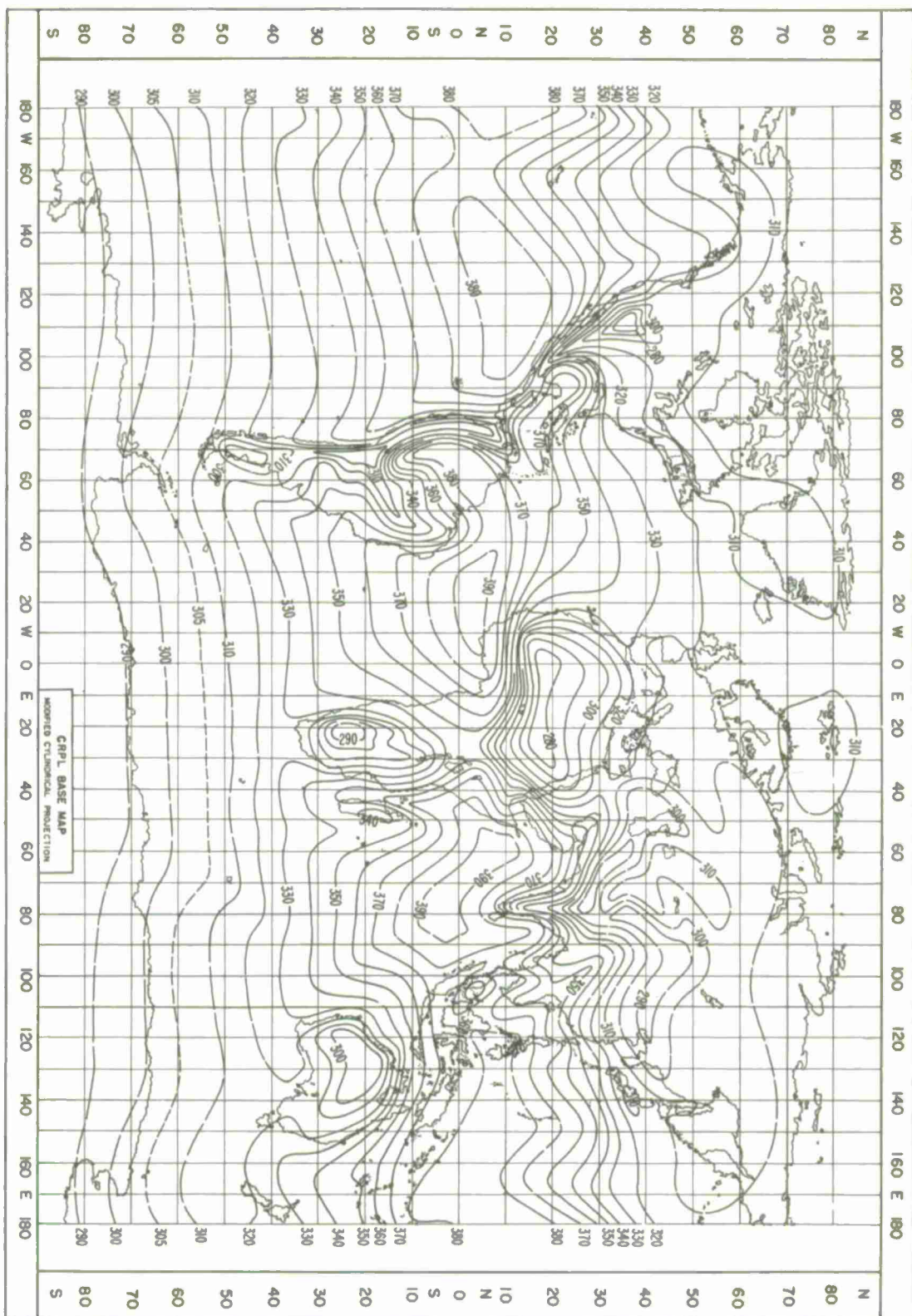
Figure 4.1

EFFECTIVE EARTH'S RADIUS, a, VERSUS SURFACE REFRACTIVITY, N_S
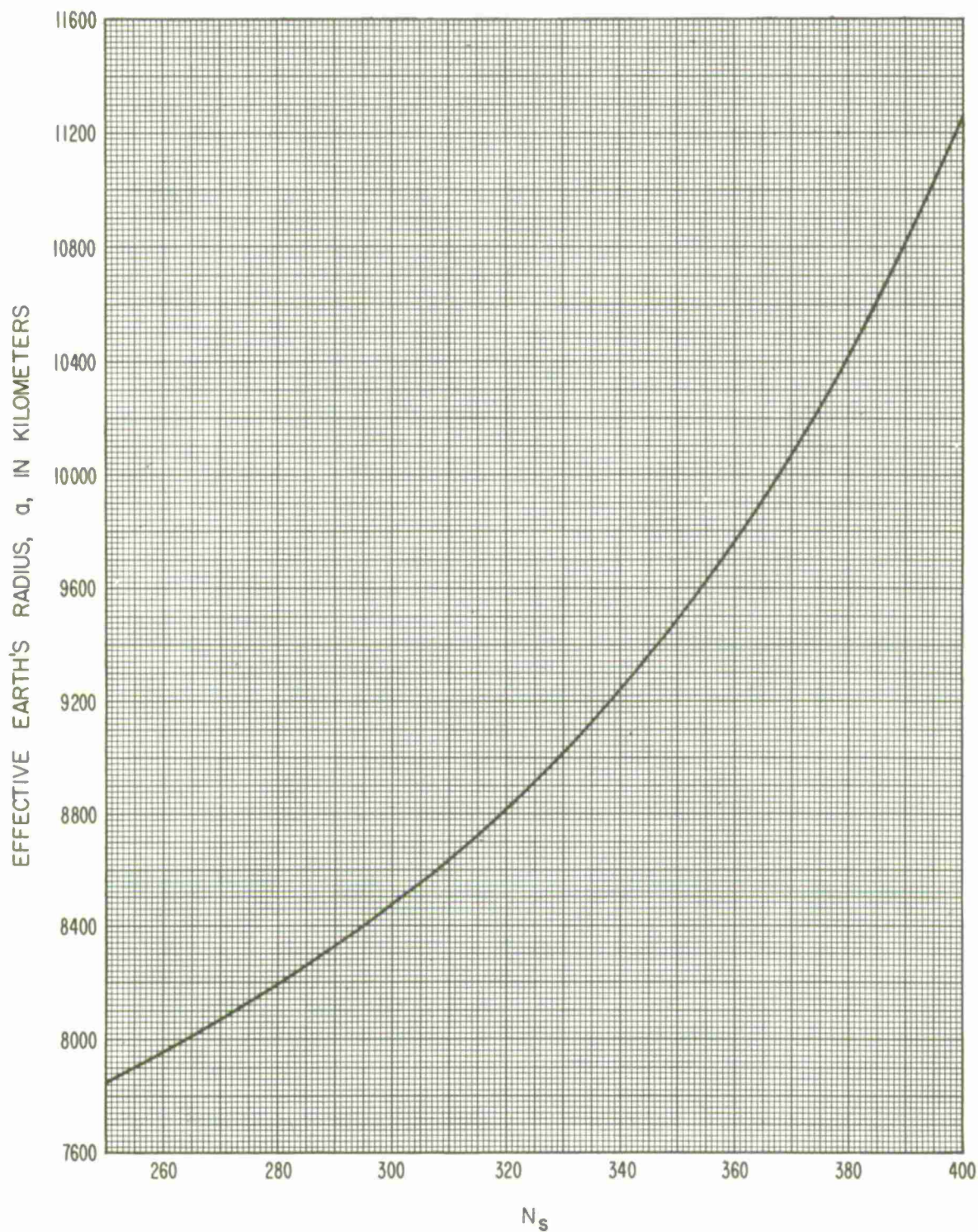
Figure 4.2

5. TRANSMISSION LOSS PREDICTION METHODS FOR WITHIN-THE-HORIZON PATHS

Ground wave propagation over a smooth spherical earth of uniform ground conductivity and dielectric constant, and with a homogeneous atmosphere, has been studied extensively. Some of the results were presented in CCIR Atlases [1955, 1959]. Recent work by Bachynski [1959, 1960, 1963], Wait [1963], Furutsu [1963], and others considers irregularities of electrical ground constants and of terrain. A distinction is made here between the roughness of terrain which determines the proportion between specular and diffuse reflection of radio waves, and large scale irregularities whose average effect is accounted for by fitting a straight line or curve to the terrain.

A comprehensive discussion of the scattering of electromagnetic waves from rough surfaces is given in a recent book by Beckmann and Spizzichino [1963]. Studies of reflection from irregular terrain as well as absorption, diffraction, and scattering by trees, hills, and man-made obstacles have been made by Beckmann [1957], Biot [1957a, b], Kalinin [1957, 1958], Kühn [1958], McGavin and Maloney [1959], McPetrie and Ford [1946], McPetrie and Saxton [1942], Saxton and Lane [1955], Sherwood and Ginzton [1955], and many other workers. Examples of studies of reflection from an ocean surface may be found in papers by Beard, Katz and Spetner [1956], and Beard [1961].

If two antennas are intervisible over the effective earth defined in section 4, geometric optics is ordinarily used to estimate the attenuation A relative to free space, provided that the great circle path terrain visible to both antennas will support a substantial amount of reflection and that it is reasonable to fit a straight line or a convex curve of radius a to this portion of the terrain. Reflections from hillsides or obstacles off the great circle path between two antennas sometimes contribute a significant amount to the received signal. Discrimination against such off-path reflections may reduce multipath fading problems, or in other cases antenna beams may be directed away from the great circle path in order to increase the signal level by taking advantage of off-path reflection or knife-edge diffraction. For short periods of time, over some paths, atmospheric focusing or defocusing will lead to somewhat smaller or much greater values of line-of-sight attenuation than the long-term median values predicted for the average path by the methods of this section.

5.1 Line-of-Sight Propagation Over a Smooth or Uniformly Rough Spherical Earth

The simplest ray optics formulas assume that the field at a receiving antenna is made up to two components, one associated with a direct ray having a path length r_o, and the other associated with a ray reflected from a point on the surface, with equal grazing angles ψ. The reflected ray has a path length $r_1 + r_2$. The field arriving at the receiver via the direct ray differs from the field arriving via the reflected ray by a phase angle which is a function of the

path length difference, $\Delta r = r_1 + r_2 - r_\delta$, illustrated in figure 5.1. The reflected ray field is also modified by an effective reflection coefficient R_e and associated phase lag $(\pi - c)$, which depend on the conductivity, permittivity, roughness, and curvature of the reflecting surface, as well as upon the ratio of the products of antenna gain patterns in the directions of direct and reflected ray paths.

Let g_{o1} and g_{o2} represent the directive gain for each antenna in the direction of the other, assuming antenna polarizations to be matched. Similar factors g_{r1} and g_{r2} are defined for each antenna in the direction of the point of ground reflection. The effective reflection coefficient R_e is then

$$R_e = DR \left(\frac{g_{r1} g_{r2}}{g_{o1} g_{o2}} \right)^{1/2} \exp \left(\frac{-0.6 \, \sigma_h \sin \psi}{\lambda} \right) \qquad (5.1)$$

where the divergence factor D allows for the divergence of energy reflected from a curved surface, and may be approximated as

$$D = \left[1 + \frac{2 d_1 d_2}{a \, d \tan \psi} \right]^{-1/2} \qquad (5.2)$$

An expression for the divergence factor, D, based on geometric optics was derived by Riblet and Barker, [1948]. The term R represents the magnitude of the theoretical coefficient, $R \exp[-i(\pi - c)]$, for reflection of a plane wave from a smooth plane surface of a given conductivity and dielectric constant. In most cases c may be set equal to zero and R is very nearly unity. A notable exception for vertical polarization over sea water is discussed in annex III. Values of R and c vs ψ are shown on figures III.1 to III.8 for both vertical and horizontal polarization over good, average, and poor ground, and over sea water.

The grazing angle ψ and the other geometrical parameters d, d_1, d_2, and a are shown on figure 5.1. The terrain roughness factor, σ_h, defined in section 5.1.2, and the radio wave length, λ, are expressed in the same units. The exponent $(\sigma_h \sin \psi)/\lambda$ is Rayleigh's criterion of roughness.

If the product $DR \exp(-0.6 \, \sigma_h \sin \psi/\lambda)$ is less than $\sqrt{\sin \psi}$, and is less than 0.5, ground reflection may be assumed to be entirely diffuse and R_e is then expressed as

$$R_e = \left[\frac{g_{r1} g_{r2}}{g_{o1} g_{o2}} \sin \psi \right]^{1/2} \qquad (5.3)$$

where terrain factors D, R and σ_h are ignored. The factor $g_{r1} g_{r2} / g_{o1} g_{o2}$ in (5.3) makes R_e approach zero when narrow-beam antennas are used to discriminate against ground reflections.

For a single ground reflection, the attenuation relative to free space may be obtained from the general formula

$$A - G_p = -10 \log \left\{ g_{o1} g_{o2} \left[1 + R_e^2 - 2 R_e \cos \left(\frac{2\pi \Delta r}{\lambda} - c \right) \right] \right\} \text{ db} \qquad (5.4)$$

where the path antenna gain G_p may not be equal to the sum of the maximum antenna gains. At frequencies above 1 GHz an estimate of losses due to atmospheric absorption as shown in (3.4) should be added to A as computed by (5.4) or (5.5).

Over a smooth perfectly-conducting surface, $R_e = 1$ and $c = 0$. Assuming also that free space antenna gains are realized, so that $G_p = 10 \log (g_{o1} g_{o2})$, the attenuation relative to free space is

$$A = -6 - 10 \log \sin^2 (\pi \Delta r / \lambda) \text{ db} \qquad (5.5)$$

Exact formulas for computing Δr are given in annex III. The appropriate approximations given in (5.9) to (5.13) suffice for most practical applications. If Δr is less than 0.12λ, (5.4) may underestimate the attenuation and one of the methods of section 5.2 should be used.

Section 5.1.1 shows exact formulas for antenna heights h_1' and h_2' above a plane earth, or above a plane tangent to the earth at the point of reflection. The grazing angle ψ is then defined by

$$\tan \psi = h_1'/d_1 = h_2'/d_2 \qquad (5.6)$$

where heights and distances are in kilometers and d_1 and d_2 are distances from each antenna to the point of specular reflection:

$$d_1 + d_2 = d , \quad d_1 = d(1 + h_2'/h_1')^{-1} , \quad d_2 = d(1 + h_1'/h_2')^{-1} \qquad (5.7)$$

The distances d_1 and d_2 may be approximated for a spherical earth by substituting antenna heights h_1 and h_2 above the earth for the heights h_1' and h_2' in (5.7). Then these heights may be calculated as

$$h_1' = h_1 - d_1^2/(2a) , \quad h_2' = h_2 - d_2^2/(2a) \qquad (5.8)$$

for an earth of effective radius a, and substituted in (5.7) to obtain improved estimates of d_1 and d_2. Iterating between (5.7) and (5.8), any desired degree of accuracy may be obtained.

The path length difference between direct and ground reflected rays is

$$\Delta r = \sqrt{d^2 + \left(h_1' + h_2'\right)^2} - \sqrt{d^2 + \left(h_1' - h_2'\right)^2} \cong 2 h_1' h_2'/d \qquad (5.9)$$

where the approximation in (5.9) is valid for small grazing angles.

Referring to (5.5) the greatest distance, d_o, for which A is zero, (assuming that $R_e = 1$ and that free space gains are realized) occurs when $\Delta r = \lambda/6$. From (5.9) $\Delta r \cong 2 h_1' h_2'/d$; therefore:

$$d_o = 12 \, h_1' \, h_2'/\lambda \qquad (5.10a)$$

This equation may be solved graphically, or by iteration, choosing a series of values for d_o, solving (5.8) for h_1', h_2', and testing the equality in (5.10a).

For the special case of equal antenna heights over a spherical earth of radius a, the distance d_o may be obtained as follows:

$$\Delta r = \lambda/6 = \frac{2}{d_o} \left[h - d_o^2/(8a) \right]^2 = 2 h^2/d_o - h d_o/(2a) + d_o^3/(32 a^2) \qquad (5.10b)$$

where

$$d_1 = d_2 = d/2, \qquad h_1 = h_2 = h, \quad \text{and} \quad h' = h - d_o^2/(8a)$$

For this special case where $h_1 = h_2$ over a smooth spherical earth of radius a, the angle ψ may be defined as

$$\tan \psi = 2 h/d - d/(4a) \qquad (5.11a)$$

and

$$\Delta r = d(\sec \psi - 1) = d \left[\sqrt{1 + \tan^2 \psi} - 1 \right] \qquad (5.11b)$$

Let θ_h represent the angle of elevation of the direct ray r_o relative to the horizontal at the lower antenna, h_1, assume that $h_1 << h_2$, $h_1 << 9 a \psi^2/2$, and that the grazing angle, ψ, is small; then, over a spherical earth of effective radius a,

$$\Delta r \cong 2 h_1 \sin \psi \cong h_1 \left[\sqrt{\theta_h^2 + 4 h_1/(3a)} + \theta_h \right] \qquad (5.12)$$

whether θ_h is positive or negative. For $\theta_h = 0$, $d_1 \cong 2 h_1/(3\psi)$.

Two very useful approximations for Δr are

$$\Delta r = 2 \psi^2 d_1 d_2 / d \cong 2 h_1 \sin \psi \text{ kilometers} \qquad (5.13)$$

and the corresponding expressions for the path length difference in electrical radians and in electrical degrees are

$$2\pi\Delta r/\lambda = 41.917 f h_1' h_2'/d = 41.917 f \psi^2 d_1 d_2/d \cong 42 f h_1 \sin \psi \quad \text{radians} \qquad (5.14a)$$

$$360\Delta r/\lambda = 2401.7 f h_1' h_2'/d = 2401.7 f \psi^2 d_1 d_2/d \cong 2402 f h_1 \sin \psi \quad \text{degrees} \qquad (5.14b)$$

where f is the radio frequency in MHz, and all heights and distances are in kilometers. The last approximation in (5.13) should be used only if h_1 is small and less than $h_2/20$, as it involves neglecting $d_1^2/(2a)$ relative to h_1 in (5.8) and assuming that $d_2 \cong d$.

As noted following (5.5), ray optics formulas are limited to grazing angles such that $\Delta r > 0.06 \lambda$. With this criterion, and assuming $R_e = 1$, the attenuation A is 15 db for the corresponding minimum grazing angle

$$\psi_m \cong \sqrt{0.03 \lambda d/(d_1 d_2)} \text{ radians}$$

where antennas are barely intervisible. A comparison with the CCIR Atlas of smooth-earth diffraction curves shows that the attenuation relative to free space varies from 10 to 20 decibels for a zero angular distance ($\theta = 0$, $\psi = 0$) except for extremely low antennas.

Figure 5.1a shows how rays will bend above an earth of actual radius $a_o = 6370$ kilometers, while figure 5.1b shows the same rays drawn as straight lines above an earth of effective radius a. Antenna heights above sea level, h_{ts} and h_{rs}, are usually slightly greater than the effective antenna heights h_1' and h_2', defined in 5.1.1. This difference arises from two circumstances: the smooth curve may be a curve-fit to the terrain instead of representing sea level, and straight rays above an effective earth overestimate the ray bending at high elevations. This latter correction is insignificant unless d is large.

5.1.1 A Curve-Fit to Terrain

A smooth curve is fitted to terrain visible from both antennas. It is used to define antenna heights h_1' and h_2', as well as to determine a single reflection point where the angle of incidence of a ray r_1 is equal to the angle of reflection of a ray r_2 in figure 5.1. This curve is also required to obtain the deviation, σ_h, of terrain heights used in computing R_e in (5.1). Experience has shown that both h_1' and h_2' should exceed 0.16λ for the following formulas to be applicable. For other prediction methods, see subsection 5.2.

First, a straight line is fitted by least squares to equidistant heights $h_i(x_i)$ above sea level, and $x_i^2/(2a)$ is then subtracted to allow for the sea level curvature $1/a$ illustrated in figure 6.4. The following equation describes a straight line $h(x)$ fitted to 21 equidistant values of $h_i(x_i)$ for terrain between $x_i = x_0$ and $x_i = x_{20}$ kilometers from the transmitting antenna. The points x_0 and x_{20} are chosen to exclude terrain adjacent to either antenna which is not visible from the other:

$$h(x) = \overline{h} + m(x - \overline{x}) \tag{5.15a}$$

$$\overline{h} = \frac{1}{21} \sum_{i=0}^{20} h_i , \quad \overline{x} = \frac{x_0 + x_{20}}{2} , \quad m = \frac{2 \sum_{i=0}^{20} h_i(i-10)}{77(x_{20} - x_0)} \tag{5.15b}$$

Smooth modified terrain values given by

$$y(x) = h(x) - x^2/(2a) \tag{5.16}$$

will then define a curve of radius a which is extrapolated to include all values of x from $x = 0$ to $x = d$, the positions of the antennas.

The heights of the antennas above this curve are

$$h_1' = h_{ts} - h(0) , \quad h_2' = h_{rs} - h(d) \tag{5.17}$$

If h_1' or h_2' is greater than one kilometer, a correction term, Δh, defined by (6.12) and shown on figure 6.7 is used to reduce the value given by (5.17).

Where terrain is so irregular that it cannot be reasonably well approximated by a single curve, σ_h is large and $R_e = 0$, not because the terrain is very rough, but because it is irregular. In such a situation, method 3 of section 5.2 may be useful.

5.1.2 The terrain roughness factor, σ_h

The terrain roughness factor σ_h in (5.1) is the root-mean-square deviation of modified terrain elevations, y_i, relative to the smooth curve defined by (5.16), within the limits of the first Fresnel zone in the horizontal reflecting plane. The outline of a first Fresnel zone ellipse is determined by the condition that

$$r_{11} + r_{21} = r_1 + r_2 + \lambda/2$$

where $r_{11} + r_{21}$ is the length of a ray path corresponding to reflection from a point on the edge of the Fresnel zone, and $r_1 + r_2$ is the length of the reflected ray for which angles of incidence and reflection are equal. Norton and Omberg [1947] give general formulas for determining a first Fresnel zone ellipse in the reflecting plane. Formulas are given in annex III for calculating distances x_a and x_b from the transmitter to the two points where the first Fresnel ellipse cuts the great circle plane.

A sample calculation of σ_h is given in Example 1 of Annex III.

5.2 Line-of-Sight Propagation over Irregular and Cluttered Terrain

Where ray optics formulas described in section 5.1 are not applicable, a satisfactory estimate of line-of-sight transmission loss may sometimes be made by one of the following methods:

1. If a slight change in the position of either antenna results in a situation where ray optics formulas may be used, then A may be estimated by extrapolation or interpolation. A useful set of calculations for $\theta = 0$ is given by Domb and Pryce [1947].

2. Instead of a single curve fit to terrain as in 5.1, in some cases the method may be extended to multiple curve fits and multiple reflections from these curves.

3. If terrain is so irregular it cannot be reasonably well approximated by a single curve, the line-of-sight knife-edge formulas of section 7 may be applicable.

4. Interpolation between curves in an atlas, or standard propagation curves such as those given in appendix I, may provide a satisfactory estimate.

5. Empirical curves drawn through data appropriate for the problem of interest may be useful. For example, the dashed curves of figures I.1 - I.3 show how values of attenuation relative to free space vary with distance and frequency for a large sample of recordings of television signals over random paths. The data shown in figures I.1 - I.4 correspond to a more careful selection of receiving locations and to a greater variety of terrain and climatic conditions.

The effects of refraction, diffraction, and absorption by trees, hills, and man-made obstacles are often important, especially if a receiving installation is low or is surrounded by obstacles. Absorption of radio energy is probably the least important of these three factors except in cases where the only path for radio energy is directly through some building material or where a radio path extends for a long distance through trees.

Studies made at 3000 MHz indicate that stone buildings and groups of trees so dense that the sky cannot be seen through them should be regarded as opaque objects around which diffraction takes place [McPetrie and Ford, 1946]. At 3000 MHz the loss through a 23-centimeter thick dry brick wall was 12 db and increased to 46 db when the wall was thoroughly soaked with water. A loss of 1.5 db through a dry sash window, and 3 db loss through a wet one were usual values.

The only objects encountered which showed a loss of less than 10 db at 3000 MHz were thin screens of leafless branches, the trunk of a single tree at a distance exceeding 30 meters, wood-framed windows, tile or slate roofs, and the sides of light wooden huts. Field strengths obtained when a thick belt of leafless trees is between transmitter and receiver are within about 6 db of those computed assuming Fresnel diffraction over an obstacle slightly lower than the trees. Loss through a thin screen of small trees will rarely exceed 6 db if the transmitting antenna can be seen through their trunks. If sky can be seen through the trees, 15 db is the greatest expected loss.

The following empirical relationship for the rate of attenuation in woods has been given by Saxton and Lane [1955]:

$$A_W = d(0.244 \log f - 0.442) \quad \text{decibels}, \qquad (f > 100 \text{ MHz}) \tag{5.18}$$

where A_W is the absorption in decibels through d meters of trees in full leaf at a frequency f megahertz.

The situation with a high and a low antenna in which the low antenna is located a small distance from and at a lower height than a thick stand of trees is quite different from the situation in which both antennas may be located in the woods. Recent studies at approximately 500 MHz show the depression of signal strengths below smooth earth values as a function of clearing depth, defined as the distance from the lower antenna to the edge of the woods [Head, 1960]. Expressing this empirical relation in terms of a formula:

$$\Delta_C = 52 - 12 \log d_c \quad \text{decibels} \tag{5.19}$$

where Δ_C is the depression of the field strength level below smooth earth values and d_c is the clearing depth in meters.

A particularly interesting application of some of the smooth-earth formulas given in this section is the work of Lewin [1962] and others in the design of space-diversity configurations to overcome phase interference fading over line-of-sight paths. Diffraction theory may be used to establish an optimum antenna height for protection against long-term power fading, choosing for instance the minimum height at which the attenuation below free space is 20 db for a horizontally uniform atmosphere with the maximum positive gradient of refractivity expected to be encountered. Then the formulas of this section will determine the optimum diversity spacing required to provide for at least one path a similar 20 db protection against multipath from direct and ground-reflected components throughout the entire range of refractivity gradients expected. In general, the refractive index gradient will vary over wider ranges on over-water paths [Ikegami, 1964].

GEOMETRY FOR WITHIN-THE-HORIZON PATHS

(a)

(b)
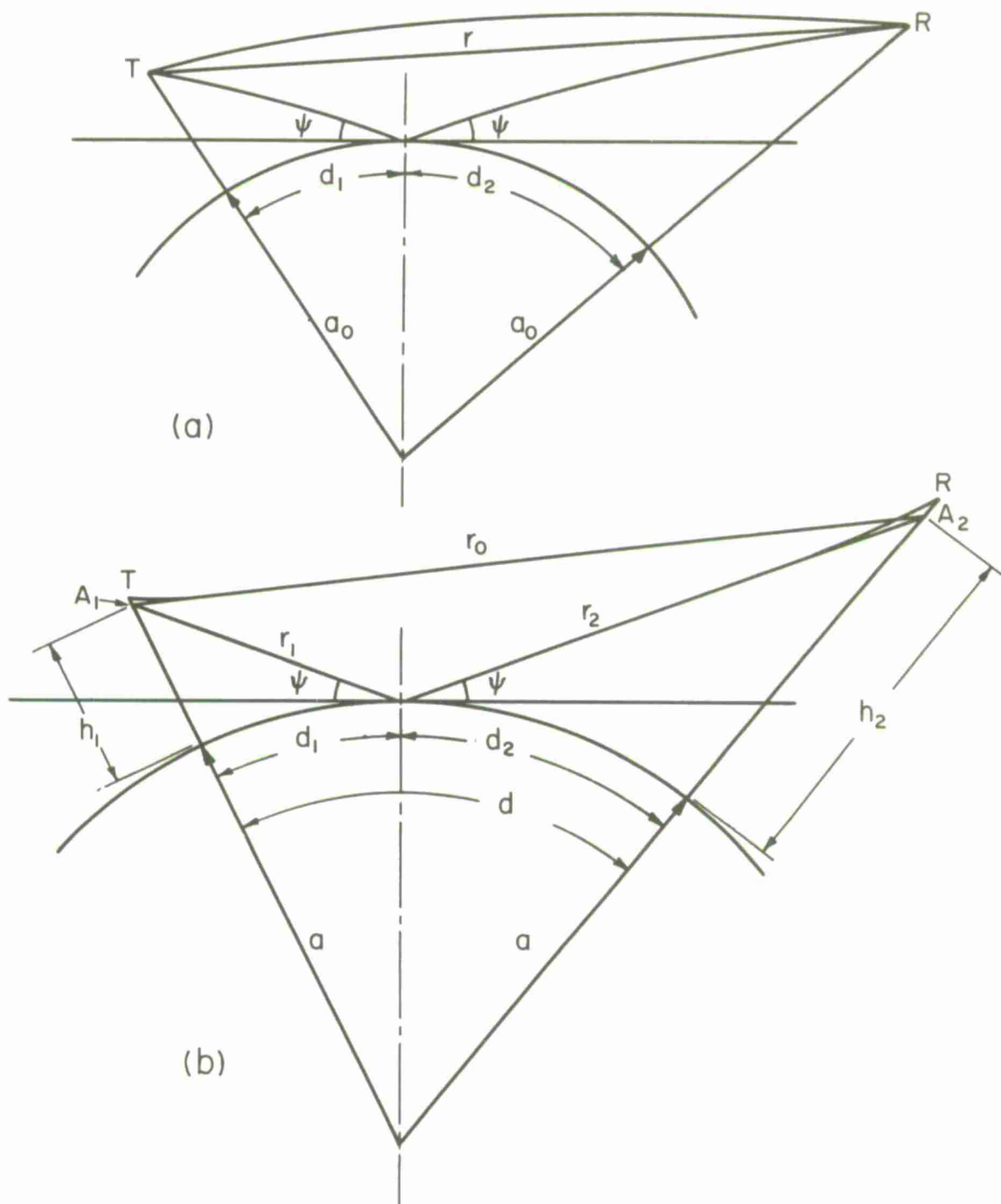
Figure 5.1

6. DETERMINATION OF ANGULAR DISTANCE FOR TRANSHORIZON PATHS

The angular distance, θ, is the angle between radio horizon rays in the great circle plane defined by the antenna locations. This important parameter is used in diffraction theory as well as in forward scatter theory. Angular distance depends upon the terrain profile, as illustrated in figure 6.1, and upon the bending of radio rays in the atmosphere. Figure 6.1 assumes a linear dependence on height of the atmospheric refractive index, n, which implies a nearly constant rate of ray refraction. If heights to be considered are less than one kilometer above the earth's surface, the assumption of a constant effective earth's radius, a, makes an adequate allowance for ray bending. Atmospheric refractivity $N = (n-1) \times 10^{6}$ more than one kilometer above the earth's surface, however, is assumed to decay exponentially with height [Bean and Thayer, 1959]. This requires corrections to the effective earth's radius formulas, as indicated in the following subsections.

To calculate θ, one must first plot the great circle path and determine the radio horizons.

6.1 Plotting a Great Circle Path

For distances less than 70 kilometers, the great circle path can be approximated by a rhumb line, which is a line intersecting all meridians at the same angle. For greater distances, the organization of a map study is illustrated on figure 6.2. Here, a rhumb line is first plotted on an index map to show the boundaries of available detailed topographic sheets. Segments of the actual great circle path are later plotted on these detailed maps.

The spherical triangle used for the computation of points on a great circle path is shown on figure 6.3, where PAB is a spherical triangle, with A and B the antenna terminals, and P the north or south pole. B has a greater latitude than A, and P is in the same hemisphere. The triangle shown is for the northern hemisphere but may readily be inverted to apply to the southern hemisphere. B' is any point along the great circle path from A to B, and the triangle PAB' is the one actually solved. The latitudes of the points are denoted by Φ_A, Φ_B, and $\Phi_{B'}$, while C and C' are the differences in longitude between A and B and A and B', respectively. Z and Z' are the corresponding great circle path lengths. The following formulas are practical for hand computations as well as for automatic digital computers. Equations (6.1) to (6.4) have been taken, in this form, from a well-known reference book [I. T. and T., 1956], where they appear on pages 730-739.

The initial bearing (X from terminal A, and Y from terminal B) are measured from true north, and are calculated as follows:

$$\tan \frac{Y - X}{2} = \cot \frac{C}{2} \left[\left(\sin \frac{\Phi_B - \Phi_A}{2} \right) \middle/ \left(\cos \frac{\Phi_B + \Phi_A}{2} \right) \right] \tag{6.1}$$

$$\tan \frac{Y + X}{2} = \cot \frac{C}{2} \left[\left(\cos \frac{\Phi_B - \Phi_A}{2} \right) \bigg/ \left(\sin \frac{\Phi_B + \Phi_A}{2} \right) \right] \qquad (6.2)$$

$$\frac{Y + X}{2} + \frac{Y - X}{2} = Y, \quad \text{and} \quad \frac{Y + X}{2} - \frac{Y - X}{2} = X \qquad (6.3)$$

The great circle distance, Z, is given by

$$\tan \frac{Z}{2} = \tan \frac{\Phi_B - \Phi_A}{2} \left[\left(\sin \frac{Y + X}{2} \right) \bigg/ \left(\sin \frac{Y - X}{2} \right) \right] \qquad (6.4)$$

To convert the angle Z obtained in degrees from (6.4) to units of length, the following is used, based on a mean sea level earth's radius of 6370 km:

$$d_{km} = 111.18 \, Z^\circ \qquad (6.5)$$

The following formulas show how to calculate either the latitude or the longitude of a point on the great circle path, when the other coordinate is given. The given coordinates correspond to the edges of detailed maps, and to intermediate points usually about 7.5 minutes apart, so that straight lines between points will adequately approximate a great circle path.

For predominantly east-west paths, calculate the latitude $\Phi_{B'}$ for a given longitude difference C':

$$\cos Y' = \sin X \sin C' \sin \Phi_A - \cos X \cos C' \qquad (6.6)$$

$$\cos \Phi_{B'} = \sin X \cos \Phi_A / \sin Y' \qquad (6.7)$$

For predominantly north-south paths, calculate the longitude difference C' for a given latitude $\Phi_{B'}$:

$$\sin Y' = \sin X \cos \Phi_A / \cos \Phi_{B'} \qquad (6.8)$$

$$\cot \frac{C'}{2} = \tan \frac{Y' - X}{2} \left[\left(\cos \frac{\Phi_{B'} + \Phi_A}{2} \right) \bigg/ \left(\sin \frac{\Phi_{B'} - \Phi_A}{2} \right) \right] \qquad (6.9)$$

Where the bearing of a path is close to 45 degrees, either method may be used.

6.2 Plotting a Terrain Profile and Determining the Location of Radio Horizon Obstacles

This subsection explains how to determine the sea level arc distance, $d_{Lt, r}$ from an antenna to its radio horizon obstacle, and the height, $h_{Lt, r}$ of this obstacle above mean sea level. The horizon obstacles are represented by the points (d_{Lt}, h_{Lt}) and (d_{Lr}, h_{Lr}) in the great circle plane containing the antennas. These points may be determined by the tops of high buildings, woods, or hills, or may be entirely determined by the bulge of the earth itself. All of the predictions of this paper replace the earth by a cylinder whose elements are perpendicular to the great circle plane and whose cross-section is in general irregular and determined by the antenna and horizon locations in the great circle plane. When the difference in elevations of antenna and horizon greatly exceeds one kilometer, ray tracing is necessary to determine the location of radio horizons accurately [Bean and Thayer, 1959].

Elevations h_i of the terrain are read from topographic maps and tabulated versus their distances x_i from the transmitting antenna. The recorded elevations should include those of successive high and low points along the path. The terrain profile is plotted on linear graph paper by modifying the terrain elevations to include the effect of the average curvature of the radio ray path and of the earth's surface. The modified elevation y_i of any point h_i at a distance x_i from the transmitter along a great circle path is its height above a plane which is horizontal at the transmitting antenna location:

$$y_i = h_i - x_i^2 / (2a) \tag{6.10}$$

where the effective earth's radius, a, in kilometers is calculated using (4.4), or is read from figure 4.2 as a function of N_s. The surface refractivity, N_s, is obtained from (4.3), where N_o is estimated from the map on figure 4.1.

A plot of y_i versus x_i on linear graph paper is the desired terrain profile. Figure 6.4 shows the profile for a line-of-sight path. The solid curve near the bottom of the figure indicates the shape of a surface of constant elevation (h = 0 km). Profiles for a path with one horizon common to both antennas and for a path with two radio horizons are shown in figures 6.5 and 6.6. The vertical scales of these three figures are exaggerated in order to provide a sufficiently detailed representation of terrain irregularities. Plotting terrain elevations vertically instead of radially from the earth's center leads to negligible errors where vertical changes are small relative to distances along the profile.

On a cartesian plot of y_i versus x_i, as illustrated in figures 6.4, 6.5, and 6.6, the ray from each antenna to its horizon is a straight line, provided the difference in antenna and horizon elevations is less than one kilometer. Procedures to be followed where this is not the case are indicated in the next subsection.

6.3 Calculation of Effective Antenna Heights for Transhorizon Paths

If an antenna is located on another structure, or on a steep cliff or mountainside, the height of this structure, cliff, or mountain above the surrounding terrain should be included as part of the antenna height. To obtain the effective height of the transmitting antenna, the average height above sea level $\bar{h}_t$ of the central 80 per cent of the terrain between the transmitter and its horizon is determined. The following formula may be used to compute $\bar{h}_t$ for 31 evenly spaced terrain elevations h_{ti} for $i = 0, 1, 2, \cdots 30$, where h_{t0} is the height above sea level of the ground below the transmitting antenna, and, $h_{t30} = h_{Lt}$:

$$\bar{h}_t = \frac{1}{25} \sum_{i=3}^{27} h_{ti} \, , \quad h_t = h_{ts} - \bar{h}_t \quad \text{for} \quad \bar{h}_t < h_{t0} \, ; \tag{6.11a}$$

otherwise

$$h_t = h_{ts} - h_{t0} \tag{6.11b}$$

where h_{ts} is the height of the transmitting antenna above mean sea level. The height h_r is similarly defined.

If h_t or h_r as defined above is less than one kilometer, $h_{te} = h_t$ or $h_{re} = h_r$. For antennas higher than one kilometer, a correction Δh, read from figure 6.7, is used to reduce h_t or h_r to the value h_{te} or h_{re}:

$$h_{te} = h_t - \Delta h(h_t, N_s) \, , \quad h_{re} = h_r - \Delta h(h_r, N_s) \tag{6.12}$$

The correction Δh was obtained by ray tracing methods described by Bean and Thayer [1959]. For a given effective earth's radius, the effective antenna height h_{te} corresponding to a given horizon distance d_{Lt} is smaller than the actual antenna height, h_t. Over a smooth spherical earth with $h_{te} < 1$ km and $h_{re} < 1$ km, the following approximate relationship exists between effective antenna heights and horizon distances:

$$h_{te} = d_{Lt}^2/(2a) \, , \quad h_{re} = d_{Lr}^2/(2a) \tag{6.13a}$$

If the straight line distance r between antennas is substantially different from the sea level arc distance d, as in communication between an earth terminal and a satellite, the effective antenna heights must satisfy the exact relation:

$$h_{te} = a[\sec(d_{Lt}/a) - 1] \, , \quad h_{re} = a[\sec(d_{Lr}/a) - 1] \tag{6.13b}$$

6.4 Calculation of the Angular Distance, θ

The angular distance, θ, is the angle between horizon rays in the great circle plane, and is the minimum diffraction angle or scattering angle unless antenna beams are elevated. Calculations for cases where the antenna beams are elevated are given in annex III.

In calculating the angular distance, one first calculates the angles θ_{et} and θ_{er} by which horizon rays are elevated or depressed relative to the horizontal at each antenna, as shown on figure 6.1. In this report, all heights and distances are measured in kilometers, and angles are in radians unless otherwise specified. When the product $d\theta$ is less than 2,

$$\theta = \theta_{oo} = \dot{d}/a + \theta_{et} + \theta_{er} \tag{6.14}$$

where "a" in (6.14) is the effective earth's radius defined in section 4. The horizon ray elevation angles θ_{et} and θ_{er} may be measured with surveying instruments in the field, or determined directly from a terrain profile plot such as that of figure 6.5 or 6.6, but are usually computed using the following equations:

$$\theta_{et} = \frac{h_{Lt} - h_{ts}}{d_{Lt}} - \frac{d_{Lt}}{2a} , \qquad \theta_{er} = \frac{h_{Lr} - h_{rs}}{d_{Lr}} - \frac{d_{Lr}}{2a} \tag{6.15}$$

where h_{Lt}, h_{Lr} are heights of horizon obstacles, and h_{ts}, h_{rs} are antenna elevations, all above mean sea level. As a general rule, the location (h_{Lt}, d_{Lt}) or (h_{Lr}, d_{Lr}) of a horizon obstacle is determined from the terrain profile by using (6.15) to test all possible horizon locations. The correct horizon point is the one for which the horizon elevation angle θ_{et} or θ_{er} is a maximum. When the trial values are negative, the maximum is the value nearest zero. For a smooth earth,

$$\theta_{et,er} = -\sqrt{2\,h_{te,re}/a} \quad \text{for} \quad h_{te,re} < 1 \text{ km}$$

At the horizon location, the angular elevation of a horizon ray, θ_{ot} or θ_{or}, is greater than the horizon elevation angle θ_{et} or θ_{er}:

$$\theta_{ot} = \theta_{et} + d_{Lt}/a , \qquad \theta_{or} = \theta_{er} + d_{Lr}/a \tag{6.16}$$

If the earth is smooth, θ_{ot} and θ_{or} are zero, and $\theta \cong D_s/a$, where

$$D_s = d - d_{Lt} - d_{Lr} \tag{6.17}$$

Figure 6.8, valid only for $\theta_{ot} + \theta_{or} = 0$, is a graph of θ versus D_s for various values of surface refractivity, N_s .

In the general case of irregular terrain, the angles α_{oo} and β_{oo} shown in figure 6.1 are calculated using the following formulas:

$$\alpha_{oo} = \frac{d}{2a} + \theta_{et} + \frac{h_{ts} - h_{rs}}{d} \tag{6.18a}$$

$$\beta_{oo} = \frac{d}{2a} + \theta_{er} + \frac{h_{rs} - h_{ts}}{d} \tag{6.18b}$$

These angles are positive for beyond-horizon paths. To allow for the effects of a non-linear refractivity gradient, α_{oo} and β_{oo} are modified by corrections $\Delta\alpha_o$ and $\Delta\beta_o$ to give the angles α_o and β_o whose sum is the angular distance, θ, and whose ratio defines a path asymmetry factor s:

$$\alpha_o = \alpha_{oo} + \Delta\alpha_o \tag{6.19a}$$

$$\beta_o = \beta_{oo} + \Delta\beta_o \tag{6.19b}$$

$$0 = \alpha_o + \beta_o \,, \qquad s = \alpha_o / \beta_o \tag{6.19c}$$

The corrections $\Delta\alpha_o$ and $\Delta\beta_o$ are functions of the angles θ_{ot} and θ_{or}, (6.16), and of the distances d_{st} and d_{sr} from each horizon obstacle to the crossover of horizon rays. These distances are approximated as

$$d_{st} = d\beta_{oo} / \theta_{oo} - d_{Lt} \,, \qquad d_{sr} = d\alpha_{oo} / \theta_{oo} - d_{Lr} \tag{6.20}$$

The sum of d_{st} and d_{sr} is the distance D_s between horizon obstacles, defined by (6.17). Over a smooth earth $d_{st} = d_{sr} = D_s / 2$.

Figure 6.9, drawn for $N_s = 301$, shows $\Delta\alpha_o$ as a function of θ_{ot} and d_{st}. Similarly, $\Delta\beta_o$ is read from the figure as a function of θ_{or} and d_{sr}. For values of N_s other than 301, the values as read from the figure are multiplied by $C(N_s)$:

$$\Delta\alpha_o(N_s) = C(N_s)\,\Delta\alpha_o(301) \,, \quad \Delta\beta_o(N_s) = C(N_s)\,\Delta\beta_o(301) \tag{6.21a}$$

$$C(N_s) = (1.3\,N_s^2 - 60\,N_s) \times 10^{-5} \tag{6.21b}$$

For instance, $C(250) = 0.66$, $C(301) = 1.0$, $C(350) = 1.38$, and $C(400) = 1.84$. Figure 6.10 shows $C(N_s)$ plotted versus N_s.

For small $\theta_{ot, r}$ no correction $\Delta\alpha_o$ or $\Delta\beta_o$ is required for values of $d_{st, r}$ less than 100 Km. When both $\Delta\alpha_o$ and $\Delta\beta_o$ are negligible:

$$\theta = \theta_{oo} = \alpha_{oo} + \beta_{oo} \tag{6.22}$$

which is the same as (6.14).

If θ_{ot} or θ_{or} is negative, compute

$$d'_{st} = d_{st} - \left| a\,\theta_{ot} \right| \quad \text{or} \quad d'_{sr} = d_{sr} - \left| a\,\theta_{or} \right| , \tag{6.23}$$

substitute d'_{st} for d_{st} or d'_{sr} for d_{sr}, and read figure 6.9, using $\theta_{ot, r} = 0$.

If either θ_{ot} or 0_{or} is greater than 0.1 radian and less than 0.9 radian, determine $\Delta\alpha_o$ or $\Delta\beta_o$ for $\theta_{ot} = 0.1$ radian and add the additional correction term

$$N_s (9.97 - \cot\theta_{ot, r}) \left[1 - \exp\left(- 0.05\, d_{st, r}\right) \right] \times 10^{-6} \text{ radians}$$

The bending of radio rays elevated more than 0.9 radian above the horizon and passing all the way through the atmosphere is less than 0.0004 radian, and may be neglected.

Other geometrical parameters required for the calculation of expected transmission loss are defined in the sections where they are used.

Many of the graphs in this and subsequent sections assume that $s = \alpha_o/\beta_o \leq 1$, where α_o and β_o are defined by (6.19a) and (6.19b). It is therefore convenient, since the transmission loss is independent of the actual direction of transmission, to denote as the transmitting antenna whichever antenna will make s less than or equal to unity. Alternatively, s may be replaced by $1/s$ and the subscripts t and r may be interchanged in some of the formulas and graphs, as noted in later sections.

PATH GEOMETRY

SCATTER VOLUME
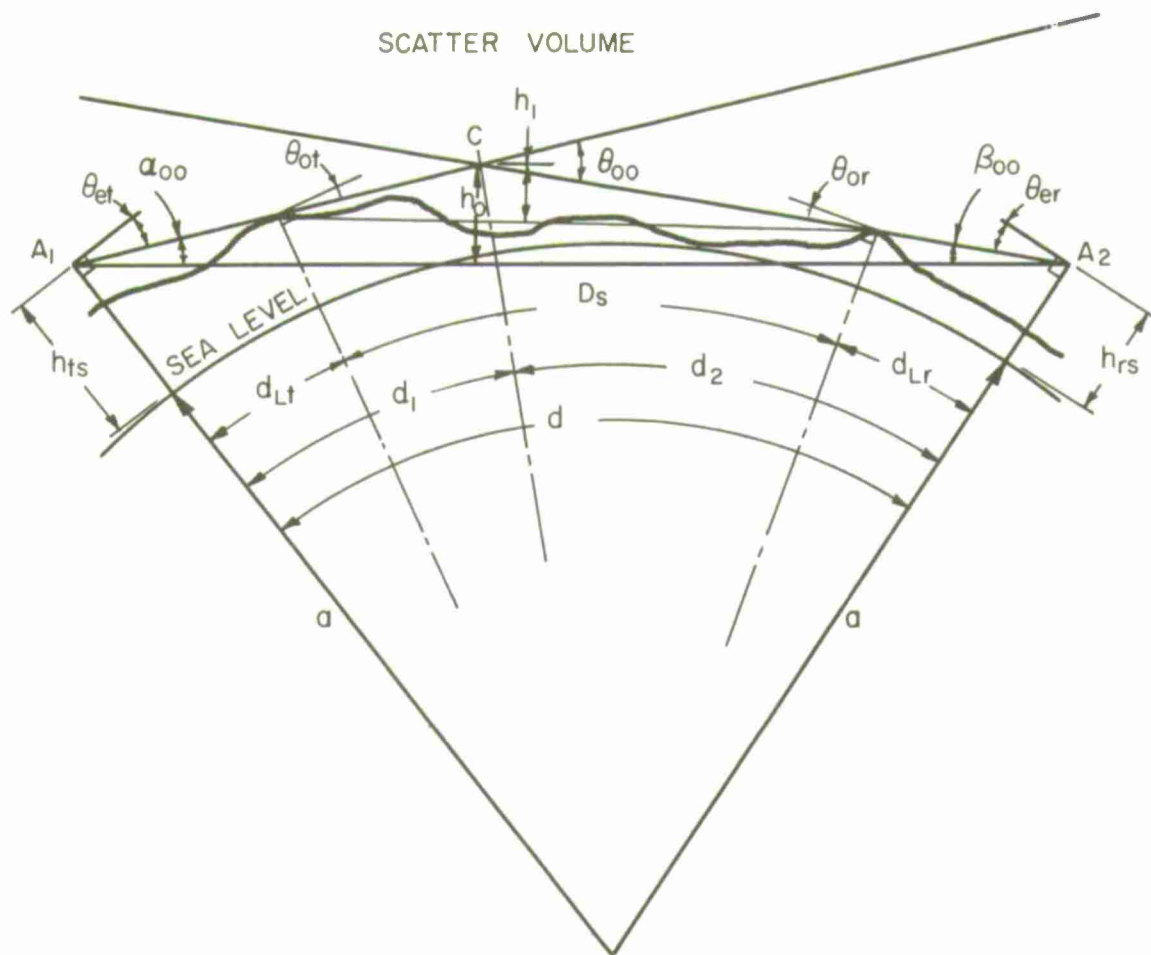
DISTANCES ARE MEASURED IN KILOMETERS ALONG A GREAT CIRCLE ARC.

$$\theta_{oo} = \frac{D_s}{a} + \theta_{ot} + \theta_{or} = \frac{d}{a} + \theta_{et} + \theta_{er}$$

Figure 6.1

TABLE MESA
RECEIVER SITE
AZIMUTH 137° 03'.108"
LONG. 105° 13' 52.3" W.
LAT. 40° 08' 53.2" N.

HASWELL
TRANSMITTER SITE
AZIMUTH 318° 22' 02.4"
LONG. 103° 09' 17.077" W.
LAT. 38° 22' 49.5" N.
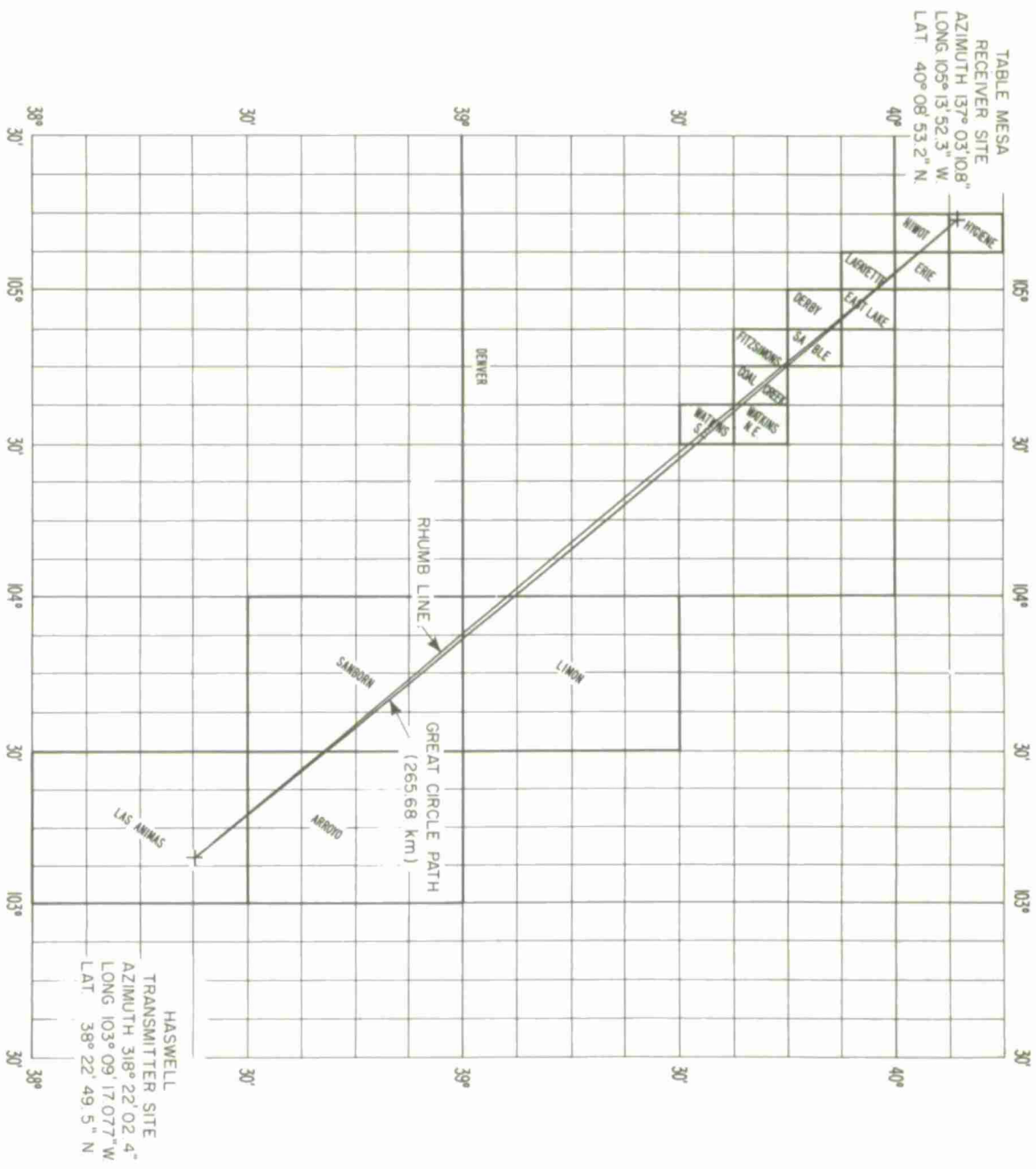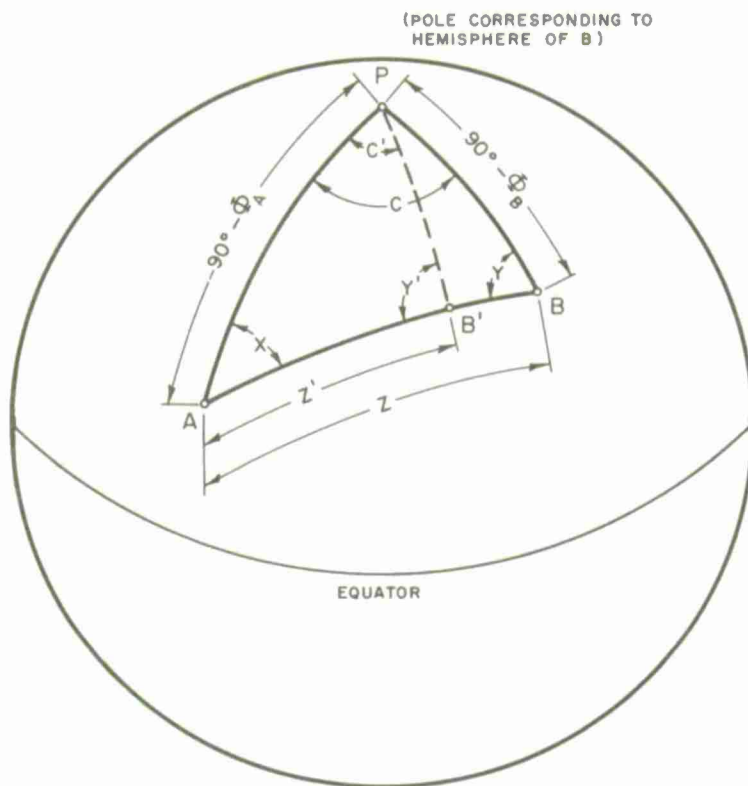
Figure 6.2

SPHERICAL TRIANGLE FOR
GREAT CIRCLE PATH COMPUTATIONS

Figure 6.3

MODIFIED TERRAIN PROFILE FOR A
LINE-OF-SIGHT PATH
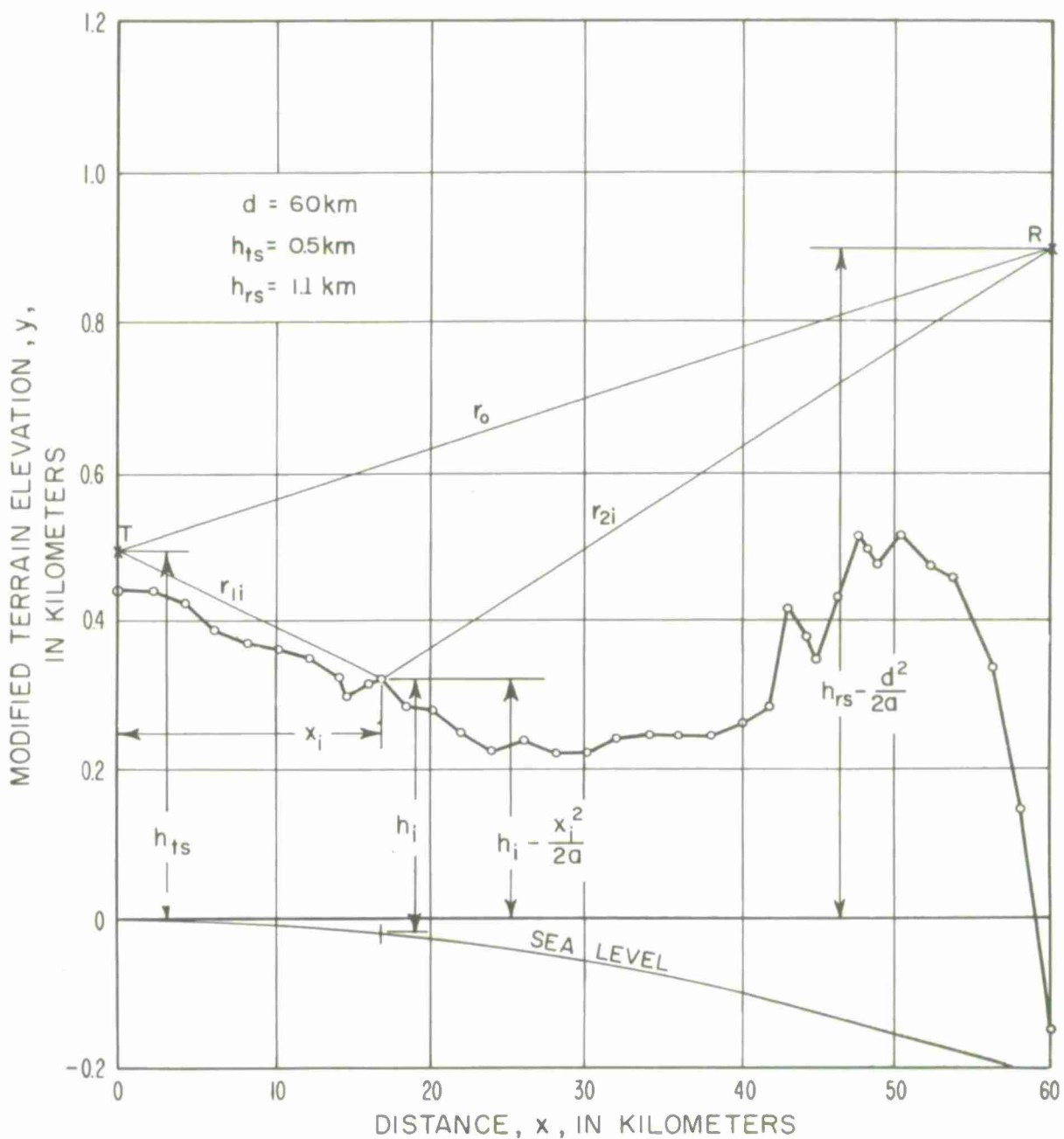
$d = 60$ km
$h_{ts} = 0.5$ km
$h_{rs} = 1.1$ km

Figure 6.4

6-11

MODIFIED TERRAIN PROFILE FOR A COMMON-HORIZON PATH

Figure 6.5

6-12

MODIFIED TERRAIN PROFILE FOR A DOUBLE-HORIZON PATH

Figure 6.6

6-13
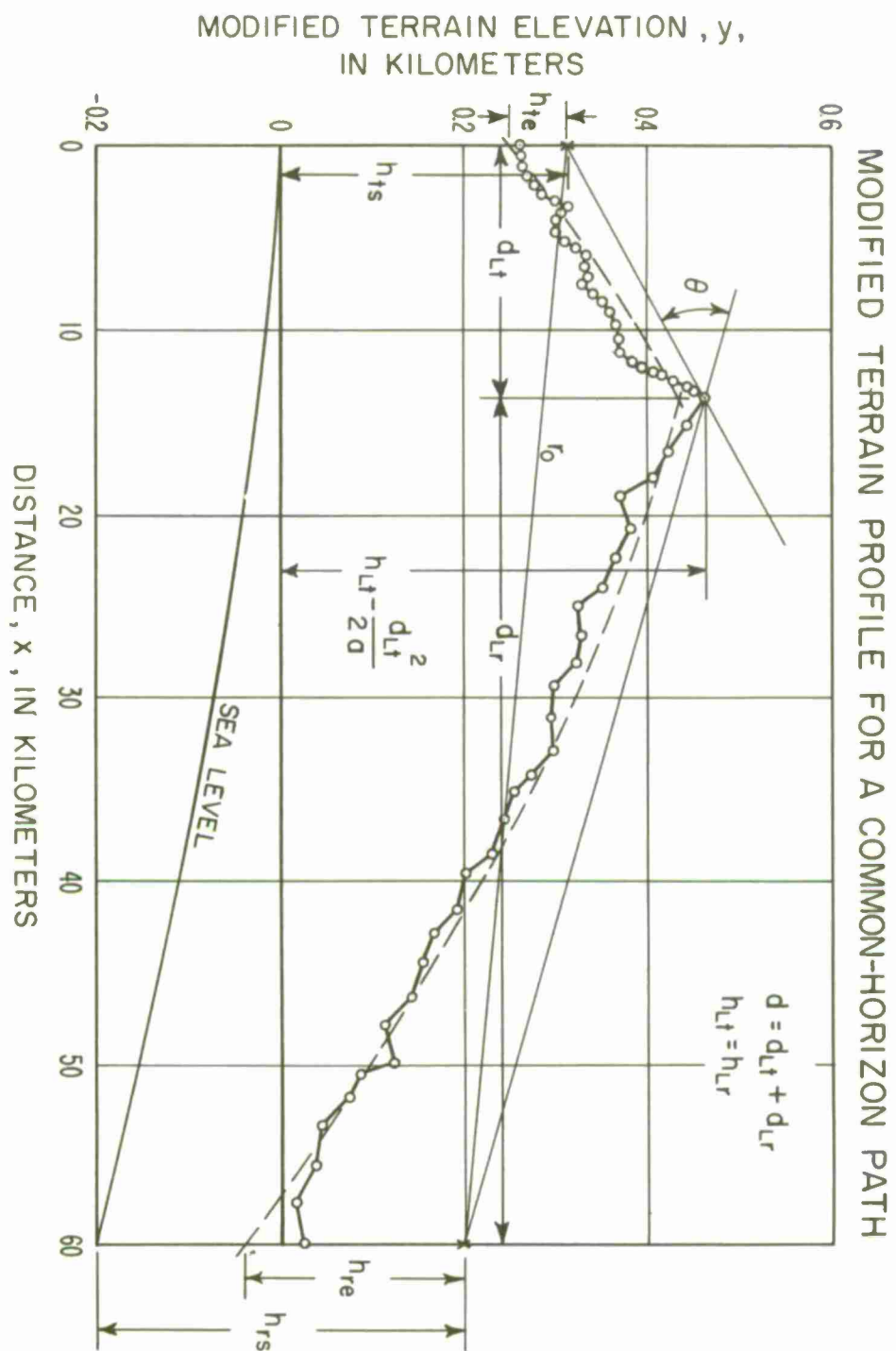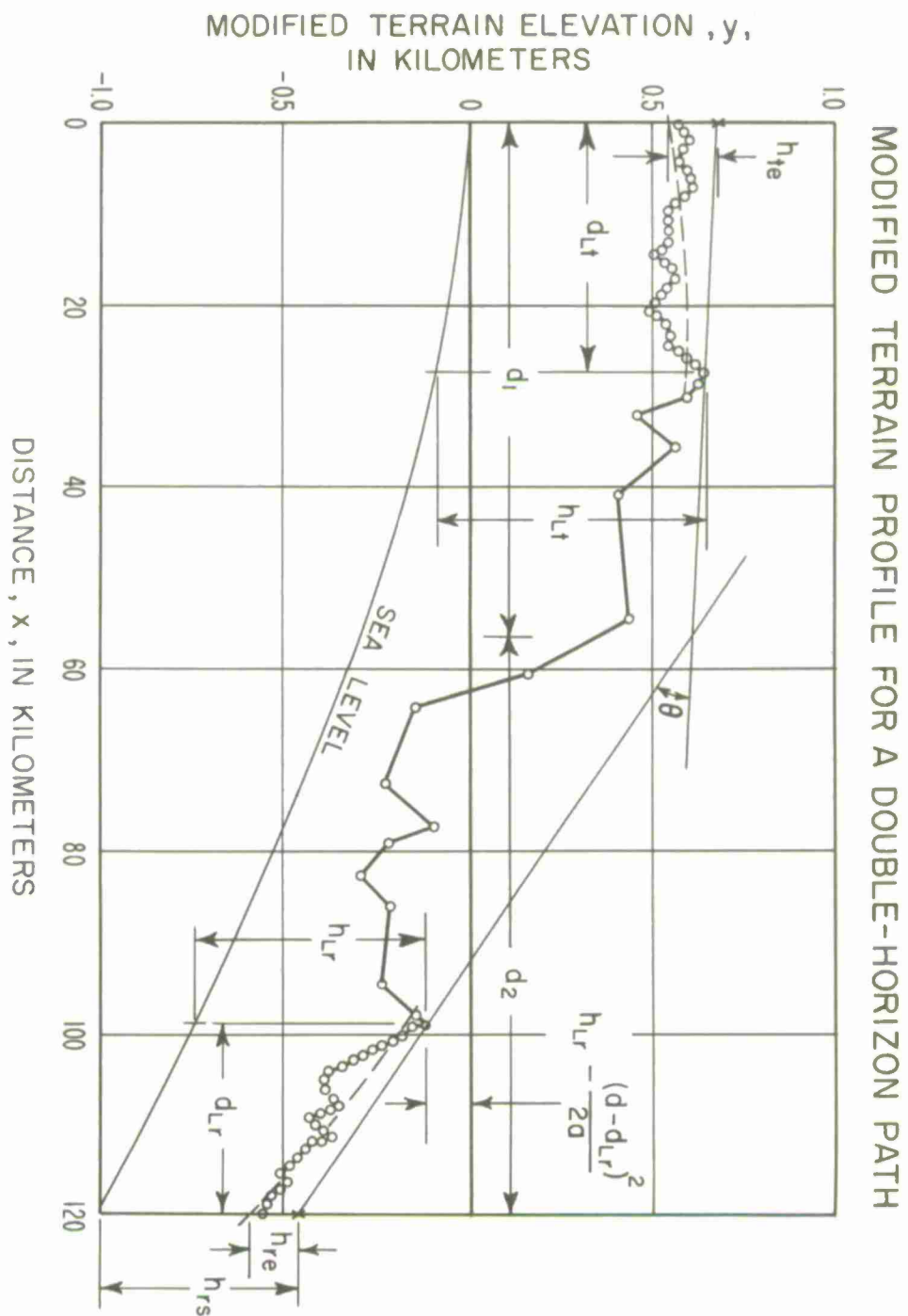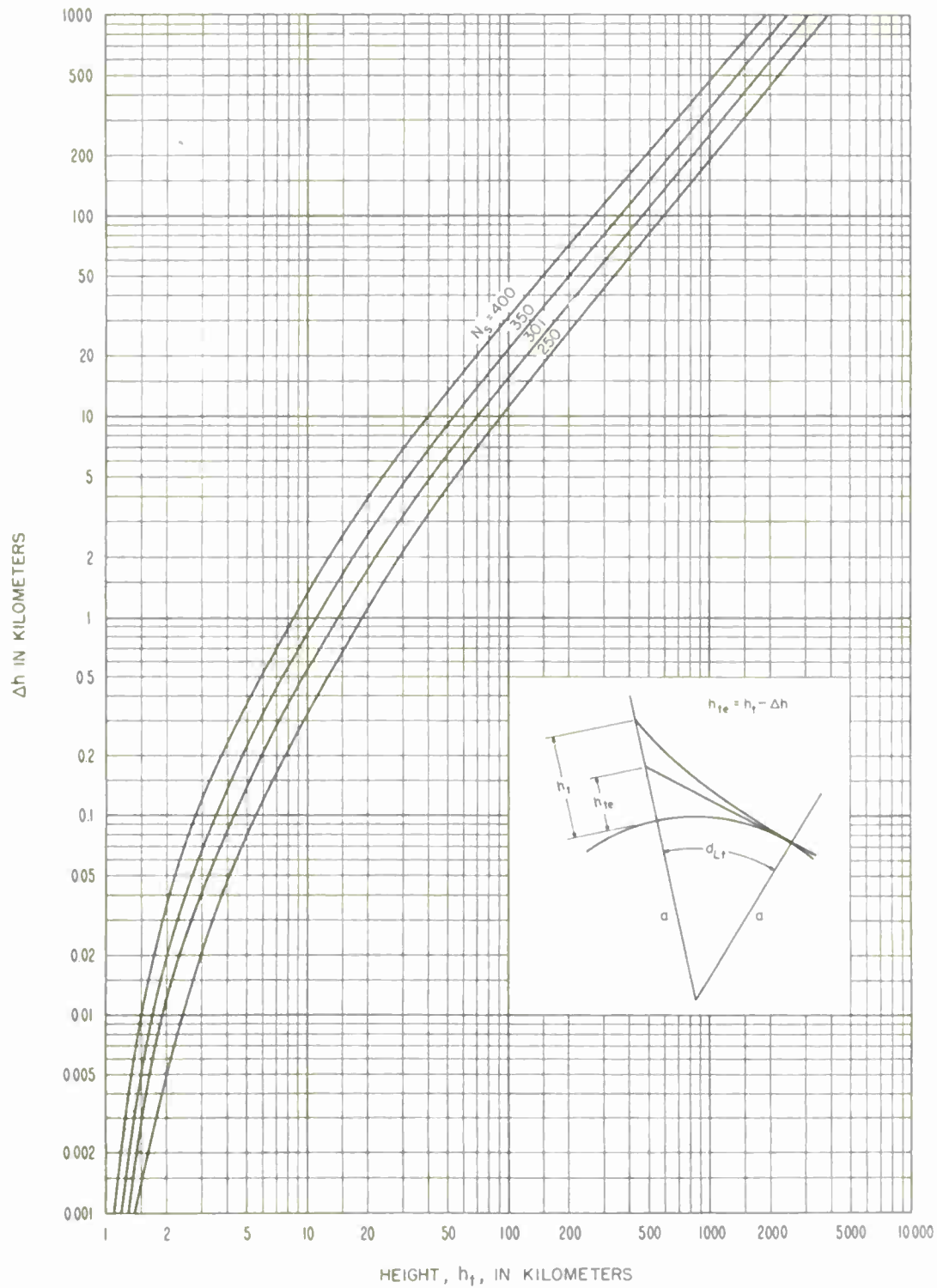
Figure 6.7

ANGULAR DISTANCE, θ, OVER A SMOOTH EARTH
VS DISTANCE BETWEEN HORIZONS, D$_S$

Figure 6.8

6-15
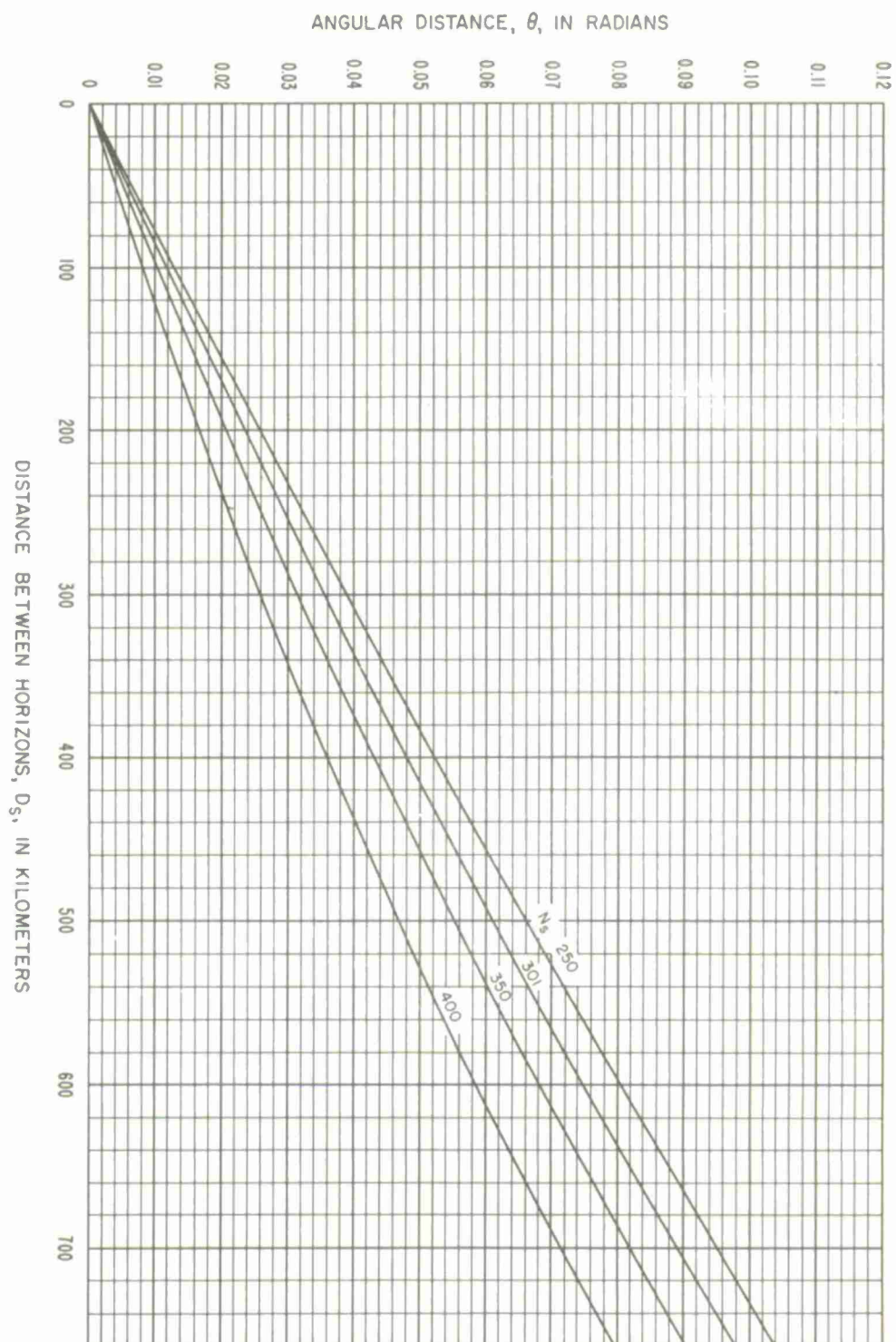
CORRECTION TERMS Δa_o, $\Delta \beta_o$ FOR $N_s = 301$
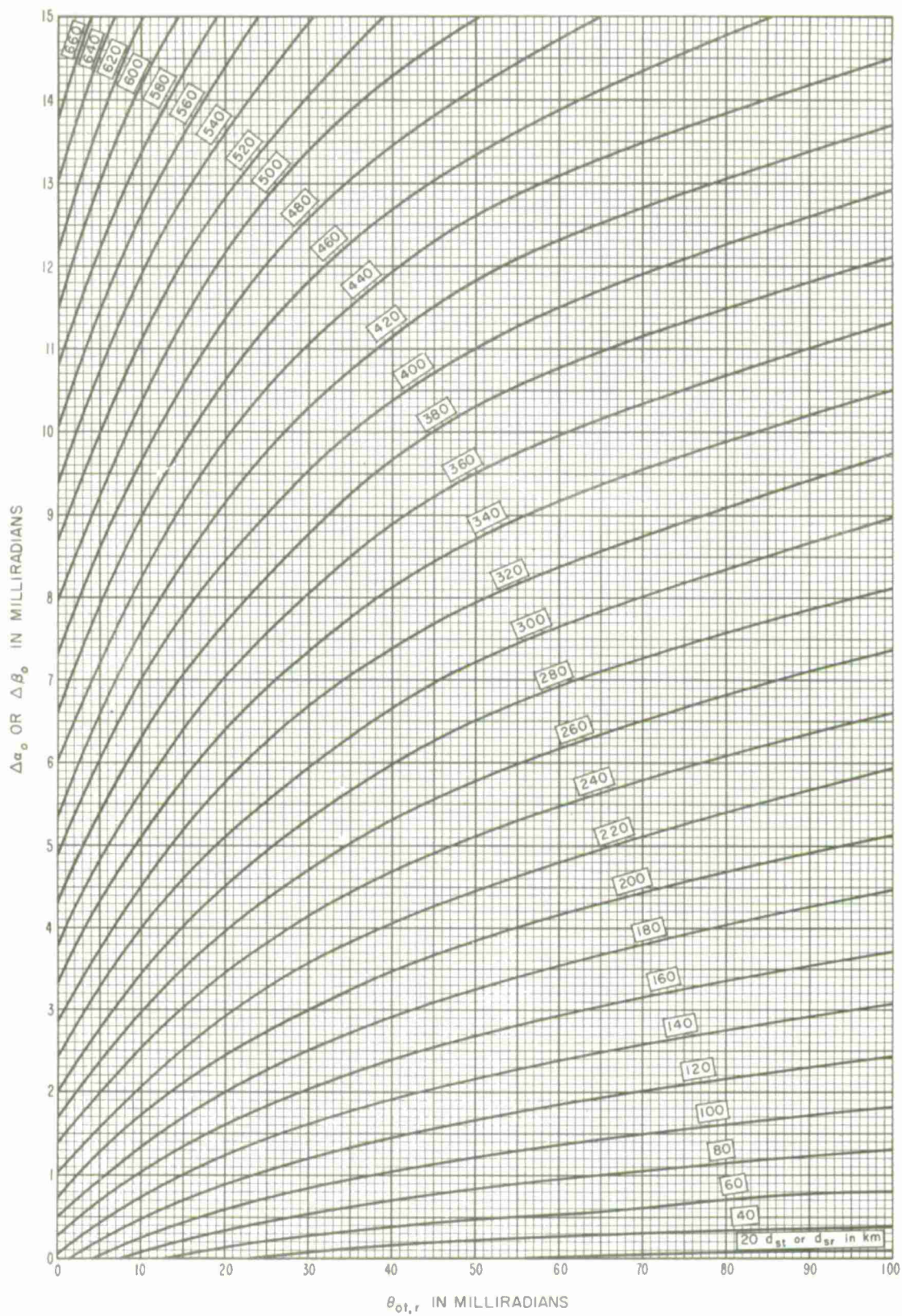
Figure 6.9

THE COEFFICIENT $C(N_S)$

$$\Delta a_0(N_S) = C(N_S) \, \Delta a_0(301)$$

$$C(N_S) = (1.3 N_S^2 - 60 N_S) \times 10^{-5}$$
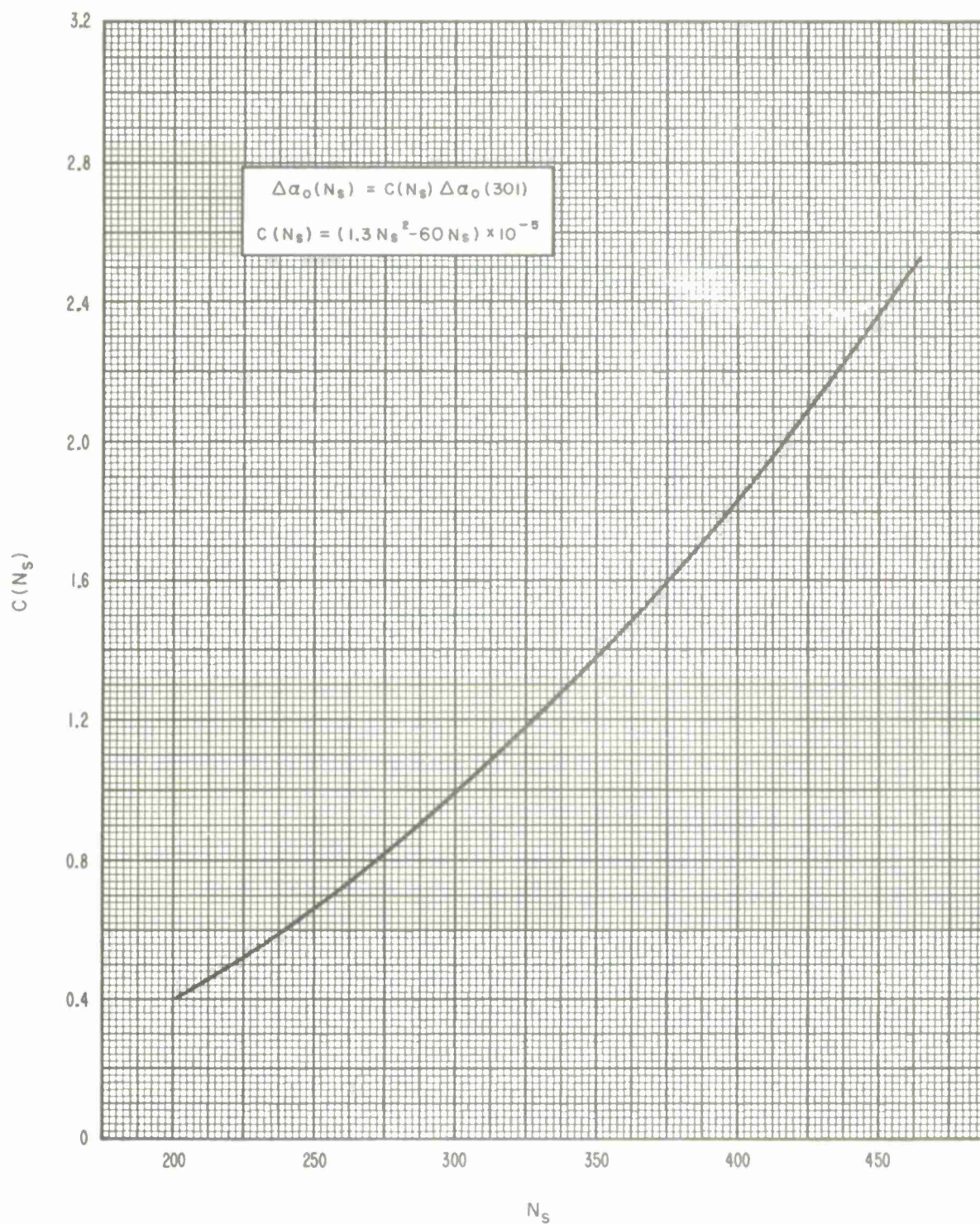
Figure 6.10

7. DIFFRACTION OVER A SINGLE ISOLATED OBSTACLE

A propagation path with a common horizon for both terminals may be considered as having a single diffracting knife edge. In some cases, reflection from terrain may be neglected as discussed in section 7.1; in other cases, ground reflections must be considered as shown in section 7.2 and appendix III. In actual situations, the common horizon may be a mountain ridge or similar obstacle, and such paths are sometimes referred to as "obstacle gain paths",[Barsis and Kirby, 1961; Dickson, Egli, Herbstreit and Wickizer, 1953; Furutsu, 1956, 1959, 1963; Kirby, Dougherty and McQuate, 1955; Rider, 1953; Ugai, 1963]. A ridge or mountain peak may not provide an ideal knife edge. The theory of "rounded obstacles" is discussed by Bachynski [1960], Dougherty and Maloney [1964], Neugebauer and Bachynski [1960], Rice [1954], Wait [1958, 1959], and Wait and Conda [1959]. Furutsu [1963] and Millington, Hewitt, and Immirzi [1962a] have recently developed tractable expressions for multiple knife-edge diffraction. In some cases, over relatively smooth terrain or over the sea, the common horizon may be the bulge of the earth rather than an isolated ridge. This situation is discussed in section 8.

7.1 Single Knife Edge, No Ground Reflections

A single diffracting knife edge where reflections from terrain may be neglected is illustrated in figure 7.1, where the wedge represents the knife edge. The diffraction loss $A(v, 0)$ is shown on figure 7.1 as a function of the parameter v, from Schelling, Burrows, and Ferrell [1933] and is defined as

$$v \equiv \pm 2\sqrt{\Delta r/\lambda} = \pm \sqrt{(2d \, \tan \alpha_o \, \tan \beta_o)/\lambda} \qquad (7.1a)$$

or in terms of frequency in MHz:

$$v = \pm 2.583 \, \theta \sqrt{f \, d_1 d_2 / d} \qquad (7.1b)$$

where the distances are all in kilometers and the angles in radians. The distance

$$\Delta r \equiv r_1 + r_2 - r_o = \theta^2 \, d_1 d_2 / (2d)$$

is discussed in section 5, and the distances d_1 and d_2 from the knife edge to the transmitter and receiver, respectively, are shown on figure 7.1. The radio wavelength, λ, is in the same units as the total path distance, d. The angles α_o, β_o, and θ are defined in section 6. In this case, $h_{Lt} = h_{Lr}$, and since $d_{st} = d_{sr} = 0$, no corrections $\Delta \alpha_o$ or $\Delta \beta_o$ are required. For the line-of-sight situation, shown in figure 7.1 and discussed in section 5.2, the angles α_o and β_o are both negative, and the parameter v is negative. For transhorizon paths, α_o and β_o are both positive and v is positive.

If v is greater than 3, A(v, 0) may be expressed by:

$$A(v, 0) \simeq 12.953 + 20 \log v \quad db \tag{7.2}$$

The basic transmission loss, L_{bd}, for a knife-edge diffraction path is given by adding A(v, 0) to the free space loss:

$$L_{bd} = L_{bf} + A(v, 0) \quad db \tag{7.3}$$

where L_{bf} is given by (2.31). For frequencies above about 1 GHz, an estimate of the loss due to absorption (3.1), should be added to (7.3) and (7.4).

If the angles α_o and β_o are small, the basic transmission loss over a knife-edge diffraction path may be written as :

$$L_{bd} = 30 \log d + 30 \log f + 10 \log \alpha_o + 10 \log \beta_o + 53.644 \quad db \tag{7.4}$$

which, however, is accurate only if $v > 3$, $d >> \lambda$, and $(d/\lambda) \tan \alpha_o \tan \beta_o > 4$.

For many paths, the diffraction loss is greater than the theoretical loss shown in (7.2), (7.3), and (7.4), because the obstacle is not a true knife edge, and because of other possible terrain effects. For a number of paths studied, the additional loss was about 10 to 20 db.

The problem of multiple knife-edge diffraction is not discussed here, but for the double knife-edge case, where diffraction occurs over two ridges, a simple technique may be used. The path is considered as though it were two simple knife-edge paths, (a) transmitter - first ridge-second ridge, and (b) first ridge-second ridge - receiver. The diffraction attenuation A(v, 0) is computed for each of these paths, and the results added to obtain the diffraction attenuation over the whole path. When the parameter v is positive and rather small for both parts of the path, this method gives excellent results. Methods for approximating theoretical values of multiple knife-edge diffraction have been developed by Wilkerson [1964].

7.2 Single Knife Edge with Ground Reflections

Theoretically, received fields may be increased by as much as 12 db due to enhancement, or deep nulls may occur due to cancellation of the signal by ground reflections. Reflection may occur on either or both sides of the diffracting edge. When an isolated knife edge forms a common horizon for the transmitter and receiver, the diffraction loss may be estimated as:

$$A = A(v, 0) - G(\overline{h}_1) - G(\overline{h}_2) \quad db \tag{7.5}$$

where

$$\overline{h}_1 = 2.2325 \ B^2(K, b^\circ) \ (f^2/a_1)^{\frac{1}{3}} \ h_{te} \cong 5.74 \ (f^2/a_1)^{\frac{1}{3}} \ h_{te} \tag{7.6a}$$

$$\overline{h}_2 = 2.2325 \ B^2(K, b^\circ) \ (f^2/a_2)^{\frac{1}{3}} \ h_{re} \cong 5.74 \ (f^2/a_2)^{\frac{1}{3}} \ h_{re}$$

$$a_1 = d_{Lt}^2/(2h_{te}), \ a_2 = d_{Lr}^2/(2h_{re}) \tag{7.6b}$$

The parameters b°, K, and $B(K, b^\circ)$ are defined in subsection 8.1. The knife-edge attenuation $A(v, 0)$ is shown on figure 7.1, and the function $G(\overline{h})$ introduced by Norton, Rice and Vogler [1955] is shown on figure 7.2. Effective antenna heights h_{te}, h_{re}, and the distances d_{Lt}, d_{Lr} are defined in section 6. In these and other formulas, f is the radio frequency in MHz.

The function $G(\overline{h}_{1,2})$ represents the effects of reflection between the obstacle and the transmitter and receiver, respectively. These terms should be used when more than half of the terrain between an antenna and its horizon cuts a first Fresnel zone ellipse which has the antenna and its horizon as focii and lies in the great circle plane. Definite criteria are not available, but in general, if terrain near the middle distance between a transmitting antenna and its horizon is closer to the ray than $0.5(\lambda d_{Lt})^{\frac{1}{2}}$ kilometers, $G(\overline{h}_1)$ should be used. The same criterion, depending on d_{Lr}, determines when $G(\overline{h}_2)$ should be used. When details of terrain are not known, an allowance for terrain effects, $G(\overline{h}_{1,2})$, should be used if $0.5(\lambda d_{Lt, Lr})^{\frac{1}{2}} > |h_{Lt, Lr} - h_{ts, rs}|/2$, where all distances and heights are in kilometers.

When the reflecting surface between the diffracting knife-edge and either or both antennas is more than the depth of a first Fresnel zone below the radio ray, and where geometric optics is applicable, the four ray knife-edge theory described in annex III may be used to compute diffraction attenuation. This method is used when details of terrain are known so that reflecting planes may be determined rather accurately. Using the four ray theory, the received field may include three reflected components, with associated reflection coefficients and ray path differences, in addition to the direct ray component.

7-3

7.3 Isolated Rounded Obstacle, No Ground Reflections

Dougherty and Maloney [1964] describe the diffraction attenuation relative to free space for an isolated, perfectly conducting, rounded knife edge. The rounded obstacle is considered to be isolated from the surrounding terrain when

$$k\,h\left[\,2/(kr)\,\right]^{\frac{1}{3}} >> 1$$

where $k = 2\pi/\lambda$, r is the radius of curvature of the rounded obstacle, and h is the smaller of the two values $[(d_{Lt}^2 + r^2)^{\frac{1}{2}} - r]$ and $[(d_{Lr}^2 + r^2)^{\frac{1}{2}} - r]$.

The diffraction loss for an isolated rounded obstacle and irregular terrain shown in figure 7.3 is defined as:

$$A(v,\rho) = A(v,0) + A(0,\rho) + U(v\rho) \quad db \tag{7.7}$$

where v is the usual dimensionless parameter defined by (7.1) and ρ is a dimensionless index of curvature for the crest radius, r in kilometers, of the rounded knife edge:

$$v\rho = 1.746\,0(fr)^{\frac{1}{3}} \tag{7.8}$$

$$\rho = 0.676\,r^{\frac{1}{3}} f^{-\frac{1}{6}}\left[\,d/(r_1 r_2)\,\right]^{\frac{1}{2}} \tag{7.9}$$

where, f is the radio frequency in MHz, d is the path distance in kilometers, and r_1, r_2 shown in figure 7.3 are the distances in kilometers from the transmitter and receiver, respectively to the rounded obstacle. For all practical applications, $r_1 r_2$ may be replaced by $d_1 d_2$. Where the rounded obstacle is the broad crest of a hill, the radius of curvature, r, for a symmetrical path is:

$$r = D_s/0 \tag{7.10}$$

where $D_s = d - d_{Lt} - d_{Lr}$ is the distance between transmitter and receiver horizons in kilometers, and θ is the angular distance in radians (6.19). Where the ratio $\alpha_o/\beta_o \neq 1$, the radius of curvature is defined in terms of the harmonic mean of radii a_t and a_r defined in the next section, (8.9), and shown in figure 8.7:

$$r = \frac{2\,D_s\,d_{st}\,d_{sr}}{0\left(d_{st}^2 + d_{sr}^2\right)} \tag{7.11}$$

In (7.7), the term $A(v,0)$ is the diffraction loss for the ideal knife edge $(r = 0)$, and is read from figure 7.1. The term $A(0,\rho)$ is the magnitude of the intercept values $(v = 0)$ for various values of ρ and is shown on figure 7.4. The last term $U(v\rho)$ is a function of the product, $v\rho$, and is shown on figure 7.5.

Arbitrary mathematical expressions, given in annex III, have been fitted to the curves of figures 7.1, 7.3, 7.4, and 7.5 for use in programming the method for a digital computer.

The diffraction loss $A(v, \rho)$ as given by (7.7) is applicable for either horizontally or vertically polarized radio waves over irregular terrain provided that the following conditions are met:

(a) the distances d, d_1, d_2, and r are much larger than λ,

(b) the extent of the obstacle transverse to the path is at least as great as the width of a first Fresnel zone:

$$\sqrt{\lambda d_{1,2} (1 - d_{1,2}/d)} \quad ,$$

(c) the components α_o and β_o of the angle θ are less than 0.175 radians, and

(d) the radius of curvature is large enough so that $(\pi r/\lambda)^{\frac{1}{3}} >> 1$.

In applying this method to computation of diffraction loss over irregular terrain, some variance of observed from predicted values is to be expected. One important source of error is in estimating the radius of curvature of the rounded obstacle, because the crests of hills or ridges are rarely smooth. Differences between theoretical and observed values are apt to be greater at UHF than at VHF.

7.4 Isolated Rounded Obstacle with Ground Reflections

If a rounded obstacle has a small radius and is far from the antennas, (7.7) may neglect important effects of diffraction or reflection by terrain features between each antenna and its horizon.

Such terrain foreground effects may be allowed for, on the average, by adding a term, $10 \exp(-2.3\rho)$ to (7.7). The effect of this term ranges from 10 db for $\rho = 0$ to 1 db for $\rho = 1$. When some information is available about foreground terrain, the $G(\overline{h}_{1,2})$ terms discussed in section 7.2 may be used if more than half of the terrain between an antenna and its horizon cuts a first Fresnel zone in the great circle plane:

$$A = A(v, \rho) - G(\overline{h}_1) - G(\overline{h}_2) \quad db \tag{7.12}$$

where $A(v, \rho)$ is defined by (7.7), $\overline{h}_1$, $\overline{h}_2$ by (7.6), and the functions $G(\overline{h}_{1,2})$ are shown on figure 7.2.

When details of terrain are known, and the reflecting surfaces between the rounded obstacle and either or both antennas are more than the depth of a first Fresnel zone below the radio ray, the geometric optics four-ray theory described in annex III may be applicable. In this case, the phase lag of the diffracted field with reference to the free space field must be considered in addition to the ray path differences of the reflected components. The phase lag $\Phi(v, \rho)$ of the diffracted field is defined as

$$\Phi(v, \rho) = 90 \, v^2 + \phi(v, 0) + \phi(0, \rho) + \phi(v\rho) \quad degrees \tag{7.13a}$$

where the functions $\phi(v, 0)$, $\phi(0, \rho)$, and $\phi(v\rho)$ are shown on figures 7.1, 7.4, and 7.5, respectively. For an ideal knife-edge, $\rho = 0$, the phase lag of the diffracted field is

$$\Phi(v, 0) = 90 \, v^2 + \phi(v, 0) \qquad \text{for } v > 0 \tag{7.13b}$$

and
$$\Phi(v, 0) = \phi(v, 0) \qquad \text{for } v \leq 0 \tag{7.13c}$$

KNIFE EDGE DIFFRACTION LOSS, A(v,0)
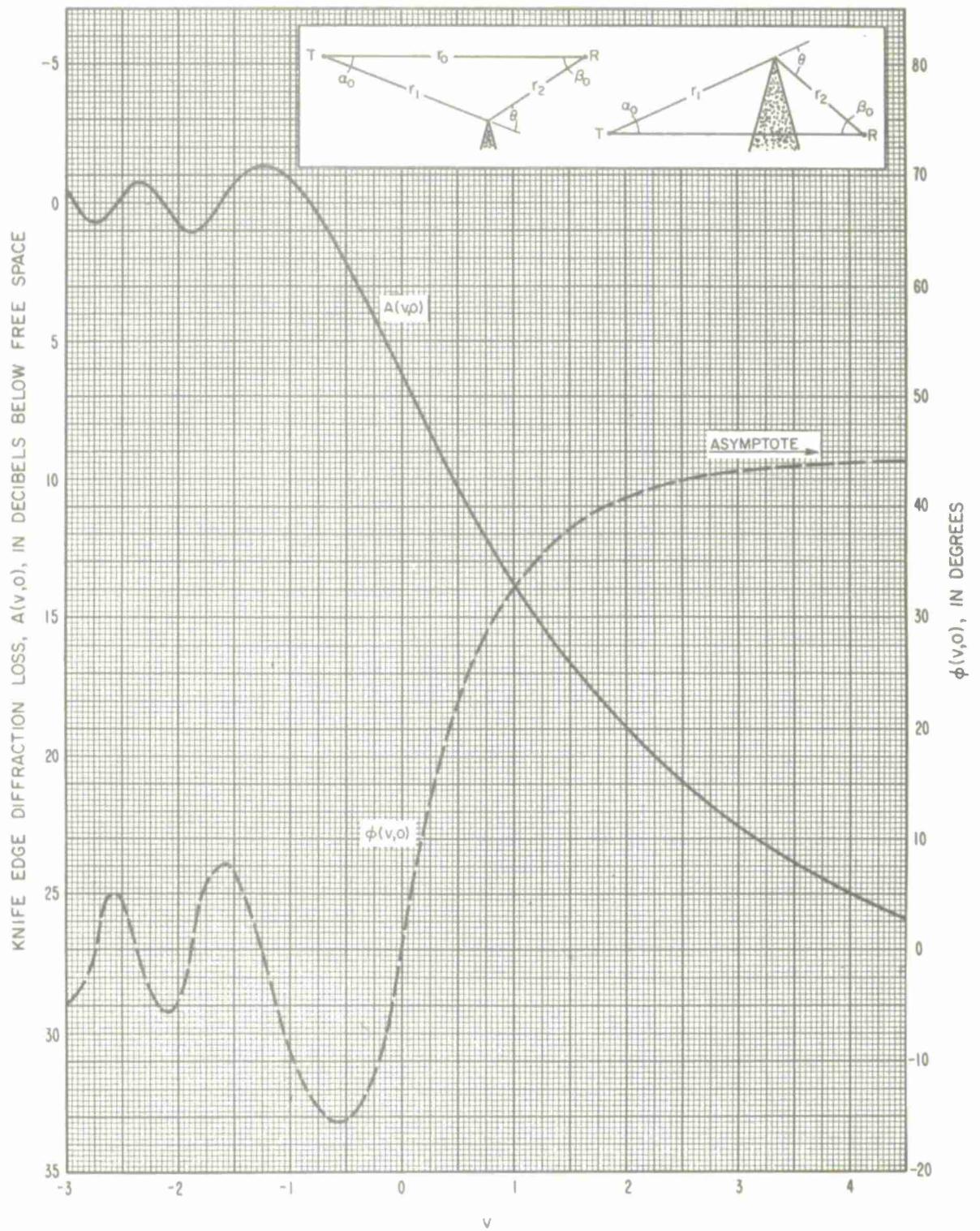
Figure 7.1

THE RESIDUAL HEIGHT GAIN FUNCTION $G(\bar{h}_{1,2})$
$0 \leq K \leq 0.1$ $b = 90°, 180°$

Figure 7.2

7-8
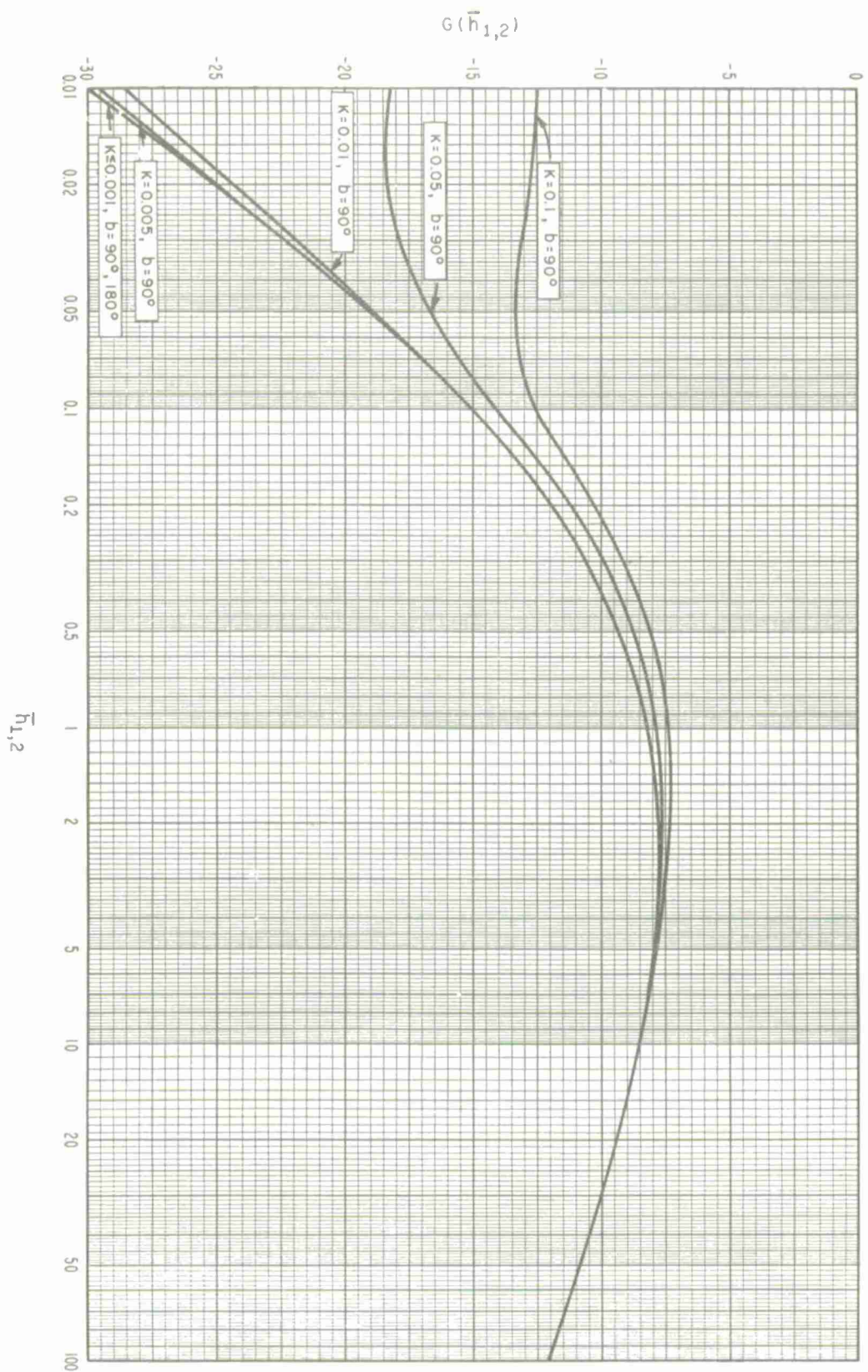
DIFFRACTION LOSS, A(v,ρ), FOR A ROUNDED OBSTACLE

Figure 7.3

7-9
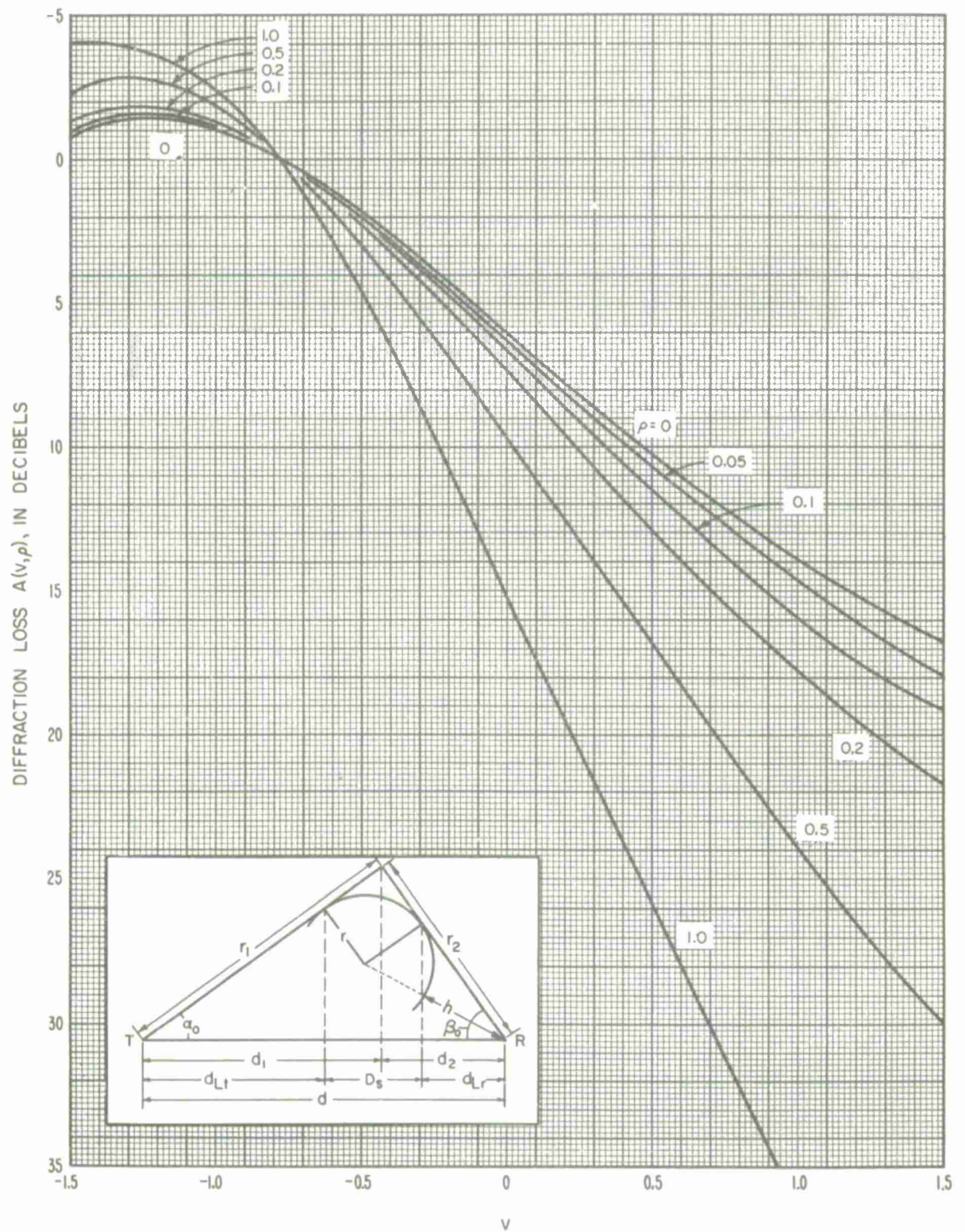
INTERCEPT MAGNITUDE AND PHASE FOR DIFFRACTION
OVER A ROUNDED OBSTACLE

$\phi(o,\rho)$

$A(o,\rho)$

A(o,ρ), IN DECIBELS

$\phi(o,\rho)$, INTERCEPT PHASE IN DEGREES

ρ
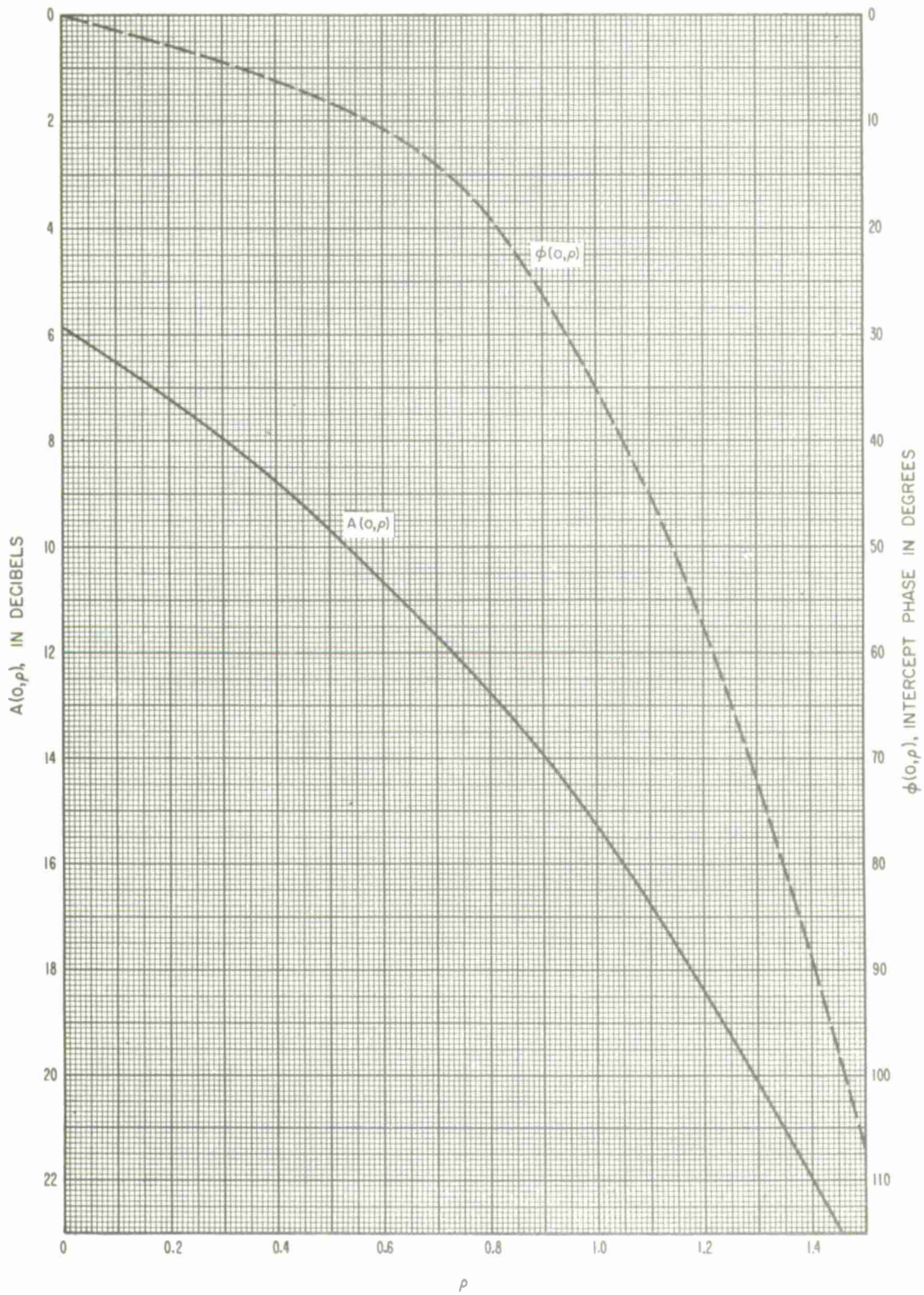
Figure 7.4

UNIVERSAL DIFFRACTION CURVE FOR A ROUNDED OBSTACLE
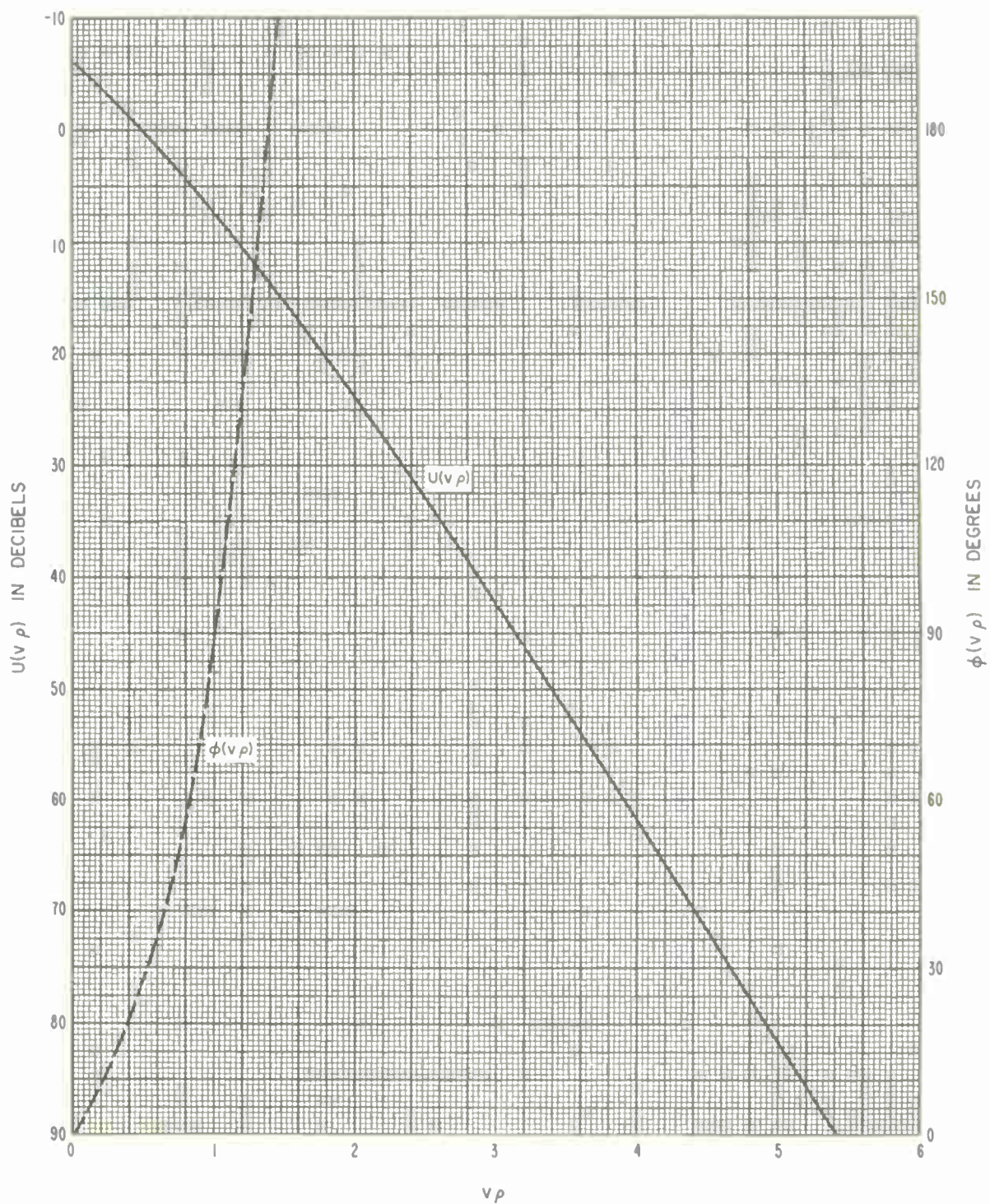
Figure 7.5

8. DIFFRACTION OVER SMOOTH EARTH AND OVER IRREGULAR TERRAIN

Diffraction attenuation over an isolated ridge or hill has been discussed in section 7. The following methods are used to compute attenuation over the bulge of the earth and over irregular terrain. The methods are applicable to the far diffraction region, where the diffracted field intensity may be determined by the first term of the Van der Pol-Bremmer residue series [Bremmer, 1949]. This region extends from near the radio horizon to well beyond the horizon. A criterion is given to determine the minimum distance for which the method may be used. In some situations the first term of the series provides a valid approximation to the diffracted field even at points slightly within line-of-sight [Vogler, 1964].

A simplified graphical method for determining ground wave attenuation over a spherical homogeneous earth in this far diffraction region was recently developed by Vogler [1964], based on a paper by Norton [1941]. The method described in section 8.1 is applicable to either horizontal or vertical polarization, and takes account of the effective earth's radius, ground constants, and radio frequency. In section 8.2, a modification of the method for computing diffraction attenuation over irregular terrain is described, and section 8.3 considers the special case of a common horizon which is not an isolated obstacle.

For frequencies above 1000 MHz, the attenuation due to gaseous absorption should be added to the diffraction loss. See (3.1) and figure 3.6.

8.1 Diffraction Attenuation over a Smooth Earth

The attenuation relative to free space may be expressed with four terms; one contains the distance dependence, two represent the dependence on antenna heights, and the fourth one depends on electromagnetic ground constants, the earth's radius, and the radio frequency:

$$A = G(x_0) - F(x_1) - F(x_2) - C_1(K, b^\circ) \quad db \qquad (8.1)$$

where

$$x_0 = d\, B_o, \qquad x_1 = d_{Lt}\, B_o, \qquad x_2 = d_{Lr}\, B_o \qquad (8.2a)$$

$$B_o = f^{\frac{1}{3}}\, C_o^2\, B(K, b^\circ), \qquad C_o = (8497/a)^{\frac{1}{3}} \qquad (8.2b)$$

The distances d, d_{Lt}, d_{Lr}, and the effective earth's radius, a, have been defined in sections 4 and 6, and f is the radio frequency in megacycles per second.

The parameters K and b° depend on polarization of the radio wave and the relative dielectric constant, ϵ, and conductivity, σ, of the ground. Figures 8.1 and 8.2 show curves of K and b° versus frequency for combinations of ϵ and σ corresponding to poor, average, and good ground, and to sea water. Figure 8.1 shows K for a = 8497 km. For other values of effective earth's radius,

$$K(a) = C_o\, K(8497) \qquad (8.3)$$

General formulas for K and b° for both horizontal and vertical polarization are given in section III.4 of annex III.

The parameter $B(K, b^\circ)$ in (8.2b) is shown as a function of K and b° in figure 8.3. The limiting value $B = 1.607$ for $K \to 0$ may be used for most cases of horizontal polarization. The parameter $C_1(K, b^\circ)$ in (8.1) is shown in figure 8.4.

The function $G(x_0)$ in (8.1) is shown on figures 8.5 and 8.6, and is defined as

$$G(x_0) = 0.05751 \, x_0 - 10 \log \, x_0 \tag{8.4}$$

and the height functions $F(x_{1,2})$ are plotted in figures 8.5 and 8.6 versus K and b°. For large values of x_1 or x_2, $F(x)$ is approximately equal to $G(x)$.

Because this method is based on only the first term of the residue series, it is limited to the following distances to insure that A is accurate within approximately 1.5 db:

$$x_0 - x_1(\Delta x_1) - x_2(\Delta x_2) > 335 , \quad \text{for } B = 1.607, \ (K \leq 0.01) \tag{8.5a}$$

$$x_0 - x_1(\Delta x_1) - x_2(\Delta x_2) > 115 , \quad \text{for } B = 0.700, \ (K \geq 10) \tag{8.5b}$$

For values of B lying between these two limits, linear interpolation between the $\Delta(x)$ curves of figure 8.6, and the two minimum values in (8.5) gives a fair approximation of the range of validity of (8.1). Using linear interpolation:

$$x_0 - x_1 \, \Delta(x_1, B) - x_2 \, \Delta(x_2, B) > x_{min} \tag{8.6}$$

where

$$x_{min} = 335 - 242.6 (1.607 - B) \tag{8.7a}$$

$$\Delta(x, B) = \Delta(x, 1.607) + 1.103 (1.607 - B) \left[\Delta(x, 0.700) - \Delta(x, 1.607) \right] \tag{8.7b}$$

$\Delta(x, 0.700)$ and $\Delta(x, 1.607)$ are the values read from the upper and lower curves of Δx in figure 8.6.

The basic diffraction transmission loss, L_{bd}, is obtained by adding the attenuation A to the free space loss L_{bf} defined by (2.31), including an allowance for atmospheric absorption when required .

8.2 Diffraction over Irregular Terrain

To compute diffraction attenuation over irregular terrain, the single effective earth's radius, a, used in (8.2) is replaced by four different radii as shown in figure 8.7. The radii a_1 and a_2 of the terrain between the antennas and their horizons, and the radii a_t and a_r of the terrain between radio horizons and the crossover point of horizon rays are defined by

$$a_1 = d_{Lt}^2/(2h_{te}), \qquad a_2 = d_{Lr}^2/(2h_{re}) \qquad (8.8)$$

$$a_t = D_s d_{st}/(\theta d_{sr}), \qquad a_r = D_s d_{sr}/(\theta d_{st}) \qquad (8.9)$$

The distances D_s, d_{st}, d_{sr}, d_{Lt}, d_{Lr}, the effective antenna heights h_{te} and h_{re}, and the angular distance θ are defined in section 6.

Four values of C_o are computed from (8.2b) with C_{o1}, C_{o2}, C_{ot}, and C_{or} corresponding to a_1, a_2, a_t, and a_r, respectively. These are used in (8.3) to obtain values of $K_{1,2,t,r}$ for the corresponding earth's radii, and $B_{1,2,t,r}$ are then read from figure 8.3 corresponding to each value of K.

The diffraction attenuation relative to free space is then:

$$A = G(x_0) - F(x_1) - F(x_2) - \overline{C}_1(K_{1,2}) + A_a \qquad (8.10)$$

where A_a is the atmospheric absorption defined by (3.1), and is negligible for frequencies less than 1 GHz, and $\overline{C}_1(K_{1,2})$ is the weighted average of $C_1(K_1,b)$ and $C_1(K_2,b)$ read from figure 8.4:

$$\overline{C}_1(K_{1,2}) = [x_1 C_1(K_1) + x_2 C_1(K_2)]/(x_1 + x_2) \qquad (8.11)$$

$$x_1 = B_1 C_{o1}^2 f^{\frac{1}{3}} d_{Lt}, \qquad x_2 = B_2 C_{o2}^2 f^{\frac{1}{3}} d_{Lr} \qquad (8.12)$$

$$x_o = \left(B_t C_{ot}^2 d_{st} + B_r C_{or}^2 d_{sr}\right) f^{\frac{1}{3}} + x_1 + x_2 \qquad (8.13)$$

$$C_{o1,o2,ot,or} = (8497/a_{1,2,t,r})^{\frac{1}{3}}, \qquad K_{1,2,t,r} = C_{o1,o2,ot,or} K(8497)$$

$$B_{1,2,t,r} = B(K_{1,2,t,r}, b^\circ)$$

This method is applicable to computation of diffraction attenuation over irregular terrain for both vertical and horizontal polarization for transhorizon paths. The method may be somewhat simplified for two special cases: diffraction over paths where $d_{st} \cong d_{sr}$, and for most paths when horizontal polarization is used.

8.2.1 Diffraction over paths where $d_{st} \cong d_{sr}$

For paths where the distances d_{st} and d_{sr} are equal, the parameter x_0 may be defined in terms of D_s and the corresponding earth's radius a_s:

$$x_0 = B_s C_{os}^2 f^{\frac{1}{3}} D_s + x_1 + x_2 \qquad (8.14)$$

$$D_s = 2 d_{st} = 2 d_{sr} , \quad a_s = D_s/\theta , \quad C_{os} = (8497/a_s)^{\frac{1}{3}} \qquad (8.15a)$$

$$K_s = C_{os} K(8497) , \quad B_s = B(K_s, b) \qquad (8.15b)$$

where x_1 and x_2 are defined by (8.12). The diffraction attenuation is then computed using (8.10).

8.2.2 For horizontal polarization

For horizontally polarized radio waves, at frequencies above 100 MHz, and with $K(a) \leq 0.001$, the parameter $B(K, b)$ approaches a constant value, $B \approx 1.607$, and $C_1(K, b) = 20.03$ db. Assuming $B = 1.607$ and $C_1 = 20.03$, the diffraction attenuation may be computed as follows:

$$A = G(x_0) - F(x_1) - F(x_2) - 20.03 \quad db \qquad (8.16a)$$

$$x_1 = 669 f^{\frac{1}{3}} d_{Lt}/a_1^2 , \quad x_2 = 669 f^{\frac{1}{3}} d_{Lr}/a_2^2 \qquad (8.16b)$$

$$x_0 = 669 f^{\frac{1}{3}} \theta^{\frac{2}{3}} D_{str} + x_1 + x_2 \qquad (8.16c)$$

where

$$D_{str} = (d_{st} d_{sr})^{\frac{1}{3}} \left(d_{st}^{\frac{1}{3}} + d_{sr}^{\frac{1}{3}} \right) \bigg/ (d_{st} + d_{sr})^{\frac{2}{3}}$$

The parameter D_{str} is shown in figure 8.8 as a function of d_{st} and d_{sr}.

For paths where $d_{st} = d_{sr}$, using horizontal polarization, the parameter x_0 simplifies to

$$x_0 = 669 f^{\frac{1}{3}} (\theta^2 D_s)^{\frac{1}{3}} + x_1 + x_2 \qquad (8.16d)$$

8.3 Single-Horizon Paths, Obstacle not Isolated

In some cases, over rather regular terrain or over the sea, a common horizon may be the bulge of the earth rather than an isolated ridge or mountain. For such paths, the path distance, d, is just the sum of d_{Lt} and d_{Lr}, and in this case, the method described in section 8.2 is simplified to one with only two earth's radii instead of four. The parameters x_1 and x_2 are defined by (8.12), and $x_0 = x_1 + x_2$. The diffraction attenuation is then computed using (8.10).

The diffraction loss predicted by this method agrees very well with observed values over a number of paths in the United Kingdom and the United States where the common horizon is not isolated.

For transhorizon paths of short to medium length, when it is not known whether diffraction or scatter is the dominant propagation mechanism, both diffraction and scatter loss should be computed. The next section shows how to compute scatter loss, and how to combine the two computed values when they are nearly equal.

THE PARAMETER K FOR AN EFFECTIVE EARTH RADIUS, a = 8497 km

CARRIER FREQUENCY IN MHz

K (a = 8497 km)

Figure 8.1

8-6
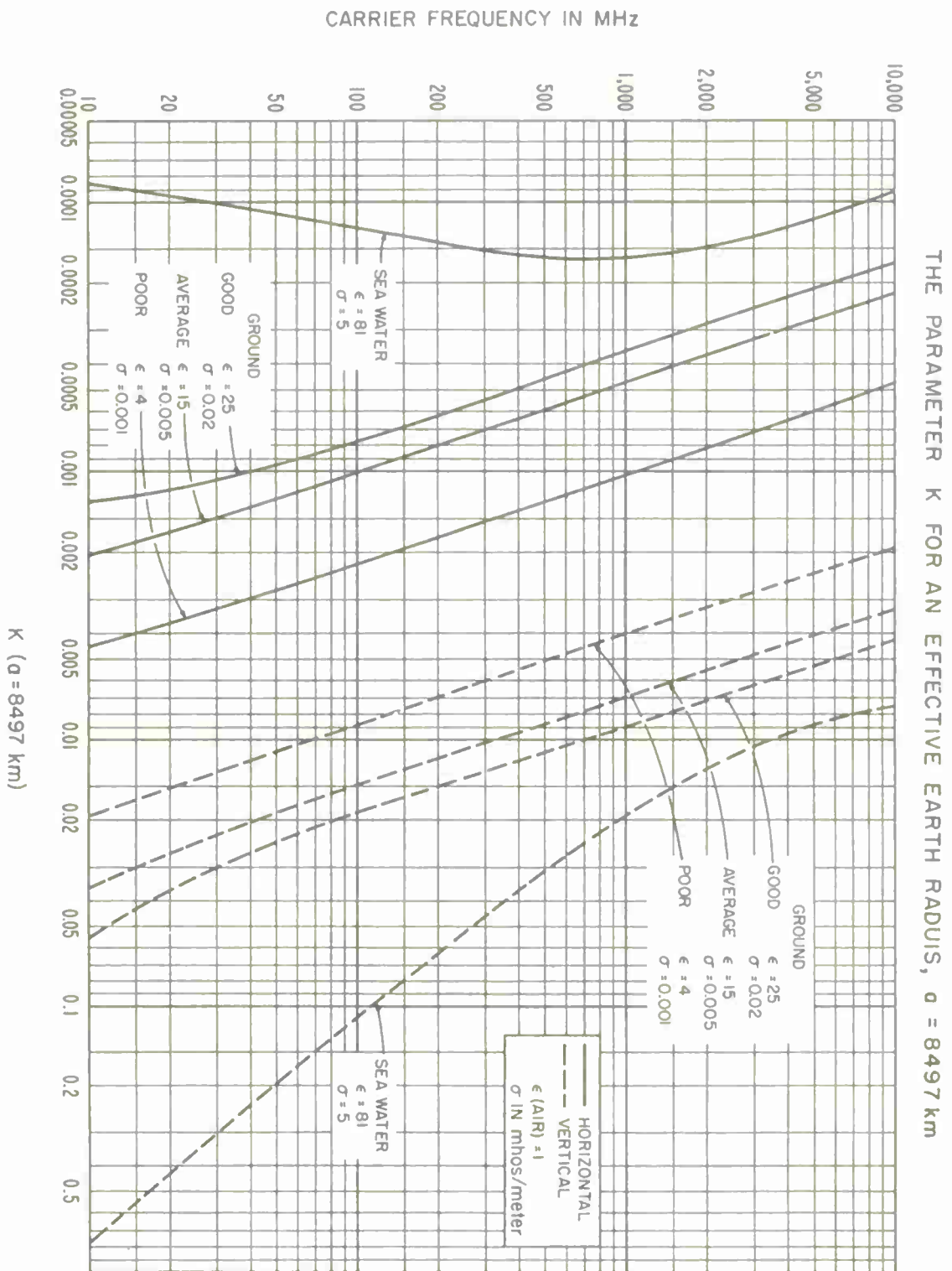
THE PARAMETER b° IN GROUND WAVE PROPAGATION

OVER A SPHERICAL EARTH

Figure 82

8-7
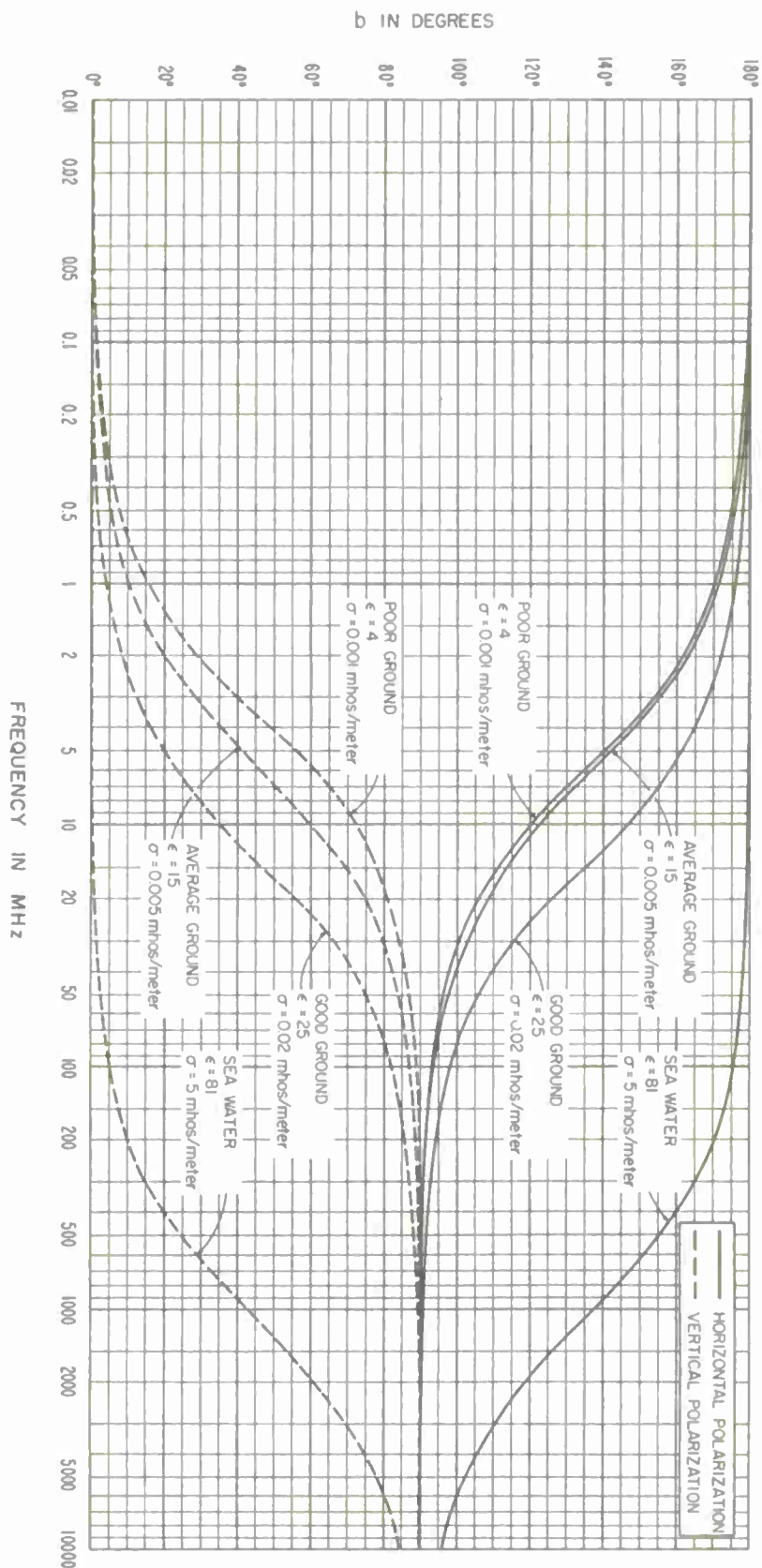
THE PARAMETER B(K,b)
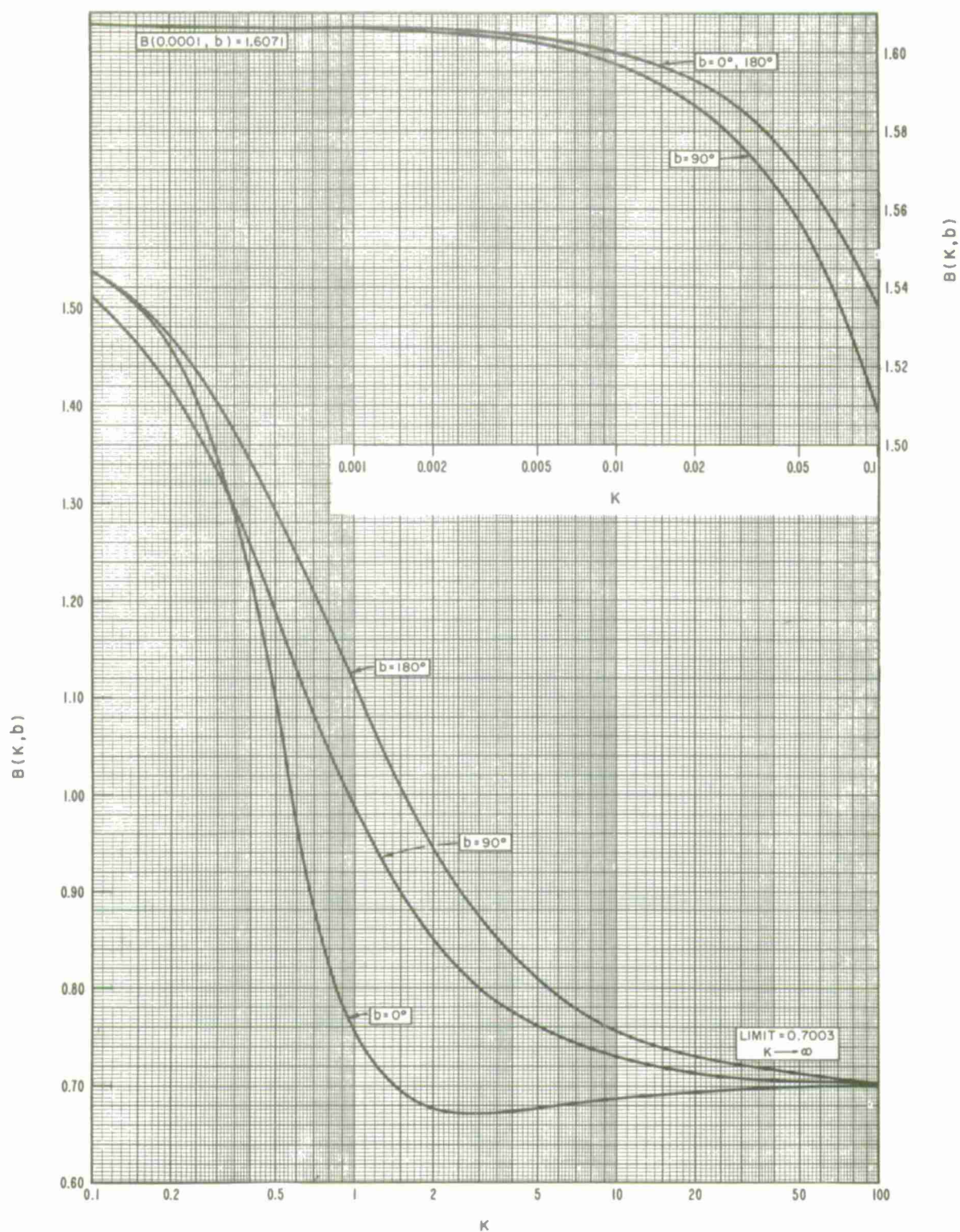
Figure 8.3

$C_1(K, b^\circ)$
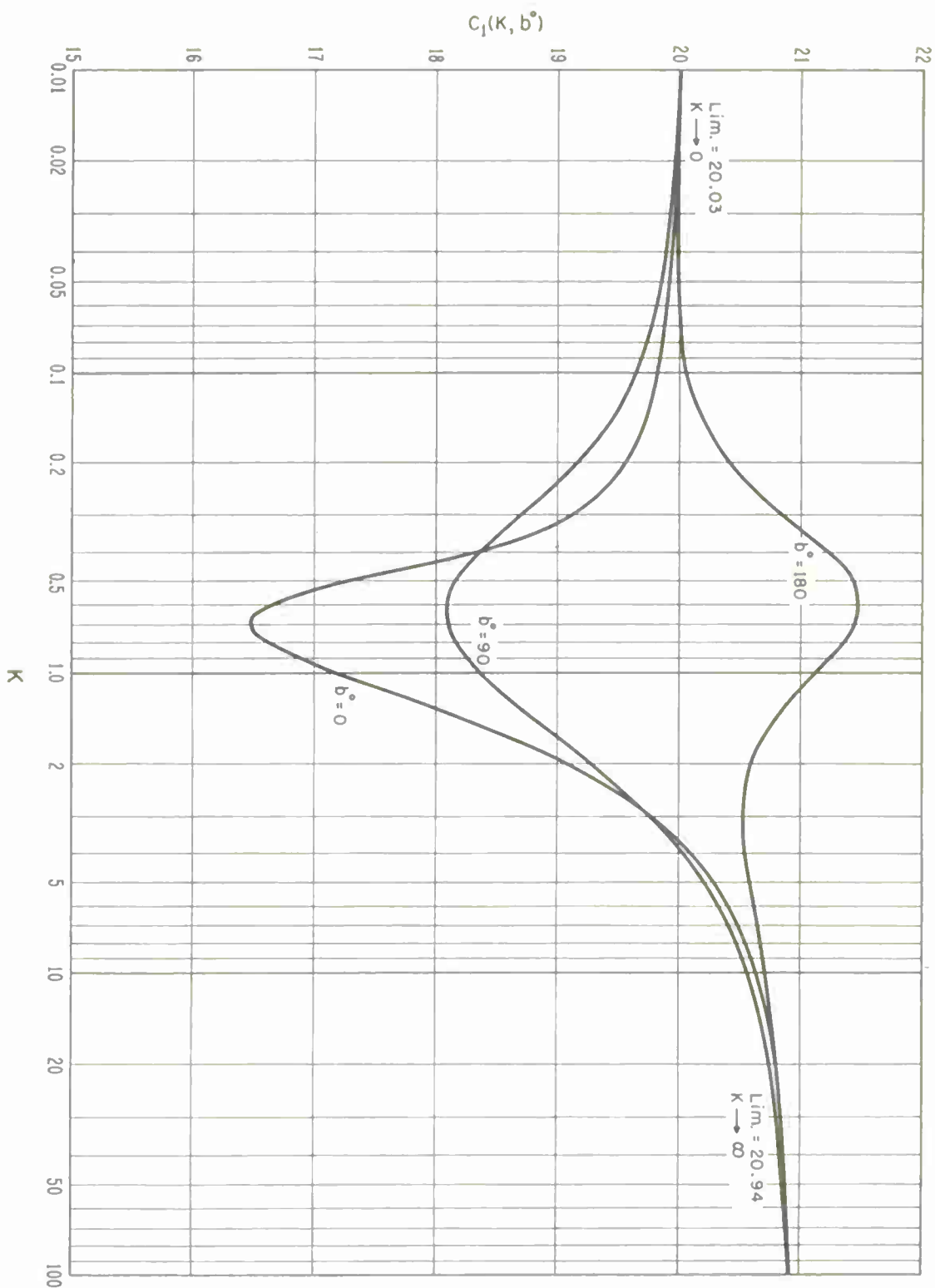
THE PARAMETER $C_1(K, b^\circ)$

Figure 8.4

THE FUNCTIONS $F(x_1,x_2)$ FOR $K \leq 0.1$ AND $G(x_0)$.
FOR LARGE x : $F(x) \sim G(x)$
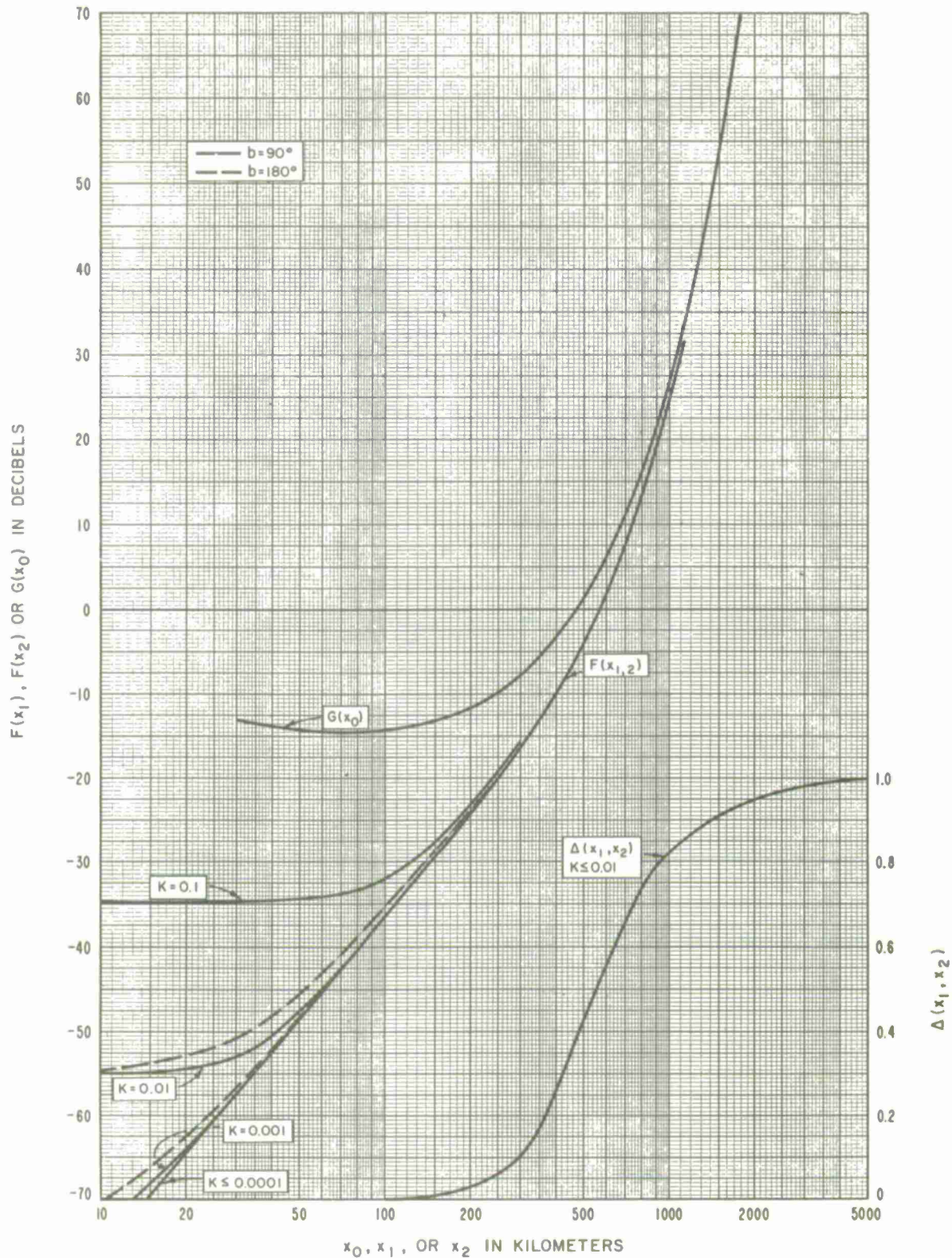
Figure 8.5

8-10
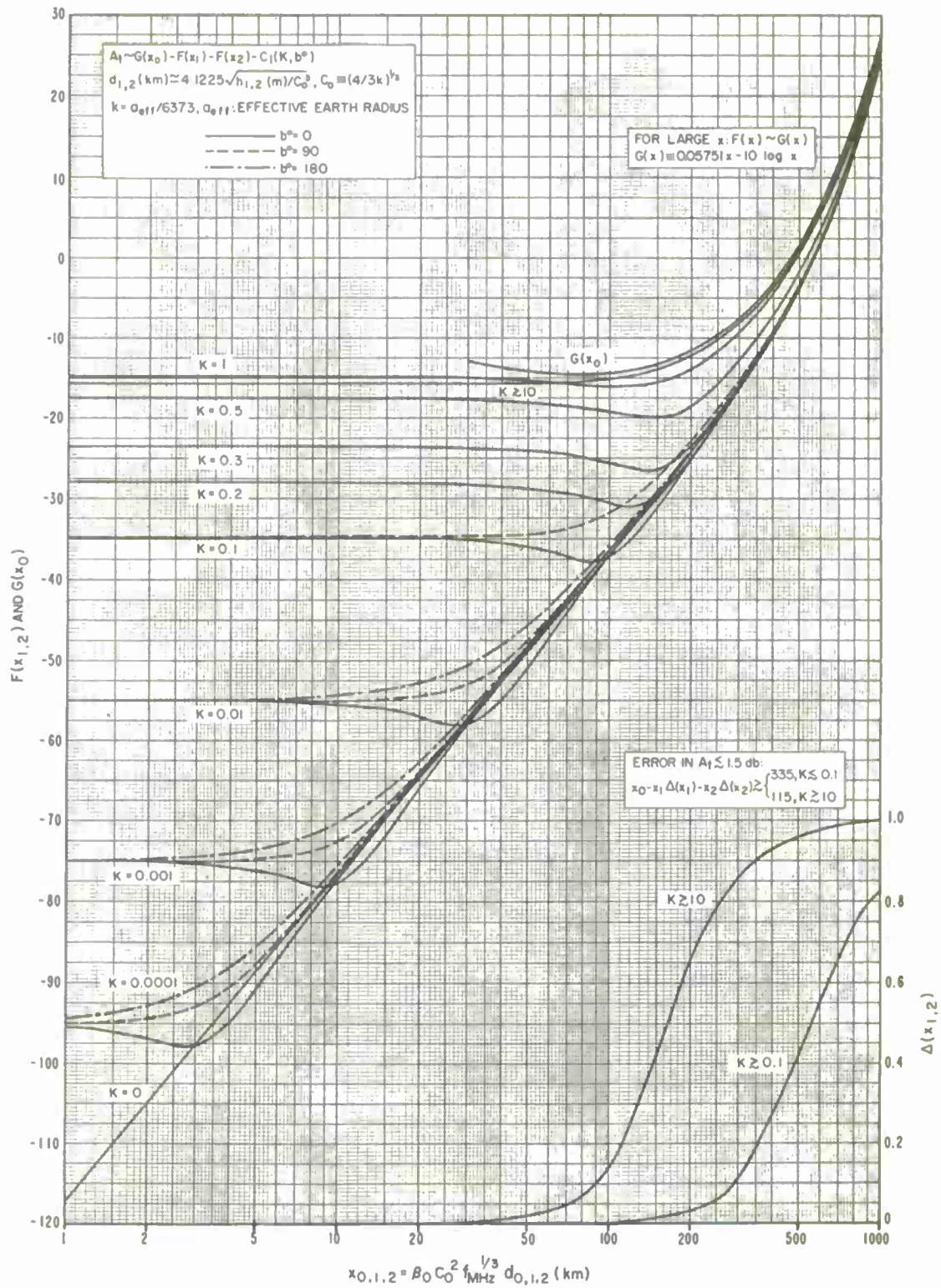
Figure 8.6

GEOMETRY FOR DIFFRACTION
OVER IRREGULAR TERRAIN

Figure 8.7

Figure 8.8

THE PARAMETER D_{str}

d_{st} (OR d_{sr}) IN KILOMETERS

$\bigcirc$ $d_{st} = d_{sr}$

D_{str}

d_{sr} (OR d_{st})
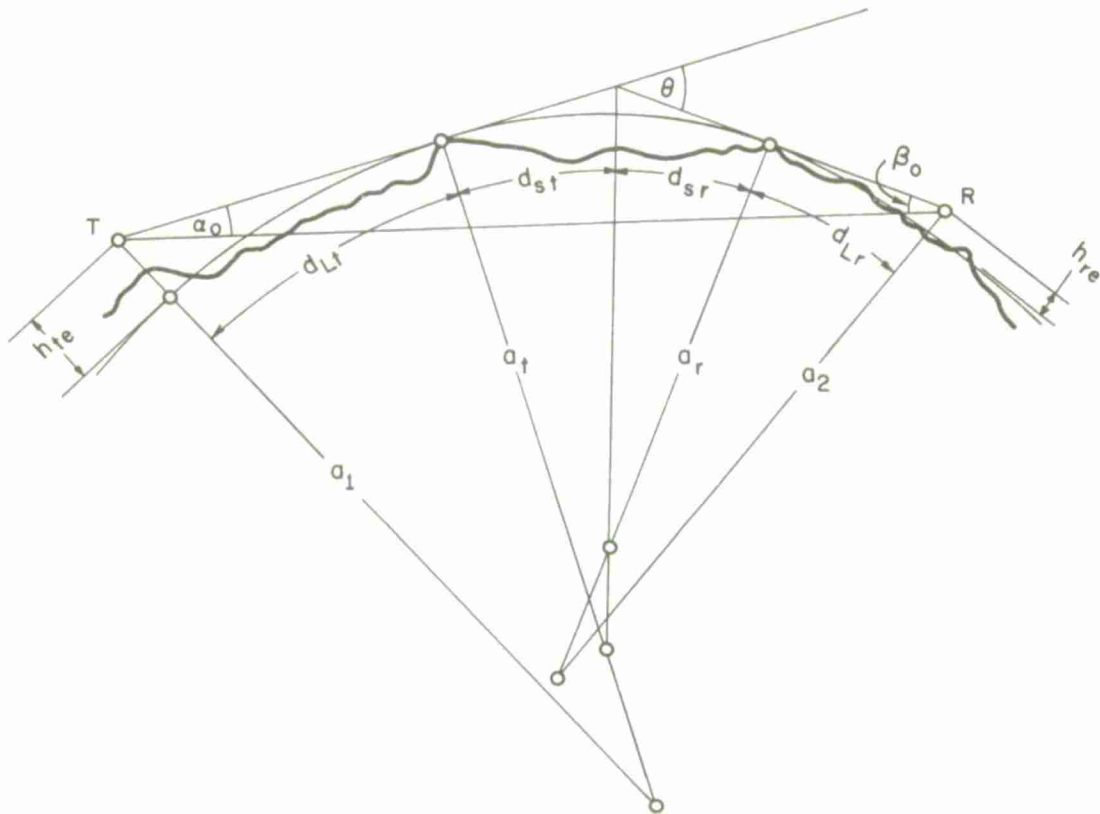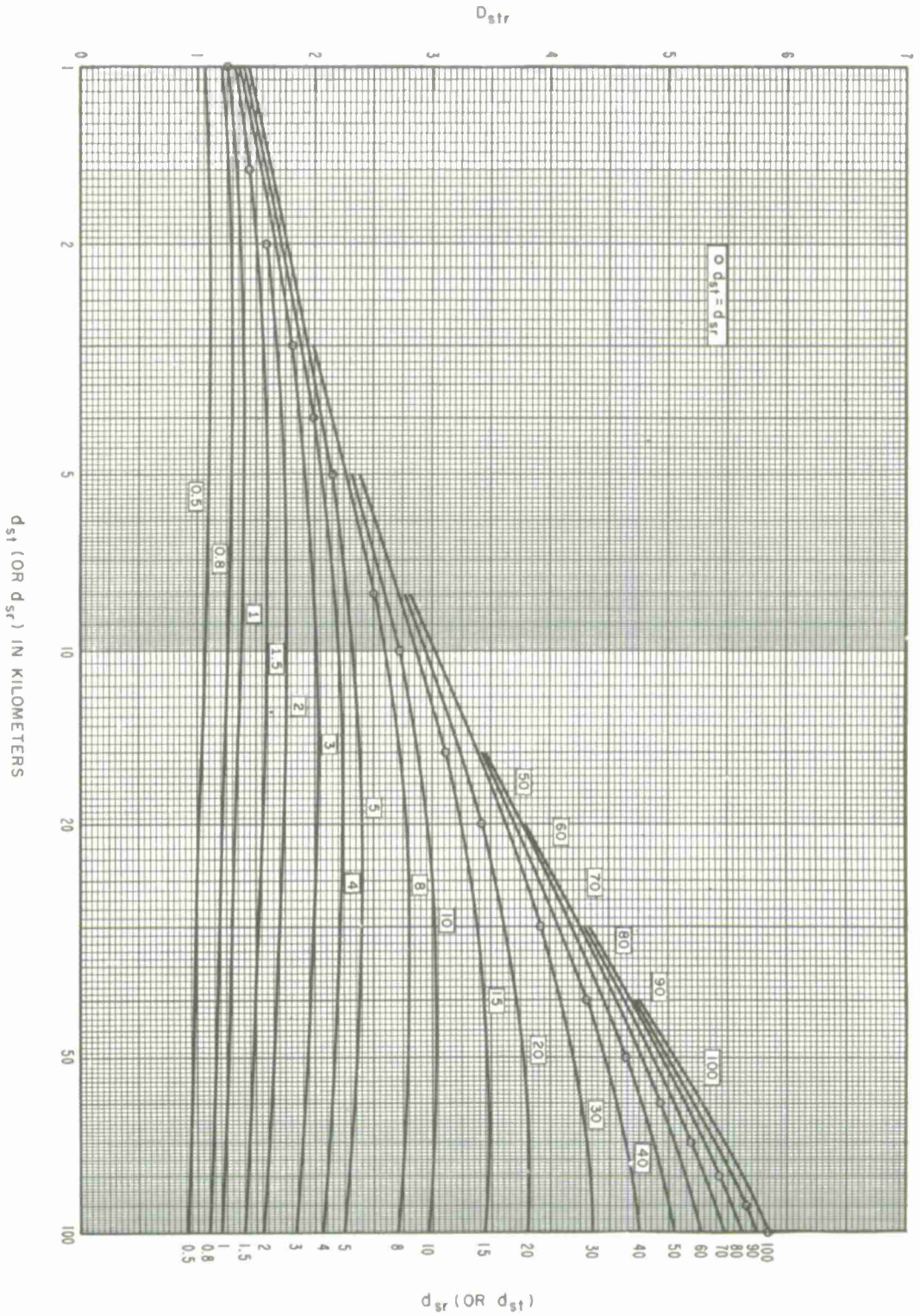
9. FORWARD SCATTER

This section gives methods for calculating reference values of long-term median radio transmission loss over paths that extend well beyond the horizon. A method is given for combining diffraction and scatter transmission loss estimates where this is appropriate. The methods of this section provide a reference median value of basic transmission loss. Empirical estimates of the median values and long-term variability of transmission loss for several climatic regions and periods of time are given in section 10 and annex III.

For long tropospheric paths the propagation mechanism is usually forward scatter, especially during times of day and seasons of the year when ducts and elevated layers are rare. Often, for other periods of time, as scattering becomes more coherent it is more properly called reflection. The examination of transmission loss variation over a particular path during some period for which detailed information about layer heights, tilts, and intensities is available can be very illuminating; see for instance Josephson and Eklund [1958]. Sometimes no distinction can be made between "forward scatter" from a turbulent atmosphere and "incoherent reflections" from patchy elevated layers. The first viewpoint is developed in papers by Pekeris [1947], Booker and Gordon [1950a, b], Megaw [1950, 1954, 1957], Millington [1958], Staras [1952, 1955], Tao [1957], Troitsky [1956, 1957a], Villars and Weisskopf [1955], Voge [1953, 1955], and Wheelon [1957, 1959], while the second viewpoint is emphasized in papers by Beckmann [1957, 1960, 1961a, b], du Castel, Misme, and Voge [1958], Friis, Crawford and Hogg [1957], Starkey, Turner, Badcoe, and Kitchen [1958], and Voge [1956, 1960]. The general prediction methods described here are for the most part consistent with either viewpoint, and agree with long-term median values for all available data. A brief discussion of forward scatter is given in Annex IV.

The reference value, L_{bsr}, of long-term median basic transmission loss due to forward scatter is

$$L_{bsr} = 30 \log f - 20 \log d + F(\theta d) - F_o + H_o + A_a \quad db \qquad (9.1)$$

For most applications the first three terms of (9.1) are sufficient for calculating L_{bsr}. In (9.1) f is the radio frequency in MHz, and d is the mean sea level arc distance in kilometers. The attenuation function $F(\theta d)$, the scattering efficiency term F_o, and the frequency gain function H_o, are discussed in the following subsections. Atmospheric absorption, A_a, defined by (3.1) and shown on figure 3.6, may be neglected at lower frequencies, but may be more than 2 db over a long path at 1000 MHz, and becomes increasingly important with increasing frequency.

For ground-based scatter links the sea level arc distance, d, and the straight line distance, r_o, between antennas are approximately equal. To estimate transmission loss between the earth and a satellite, where r_o is much greater than d, a term $20 \log(r_o/d)$

should be added to the reference value L_{bsr}.   Annex III contains a discussion of transmission loss expected when antenna beams are elevated above the horizon, or directed away from the great circle plane determined by the antenna locations.

The median forward scatter transmission loss, L_{sr}, is the basic transmission loss, L_{bsr}, minus the path antenna gain, G_p.   Section 9.4 shows how to estimate the loss in path antenna gain, L_{gp}, when there is a loss in antenna gain due to scatter. Section 9.5 shows how to combine diffraction and scatter losses. Following Arons [1956], the scattering of diffracted fields and the diffraction of scatter fields are ignored.

9.1 The Attenuation Function $F(\theta d)$

The attenuation function $F(0d)$ depends upon the most important features of the propagation path and upon the surface refractivity, N_s. The function includes a small empirical adjustment to data available in the frequency range from 100 to 1000 MHz.

For most land-based scatter links figure 9.1 may be used, where $F(\theta d)$ is plotted versus the product θd for N_s = 400, 350, 301 and 250. The path distance, d, is in kilometers and the angular distance, θ, in radians. For values of $\theta d \leq 10$ the curves of figure 9.1 are valid for all values of s. For values of θd greater than 10 the curves may be used for values of s from 0.7 to unity. For s greater than 1 use 1/s in reading the graph.

For highly asymmetrical paths with $0d > 10$, figures III.11 to III.14 of annex III are used to obtain $F(0d)$.   Annex III also contains analytical functions fitted to the curves $F(\theta d)$ for $0.7 \leq s \leq 1$ for all values of the product θd and for N_s = 250, 301, 350, and 400. Using the expressions for the function $F(\theta d)$ with N_s = 301, the reference median basic transmission loss is

For $\theta d \leq 10$:

$$L_{bsr} \cong 135.8 + 30 \log f + 30 \log \theta + 10 \log d + 0.34\, \theta d \qquad (9.2a)$$

For $10 < \theta d \leq 50$:

$$L_{bsr} \cong 131.4 + 30 \log f + 35 \log \theta + 15 \log d + 0.27\, 0d \qquad (9.2b)$$

Reference values may be computed in a similar manner for other values of N_s.

The approximations in (9.2) do not make any allowance for the frequency gain function, H_o. For usual cases of transmission at frequencies above 400 MHz the approximations in (9.2) give good results. For the higher frequencies an estimate of atmospheric absorption should be added. For lower frequencies, or low antenna heights, ground-reflected energy tends to cancel the direct ray and the approximation in (9.2) will underestimate the transmission loss.

9.2 The Frequency Gain Function, H_o

It is assumed that if antennas are sufficiently high, reflection of energy by the ground doubles the power incident on scatterers visible to both antennas, and again doubles the power scattered to the receiver. As the frequency is reduced, effective antenna heights h_{te}/λ and h_{re}/λ in wavelengths become smaller, and ground-reflected energy tends to cancel direct-ray energy at the lower part of the common volume, where scattering efficiency is greatest. The frequency gain function H_o in (9.1) is an estimate of the corresponding increase in transmission loss.

This function first decreases rapidly with increasing distance and then approaches a constant value. For $h_{te}/\lambda > 4\,a/d$ and $h_{re}/\lambda > 4\,a/d$, H_o is negligible. The upper limit of H_o as h_{te} and h_{re} approach zero is $H_o \simeq 6 + A_o$ db, where A_o is the diffraction atten-uation over a smooth earth, relative to free space, at $\theta = 0$. For frequencies up to 10 GHz. A_o may be estimated from the CCIR Atlas of Ground Wave Propagation Curves [1955, 1959]. H_o should rarely exceed 25 db except for very low antennas.

The frequency gain function, H_o, depends on effective antenna heights in terms of wave lengths, path asymmetry, and the parameter η_s shown on figure 9.2 and defined as

$$\eta_s = 0.5696\, h_o\, [\, 1 + (0.031 - 2.32\, N_s \times 10^{-3} + 5.67\, N_s^2 \times 10^{-6})\exp(-3.8\, h_o^6 \times 10^{-6})]\quad (9.3a)$$

$$h_o = s d\, \theta/(1 + s)^2\ \text{km.}\quad (9.3b)$$

The parameters r_1 and r_2 are defined as

$$r_1 = 4\pi\theta\, h_{te}/\lambda, \qquad r_2 = 4\pi\theta\, h_{re}/\lambda \quad (9.4a)$$

where θ is the angular distance in radians, and the effective antenna heights h_{te}, h_{re} are in the same units as the radio wave length, λ. In terms of frequency r_1 and r_2 may be written

$$r_1 = 41.92\,\theta\, f\, h_{te}, \qquad r_2 = 41.92\,\theta\, f\, h_{re} \quad (9.4b)$$

where θ is in radians, f in MHz, and h_{te}, h_{re} are in kilometers.

For the great majority of transhorizon paths, s is within the range $0.7 \leq s \leq 1$. The effect of very small values of s, with $\alpha_o \ll \beta_o$, may be seen in figures III.15 to III.19, which have been computed for the special case where effective transmitting and receiving an-tenna heights are equal.

a) For η_s greater than or equal to 1:

Read $H_o(r_1)$ and $H_o(r_2)$ from figure 9.3; then H_o is

$$H_o = [H_o(r_1) + H_o(r_2)]/2 + \Delta H_o \qquad (9.5)$$

where

$$\Delta H_o = 6(0.6 - \log \eta_s)\log s \log q$$

$$s = \alpha_o/\beta_o \qquad q = r_2/sr_1$$

If $\eta_s > 5$ the value of H_o for $\eta_s = 5$ is used. The correction term ΔH_o is zero for $\eta_s = 4$, $s = 1$, or $q = 1$ and reaches a maximum value, $\Delta H_o = 3.6$ db, for highly asymmetrical paths when $\eta_s = 1$. The value of ΔH_o may be computed as shown or read from the nomogram, figure 9.4. A straight line between values of s and q on their respective scales intersects the vertical line marked ①. This point of intersection when connected by a straight line to the appropriate value of η_s intersects the ΔH_o scale at the desired value.

The following limits should be applied in determining ΔH_o:

If $s \geq 10$ or $q \geq 10$, use $s = 10$ or $q = 10$.

If $s \leq 0.1$ or $q \leq 0.1$, use $s = 0.1$ or $q = 0.1$.

If $\Delta H_o \geq [H_o(r_1) + H_o(r_2)]/2$, use $H_o = H_o(r_1) + H_o(r_2)$.

If ΔH_o would make H_o negative, use $H_o = 0$.

b) For η_s less than 1:

First obtain H_o for $\eta_s = 1$ as described above, then read H_o for $\eta_s = 0$ from figure 9.5. The desired value is found by interpolation:

$$H_o(\eta_s < 1) = H_o(\eta_s = 0) + \eta_s [H_o(\eta_s = 1) - H_o(\eta_s = 0)] \qquad (9.6)$$

The case $\eta_s = 0$ corresponds to the assumption of a constant atmospheric refractive index.

A special case, $h_{te} = h_{re}$, $r_1 = r_2$, occurs frequently in systems design. For this case H_o has been plotted versus r in figures III.15 to III.19 for $\eta_s = 1, 2, 3, 4, 5$ and for $s = 0.1, 0.25, 0.5, 0.75$ and 1. For given values of η_s and s, H_o is read directly from the graphs using linear interpolation. No correction term is required. For $\eta_s < 1$ the value of $H_o(\eta_s = 1)$ is read from figure 9.3 with $r_1 = r_2$ and $H_o(\eta_s = 0)$ is read from figure 9.5 as before.

9.3 The Scattering Efficiency Correction, F_o

The correction term F_o in (9.1) allows for the reduction of scattering efficiency at great heights in the atmosphere:

$$F_o = 1.086 (\eta_s/h_o)(h_o - h_1 - h_{Lt} - h_{Lr}) \text{ db} \qquad (9.7)$$

where η_s and h_o are defined by (9.3) and h_1 is defined as

$$h_1 = s D_s \theta/(1 + s)^2, \qquad D_s = d - d_{Lt} - d_{Lr} \qquad (9.8)$$

The heights of the horizon obstacles, h_{Lt}, h_{Lr} and the horizon distances d_{Lt}, d_{Lr} are defined in section 6. All heights and distances are expressed in kilometers.

The correction term F_o exceeds 2 decibels only for distances and antenna heights so large that h_o exceeds h_1 by more than 3 kilometers.

9.4 Expected Values of Forward Scatter Multipath Coupling Loss

Methods for calculating expected values of forward scatter multipath coupling loss are given in several papers, by Rice and Daniel [1955], Booker and de Bettencourt [1955], Staras [1957], and Hartman and Wilkerson [1959]. This report uses the most general method available depending on the paper by Hartman and Wilkerson [1959].

As explained in section 2, the path antenna gain is

$$G_p = G_t + G_r - L_{gp} \quad db \qquad (9.9)$$

where G_t and G_r are free space antenna gains in decibels relative to an isotropic radiator. The influence of antenna and propagation path characteristics in determining the loss in path antenna gain or multipath coupling loss L_{gp} are interdependent and cannot be considered separately.

This section shows how to estimate only that component of the loss in path antenna gain which is due to phase incoherence of the forward scattered fields. This quantity is readily approximated from figure 9.6 as a function of η_s, defined by (9.5), and the ratio θ/Ω, where $\Omega = 2\delta$ is the effective half-power antenna beamwidth. If the antenna beamwidths are equal, $\Omega_t = \Omega_r$, and if $s = 1$, values of L_{gp} from figure 9.6 are exact. When antenna beamwidths are not equal the loss in gain may be approximated using $\Omega = \sqrt{\Omega_t \Omega_r}$.

The relation between the free-space antenna gain G in decibels relative to an isotropic radiator and the half power beamwidth $\Omega = 2\delta$ was given by (2.14) as:

$$G = 3.50 - 20 \log \delta = 9.52 - 20 \log \Omega \quad db$$

where δ and Ω are in radians.

Assuming 56% aperture efficiencies for both antennas,

$$\theta/\Omega \cong \theta(\Omega_t \Omega_r)^{-1/2} \cong 0.335\theta \exp[0.0576(G_t + G_r)] \qquad (9.10)$$

where θ is the angular distance in radians and G_t, G_r are the free space gains in decibels.

Section 2 shows that the gain for parabolic dishes with 56% aperture efficiency may be computed as (2.16):

$$G = 20 \log D + 20 \log f - 42.10 \quad db$$

where D is the diameter of the dish in meters and f is the frequency in MHz.

For dipole-fed parabolic antennas where $10 < D/\lambda < 25$, an empirical correction gives the following equation for the antenna gain (2.17):

$$G = 23.3 \log D + 23.3 \log f - 55.1 \quad db$$

The general method for calculating L_{gp} requires the following parameters:

$$\nu = \eta_s / 2, \quad \mu = \delta_r / \delta_t \tag{9.11}$$

$$\text{For } s\mu \geq 1, \ n = \alpha_o / \delta_t. \quad \text{For } s\mu \leq 1, \ n = \beta_o / \delta_r \tag{9.12a}$$

$$\hat{n} = (n + 0.03\nu)/f(\nu) \tag{9.12b}$$

$$f(\nu) = [1.36 + 0.116\nu][1 + 0.36 \exp(-0.56\nu)]^{-1} \tag{9.13}$$

where η_s, s, α_o and β_o have been defined, δ_t and δ_r are the effective half-power semi-beamwidths of the transmitting and receiving antennas, respectively, and $f(\nu)$ as defined by (9.13) is shown on figure 9.7.

Figure 9.8 shows L_{gp} versus $\hat{n}$ for various values of the product $s\mu$. For $s\mu < 1$ read figure 9.8 for $1/(s\mu)$ instead of $s\mu$.

9.5 Combination of Diffraction and Scatter Transmission Loss

For transmission paths extending only very slightly beyond line-of-sight, diffraction will be the dominant mechanism in most cases and scattering may be neglected. Conversely, for long paths, the diffracted field may be hundreds of decibels weaker than the scattered field, and thus the diffraction mechanism can be neglected. In intermediate cases, both mechanisms have to be considered and the results combined in the following manner:

Figure 9.9 shows a function, $R(0.5)$, which depends on the difference between the diffraction and scatter transmission loss. Calculate this difference $(L_{dr} - L_{sr})$ in decibels, determine $R(0.5)$ from figure 9.9 and then determine the resulting reference value of hourly median transmission loss, L_{cr}, from the relation

$$L_{cr} = L_{dr} - R(0.5) \tag{9.14}$$

If the difference between the diffracted and the scattered transmission loss values exceeds 15 db, the resulting value of L_{cr} will be equal to L_{dr} if it is smaller than L_{sr}, or to L_{sr} if this is the smaller value. In general, for most paths having an angular distance greater than 0.02 radians the diffraction calculations may be omitted; in this case, $L_{cr} = L_{sr}$.

THE ATTENUATION FUNCTION, F(θd)
d IS IN KILOMETERS AND θ IS IN RADIANS
(0.75 ≤ S ≤ 1)
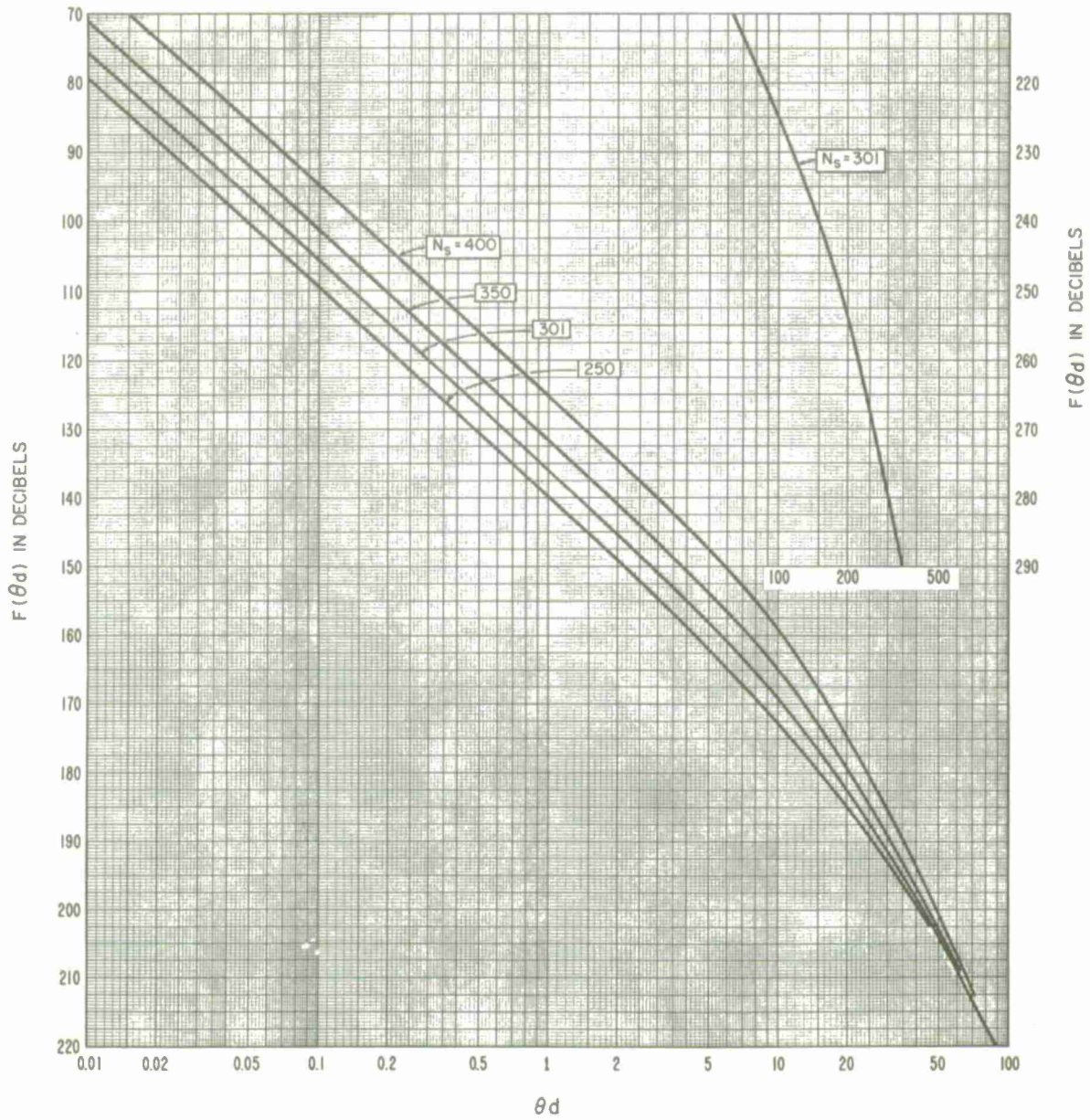
Figure 9.1

THE PARAMETER $\eta_s(h_0)$, USED TO COMPUTE H_0

$$\eta_s = 0.5696 h_0 \left[1 + (0.031 - 2.32 N_s \times 10^{-3} + 5.67 N_s^2 \times 10^{-6}) e^{-3.8 h_0^6 \times 10^{-6}} \right]$$

$$h_0 = S d\theta / (1+S)^2 \text{ km}$$

$\eta_s = 0.5696 h_0$

N_s
400
350
301
250

h_0 IN KILOMETERS
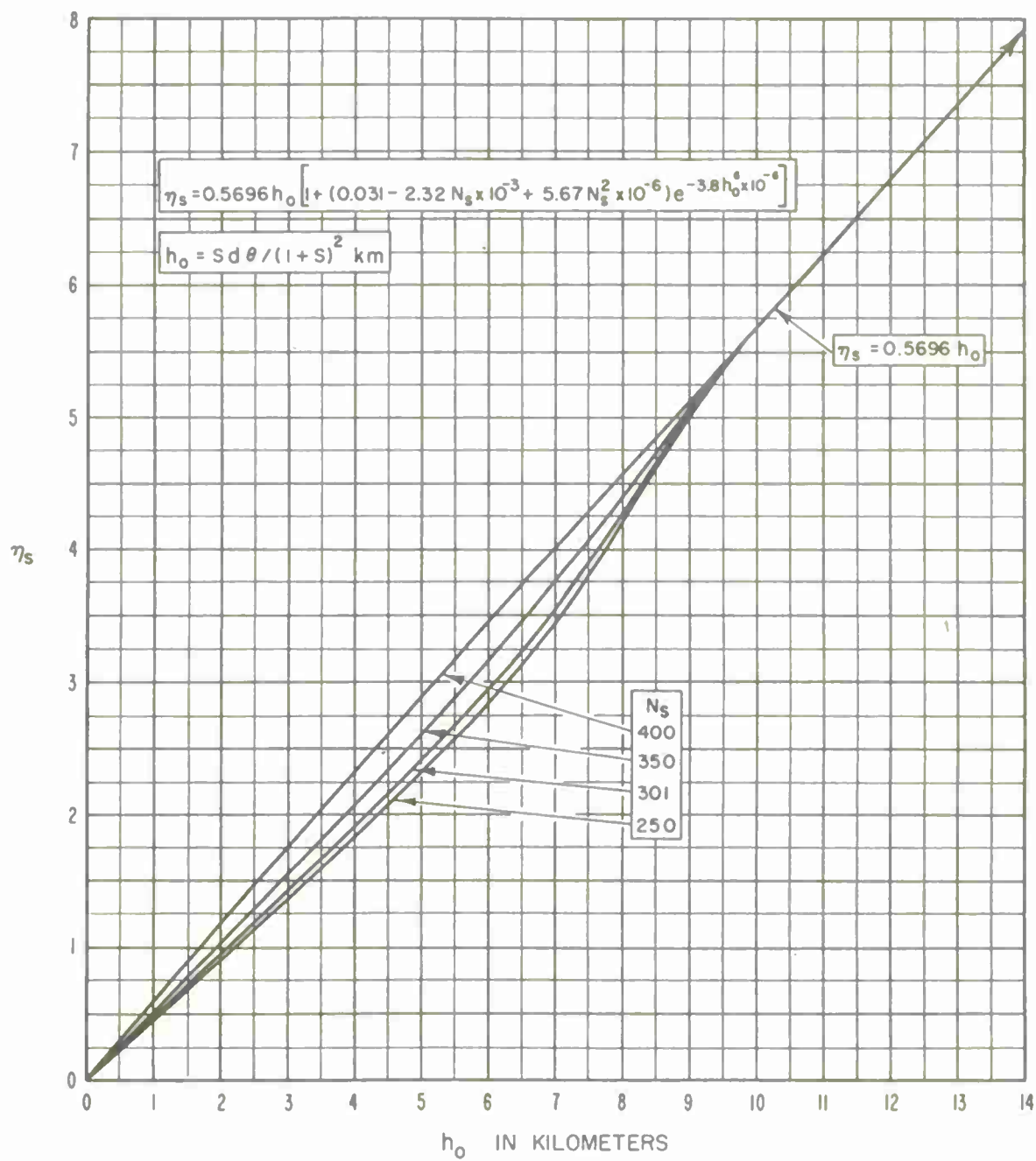
Figure 9.2

THE FREQUENCY GAIN FUNCTION, H_0
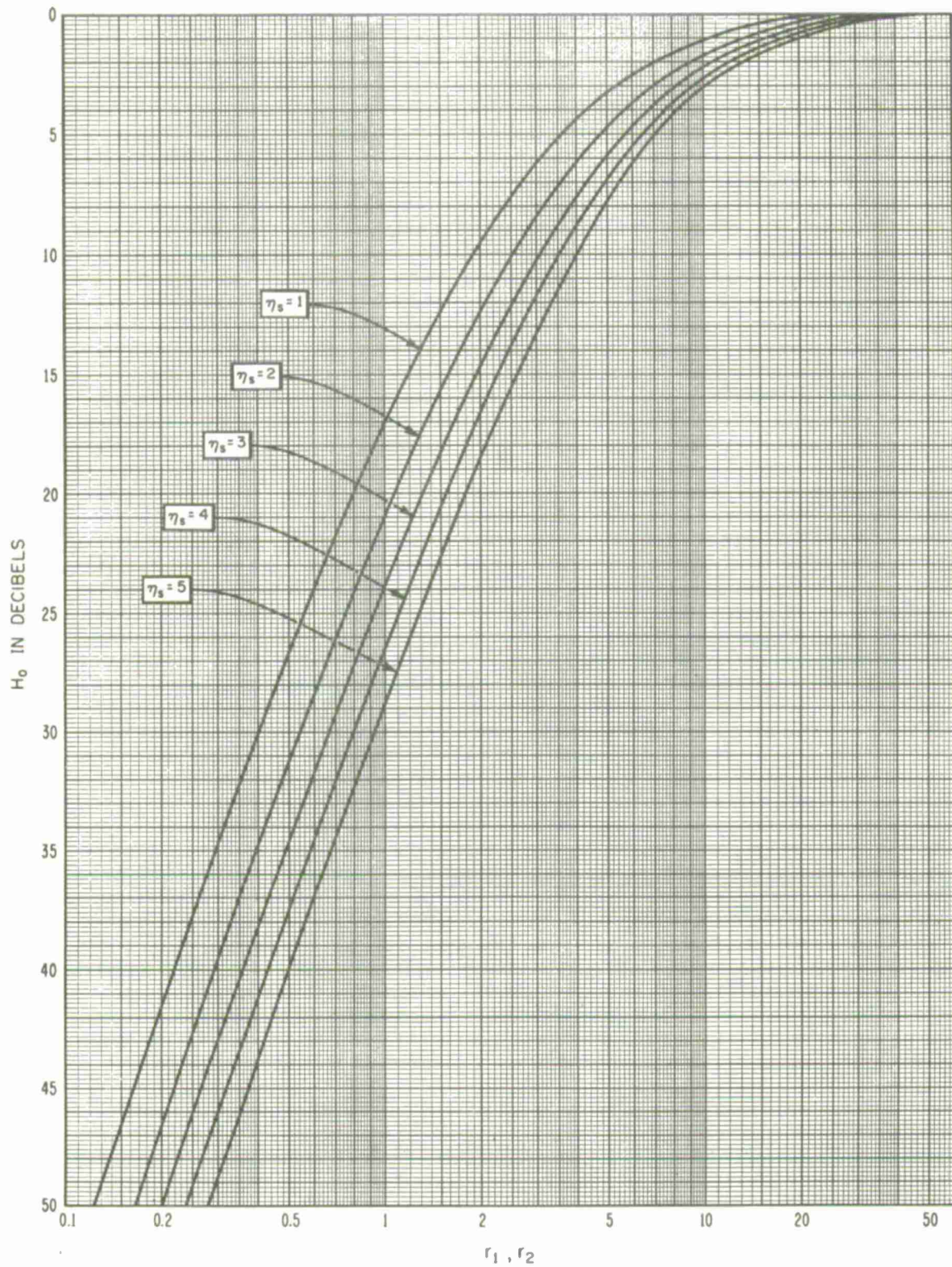
Figure 9.3

NOMOGRAM TO DETERMINE ΔH_0

$$\Delta H_0 = 6(0.6 \log \eta_s) \log s \log q$$
$$q = r_2/(s r_1), \quad s = \alpha_0/\beta_0$$
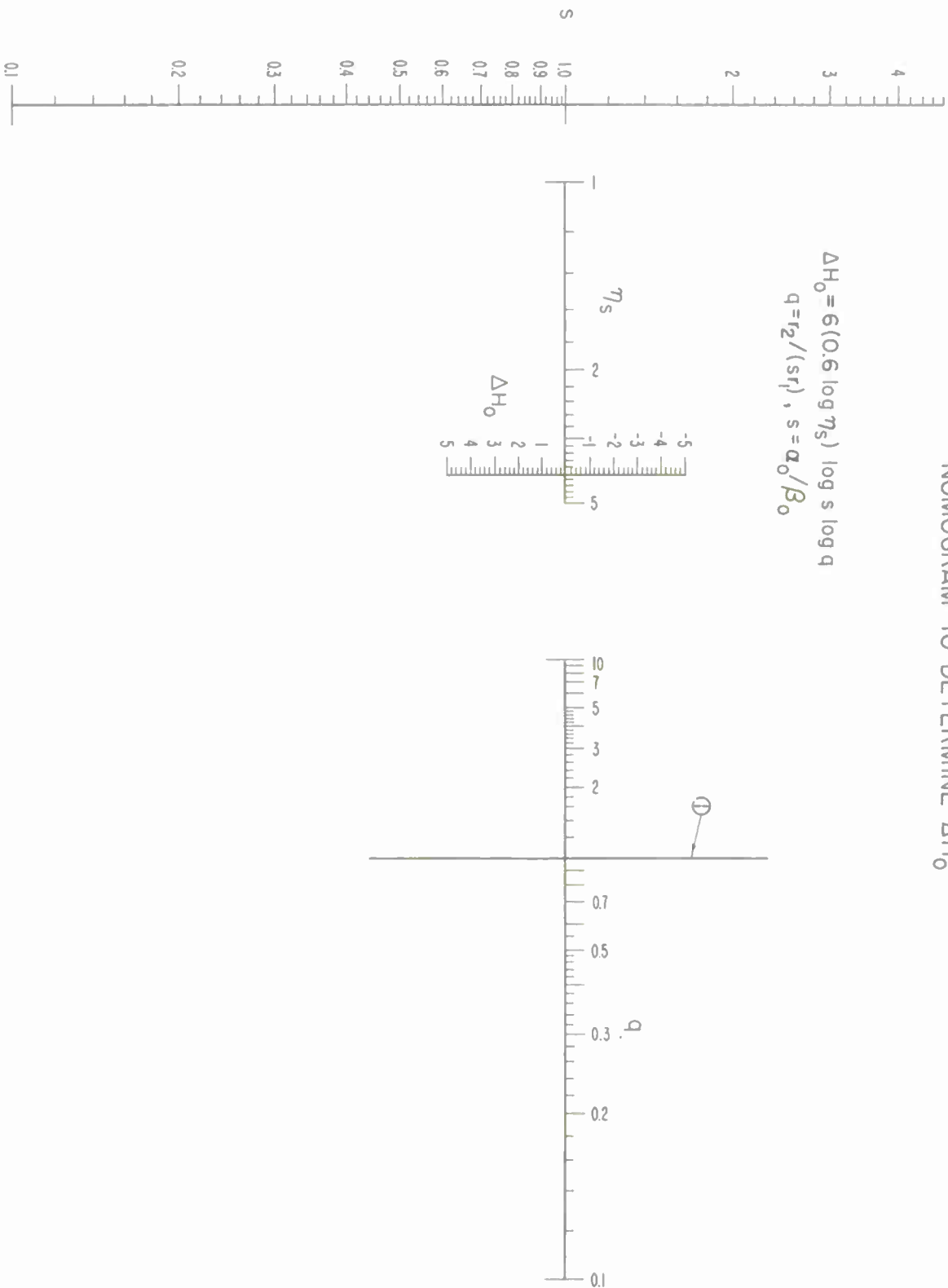
Figure 9.4

THE PARAMETER H_0 FOR $\eta_s = 0$

$(0.7 \le S \le 1)$
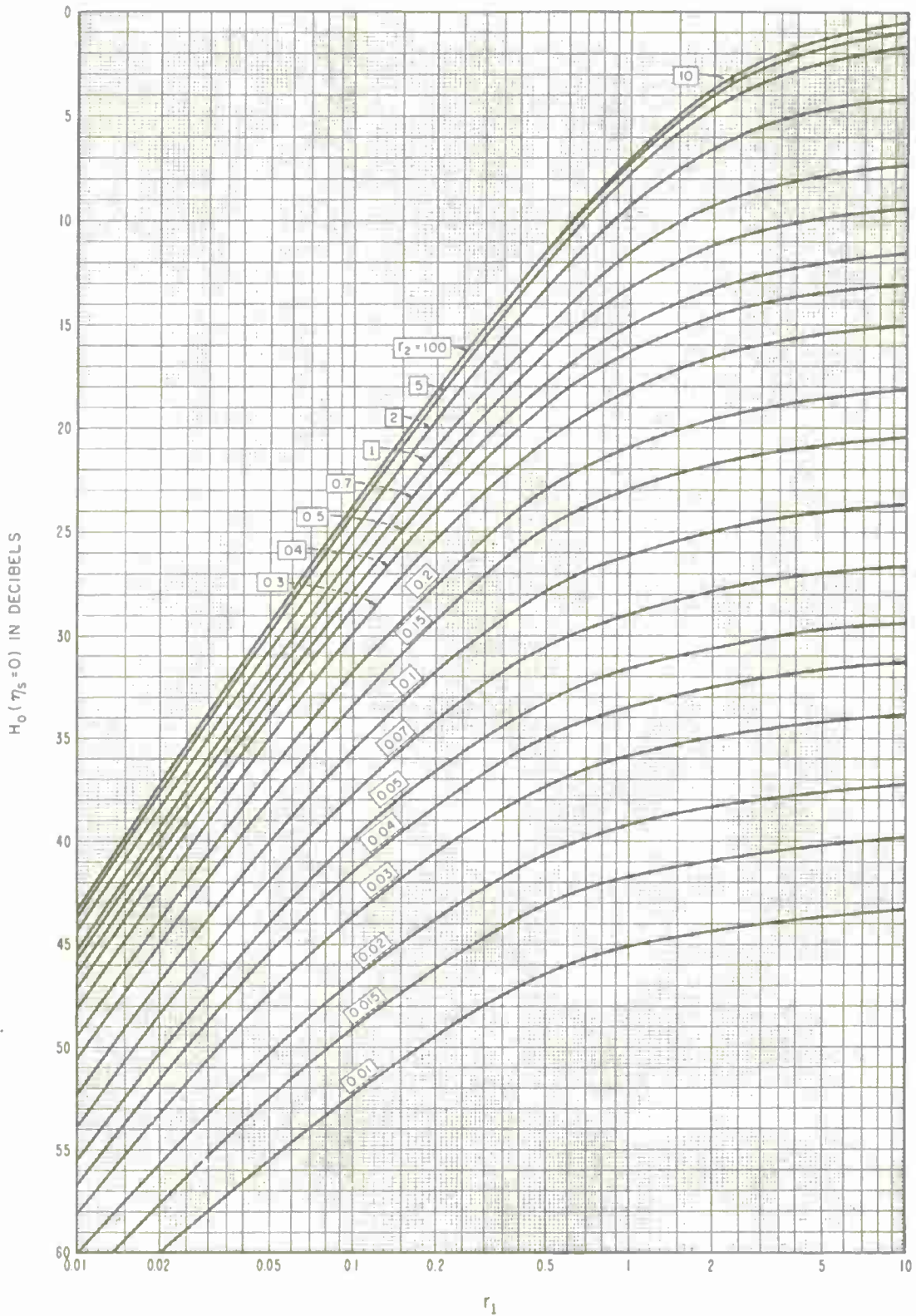
Figure 9.5

LOSS IN ANTENNA GAIN, L_{gp}
assuming equal free space gains G_t and G_r
at the terminals of a symmetrical path

$$\Omega_t = \Omega_r \quad , s=1$$

Ratio θ/Ω of angular distance θ to half-power antenna beamwidth, Ω
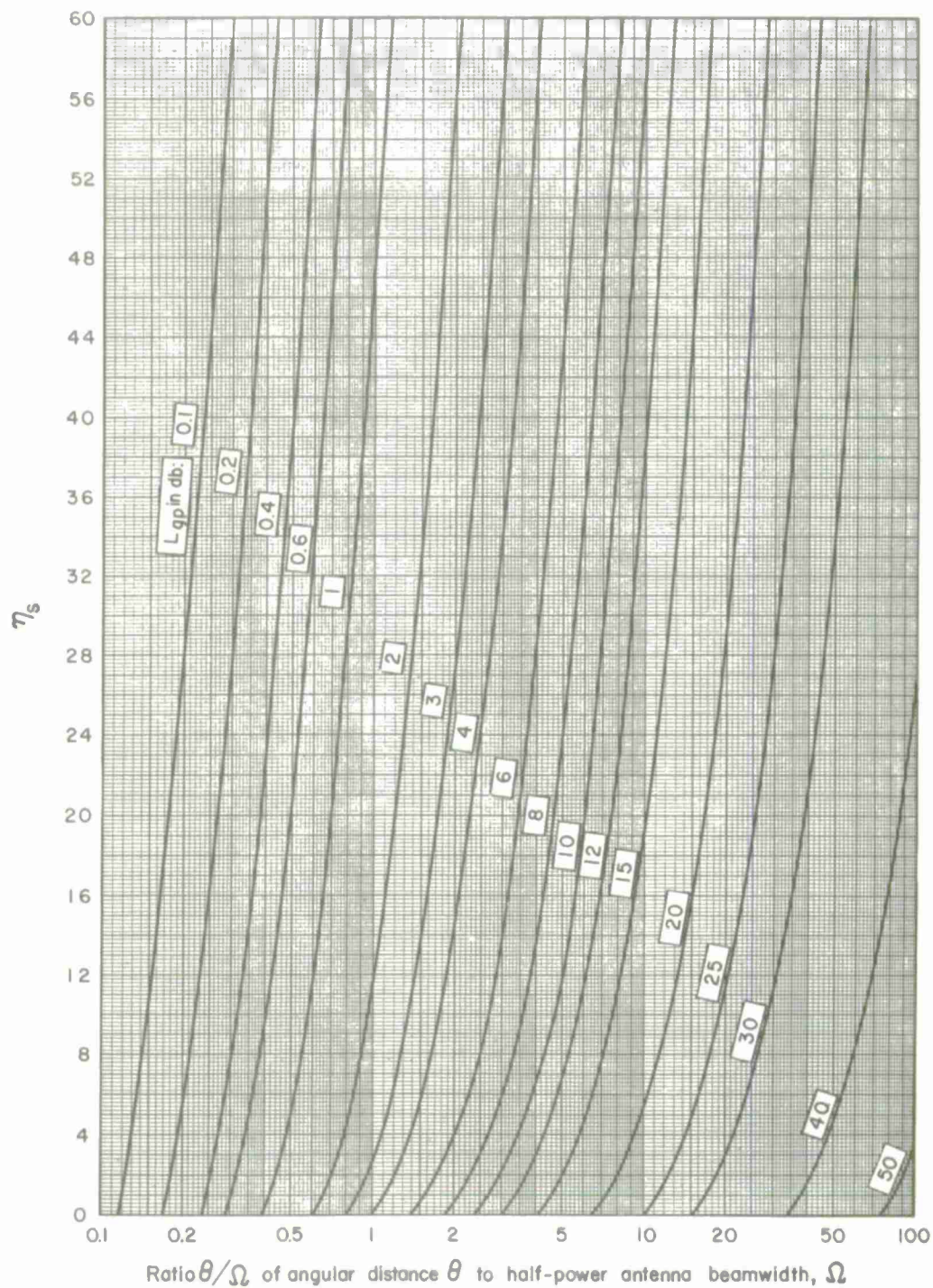
Figure 9.6

9-13

THE CONTRACTION FACTOR f(ν)

$\nu = \eta_s/2$
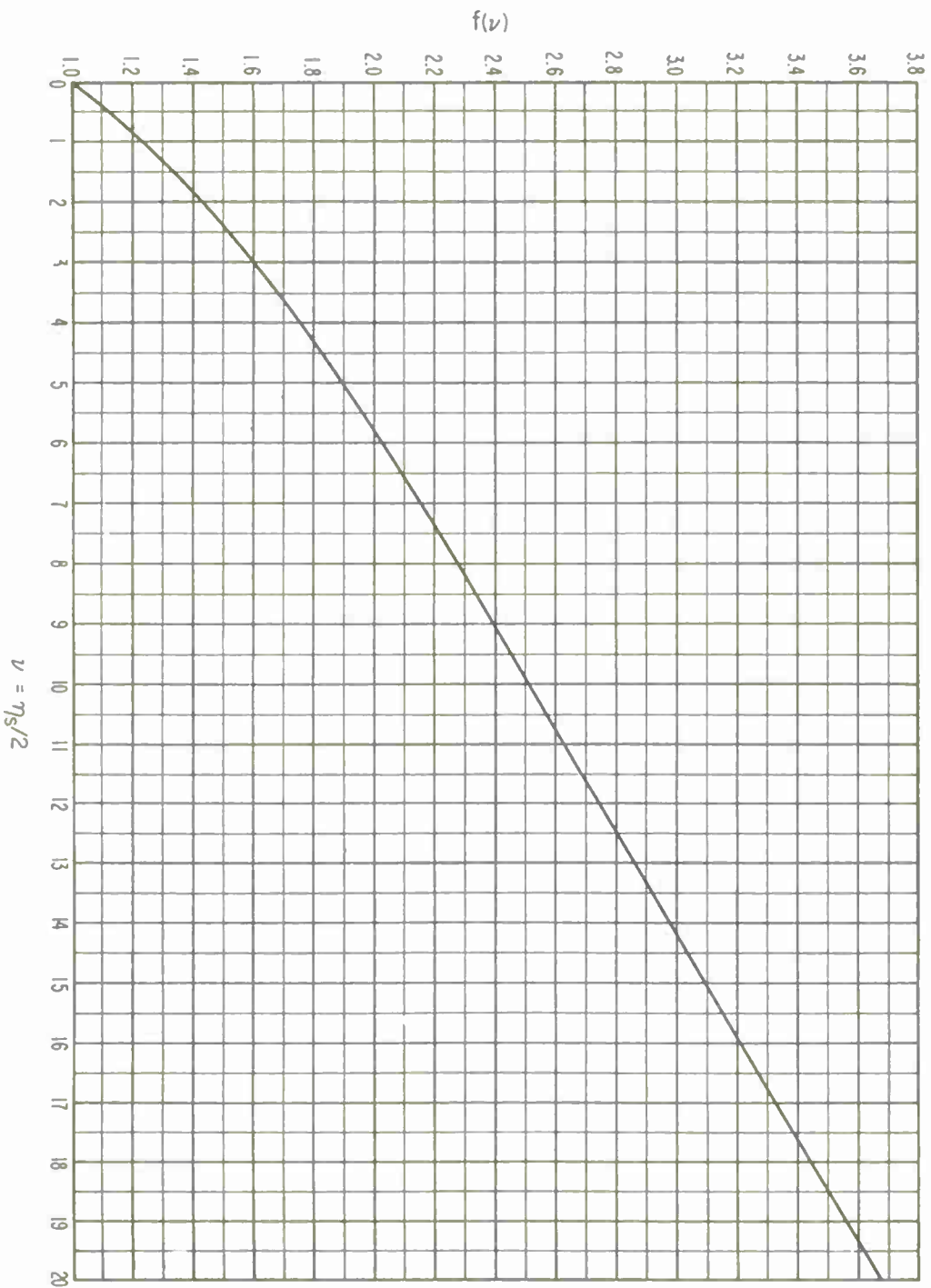
Figure 9.7

LOSS IN PATH ANTENNA GAIN vs $\hat{n}$

L_{gp} = LOSS IN PATH ANTENNA GAIN IN DECIBELS

$\hat{n}$

$s\mu = 1$
$s\mu = 2$
$s\mu = 4$
$s\mu = \infty$
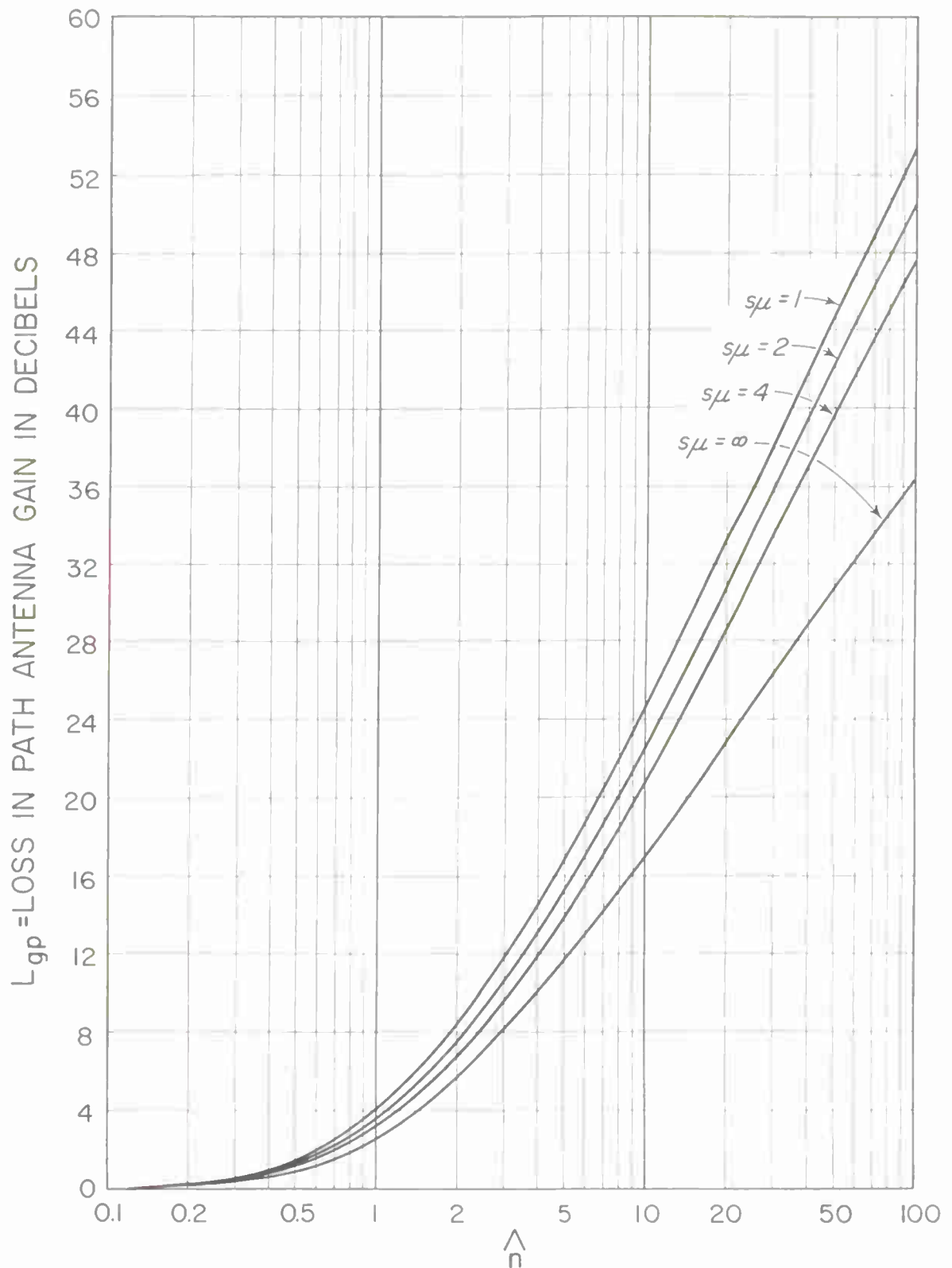
Figure 9.8
9-15

THE MEDIAN, $R_{0.5}$, FROM THE CUMULATIVE DISTRIBUTION OF THE
RESULTANT AMPLITUDE OF A CONSTANT DIFFRACTED FIELD
PLUS A RAYLEIGH DISTRIBUTED SCATTERED FIELD

$$L_{cr} = L_{dr} - R(0.5)$$

L_{dr} = BASIC TRANSMISSION LOSS CORRESPONDING TO THE DIFFRACTED FIELD.

L_{sr} = MEDIAN BASIC TRANSMISSION LOSS CORRESPONDING TO THE
RAYLEIGH DISTRIBUTED SCATTERED FIELD.

L_{cr} = MEDIAN BASIC TRANSMISSION LOSS CORRESPONDING TO THE
RESULTANT FIELD.
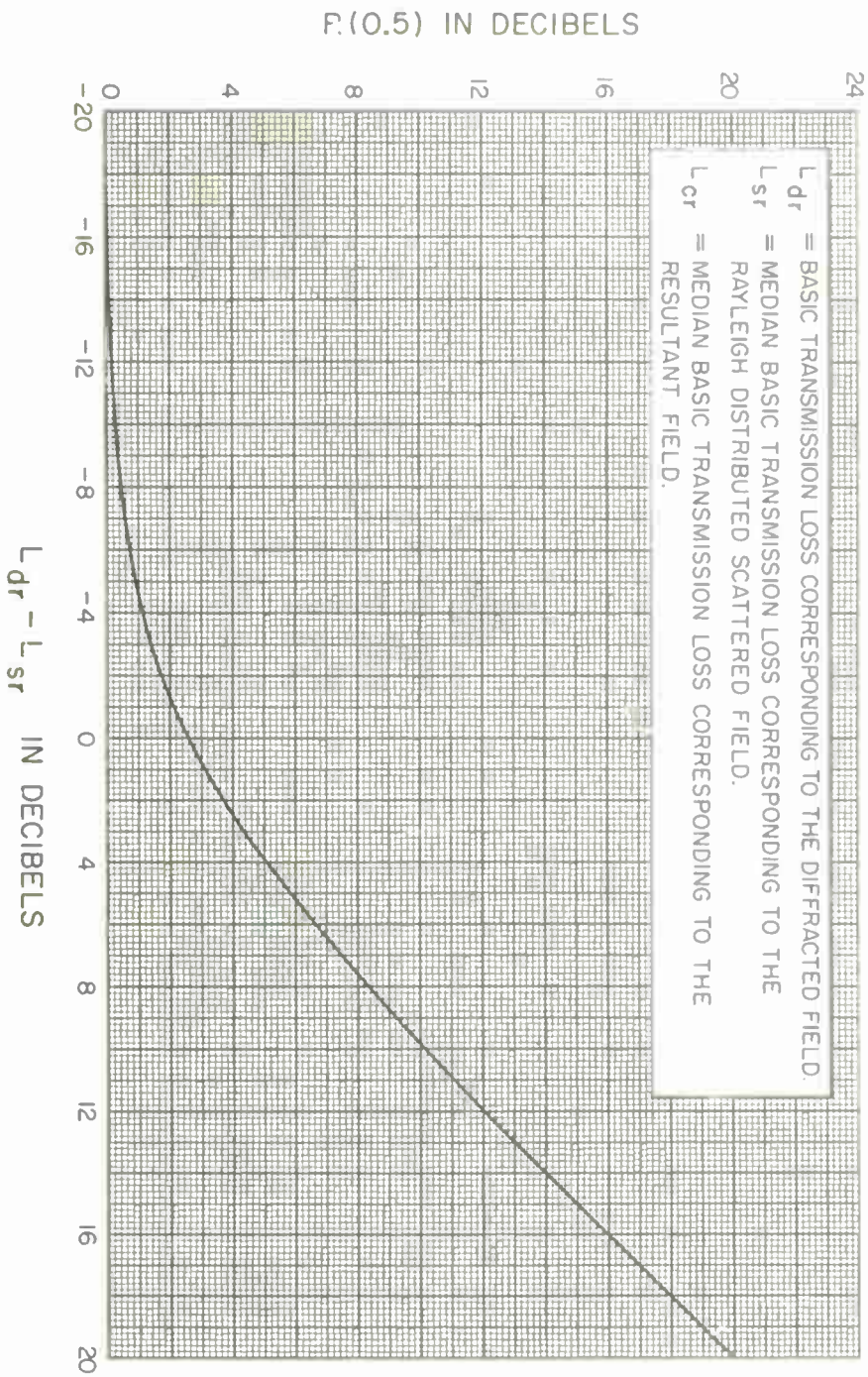
Figure 9.9

10. LONG-TERM POWER FADING

The variability of tropospheric radio transmission loss depends upon changes in the atmosphere and upon complex interrelationships between various propagation mechanisms. Short-term variability or "phase interference fading," associated with simultaneously oc- curing modes of propagation, is discussed in annex V. The effects of this type of fading ex- pected within an hour are allowed for by determining an hourly median rms-carrier-to-rms- noise ratio which defines the grade of service that will be provided. Long-term power fading, identified with the variability of hourly median values of transmission loss, is usually due to slow changes in average atmospheric refraction, in the degree of atmospheric stratification, or in the intensity of refractive index turbulence.

An estimate of the long-term power fading to be expected over a given path is impor- tant to insure adequate service over the path. The possibility that unusually high inter- fering fields may occur for an appreciable percentage of time places restrictions on ser- vices operating on the same or adjacent frequencies. The basis for the mainly empirical pre- dictions of long-term variability given here needs to be well understood in order to appreciate their value as well as their limitations.

An increase in atmospheric refraction increases long distance diffraction or forward scatter fields but may lead to multipath fading problems over short paths. Increased turbu- lence of the atmosphere may result in either an increase or a decrease of radio transmission loss depending on the geometry of a particular path and on the dominance of various propaga- tion mechanisms. Increased stratification favors propagation by reflection from elevated layers and sometimes the guiding of energy by ducts or layers. Such stratification usually increases long-distance fields but may be associated with prolonged fadeouts at short distances.

Just beyond radio line-of-sight, fading rate and fading range depend in a very complex manner on the relative importance of various propagation mechanisms. During periods of layering and ducting in the atmosphere, transmission loss shows a tendency to go into relatively deep fades, with durations from less than a minute to more than an hour. Ordinarily a dif- fraction signal fades slowly if at all, and the fades are of relatively short duration and very deep. A tropospheric forward scatter signal, on the other hand, exhibits the rapid and severe fading characteristic of the Rayleigh distribution. An intermediate type of fading results when the scattered power is nearly equal to power introduced by some mechanism such as diffrac- tion, for which the variation in time is usually very slow. Aircraft reflections introduce rapid, intense, and relatively regular fading. Meteor bursts and some types of ionospheric propagation add spikes to a paper chart record.

Space-wave fadeouts [Bean, 1954] may represent power fading due to defocusing of radio energy in some regions of space, (radio holes) accompanied by a focusing effect and

signal enhancement in other regions [Doherty, 1952; Price, 1948], or may correspond to phase interference fading phenomena. In temperate continental climates, space-wave fade-outs are likely to occur primarily at night and most frequently during the summer months; they are more frequent at UHF than at VHF, and their occurrence can be correlated with the occurrence of ground-modified refractive index profiles [Barsis and Johnson, 1962]. Such fading predominates in geographic areas where layers and ducts occur frequently. Ordinary space diversity does not appear to be helpful in overcoming this type of fading. During periods of uniform refractive-index lapse rates, prolonged fadeouts are much less intense or do not exist. Sometimes those that do exist are caused by multipath reflections which arrive in such a phase and amplitude relationship that a slight change in the lapse rate will cause a large change in the resultant field. The latter type can be overcome in most instances by either relocating the terminal antennas or by the use of space diversity.

General discussions of the time fading of VHF and UHF radio fields will be found in reports by Bullington [1950], du Castel [1957a], Chernov [1955],Grosskopf [1958], Krasil'nikov [1949], Troitski [1957b], and Ugai [1961]. Silverman [1957], discusses some of the theory of the short-term fading of scatter signals, Bremmer [1957] discusses signal distortion due to tropospheric scatter, while Beckmann [1961b] considers related depolarization phenomena.

The observed correlation of radio data with various meteorological parameters is discussed by Bean [1956, 1961], Bean and Cahoon [1957], du Castel and Misme [1957], Josephson and Blomquist [1958], Misme [1958, 1960a, b, c, 1961], Moler and Holden [1960], and Ryde [1946]. Meteorological parameters such as surface refractivity and the height gradient of refractive index have been found more useful as a basis for predicting regional changes than for predicting diurnal or seasonal variations. In this report meteorological information has been used to distinguish between climatic regions, while radio data are depended on to predict long-term variability about the computed long-term median value in each of these regions.

The basic data used in developing these estimates of long-term power fading were recorded in various parts of the world over more than a thousand propagation paths. Path distances extend from within line-of-sight to about 1000 kilometers, and frequencies range from 40 MHz to 10 GHz.

As more data are collected, particularly in regions where little information is currently available, these estimates should be re-examined and revised. Allowances should sometimes be made for predictable long-term variations in antenna gain, interference due to reflections from aircraft or satellites, and variations in equipment performance. Microwave attenuation due to rainfall, discussed in section 3, should be allowed for in estimating

the variability of transmission loss at frequencies above 5 GHz. The long-term variability of oxygen and water vapor absorption may be important above 15 GHz.

It is often desirable to specify rather precisely the conditions for which an estimate of power fading characteristics is desired. For instance, the average frequency dependence of long-term variability over a given type of profile depends critically on the relative dominance of various propagation mechanisms, and this in turn depends on climate, season, time of day, and average terrain characteristics.

Climatic regions may be defined in several different ways: (1) by geographic areas on a map, (2) by average meteorological conditions, (3) by the predominance of various propagation mechanisms or (4) by averages of available data. In various so-called "climates," at different times of day or seasons of the year, different propagation mechanisms may be dominant. For example, in a continental temperate climate the characteristics of a received signal over a given path may be quite different in the early morning hours of May than during the afternoon hours in February.

Probably the most serious obstacle to improvement of methods for predicting the characteristics of tropospheric propagation is the lack of adequate parameters for describing layers and ducts. It is important to learn how to describe atmospheric stratification well enough to predict the intensity of focusing, defocusing, and reflection as well as the percentage of time such phenomena are likely to be important for a given region, time of day or season, and radio frequency. When it becomes possible to describe the actual inhomogeneous, stratified, and turbulent atmosphere more adequately, it should also be found worthwhile to "mix" predicted cumulative distributions of transmission loss for a variety of propagation mechanisms.

Based on our current knowledge of meteorological conditions and their effects on radio propagation, the International Radio Consultative Committee[CCIR 1963f] has defined several "climates." A large amount of data is available from continental temperate and maritime temperate climates. Other climatic regions, where few data are available, are discussed in annex III. The division into climates is somewhat arbitrary, based on present knowledge of radio meteorology, and is not necessarily the same as meteorological climates [Haurwitz and Austin, 1944].

Three important effects of the atmosphere on radio propagation have been considered in defining the various climates. These are: bending of the radio rays, the effects of atmospheric turbulence, and the degree and stability of atmospheric stratification. The amount a radio ray is bent and the intensity of atmospheric turbulence are usually correlated

10-3

with the surface refractivity, N_s. The intensity and stability of various types of stratification are often not well correlated with N_s. Rather stable and extensive layers of dry warm air over relatively cool moist air tend to form ducts for VHF and UHF communication. The sharp moisture discontinuity bends the radio rays, which then tend to follow the dry-moist air interface. The phenomenon of super-refraction, associated with the occurrence of radio ducts close to the surface of the earth, is essentially a fine weather phenomenon. Inland, during fine weather, ducting is most noticeable at night. Over the sea super-refraction is most marked where the warm dry air of an adjacent land-mass is able to extend out over a comparatively cool sea. Rough terrain and high winds both tend to increase mixing in the atmosphere and consequently reduce super-refraction. Areas of divergence, usually favorable for elevated duct formation, appear to be most persistent over ocean areas from $10°$ to $40°$ north and south latitude, especially during winter months. [Moler and Holden, 1960; Randall, 1964]. Elevated ducts are usually less important for tropospheric propagation than those close to the surface.

World maps of minimum monthly mean N_o, figure 4.1, and of the annual range of monthly mean N_s, figure III.31, may be useful in deciding which climate or climates are applicable in a given region. The boundaries between various climatic regions are not well defined. In some cases it may be necessary to interpolate between the curves for two climates giving additional weight to the one whose occurrence is considered more likely.

Some important characteristics of the climatic regions for which estimates of time variability are shown, are noted below:

1. Continental Temperate characterized by an annual mean N_s of about 320 N-units with an annual range of monthly mean N_s of 20 to 40 N-units. A continental climate in a large land mass shows extremes of temperature in a "temperate" zone, such as $30°$ to $60°$ north or south latitude. Pronounced diurnal and seasonal changes in propagation are expected to occur. On the east coast of the United States the annual range of N_s may be as much as 40 to 50 N-units due to contrasting effects of arctic or tropical maritime air masses which may move into the area from the north or from the south.

2. Maritime Temperate Overland characterized by an annual mean N_s of about 320 N-units with a rather small annual range of monthly mean N_s of 20 to 30 N-units. Such climatic regions are usually located from $20°$ to $50°$ north or south latitude, near the sea, where prevailing winds, unobstructed by mountains, carry moist maritime air inland. These conditions are typical of the United Kingdom, the west coasts of North America and Europe and the northern coastal areas of Africa.

Although the islands of Japan lie within this range of latitude the climate differs in showing a much greater annual range of monthly mean N_s, about 60 N-units, the prevailing winds have traversed a large land mass, and the terrain is rugged. One would therefore not expect to find radio propagation conditions similar to those in the United Kingdom although the annual mean N_s is 310 to 320 N-units in each location. Climate 1 is probably more appropriate than climate 2 in this area. Ducting may be very important in coastal and over-sea areas of Japan.

3. <u>Maritime Temperate Oversea</u> coastal and oversea areas with the same general characteristics as those for climate 2. The distinction made is that a radio path with both horizons on the sea is considered to be an oversea path; otherwise climate 2 is used. Ducting is rather common between the United Kingdom and the European Continent, and in summer along the west coast of the United States.

4. <u>Maritime Subtropical Overland</u> characterized by an annual mean N_s of about 370 N-units with an annual range of monthly mean N_s of 30 to 60 N-units. Such climates may be found from about 10° to 30° north and south latitude, usually on lowlands near the sea with definite rainy and dry seasons. Where the land area is dry radio-ducts may be present for a considerable part of the year.

5. <u>Maritime Subtropical Oversea</u> conditions observed in coastal areas with the same range of latitude as climate 4. Typical of this climate is the northwest coast of Africa.

6. <u>Desert, Sahara</u> characterized by an annual mean N_s of about 280 N-units with year-round semiarid conditions. The annual range of monthly mean N_s may be from 20 to 80 N-units.

7. <u>Equatorial</u> maritime tropical climate with an annual mean N_s of about 360 N-units and annual range of 0 to 30 N-units. Such climates may be observed from 20° N to 20° S latitude and are characterized by monotonous heavy rains and high average summer temperatures. Typical equatorial climates occur along the Ivory Coast and in the Congo of Africa.

8. <u>Continental Subtropical</u> typified by the Sudan and monsoon climates, with an annual mean N_s of about 320 N-units and an annual range of 60 to 100 N-units. This is a hot climate with seasonal extremes of winter drought and summer rainfall, usually located from 20° to 40° N latitude.

A continental polar climate, for which no curves are shown, may also be defined. Temperatures are low to moderate all year round. The annual mean N_s is about 310 N-units with an annual range of monthly mean N_s of 10 to 40 N-units. Under polar conditions, which may occur in middle latitudes as well as in polar regions, radio propagation would be expected to show somewhat less variability than in a continental temperate climate. Long-term median values of transmission loss are expected to agree with the reference values L_{cr}.

It is difficult to predict the percentage of time that high fields due to ducting conditions may be expected to occur. Some of the better-known maritime areas of super-refraction listed by Booker [1946] are:

summer months;   a) British Isles, Atlantic coasts of France, Spain and Portugal and the Mediterrean Sea

b) Red Sea, Gulf of Aden, Persian Gulf

c) west and south coasts of Australia, New South Wales and New Zealand

d) Pacific coast of United States and Canada, Atlantic coast north of Chesapeake Bay

e) coasts of China and Japan

f) polar regions, although some sub-refraction may also be expected

all year;   a) west and southwest coast of Africa, especially marked in summer

b) west coast of India and the Bay of Bengal except during the south-west monsoon

c) northern part of the Arabian Sea, especially during the Indian hot season

d) north and northwest coasts of Australia except during the north-west monsoon

It is apparent that the most intense super-refraction is encountered in a tropical (not equa-torial) climate, in trade wind areas over the oceans, and in most of the principal deserts of the world.

High mountain areas or plateaus in a continental climate are characterized by low values of N_s and year-round semiarid conditions. The central part of Australia with its hot dry desert climate and an annual range of N_s as much as 50 to 70 N-units may be inter-mediate between climates 1 and 6.

Prediction of long-term median reference values of transmission loss, by the methods of sections 3 to 9, takes advantage of theory in allowing for the effects of path geometry and radio ray refraction in a standard atmosphere. Meteorological information is used to dis-tinguish between climatic regions. Median values of data available in each of these regions are related to the long-term reference value by means of a parameter $V(50, d_e)$ which is a function of an "effective distance," d_e, defined below. Long-term fading about the median for each climatic region is plotted in a series of figures as a function of d_e. For regions where a large amount of data is available, curves are presented that show frequency-related effects. (Seasonal and diurnal changes are given in annex III for a continental temperate climate.)

10.1 The Effective Distance, d_e

Empirical estimates of long-term power fading depend on an effective distance, d_e, which has been found superior to other parameters such as path length, angular distance, distance between actual horizons, or distance between theoretical horizons over a smooth earth. The effective distance make allowance for effective antenna heights and some allowance for frequency.

Define θ_{s1} as the angular distance where diffraction and forward scatter transmission loss are approximately equal over a smooth earth of effective radius $a = 9000$ kilometers, and define d_{s1} as $9000 \, \theta_{s1}$. Then:

$$d_{s1} = 65(100/f)^{\frac{1}{3}} \text{ km} \tag{10.1}$$

The value of d_{s1} is compared with the smooth-earth distance, d_{so}, between radio horizons:

$$d_{so} = d - 3\sqrt{2h_{te}} - 3\sqrt{2h_{re}} \text{ km} \tag{10.2}$$

where the effective antenna heights h_{te} and h_{re} are expressed in meters, the path length d in kilometers and the radio frequency f in MHz.

It has been observed that the long-term variability of hourly medians is greatest on the average for values of d_{so} only slightly greater than d_{s1}. The effective distance d_e is arbitrarily defined as:

$$d_e = 130/[1+(d_{s1}-d_{so})/d] \text{ km, for } d_{so} \leq d_{s1} \tag{10.3a}$$

$$d_e = 130 + d_{so} - d_{s1} \text{ km, for } d_{so} > d_{s1} \tag{10.3b}$$

10.2 The Functions $V(50, d_e)$ and $Y(p, d_e)$

The predicted median long-term transmission loss for a given climatic region $L_n(50)$, characterized by a subscript n, is related to the calculated long-term reference value L_{cr} by means of the function $V(50, d_e)$

$$L_n(50) = L_{cr} - V_n(50, d_e) \quad db \tag{10.4}$$

where $L_n(50)$ is the predicted transmission loss exceeded by 50 percent of all hourly medians in a given climatic region. $V_n(50, d_e)$ is shown on figure 10.1 for several climates as a function of the effective distance d_e. For the special case of forward scatter during winter afternoons in a temperate continental climate, $V(50) = 0$ and $L(50) = L_{cr}$. In all other cases, the calculated long-term reference value L_{cr} should be adjusted to the median $L_n(50)$ for the particular climatic region or time period considered. The function $F(\theta d)$ in the scatter prediction of a long-term reference median contains an empirical adjustment to data. The term $V(50, d_e)$ provides a further adjustment to data for all propagation mechanisms and for different climatic regions and periods of time.

In general, the transmission loss exceeded (100-p) percent of the time is

$$L_n(p) = L_n(50) - Y_n(p, d_e) \quad db \tag{10.5}$$

where $Y_n(p, d_e)$ is the variability of $L_n(p)$ relative to its long-term median value $L_n(50)$. For a specified climatic region and a given effective distance, the cumulative distribution of transmission loss may be obtained from (10.5). In a continental temperate climate transmission loss is often nearly log-normally distributed. The standard deviation may be as much as twenty decibels for short transhorizon paths where the mechanisms of diffraction and forward scatter are about equally important. When a propagation path in a maritime temperate climate is over water, a log-normal distribution may be expected from $L(50)$ to $L(99.9)$, but considerably higher fields are expected for small percentages of time when pronounced superrefraction and ducting are present.

10.3 Continental Temperate Climate

Data from the U.S.A., West Germany, and France provide the basis for predicting long-term power fading in a continental temperate climate. More than half a million hourly median values of basic transmission loss recorded over some two hundred paths were used in developing these estimates.

Figure 10.2 shows basic estimates $Y_o(p)$ of variability in a continental temperate climate. Curves are drawn for 10 and 90 percent of all hours of the day for summer, winter and all year for a "typical" year. In the northern temperate zone, "summer" extends from May through October and "winter" from November through April.

A "frequency factor" $g(p, f)$ shown in figure 10.3 adjusts the predicted variability to allow for frequency-related effects:

$$Y(p) = Y_o(p, d_e)g(p, f) \qquad (10.6)$$

The function $g(p, f)$ shows a marked increase in variability as frequency is increased above 100 MHz to a maximum at 400 to 500 MHz. Variability then decreases till values at 1 or 2 GHz are similar to those expected at 100 MHz. The empirical curves $g(p, f)$ should not be regarded as an estimate of the dependence of long-term variability on frequency, but represent only an average of many effects, some of which are frequency-sensitive. The apparent frequency dependence is a function of the relative dominance of various propagation mechanisms, and this in turn depends on climate, time of day, season, and the particular types of terrain profiles for which data are available. For example, a heavily forested low altitude path will usually show greater variability than that observed over a treeless high altitude prairie, and this effect is frequency sensitive. An allowance for the year-to-year variability is also included in $g(p, f)$. Data summarized by Williamson et al [1960] show that L(50) varies more from year to year than $Y(p)$. Assuming a normal distribution of L within each year and of L(50) from year to year, L would be normally distributed with a median equal to L(50) for a "typical" year. $Y(p)$ is then increased by a constant factor, which has been included in $g(p, f)$.

Estimates of Y(10) and Y(90) are obtained from figures 10.2, 10.3 and from equation 10.6). These estimates are used to obtain a predicted cumulative distribution using the following ratios:

$$Y(0.01) = 3.33\ Y(10) \qquad\qquad Y(99.99) = 2.90\ Y(90)$$
$$Y(0.1)\ \ = 2.73\ Y(10) \qquad\qquad Y(99.9)\ \ = 2.41\ Y(90) \qquad (10.7)$$
$$Y(1)\ \ \ \ \ = 2.00\ Y(10) \qquad\qquad Y(99)\ \ \ \ \ = 1.82\ Y(90)$$

For example, assume $f = 100$ MHz, $d_e = 110$ km, and a predicted reference median basic transmission loss, $L_{bcr} = 180$ db, so that $V(50, d_e) = 1.9$ db, (figure 10.1), $Y_o(10, d_e) = 8$ db, and $Y_o(90, d_e) = -5.8$ db, (figure 10.2), $g(10, f) = g(90, f) = 1.05$ (figure 10.3). Then $Y(10) = 1.05 \, Y_o(10) = 8.5$ db, and $Y(90) = 1.05 \, Y_o(90) = -6.1$ db. Using the ratios given above:

$Y(0.01) = 28.3$, $Y(0.1) = 23.2$, $Y(1) = 17.0$, $Y(10) = 8.5$,

$Y(99.99) = -17.7$, $Y(99.9) = -14.7$, $Y(99) = -11.1$, $Y(90) = -6.1$.

The median value is

$$L_b(50) = L_{bcr} - V(50) = 178.1 \text{ db}$$

and the predicted distribution of basic transmission loss is;

$L(0.01) = 149.8$, $L(0.1) = 154.9$, $L(1) = 161.1$, $L(10) = 169.6$, $L(50) = 178.1$, $L(90) = 184.2$, $L(99) = 189.2$, $L(99.9) = 192.8$ and $L(99.99) = 195.8$ db.

These values are plotted as a function of time availability, p, on figure 10.4 and show a complete predicted cumulative distribution of basic transmission loss.

For antennas elevated above the horizon, as in ground-to-air or earth-to-space communication, less variability is expected. This is allowed for by a factor $f(\theta_h)$ discussed in annex III. For transhorizon paths $f(\theta_h)$ is unity and does not affect the distribution. For line-of-sight paths $f(\theta_h)$ is nearly unity unless the angle of elevation exceeds 0.15 radians.

Allowance must sometimes be made for other sources of power fading such as attenuation due to rainfall or interference due to reflections from aircraft that may not be adequately represented in available data. For example, at microwave frequencies the distribution of water vapor, oxygen, rain, snow, clouds and fog is important in predicting long-term power fading. Let Y_1, $Y_2 - - - Y_n$ represent estimates corresponding to each of these sources of variability, and let ρ_{ij} be the correlation between variations due to sources i and j. Then the total variability is approximated as:

$$Y^2(p) = \sum_{i=1}^{m} Y_i^2(p) + 2 \sum_{\substack{i,j=1 \\ i<j}}^{m} Y_i Y_j \rho_{ij} \qquad (10.8)$$

where $Y(p)$ is positive for $p < 50$ percent, zero for $p = 50$ percent, and negative for $p > 50$ percent. Section 3 shows how to estimate $Y_a(p)$ and $Y_r(p)$ for atmospheric absorption by oxygen and water vapor, and for rain absorption respectively. Let ρ_{1a} be the correlation between variations Y of available data and variations Y_a due to microwave absorption by

oxygen and water vapor. Let ρ_{1r} be the correlation between Y and Y_r. Assuming that $\rho_{1a} = 1$, $\rho_{1r} = 0.5$, and $\rho_{ar} = 0$,

$$Y^2(p) = (Y + Y_a)^2 + Y_r^2 + Y\,Y_r \qquad (10.9)$$

This method was used to allow for the effects of rainfall at frequencies above 5 GHz, for 99 and 99.99 percent of all hours in figures I.6 to I.11 of annex I.

Figures 10.5 to 10.10 show variability, $Y(p)$ about the long-term median value as a function of d_e for period of record data in the following frequency groups; 40-88, 88-108, 108-250, 250-450, 450-1000, and > 1000 MHz. The curves on the figures show predicted values of $Y(p)$ for all hours of the year at the median frequency in each group. These medians are: 47.1, 98.7, 192.8, 417, 700, and 1500 MHz for data recorded in a continental temperate climate. Equation (10.6) and figures 10.2 and 10.3 were used to obtain the curves in figures 10.5 to 10.10.

An analytic function fitted to the curves of $V(50, d_e)$ and $Y_o(p, d_e)$ is given in annex III. Diurnal and seasonal variations are also discussed and functions listed to predict variability for several times of day and seasons.

10.4 Maritime Temperate Climate

Studies made in the United Kingdom have shown appreciable differences between propagation over land and over sea, particularly at higher frequencies. Data from maritime temperate regions were therefore classified as overland and oversea, where oversea paths are categorized as having the coastal boundaries within their radio horizons. Paths that extend over a mixture of land and sea are included with the overland paths.

The data were divided into frequency groups as follows:

Bands I and II	(40-100 MHz)
Band III	(150-250 MHz)
Bands IV and V	(450-1000 MHz).

Long-term variability of the data for each path about its long-term median value is shown as a function of effective distance in figures 10.11 to 10.16. Curves were drawn through medians of data for each percentage of time $p = 0.01, 0.1, 1, 10, 90, 99, 99.9, 99.99$. Figures 10.11 to 10.16 show that it is not practical to use a formula like (10.6) for the maritime temperate climate, because the frequency factor $g(p, f) = Y/Y_o$ is not independent of d_e, as it is in the case of the continental temperate climate. The importance of tropospheric ducting in a maritime climate is mainly responsible for this difference.

These figures demonstrate greater variability oversea than overland in all frequency groups. The very high fields noted at UHF for small percentages of time are due to persistent layers and ducts that guide the radio energy. In cases of propagation for great distances over water the fields approach free space values for small percentages of time. Curves have been drawn for those distance ranges where data permitted reasonable estimates. Each curve is solid where it is well supported by data, and is dashed for the remainder of its length.

10.5 Other Climates

A limited amount of data available from other climatic regions has been studied, [CCIR 1963f] . Curves showing predicted variability in several climatic regions are shown in annex III, figures III. 25 to III. 29.

At times it may be necessary to predict radio performance in an area where few if any measurements have been made. In such a case, estimates of variability are based on whatever is known about the meteorological conditions in the area, and their effects on radio propagation, together with results of studies in other climatic regions. If a small amount of radio data is available, this may be compared with predicted cumulative distributions of transmission loss corresponding to somewhat similar meteorological conditions. In this way estimates for relatively unknown areas may be extrapolated from what is known.

10.6 Variability for Knife-Edge Diffraction Paths

The variability of hourly medians for knife-edge diffraction paths can be estimated by considering the path as consisting of two line-of-sight paths in tandem. The diffracting knife-edge then constitutes a common terminal for both line-of-sight paths. The variability of hourly median transmission loss for each of the paths is computed by the methods of this section and characterized by the variability functions

$$V_1(p) = V_1(50) + Y_1(p) \quad db$$

$$V_2(p) = V_2(50) + Y_2(p) \quad db$$

During any particular hour, the total variability function V for the diffraction path would be expected to be the sum of V_1 plus V_2. To obtain the cumulative distribution of all values of V applicable to the total path a convolution of the individual variables V_1 and V_2 may be employed [Davenport and Root, 1958].

Assuming that V_1 and V_2 are statistically independent variables, their convolution is the cumulative distribution of the variable $V = V_1 + V_2$. The cumulative distribution of V may be obtained by selecting n equally-spaced percentage values from the individual distributions of $V_1(p)$ and $V_2(p)$ calculating all possible sums $V_k = V_{1i} + V_{2j}$ and forming the cumulative distribution of all values V_k obtained in this manner.

Another method of convolution that gives good results requires the calculation and ordering of only n, instead of n^2, values of V. As before $V_1(p)$ and $V_2(p)$ are obtained for n equally spaced percentages. Then one set is randomly ordered compared to the other so that the n sums $V = V_1 + V_2$ are randomly ordered. The cumulative distribution of these sums then provides the desired convolution of V_1 and V_2. If the distribution of $V_1 - V_2$ is desired this is the convolution of V_1 and $-V_2$.

THE FUNCTION V(50, d_e) FOR 8 CLIMATIC REGIONS

$L(50) = L_{cr} - V(50, d_e)$ db

V(50, d_e) IN DECIBELS

d_e IN KILOMETERS

CLIMATES

1. CONTINENTAL TEMPERATE
2. MARITIME TEMPERATE OVERLAND
3. MARITIME TEMPERATE OVERSEA
4. MARITIME SUBTROPICAL OVERLAND

5. MARITIME SUBTROPICAL OVERSEA
6. DESERT, SAHARA
7. EQUATORIAL
8. CONTINENTAL SUBTROPICAL

Figure 10.1

10-14
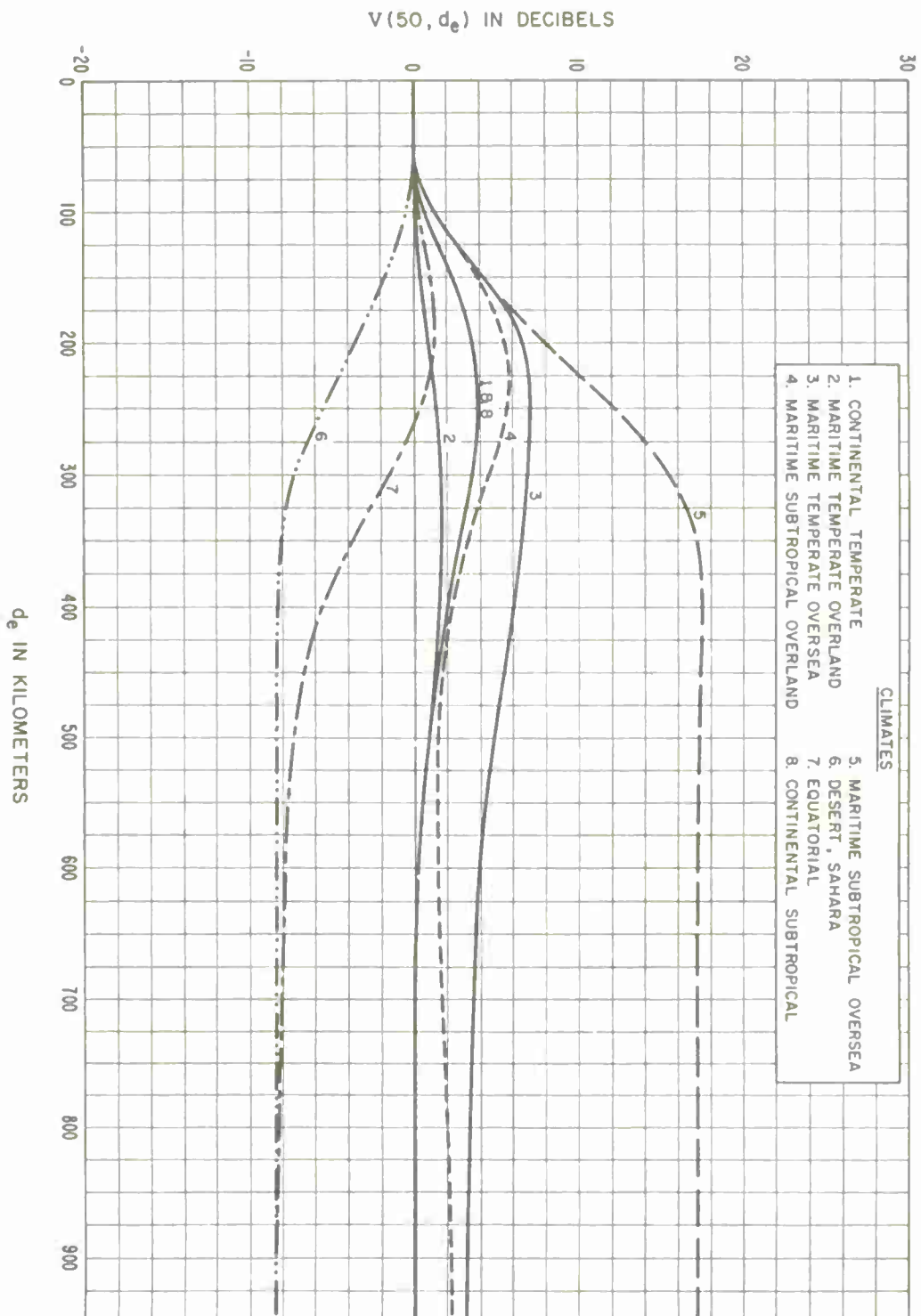
LONG-TERM POWER-FADING FUNCTION Y_0
CONTINENTAL TEMPERATE CLIMATE

Figure 10.2

EQUIVALENT DISTANCE, d_e, IN KILOMETERS

$Y_0(90, d_e)$ IN db

$Y_0(10, d_e)$ IN db

SUMMER

ALL HOURS

WINTER

WINTER

SUMMER AND ALL HOURS

$Y_0(90)$

$Y_0(10)$
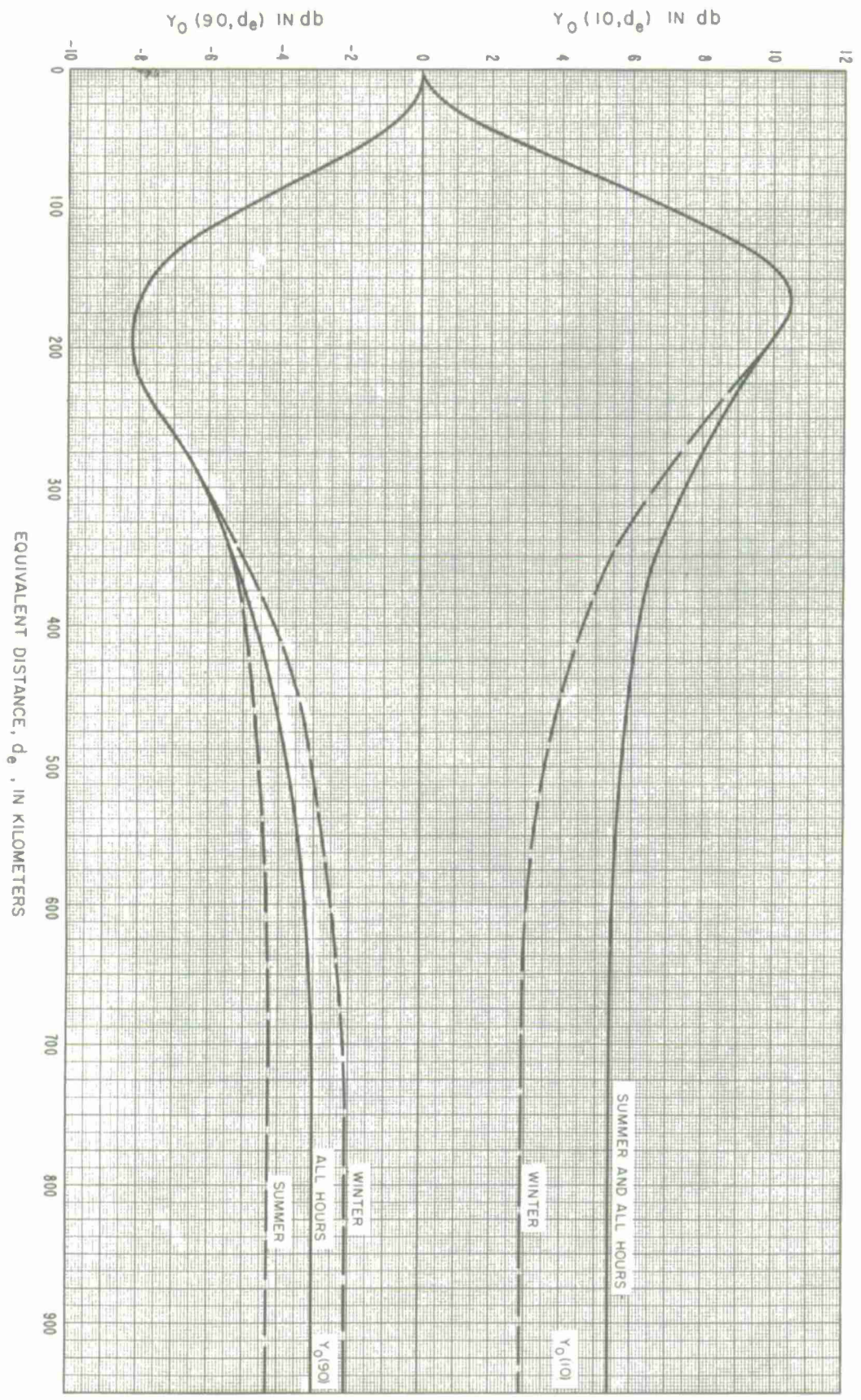
POWER FADING ADJUSTMENT FACTOR g(p,f)
BASED ON U.S. OVERLAND DATA
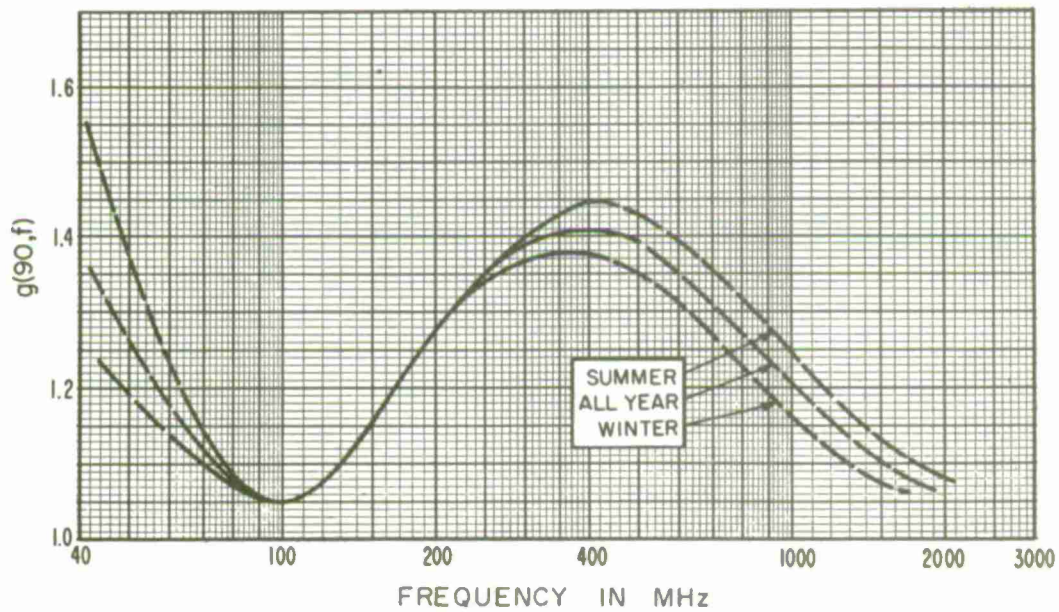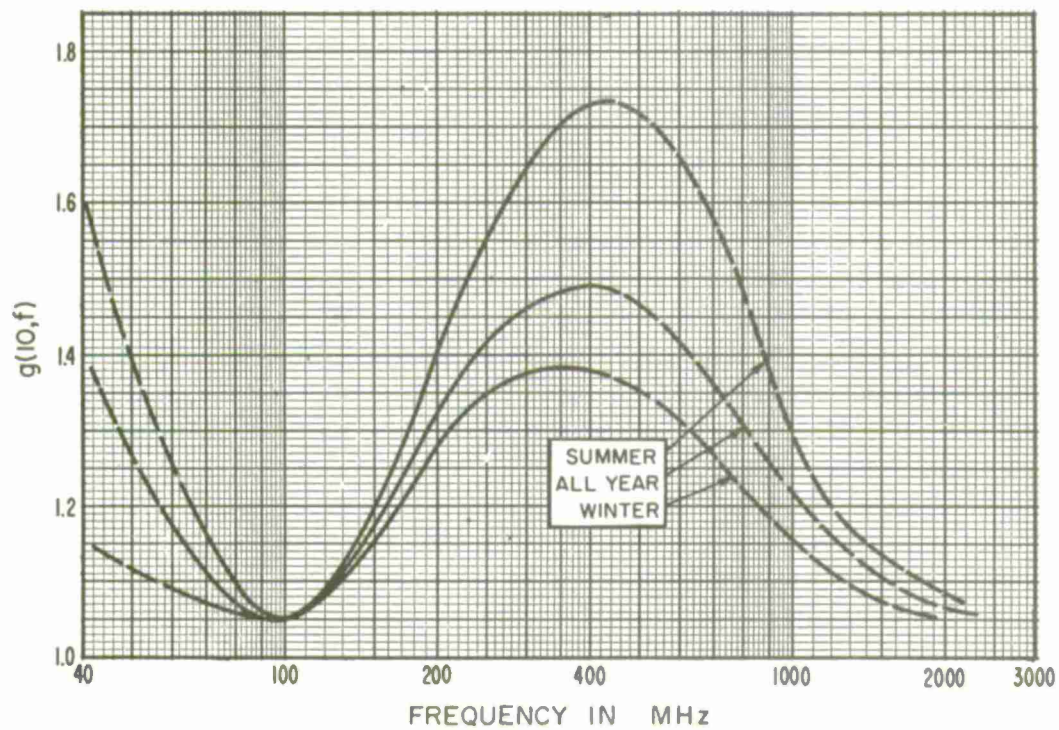
Figure 10.3

EXAMPLE OF A CUMULATIVE DISTRIBUTION $L_b(p)$ VERSUS p
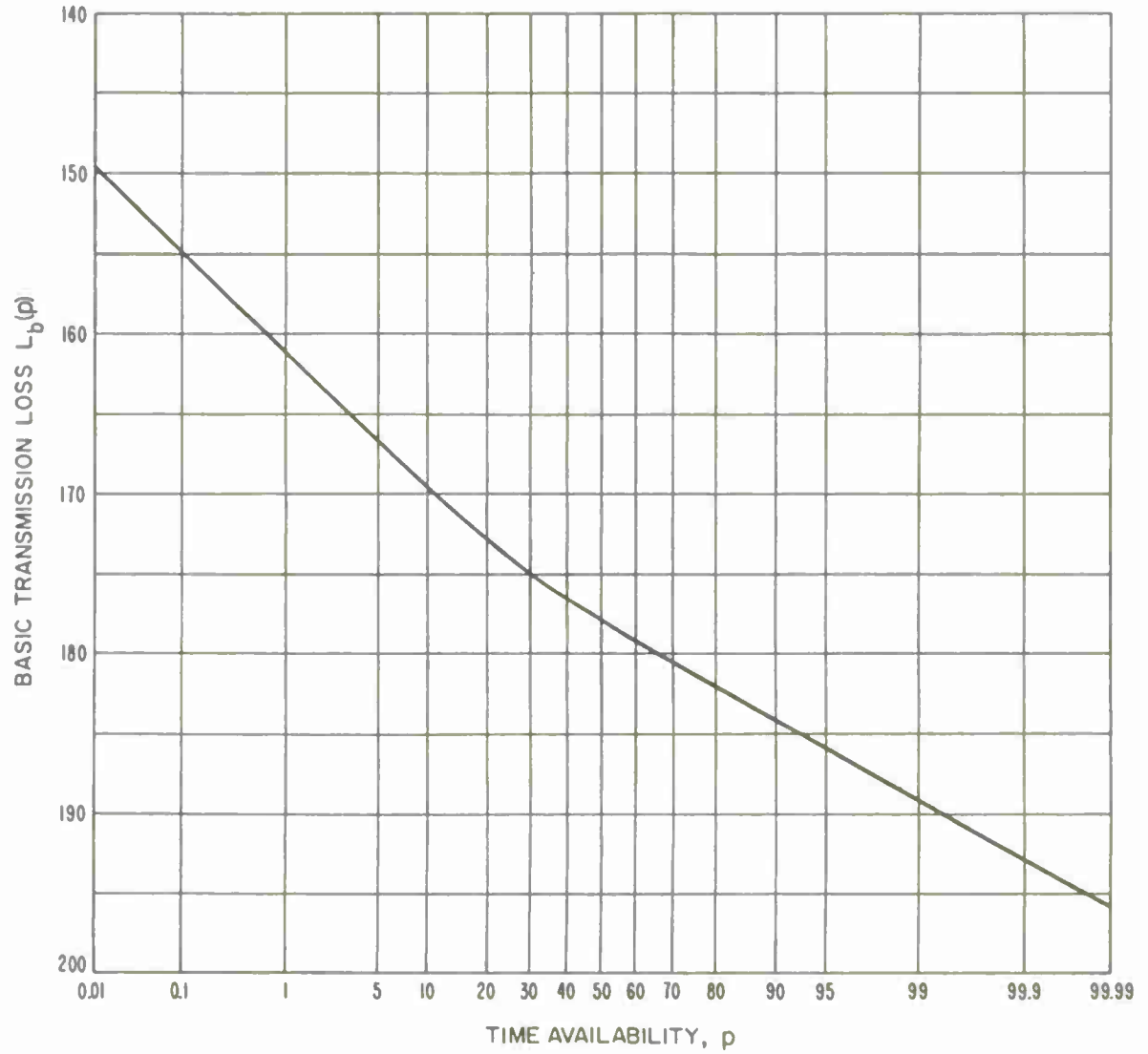
Figure 10.4

LONG-TERM POWER FADING
CONTINENTAL TEMPERATE CLIMATE, 40 - 88 MHz

Y(p) = VARIABILITY ABOUT THE LONG-TERM MEDIAN, IN DECIBELS

EFFECTIVE DISTANCE, d_e, IN KILOMETERS

Figure 10.5

DATA FROM CONTINENTAL U.S.A.
MEDIAN FREQUENCY = 47.1 MHz

•	Y(0.01),	Y(99.99)
▲	Y(0.1) ,	Y(99.9)
×	Y(1) ,	Y(99)
○	Y(10) ,	Y(90)

CURVES SHOW PREDICTED VALUES OF Y(p)

Y(0.01) = 3.33 Y(10)   Y(99.99) = 2.90 Y(90)
Y(0.1) = 2.73 Y(10)   Y(99.9) = 2.41 Y(90)
Y(1) = 2.00 Y(10)   Y(99) = 1.82 Y(90)
Y(10) = 1.30 Y_0(10, d_e)   Y(90) = 1.29 Y_0(90, d_e)
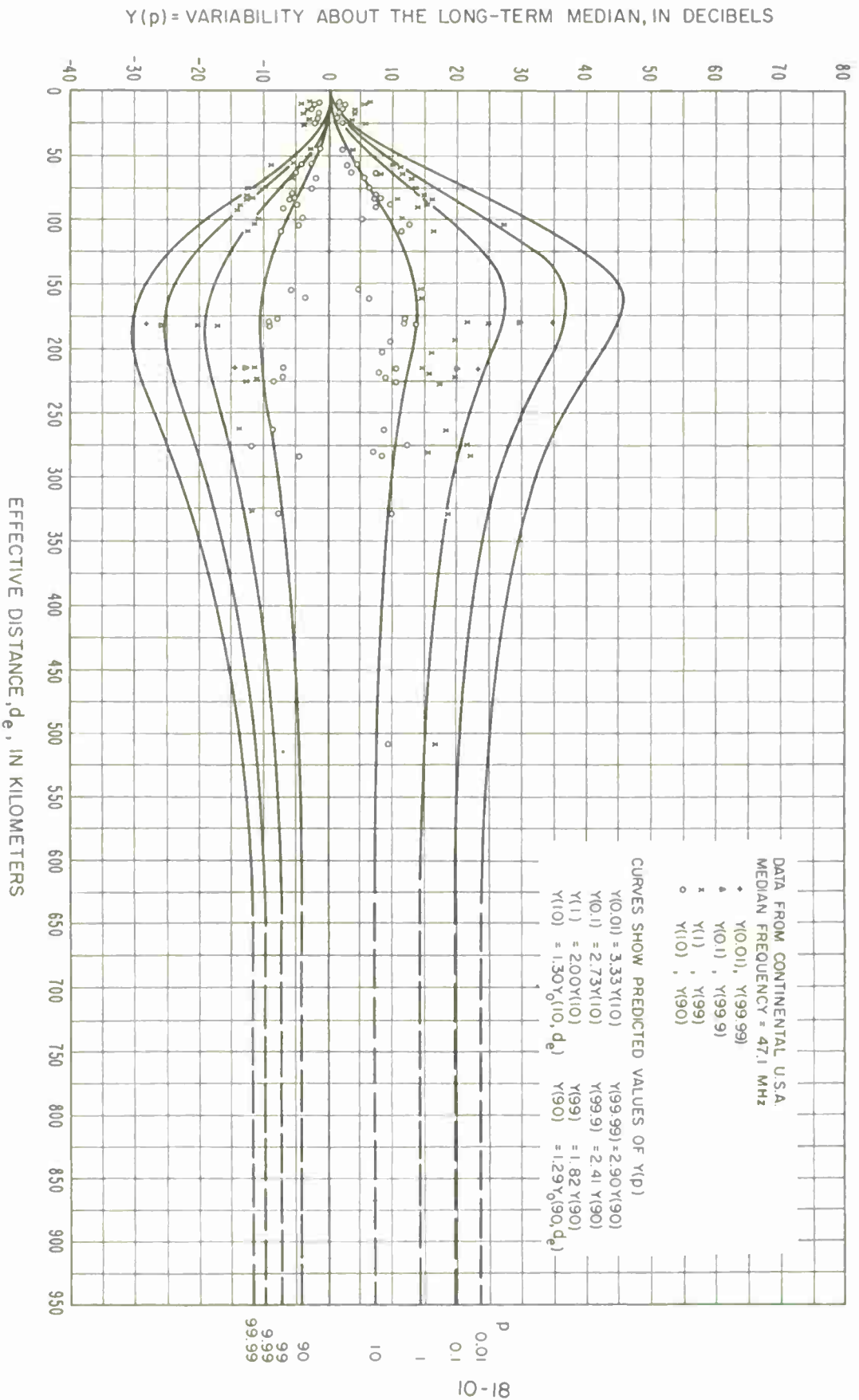
LONG–TERM POWER FADING
CONTINENTAL TEMPERATE CLIMATE, 88–108 MHz

Y(p) = VARIABILITY ABOUT THE LONG–TERM MEDIAN, IN DECIBELS

EFFECTIVE DISTANCE, d$_e$, IN KILOMETERS

Figure 10.6

DATA FROM CONTINENTAL U.S.A.
MEDIAN FREQUENCY = 98.7 MHz

- + Y(0.01), Y(99.99)
- ▲ Y(0.1) , Y(99.9)
- ✕ Y(1) , Y(99)
- ○ Y(10) , Y(90)

CURVES SHOW PREDICTED VALUES OF Y(p)

Y(0.01) = 3.33 Y(10)   Y(99.99) = 2.90 Y(90)
Y(0.1) = 2.73 Y(10)   Y(99.9) = 2.41 Y(90)
Y(1) = 2.00 Y(10)   Y(99) = 1.82 Y(90)
Y(10) = 1.05 Y$_o$(10, d$_e$)   Y(90) = 1.05 Y$_o$(10, d$_e$)
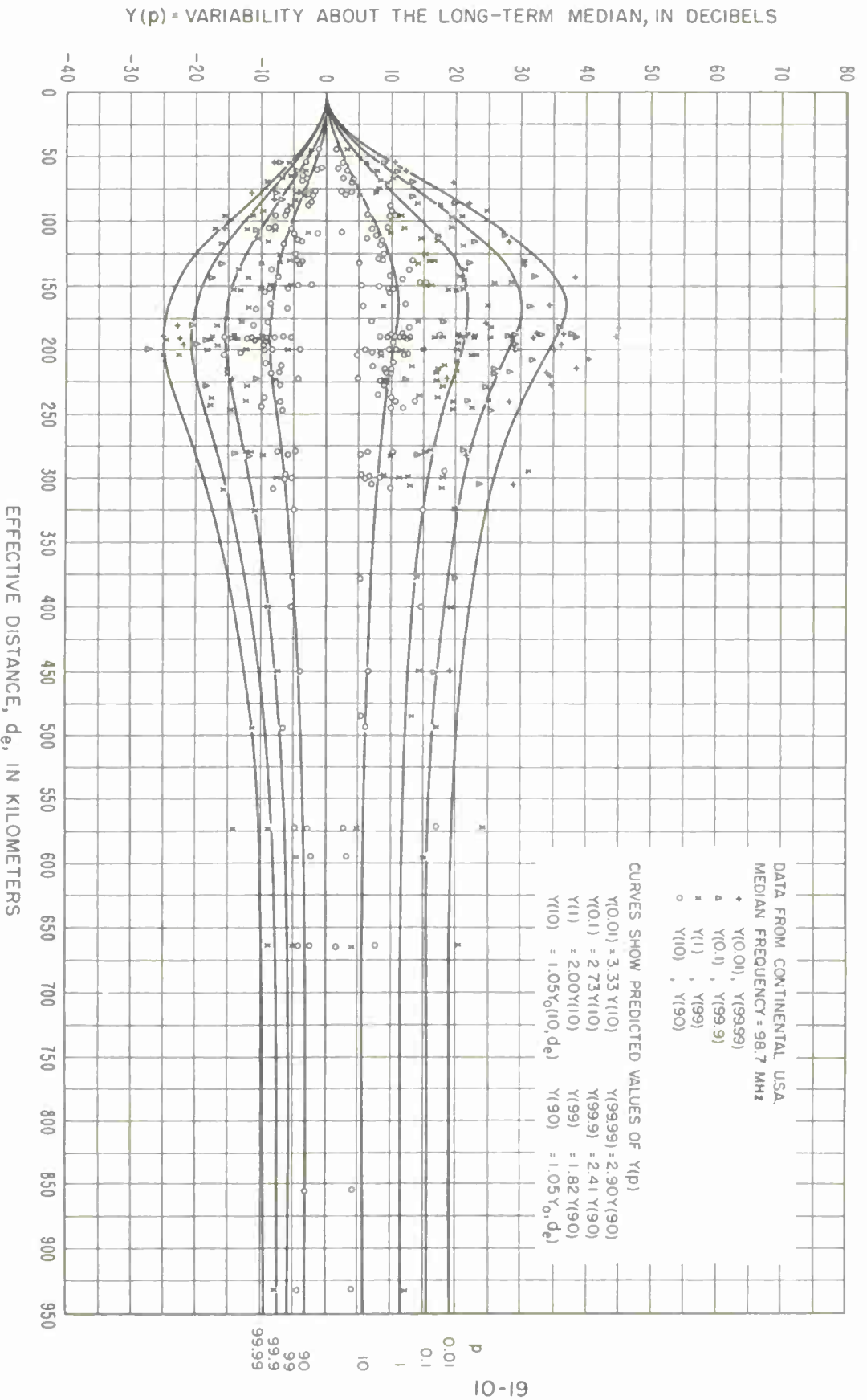
LONG-TERM POWER FADING
CONTINENTAL TEMPERATE CLIMATE, 108-250 MHz

Y(p) = VARIABILITY ABOUT THE LONG-TERM MEDIAN, IN DECIBELS

EFFECTIVE DISTANCE, d_e, IN KILOMETERS

Figure 10.7

DATA FROM CONTINENTAL U.S.A.
MEDIAN FREQUENCY = 192.8 MHz

+ Y(0.01), Y(99.99)
▲ Y(0.1), Y(99.9)
x Y(1) , Y(99)
○ Y(10) , Y(90)

CURVES SHOW PREDICTED VALUES OF Y(p)

Y(0.01) = 3.33 Y(10)   Y(99.99) = 2.90Y(90)
Y(0.1) = 2.73Y(10)   Y(99.9) = 2.41 Y(90)
Y(1) = 2.00Y(10)   Y(99) = 1.82 Y(90)
Y(10) = 1.30Y_0(10, d_e)   Y(90) = 1.26Y_0(90,d_e)

10-20
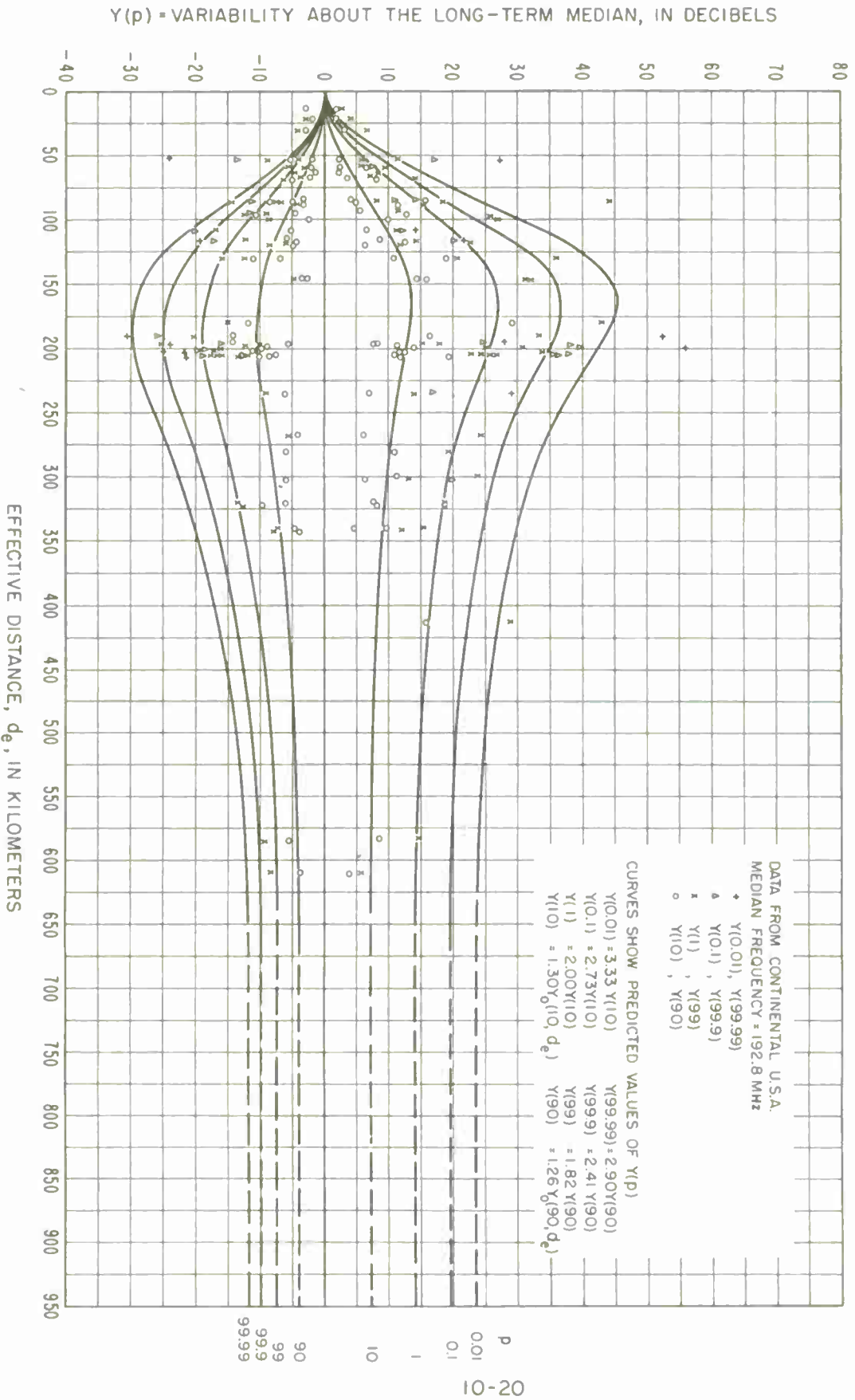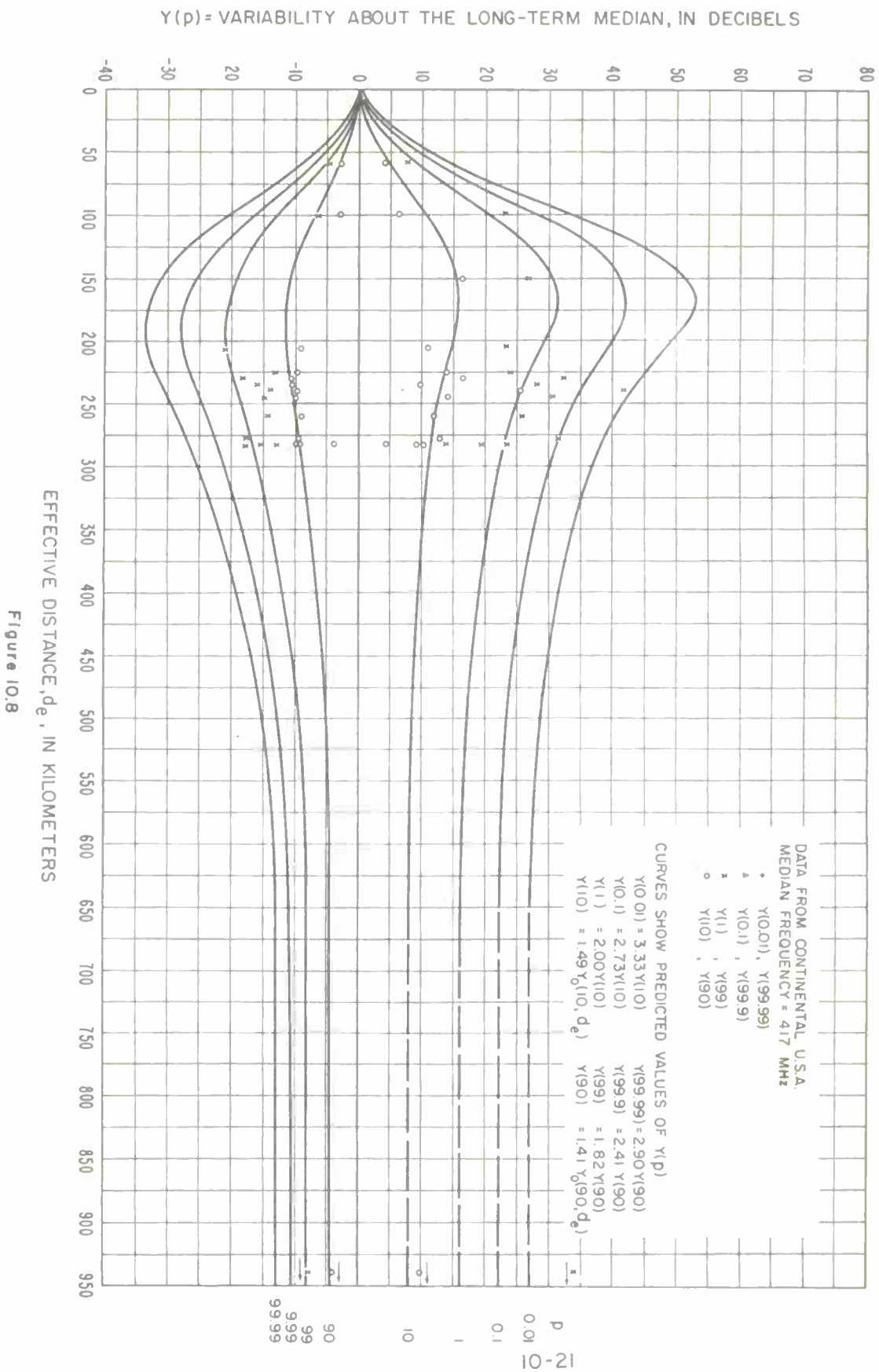
LONG-TERM POWER FADING
CONTINENTAL TEMPERATE CLIMATE, 250-450 MHz

Y(p) = VARIABILITY ABOUT THE LONG-TERM MEDIAN, IN DECIBELS

EFFECTIVE DISTANCE, d_e, IN KILOMETERS

Figure 10.8

DATA FROM CONTINENTAL U.S.A.
MEDIAN FREQUENCY = 417 MHz

•	Y(0.01), Y(99.99)
▲	Y(0.1), Y(99.9)
×	Y(1), Y(99)
○	Y(10), Y(90)

CURVES SHOW PREDICTED VALUES OF Y(p)

Y(0.01) = 3.33 Y(10)	Y(99.99) = 2.90 Y(90)
Y(0.1) = 2.73 Y(10)	Y(99.9) = 2.41 Y(90)
Y(1) = 2.00 Y(10)	Y(99) = 1.82 Y(90)
Y(10) = 1.49 Y_0(10, d_e)	Y(90) = 1.41 Y_0(90, d_e)

LONG-TERM POWER FADING
CONTINENTAL TEMPERATE CLIMATE, 450-1000 MHz

DATA FROM CONTINENTAL U.S.A.
MEDIAN FREQUENCY = 700 MHz

+   Y(0.01), Y(99.99)
▲   Y(0.1) , Y(99.9)
×   Y(1) , Y(99)
○   Y(10) , Y(90)

CURVES SHOW PREDICTED VALUES OF Y(p)

Y(0.01) = 3.33 Y(10)   Y(99.99) = 2.90 Y(90)
Y(0.1) = 2.73 Y(10)   Y(99.9) = 2.41 Y(90)
Y(1) = 2.00 Y(10)   Y(99) = 1.82 Y(90)
Y(10) = 1.36 Y₀(10,dₑ)   Y(90) = 1.31 Y₀(90,dₑ)

Y(p) = VARIABILITY ABOUT THE LONG-TERM MEDIAN, IN DECIBELS

EFFECTIVE DISTANCE, dₑ, IN KILOMETERS

Figure 10.9

10-22

Y(p) = VARIABILITY ABOUT THE LONG-TERM MEDIAN, IN DECIBELS
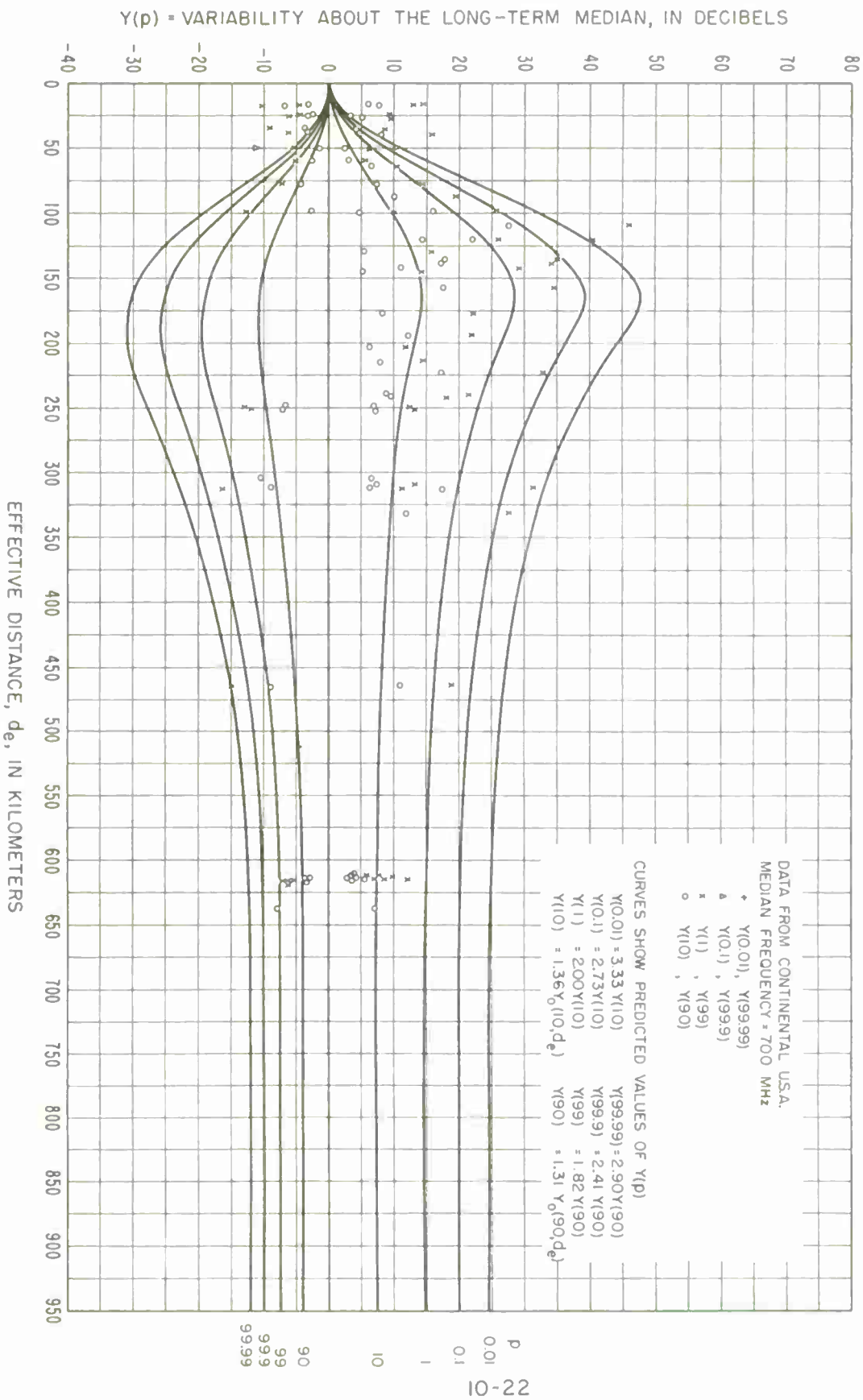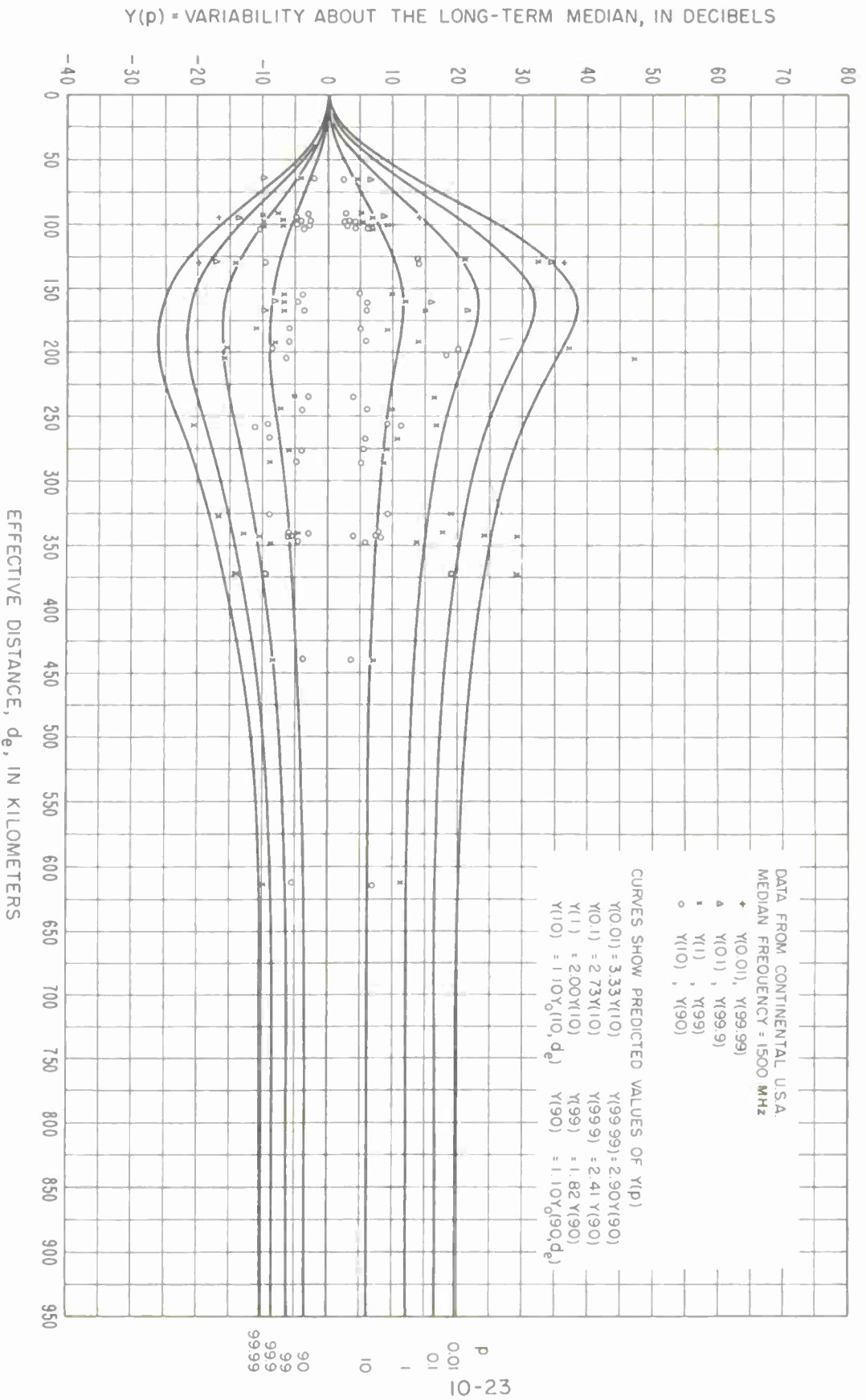
LONG-TERM POWER FADING

CONTINENTAL TEMPERATE CLIMATE, FREQ >1000 MHz

DATA FROM CONTINENTAL U.S.A.
MEDIAN FREQUENCY = 1500 MHz

+ Y(0.01), Y(99.99)
△ Y(0.1) , Y(99.9)
× Y(1) , Y(99)
○ Y(10) , Y(90)

CURVES SHOW PREDICTED VALUES OF Y(p)

Y(0.01) = 3.33 Y(10)   Y(99.99) = 2.90 Y(90)
Y(0.1) = 2.73 Y(10)   Y(99.9) = 2.41 Y(90)
Y(1) = 2.00 Y(10)   Y(99) = 1.82 Y(90)
Y(10) = 1.10 Y_0(10, d_e)   Y(90) = 1.10 Y_0(90, d_e)

EFFECTIVE DISTANCE, d_e, IN KILOMETERS

Figure 10.10

p
0.01
0.1
1
10
90
99
99.9
99.99

10-23

Y(p) = VARIABILITY ABOUT THE LONG-TERM MEDIAN, IN DECIBELS

LONG-TERM POWER FADING

MARITIME TEMPERATE CLIMATE OVERLAND, BANDS I AND II (40 – 100 MHz)

DATA FROM UNITED KINGDOM

+   Y(0.01) , Y(99.99)
▲   Y(0.1) , Y(99.9)
×   Y(1) , Y(99)
○   Y(10) , Y(90)

EFFECTIVE DISTANCE, d_e , IN KILOMETERS

Figure 10.11

10-24
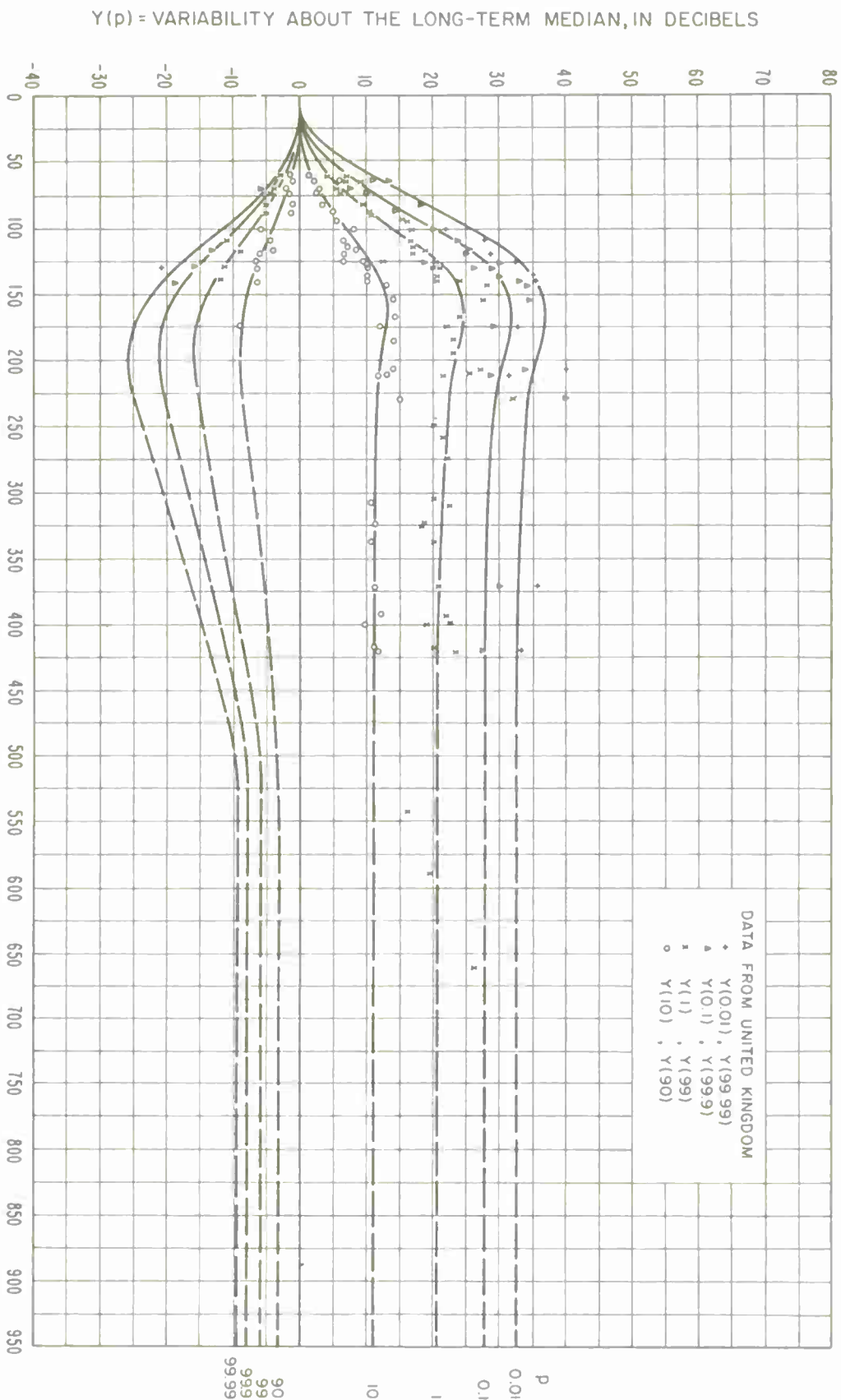
LONG-TERM POWER FADING

MARITIME TEMPERATE CLIMATE OVERSEA, BANDS I AND II (40-100 MHz)

Y(p)= VARIABILITY ABOUT THE LONG-TERM MEDIAN, IN DECIBELS

EFFECTIVE DISTANCE, de, IN KILOMETERS

DATA FROM UNITED KINGDOM

· Y(0.01), Y(99.99)
▲ Y(0.1) , Y(99.9)
■ Y(1) , Y(99)
○ Y(10) , Y(90)

Figure 10.12

10-25

Y(p) = VARIABILITY ABOUT THE LONG-TERM MEDIAN, IN DECIBELS

LONG-TERM POWER FADING
MARITIME TEMPERATE CLIMATE OVERLAND, BAND III (150-250 MHz)

EFFECTIVE DISTANCE, d_e, IN KILOMETERS

Figure 10.13

DATA FROM UNITED KINGDOM

. Y(0.01), Y(99.99)
▲ Y(0.1) , Y(99.9)
× Y(1) , Y(99)
○ Y(10) , Y(90)

10-26

Y(p) = VARIABILITY ABOUT THE LONG-TERM MEDIAN, IN DECIBELS
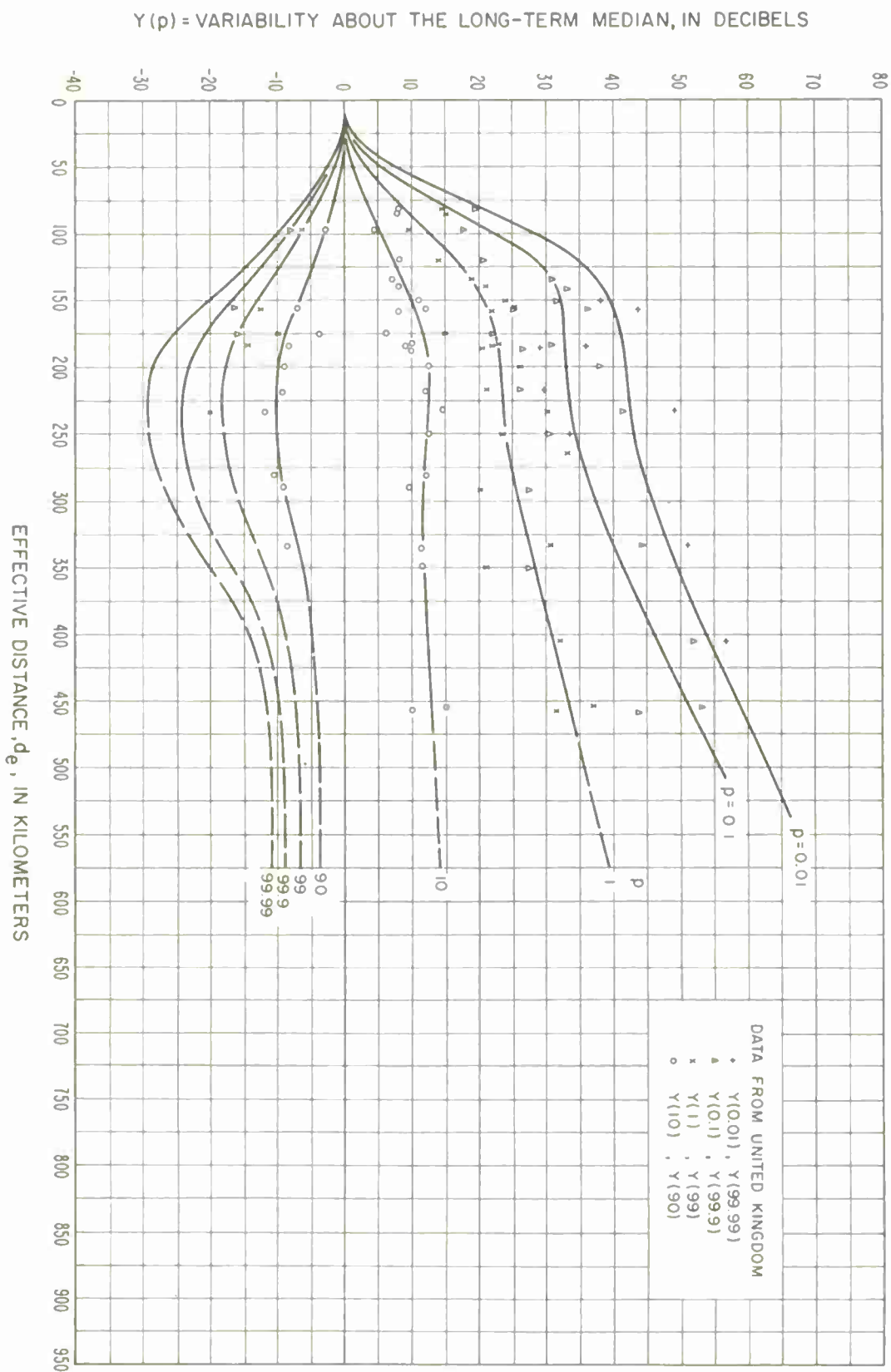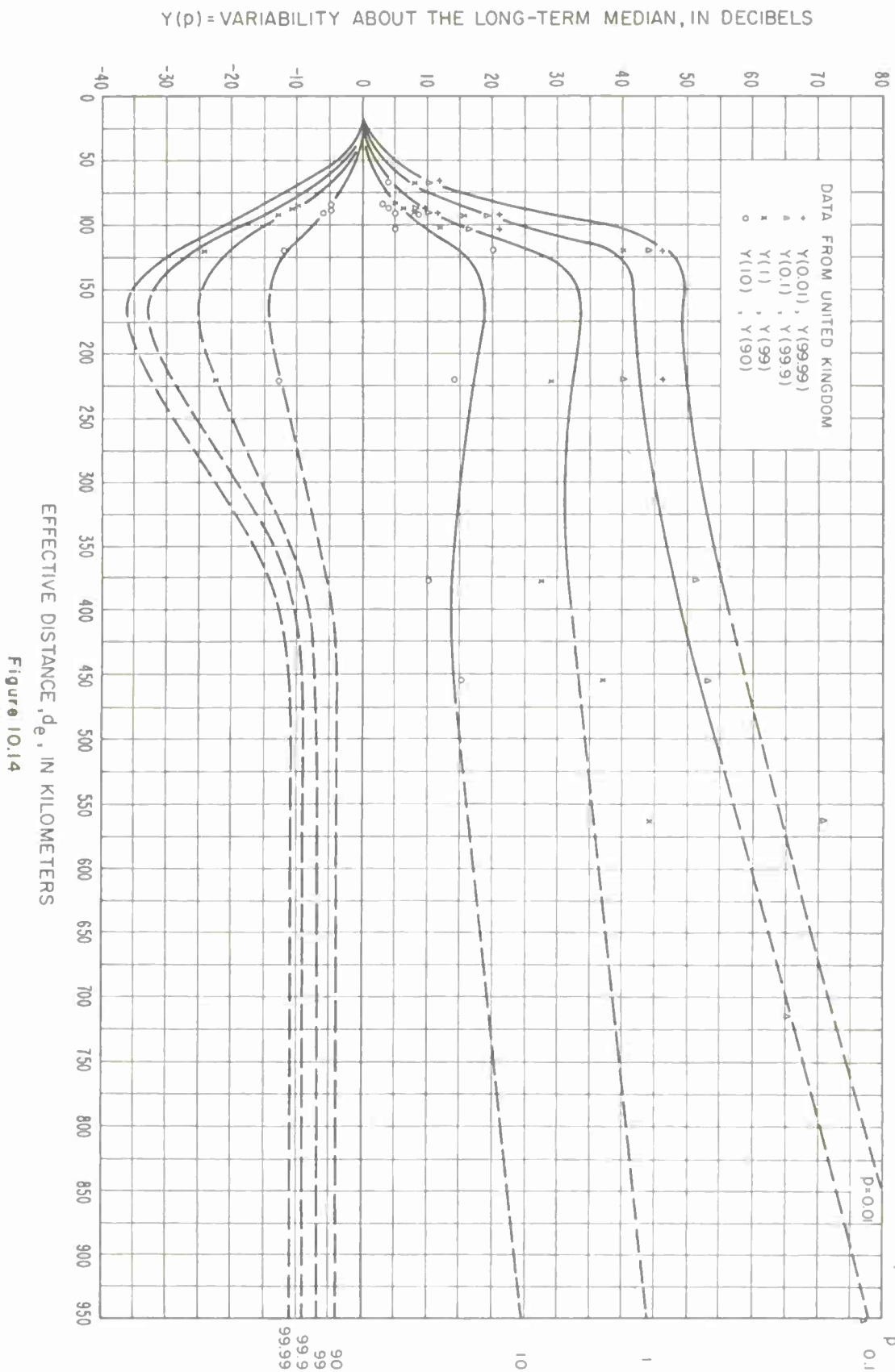
LONG-TERM POWER FADING

MARITIME TEMPERATE CLIMATE OVERSEA, BAND III (150-250 MHz)

DATA FROM UNITED KINGDOM

+	Y(0.01) , Y(99.99)
▲	Y(0.1) , Y(99.9)
✕	Y(1) , Y(99)
○	Y(10) , Y(90)

EFFECTIVE DISTANCE, d_e, IN KILOMETERS

Figure 10.14

10-27

Y(p) = VARIABILITY ABOUT THE LONG-TERM MEDIAN, IN DECIBELS

LONG-TERM POWER FADING

MARITIME TEMPERATE CLIMATE OVERLAND, BANDS IV AND V (450-1000 MHz)

EFFECTIVE DISTANCE, d_e, IN KILOMETERS

Figure 10.15

DATA FROM UNITED KINGDOM

•	Y(0.01) , Y(99.99)
▲	Y(0.1) , Y(99.9)
⋊	Y(1) , Y(99)
○	Y(10) , Y(90)

p=0.01

p=0.1

p=1

10

p

99.99
99.9
99
90

Y(p) = VARIABILITY ABOUT THE LONG-TERM MEDIAN, IN DECIBELS
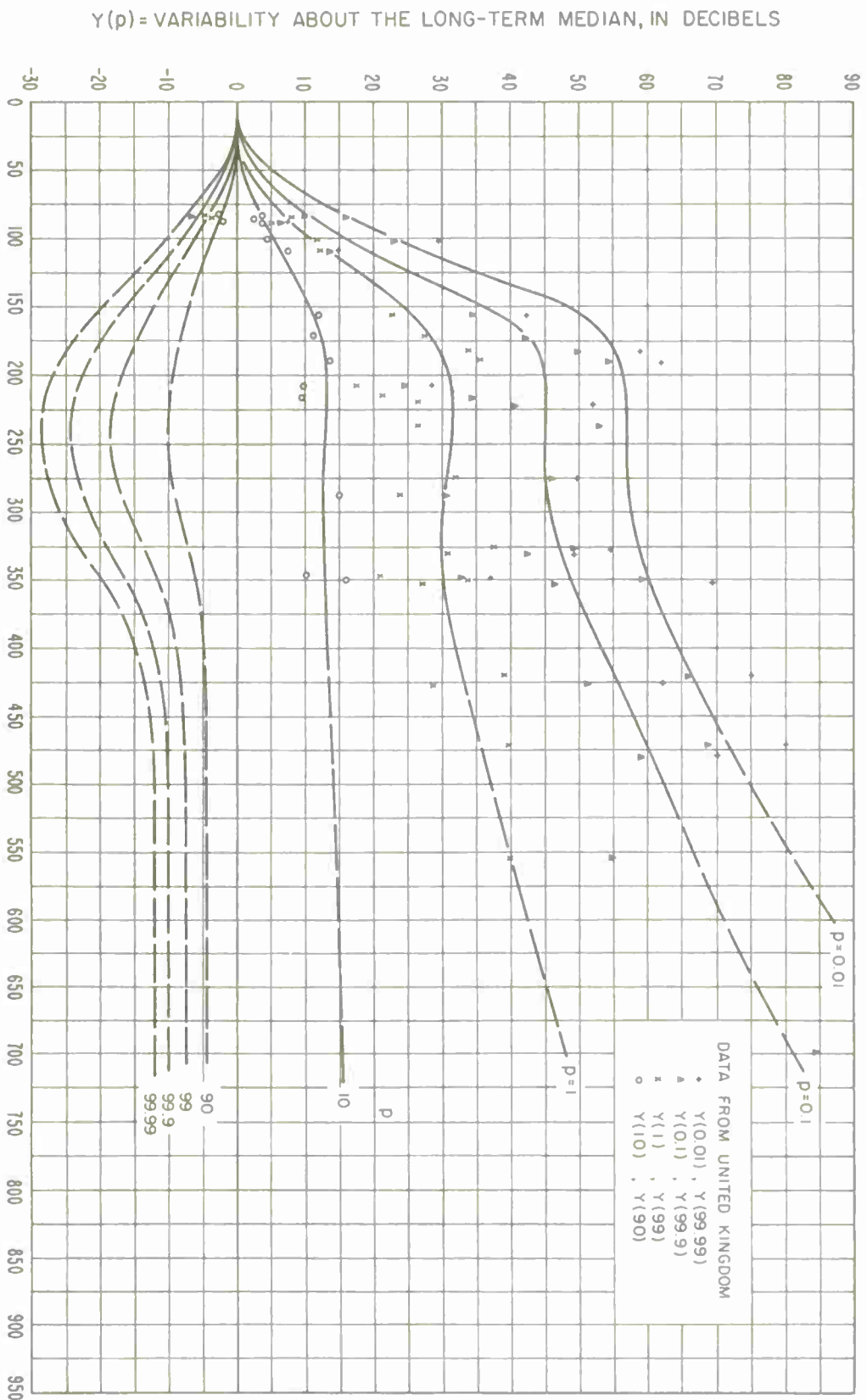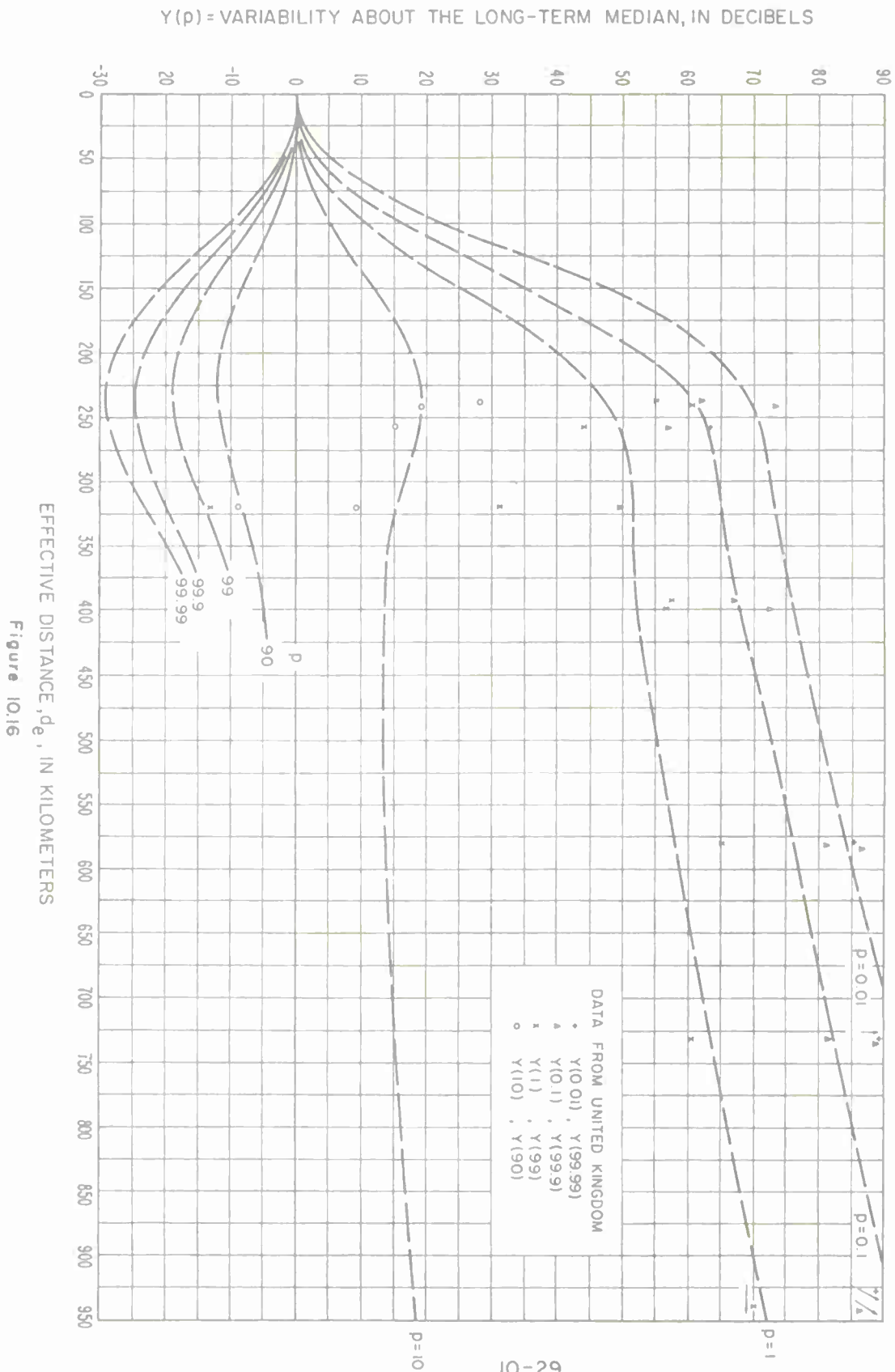
LONG-TERM POWER FADING

MARITIME TEMPERATE CLIMATE OVERSEA, BANDS IV AND V (450-1000 MHz)

EFFECTIVE DISTANCE, d_e, IN KILOMETERS

Figure 10.16

DATA FROM UNITED KINGDOM

•	Y(0.01), Y(99.99)
▲	Y(0.1), Y(99.9)
×	Y(1), Y(99)
○	Y(10), Y(90)

11. REFERENCES

The references given below include only selected papers referred to in the text of this report. A comprehensive survey of work in the field of tropospheric propagation, and an extensive bibliography will be found in the following report:

Shkarofsky, I. P. (March 1958), Tropospheric scatter propagation, Res. Rpt. No. 7-200-1, RCA Victor Co., Ltd. Res. Labs, Montreal, Canada.

Four recent bibliographies are:

Abbott, R. L. (Nov. 1960), Bibliography of tropospheric radio wave scattering, NBS Tech. Note No. 80.

Abbott, R. L., and E. R. Westwater (Dec. 1961), Bibliography of microwave thermal emissions by atmospheric gases, Private Communication.

Nupen, Wilhelm (1964), Bibliography on propagation of radio waves through the troposphere, NBS Tech. Note No. 304.

Dougherty, H. T. (Aug. 1964), Bibliography of fading on microwave line-of-sight tropospheric propagation paths and associated subjects, NBS Tech. Note No. 302.

Anderson, L. J., and E. E. Gossard (Oct. 1953a), The effect of the oceanic duct on microwave propagation, Am. Geophys. Union Trans. 34, No. 5, 695-700.

Anderson, L. J., and E. E. Gossard (Jan. 1953b), Prediction of the nocturnal duct and its effect on UHF, Proc. IRE 41, No. 1, 136-139.

Arons, L. D. (Oct. 1956), An analysis of radio-wave scattering in the diffraction region, Cornell University E. E. Report 312.

Artman, J. O., and J. P. Gordon (Dec. 1954), Absorption of microwaves by oxygen in the millimeter wavelength region, Phys. Rev. 96, No. 5, 1237-1245.

Bachynski, M. P. (1959), Microwave propagation over rough surfaces, RCA Review 20, No. 2, 308-335.

Bachynski, M. P. (July-Aug. 1960), Propagation at oblique incidence over cylindrical obstacles, J. Res. NBS 64D (Radio Prop.), No. 4, 311-315.

Bachynski, M. P. (March 1963), Scale model investigations of electromagnetic wave propagation over natural obstacles, RCA Review 24, No. 1, 105-144.

Barghausen, A. F., F. O. Giraud, R. E. McGavin, S. Murahata, and R. W. Wilber (Jan. 1963), Equipment characteristics and their relation to system performance for tropospheric communication circuits, NBS Tech. Note 103.

Barsis, A. P., and M. E. Johnson (Nov. - Dec. 1962), Prolonged space-wave fade-outs in tropospheric propagation, J. Res. NBS 66D (Radio Prop.), No. 6, 681-694.

Barsis, A. P., and R. S. Kirby (Sept. - Oct. 1961), VHF and UHF signal characteristics observed on a long knife-edge diffraction path, J. Res. NBS 65D (Radio Prop.), No. 5, 437-448.

Barsis, A. P., K. A. Norton, P. L. Rice, and P. H. Elder (Aug. 1961), Performance predictions for single tropospheric communication links and for several links in tandem, NBS Tech. Note 102. (See also IRE Transactions on Communication Systems CS-10, No. 1, 2-22, March 1962).

Batchelor, G. K. (1947), Kolmogoroff's theory of locally isotropic turbulence, Proc. Camb. Phil. Soc. 43, 533-559.

Batchelor, G. K. (1953), The theory of homogeneous turbulence, (Cambridge University Press).

Bean, B. R. (May 1954), Prolonged space-wave fadeouts at 1,046 Mc observed in Cheyenne Mountain propagation program, Proc. IRE 42, No. 5, 848-853.

Bean, B. R. (1956), Some meteorological effects on scattered VHF radio waves, IRE Trans. Comm. Syst., CS 4(1), 32-38.

Bean, B. R. (July-Aug. 1959), Climatology of ground-based radio ducts, J. Res. NBS 63D (Radio Prop.), No. 1, 29-34.

Bean, B. R. (1961), Concerning the bi-exponential nature of the tropospheric radio refractive index, Beiträge zur Physik der Atmosphäre 34, No. 1/2, 81-91.

Bean, B. R., and R. L. Abbott (1957), Oxygen and water vapor absorption of radio waves in the atmosphere, Geofisica Pura e Applicata - Milano 37, 127-134.

Bean, B. R., and B. A. Cahoon (Nov. 1957), The use of surface observations to predict the total atmospheric bending of radio rays at small elevation angles, Proc. IRE 45, No. 11, 1545-1546.

Bean, B. R., J. D. Horn, and A. M. Ozanich, Jr. (Nov. 1960), Climatic charts and data of the radio refractive index for the United States and the world, NBS Monograph No. 22.

Bean, B. R., J. D. Horn, and L. P. Riggs (Oct. 1962), Synoptic radio meteorology, NBS Tech. Note 98.

Bean, B. R., and G. D. Thayer (May 1959), Models of the atmospheric radio refractive index, Proc. IRE 47, No. 5, 740-755.

Beard, C. I. (September 1961, Coherent and incoherent scattering of microwaves from the ocean, IRE Trans. Ant. Prop. AP-9, 470-483.

Beard, C. I., I. Katz, and L. M. Spetner (April 1956), Phenomenological vector model of microwave reflection from the ocean, IRE Trans. Ant. Prop. AP-4, No. 2, 162-167.

Beckmann, P. (1957), A new approach to the problem of reflection from a rough surface, Acta, Tech. Ceskosl. Akad. 2, 311-355; see also pp. 323-335, (1959).

Beckmann, P. (1960), A generalized Rayleigh distribution and its application to tropospheric propagation, Electromagnetic Wave Propagation, (Symposium, Liege, 1958), (Academic Press, London, 445-449).

Beckmann, P. (1961a), The statistical distribution of the amplitude and phase of a multiply scattered field, Inst. Rad. Eng. and Elec., Czechoslovak Akad. Sci., Paper No. 18. See also NBS Jour. Res. 66D, (Radio Propagation), pp. 231-240, 1962.

Beckmann, P. (1961b), The depolarization of electromagnetic waves scattered from rough surfaces, Inst. Rad. Eng. and Elect., Czechoslovak Akad. Sci., Paper No. 19.

Beckmann, P. (September 1964), Rayleigh distribution and its generalization, NBS Jour. Res. 68D, (Radio Science), No. 9, pp. 927-932.

Beckmann, P. and A. Spizzichino (1963), The scattering of Electromagnetic waves from rough surfaces, International Series of Monographs on Electromagnetic Waves, Vol. 4, (Pergamon Press, New York, N.Y.).

Biot, M. A. (Dec. 1957a), Some new aspects of the reflection of electromagnetic waves on a rough surface, J. Appl. Phys. 28, No. 12, 1455-1463.

Biot, M. A. (Nov. 1957b), Reflection on a rough surface from an acoustic point source, J. Acoust. Soc. Am. 29, No. 11, 1193-1200.

Booker, H. G. (1946), Elements of radio meteorology: How weather and climate cause unorthodox radar vision beyond the geometrical horizon, J. Inst. Elec. Engrs. (London) 93, Pt. III-A, No. 1, 69-78.

Booker, H. G., and J. T. de Bettencourt (Mar. 1955), Theory of radio transmission by tropospheric scattering using very narrow beams, Proc. IRE 43, No. 3, 281-290.

Booker, H. G., and W. E. Gordon (Sept. 1950a), Outline of a theory of radio scattering in the troposphere, J. Geophys. Res. 55, No. 3, 241-246; see also Proc. IRE 38, No. 4, 401, (April, 1950b).

Booker, H. G., and W. Walkinshaw (April 1946), The mode theory of tropospheric refraction and its relation to waveguides and diffraction, Report on Conference on Meteorological Factors in Radio Wave Propagation (The Phys. Soc., and the Royal Met. Soc., London), 80-127.

Bray, W. J., F. Hopkins, A. Kitchen, and J. A. Saxton (Jan. 1955), Review of long-distance radio-wave propagation above 30 Mc/s, Proc. IEE, Paper No. 1782R, Pt. B, 102, 87-95.

Bremmer, H. (1949), Terrestrial radio waves; theory of propagation, (Elsevier Publishing Co., Amsterdam and New York, N. Y.).

Bremmer, H. (Sept. 1957), Distortion in tropospheric scatter, Phillips Telecomm. Rev. 18, No. 3, 137-154.

Bremmer, H. (May 1959), On the theory of the fading properties of a fluctuating signal imposed on a constant signal, NBS Circular 599.

Bugnolo, D. S. (July 1958), Multiple scattering of electromagnetic radiation and the transport equation of diffusion, IRE Trans. Ant. Prop. AP-6, No. 3, 310.

Bullington, K. (Jan. 1950), Radio propagation variations at VHF and UHF, Proc. IRE 38, No. 1, 27-32.

Bullington, K. (Oct. 1955), Characteristics of beyond-the-horizon radio transmission, Proc. IRE 43, No. 10, 1175-1180.

Bussey, H. E. (July 1950), Microwave attenuation statistics estimated from rainfall and water vapor statistics, Proc. IRE 38, No. 7, 781-785.

CCIR (1955), Atlas of ground wave propagation curves for frequencies between 30 Mc/s and 300 Mc/s, ITU, Geneva.

CCIR (1959), Atlas of ground wave propagation curves for frequencies between 30 and 10,000 Mc/s (Vertical polarization only; prepared by the Radio Research Laboratories, Ministry of Postal Services, Tokyo, Japan, January 1958), ITU, Geneva.

CCIR (1963a), The concept of transmission loss in studies of radio systems, Documents of the Xth Plenary Assembly, ITU, Geneva, Vol. III, Recommendation 341, 29-31.

CCIR (1963b), Transmission loss in studies of radio systems, Documents of the Xth Plenary Assembly, ITU, Geneva, Vol. III, Report 112, 84-89.

CCIR (1963c), Optimum use of the radio spectrum, Documents of the Xth Plenary Assembly, ITU, Geneva, Vol. III, Resolution 1, 111.

CCIR (1963d), Line frequencies or bands of interest to radioastronomy and related sciences, in the 30 - 300 Gc/s range arising from natural phenomena, Documents of the Xth Plenary Assembly, ITU, Geneva, Vol. IV, Report 223, 304-307.

CCIR (1963e), Reference atmospheres, Documents of the Xth Plenary Assembly, ITU, Geneva, Vol. II, Report, 231, 74-75.

CCIR (1963f), Estimation of tropospheric-wave transmission loss, Documents of the Xth Plenary Assembly, ITU, Geneva, Vol. II, Report 244, 191-213.

CCIR (1963g), Propagation curves for VHF/UHF broadcasting in the African Continent, Documents of the Xth Plenary Assembly, ITU, Geneva, Vol. III, Report 240, 143-181.

CCIR (1963h), VHF and UHF propagation curves for the frequency range from 40 Mc/s to 1000 Mc/s - Broadcasting and mobile services, Documents of the Xth Plenary Assembly, ITU, Geneva, Vol. II, Recommendation 370, 24-36.

CCIR (1963i), Communication satellite systems-frequency sharing between communication satellites systems and terrestrial services, Documents of the Xth Plenary Assembly, ITU, Geneva, Vol. IV, Report 209, 221-232.

CCIR (1963j), Influence of the atmosphere on wave propagation, Documents of the Xth Plenary Assembly, ITU, Geneva, Vol. II, Report 233, 76-120.

CCIR (1963k), Propagation data required for radio relay systems, Documents of the Xth Plenary Assembly, ITU, Geneva, Vol. II, Report 242, 182-187.

CCIR (1963ℓ), Fading of signals propagated by the ionosphere, Documents of the Xth Plenary Assembly, ITU, Geneva, Vol. II, Report 266, 327-334.

CCIR (1963m), Terms and definitions, Documents of the Xth Plenary Assembly, ITU, Geneva, Vol. I, Report 321, 239.

CCIR (1964), Optimum use of the radio frequency spectrum, Document being prepared for the XIth Plenary Assembly, in accordance with Resolution 1 of the Xth Plenary Assembly, ITU, Geneva, Vol. III, 111.

Chernov, L. A. (Jan. - June 1955), Correlation of amplitude and phase fluctuations for wave propagation in a medium with random irregularities, Akust. Zh. 1, 89; translation in Soviet Phys. - Acoust. 1, No. 1-2, 94-101.

Christiansen, W. N. (1947), Rhombic antenna arrays, A.W.A. Tech. Rev. [Amal. Wireless Australia] 7, No. 4, 361-383.

Clemow, D. B., and E. H. Bruce-Clayton (Jan. 1963), Long range VHF air/ground communications, Brit. IRE J. 25, No. 1, 17-32.

Cozzens, D. E. (June 1962), Nomograph for determining paraboloidal gain as a function of feed pattern and angular aperture, Microwave J. V, No. 6, 58-59.

Crawford, A. B., and D. C. Hogg (July 1956), Measurement of atmospheric attenuation at millimeter wavelengths, Bell Syst. Tech. J. 35, 907-916.

Crawford, A. B., D. C. Hogg, and W. H. Kummer (Sept. 1959), Studies in tropospheric propagation beyond the horizon, Bell Syst. Tech. J. 38, No. 5, 1067-1178.

Crichlow, W. Q., D. F. Smith, R. N. Morton, and W. R. Corliss (Aug. 1955), Worldwide radio noise levels expected in the frequency band 10 Kc to 100 Mc, NBS Circular 557.

Crysdale, J. H. (July 1958), Comparison of some experimental terrain diffraction losses with predictions based on Rice's theory for diffraction by a parabolic cylinder, IRE Trans. Ant. Prop. AP-6, No. 3, 293-295.

Crysdale, J. H., J. W. B. Day, W. S. Cook, M. E. Psutka, and P. E. Robillard (April 1957), An experimental investigation of the diffraction of electromagnetic waves by a dominating ridge, IRE Trans. Ant. Prop. AP-5, No. 2, 203-210.

Davenport, W. B., and W. L. Root (1958), An introduction to the theory of random signals and noise, McGraw-Hill Book Co., Inc., New York, Chapter 3

deJager, C. (1952), The spectrum of turbulence in the earth's upper atmosphere, Mem. Soc. Roy. des Sci., Liege 12, 223-252.

Dickson, F. H., J. J. Egli, J. W. Herbstreit, and G. S. Wickizer (Aug. 1953), Large reductions of VHF transmission loss and fading by the presence of a mountain obstacle in beyond-line-of-sight paths, Proc. IRE 41, No. 8, 967-969. See also subsequent correspondence by Crysdale and rebuttal by Dickson, et al., in Proc. IRE 43, No. 5, 627-628 (May 1955).

Doherty, L. H. (Sept. 1952), Geometrical optics and the field at a caustic with applications to radio wave propagation between aircraft, Cornell University School of Electrical Engineering Research Report EE-138.

Dolukhanov, M. P. (1957), Investigations into the propagation of radio waves over the earth's surface in the USSR., Radio Engr. and Electronics (USSR) 2, No. 11, 39-61.

Domb, C., and M. H. L. Pryce (Sept. 1947), The calculation of field strengths over a spherical earth, IEE 94, Part III, No. 31, 325-339.

Dougherty, H. T., and L. J. Maloney, (Feb. 1964) The application of diffraction by convex surfaces to irregular terrain situations, J. Res. NBS 68D (Radio Science), No. 2, 239-250.

duCastel, F. (May 1957a), Different types of fluctuations of tropospheric fields and their physical interpretation, L'Onde Electrique 37, No. 362, 501-506.

duCastel, F. (Nov. 1957b), The use of ultra short waves for long distance telephone links in Africa (Results of Tests in the Cameroons), L'Onde Electrique 37, No. 368, 1025-1035.

duCastel, F. (Nov.-Dec. 1960), Experimental results from transhorizon tropospheric propagation, Ann des Télécomm. 15, No. 11-12, 255-259.

duCastel, F., and P. Misme (Nov. 1957), Elements of radio climatology, L'Onde Electrique 37, No. 368, 1045-1052.

duCastel, F., P. Misme, and J. Voge (March 1958), Reflection of an electromagnetic wave from an atmospheric layer with variable index of refraction, C. R. Acad., Sci. Fr. 246, No. 12, 1838-1840.

duCastel, F., P. Misme, A. Spizzichino, and J. Voge (1962), On the role of the process of reflection in radio wave propagation, J. Res. NBS 66D (Ra. .a rд-), .lo. 3, 273-284.

Dutton, E. J. (June 1961), On the climatology of ground-based radio ducts and associated fading regions, NBS Tech. Note 96.

Dutton, E. J., and G. D. Thayer (Oct. 1961), Techniques for computing refraction of radio waves in the troposphere, NBS Tech. Note 97.

Fengler, G. (1964), Untersuchungen der elektromagnetischen wellenausbreitung im 500 MHZ-bereich über land unter besonderer berücksichtigung der meteorologischen, Berichte des Instituts für Radiometeorologie und Maritime Meteorologie an der Universität Hamburg, Report No. 8.

Fengler, G., J. Jeske, and G. Stilke, Radiometeorological papers II, Berichte des Instituts für Radiometeorologie und Maritime Meteorologie an der Universität Hamburg, Report No. 9.

Florman, E. F., and J. J. Tary (Jan. 1962), Required signal-to-noise ratios, RF signal power, and bandwidth for multichannel radio communications systems, NBS Tech. Note 100.

Fok, V. A., L. A. Vainshtein, and M. G. Belkina (1958), Radiowave propagation in surface tropospheric ducts, Radio Eng. Electron. (USSR), 3, No. 12, 1-27.

Friend, A. W. (June 1945), A summary and interpretation of ultra high frequency wave propagation data collected by the late Ross A. Hull, Proc. IRE 33, 358.

Friis, H. T., A. B. Crawford, and D. C. Hogg (May 1957), A reflection theory for propagation beyond the horizon, Bell Syst. Tech. J. 36, No. 3, 627-644.

Furutsu, K. (1956), On the multiple diffraction of electromagnetic waves by spherical mountains, J. Radio Res. Labs., Tokyo 3, 331.

Furutsu, K (1959), Wave propagation over an irregular terrain, I, II, III, J. Radio Res. Labs., Tokyo 4, 135, 349 (1957), and 6, 71 (1959).

Furutsu, K. (Jan. - Feb. 1963), On the theory of radio wave propagation over inhomogeneous earth, J. Res. NBS 67D (Radio Prop.), No. 1, 39-62.

Grosskopf, J. (June 1956), On the existing condition of research in the realm of tropospherically scattered radiation, Nachrtech. Z. 9, No. 6, 272-279.

Grosskopf, J. (Nov. 1958), Some remarks on the analysis of fading in the meter and decimeter range, Nachrtech. Z. 11, No. 11, 577-586.

Gunn, K. L. S., and T. W. R. East (Oct. 1954), The microwave properties of precipitation particles, Quart. J. Roy. Meteorol. Soc. (London) 80, 522-545.

Harper, A. E. (1941), Rhombic antenna design, (D. van Nostrand Co., Princeton, N. J.).

Hartman, W. J. (May 1963), Path antenna gain and comments on "Properties of 400 Mcps long-distance tropospheric circuits," Proc. IEEE 51, No. 5, 847-848.

Hartman, W. J., and R. E. Wilkerson (Nov. - Dec. 1959), Path antenna gain in an exponential atmosphere, J. Res. NBS 63D (Radio Prop.), No. 3, 273-286.

Hathaway, S. D., and H. W. Evans (Jan. 1959), Radio attenuation at 11 k Mc and some implications affecting relay system engineering, Bell Syst. Tech. J. 38, No. 1, 73-97.

Haurwitz, B. and J. M. Austin [1944], Climatology, McGraw-Hill Co. Inc., New York.

Hay, H. G., and R. S. Unwin (Dec. 1952), Tropospheric wave propagation in a duct of nonuniform height, Phys. Soc. London Proc. 65, No. 396b, 981-989.

Head, H. T. (June 1960), The influence of trees on television field strengths at ultra-high frequencies, Proc. IRE 48, No. 6, 1016-1020.

Heisenberg, W. (Dec. 1948), On the theory of statistical and isotropic turbulence, Proc. Roy. Soc. London A 195, 402-406.

Herbstreit, J. W., and P. L. Rice (Sept. 1959), Survey of Central Radio Propagation Laboratory research in tropospheric propagation, 1948-1956, NBS Tech. Note No. 26.

Hirai, Masaichi (May 1961a), Multipath properties of tropospheric propagation of very short radio waves beyond the horizon, Jour. Radio Res. Lab., Japan 8, No. 37, 147-174.

Hirai, Masaichi (Sept. 1961b), Diversity effects in spaced-antenna reception of tropospheric scatter waves, Jour. Radio Res. Lab., Japan 8, 301-329.

Hitchcock, R. J., and P. A. C. Morris (July 1961), The HF band: Is a new look required? Wireless World, 375-378.

Hogg, D. C., and W. W. Mumford (March 1960), The effective noise temperature of the sky, Microwave J. 3, 80-84.

Hogg, D. C., and R. A. Semplak (Sept. 1961), The effect of rain and water vapor on sky noise at centimeter wavelengths, Bell Syst. Tech. J. 40, No. 5, 1331-1348.

Ikegami, F. (July 1959), Influence of an atmospheric duct on microwave fading, IRE Trans. Ant. Prop. AP-7, No. 3, 252-257.

Ikegami, F. (May-June 1964), Radiometeorological effects in propagation over the sea and islands, Rev. Elect. Commun. Lab., Tokyo, ET-12, 5-324312-324.

International Telephone and Telegraph Corporation (1956), Reference data for radio engineers, Fourth Edition, (ITT, New York).

Janes, H. B., and P. I. Wells (Oct. 1955), Some tropospheric scatter propagation measurements near the radio horizon, Proc. IRE 43, No. 10, 1336-1340.

Jasik, H. (1961), Antenna Engineering Handbook, (McGraw Hill).

Johnson, M. A. (1958), A review of tropospheric scatter propagation theory and its application to experiment, Proc. IEE 105B, Suppl. 8, 165-176.

Josephson, B., and A. Blomquist (April 1958), The influence of moisture in the ground, temperature and terrain on ground wave propagation in the VHF band, IRE Trans. Ant. Prop. AP-6, No. 2, 169-172.

Josephson, B., and G. Carlson (April 1958), Distance dependence, fading characteristics and pulse distortion of 3000 Mc trans-horizon signals, IRE Trans. Ant. Prop. AP-6, No. 2, 173-175.

Josephson, B., and F. Eklund (April 1958), Some microwave propagation experiences from a just-below-horizon path, IRE Trans. Ant. Prop. AP-6, No. 2, 176-178.

Jowett, J. K. S. (Jan. 1958), The measurement and prediction of VHF tropospheric field strengths at distances beyond the horizon, Proc. IEE 105B, Supp. 8, 91-96, and 122-126, Paper No. 2500R.

Joy, W. R. R. (Jan. 1958a), The long-range propagation of radio waves at 10 cm wavelength, Proc. IEE 105B, Supp. 8, 153-157, Paper No. 2522R.

Joy, W. R. R. (1958b), Radio propagation far beyond the horizon at about 3.2 cm wavelength, Proc. IEE 105B, Supp. 8, 158-164 and 184-188, Paper No. 2528R.

Kales, M. L. (May 1951), Elliptically polarized waves and antenna, Proc. IRE 39, No. 5, 544-549.

Kalinin, A. I. (1957), Approximate methods of computing the field strength of ultra short waves with consideration of terrain relief, Radio Eng. 12, No. 4, 13-26, Radiotekhn. i Elektron. 12, No. 4, 13-23.

Kalinin, Iu. K (1958), Perturbation of plane radio wave by inhomogeneities of the earth's surface, Radiotech. and Elecktron 3, 557-561, Translation in Radio Engineering and Electronics 3, No. 4, 143-149.

Kerr, D. E. (1964), Propagation of short radio waves, MIT Radiation Laboratory Series 13, (Boston Technical Publishers, Inc., Lexington, Mass.).

Kirby, R. S., H. T. Dougherty, and P. L. McQuate (Oct. 1955), Obstacle gain measurements over Pike's Peak at 60 to 1046 Mc/s, Proc. IRE 43, No. 10, 1467-1472.

Kirby, R. S., P. L. Rice, and L. J. Maloney (Oct. 1961), Characteristics of point-to-point tropospheric propagation and siting considerations, NBS Tech. Note No. 95.

Kitchen, F. A., and I. J. Richmond (March 1957), Some characteristics of long distance scatter transmissions (two parts), British Comm. and Electr. 4, No. 2, 74-78 (Feb. 1957); 4, No. 3, 146-148, (March 1957).

Kitchen, F. A., E. G. Richards, and I. J. Richmond (Jan. 1958), Some investigations of metre-wave radio propagation in the transhorizon region, Proc. IEE 105B, Supp. 8, 106-116, Paper No. 2509R.

Kitchen, F. A., W. R. R. Joy, and E. G. Richards (Aug. 1958), Influence of the semi-permanent low-level ocean duct on centimetre wave scatter propagation beyond the horizon, Nature 182, No. 4632, 385-386.

Kolmogoroff, A. N. (1941), Dissipation of energy in locally isotropic turbulence, Comptes Rendus (Doklady) de l'Acadamie des Sciences de l'USSR 32, No. 1, 16-18.

Krasil'nikov, V. A. (1949), The effect of variations of the coefficient of refraction in the atmosphere upon the propagation of ultra-short waves, Izvest. Akad. Nauk.S.S.S.R. Sev. Geografi Geofiz 13, No. 1, 33-57 (in Russian).

Kühn, V. (Feb. and May 1958), Propagation investigation of the effect of various types of terrain in frequency bands I, II, and III, Tech. Comm. Lab. for Commercial Radio and Telev., BRF, DDR.

Lane, J. A., and J. A. Saxton (July 1952), Dielectric dispersion in pure polar liquids at very high radio frequencies, Proc. Roy. Soc. A213, 400-408.

Laws, J. O., and D. A. Parsons (Apr. 1943), The relation of raindrop-size to intensity, Trans. Amer. Geophys. Union 24, 452-460.

Lewin, L. (July 1962), Diversity reception and automatic phase correction, Proc. IEE 109, Part B, No. 46, 295-304.

McGavin, R. E. (May 1962), A survey of the techniques for measuring the radio refractive index, NBS Tech. Note 99.

McGavin, R.E., and L. J. Maloney (Sept.-Oct. 1959), Study at 1046 Mc/s of the reflection coefficient of irregular terrain at grazing angles, J. Res. NBS 63D (Radio Prop.), No. 2, 235-248.

McPetrie, J. S., and J. A. Saxton (Sept. 1942), Diffraction of ultra-short radio waves, Nature 150, 292.

McPetrie, J. S., and L. H. Ford (1946), Some experiments on the propagation over land of radiation of 9.2 cm wavelength, especially on the effect of obstacles, Proc. IEE 93, Pt. 3-A, Nos. 1-4, 531-538.

Megaw, E. C. S. (Dec. 1950), Scattering of electromagnetic waves by atmospheric turbulence, Nature 166, 1100-1104.

Megaw, E. C. S. (April 1954), Interpretation of stellar scintillation, Quart. J. Roy. Met. Soc. 80, 248-251.

Megaw, E. C. S. (Sept. 1957), Fundamental radio scatter propagation theory, Proc. IEE, Pt. C 104, No. 6, 441-455, see also Monograph 236R, May 1957.

Merkulov, V. V. (1957), On the theory of propagation of electromagnetic waves in media with random inhomogeneities in the index of refraction, Soviet Physics: Tech. Phys. 2, 958-961, J. Electro-Tech. Phys. 27, No. 5, 1051.

Millington, G. (May 1958), Tropospheric scatter propagation, Electronic Eng. 30, No. 363, 248-252.

Millington, G., R. Hewitt, and F. S. Immirzi (Sept. 1962a), Double knife-edge diffraction in field strength predictions, Proc. IEE 109, Part C, No. 16, 419-429. See also IEE Monograph No. 507E (Mar. 1962).

Millington, G., R. Hewitt, and F. S. Immirzi (Sept. 1962b), The Fresnel surface integral, Proc. IEE 109, Part C, 430-437. See also IEE Monograph No. 508E (Mar. 1962).

Millington, G., and G. A. Isted (July 1950), Ground wave propagation over an inhomogeneous, smooth earth, Part 2: Experimental evidence and practical implications, Proc. IEE, Part III 97, No. 48, 209.

Misme, P. (July 1958), The correlation between the electric field at a great distance and a new radiometeorological parameter, Trans. IRE Trans. Ant. Prop. AP-6, No. 3, 289-292.

Misme, P. (March-April 1960a), The equivalent gradient direct measurements and theoretical calculations, Ann. des Télécomm. 15, Nos. 3-4, 92-99.

Misme, P. (Aug. 1960b), Comments on "Models of the atmospheric radio refractive index," Proc. IRE 48, No. 8, 1498-1501.

Misme, P. (Nov.-Dec. 1960c), Some aspects of radiometeorology and radioclimatology, Ann. des Télécomm. 15, No. 11-12, 266-273.

Misme, P. (May-June 1961), The influence of the equivalent gradient and atmospheric stability on transhorizon paths in the Sahara and the Congo, Ann. des Télécomm. 16, Nos. 5-6, 110-116.

Moler, W. F., and D. B. Holden (Jan.-Feb. 1960), Tropospheric scatter propagation and atmospheric circulations, J. Res. NBS 64D (Radio Prop.), No. 1, 82-94.

Nakagami, M. (Oct. 1940), Study on the resultant amplitude of many vibrations whose phases and amplitudes are random, Nippon Elec. Comm. Eng. 22, 69-92.

National Bureau of Standards (1954), Applied Mathematics Series 32, Table of the sine and cosine integrals for arguments from 10 - 100.

National Bureau of Standards (June 1964), Applied Mathematics Series 55, Handbook of Mathematical Functions.

Neugebauer, H. E. J., and M. P. Bachynski (July-Aug. 1960), Diffraction by smooth conical obstacles, J. Res. NBS 64D (Radio Prop.), No. 4, 317-329.

Newton, R. G., and T. F. Rogers (Nov. 1953), Dependence of total microwave atmospheric absorption on propagation path elevation, Air Force Cambridge Report AFCRC Tech. 53-54A.

Nomura, Y. A., and K. Takaku (Aug. 1955), On the propagation of electromagnetic waves in an inhomogeneous atmosphere, J. Phys. Soc. Japan 10, No. 8, 700-714.

Norton, K. A. (Dec. 1941), The calculation of ground-wave field intensity over a finitely conducting spherical earth. Proc. IRE 29, No. 12, 623-639.

Norton, K. A. (1950), Addendum to Reference E to the report of Ad Hoc Committee of the F.C.C. for the Evaluation of the Radio Propagation Factors Concerning the TV and FM Broadcasting Services in the Frequency Range Between 50 and 250 Mc/s. (See Norton and Fine reference below.)

Norton, K. A. (Jan, 1953), Transmission loss in radio propagation, Proc. IRE 41, No. 1, 146-152.

Norton, K. A. (July-Aug. 1959), System loss in radio wave propagation, J. Res. NBS 63D (Radio Prop.), No. 1, 53-73.

Norton, K. A. (July 1960), Carrier frequency dependence of the basic transmission loss in tropospheric forward scatter propagation, J. Geophys. Res. 65, No. 7, 2029-2045.

Norton, K. A. (1962), Efficient use of the radio spectrum, NBS Tech. Note 158.

Norton, K. A., and E. C. Barrows (1964), Observed vertical wavenumber spectra of refractivity near the ground, to be published.

Norton, K. A., and H. Fine (Aug. 1, 1949), A study of methods for the efficient allocation of radio frequencies to broacasting services operating in the range above 50 Mc, Reference E to the Report of Ad Hoc Committee of the F.C.C. for the Evaluation of the Radio Propagation Factors Concerning the TV and FM Broadcasting Services in the Frequency Range Between 250 Mc/s.

Norton, K. A., and A. C. Omberg (Jan. 1947), The maximum range of a radar set, Proc. IRE 35, No. 1, 4-24.

Norton, K. A., P. L. Rice, H. B. Janes, and A. P. Barsis (Oct. 1955), The rate of fading in propagation through a turbulent atmosphere, Proc. IRE 43, No. 10, 1341-1353.

Norton, K. A., P. L. Rice, and L. E. Vogler (Oct. 1955), The use of angular distance in estimating transmission loss and fading range for propagation through a turbulent atmosphere over irregular terrain, Proc. IRE 43, No. 10, 1488-1526.

Norton, K. A., H. Staras, and M. Blum (Feb. 1952), A statistical approach to the problem of multiple radio interference to FM and television service, IRE Trans. Ant. Prop. AP-1, 43-49.

Norton, K. A., L. E. Vogler, W. V. Mansfield, and P. J. Short (Oct. 1955), The probability distribution of the amplitude of a constant vector plus a Rayleigh-distributed vector, Proc. IRE 43, No. 10, 1354-1361.

Obukhov, A. M. (1941), On the distribution of energy in the spectrum of turbulent flow, Bull. Acad. Sci. USSR Geo. and Geophys. Ser. 4-5, 453. See also Comptes Rendus (Doklady) L'Academie des Sciences de l'USSR 32, No. 1, 19 (1941).

Obukhov, A. M. (1953), On the effect of inhomogeneities of the atmosphere on sound and light propagation, Bull. Acad. Sci. USSR, Geog. and Geophys. Ser. 2, 155.

Onoe, M., M. Hirai, and S. Niwa (April 1958), Results of experiments of long distance overland propagation of ultra-short waves, J. Radio Res. Lab. (Tokyo) 5, No. 20, 79-94.

Onoe, M. and K. Nishikori (Oct. 1957), Microwave propagation over the sea beyond the line of sight, Radio Res. Lab. J. 4, No. 18, 395-406.

Pearcey, T. (1956), Table of the Fresnel integral, (Cambridge Univ. Press, New York, N. Y.).

Pekeris, C. L. (Feb. 1947), Note on scattering of radiation in an inhomogeneous medium, Phys. Rev. 71, No. 3, 268-269.

Perlat, A., and J. Voge (Dec. 1953), Attenuation of centimeter and millimeter waves by the atmosphere, Ann. des Télécomm. 8, No. 12, 395-407.

Price, W. L. (July 1948), Radio shadow effects produced in the atmosphere by inversions, Proc. Phys. Soc. London 61, No. 343, 59-78.

Randall, D. L. (1964), A summary of tropospheric radio duct meteorology at V.H.F. and UHF as observed on a trip around the world, World Conference on Radio Meteorology Boulder, Colorado, September 14-18.

Rayleigh, Lord (Aug. 1880), On the resultant of a large number of vibrations of the same pitch and of arbitrary phase, Phil. Mag. 10, 73-78.

Riblet, H. J., and C. B. Barker (1948), A general divergence formula, J. Appl. Phys. 19, 63.

Rice, P. L., and F. T. Daniel (Apr. 1955), Radio transmission loss vs. distance and antenna height at 100 Mc, Trans. IRE Ant. Prop. AP-3, No. 2, 59-62.

Rice, P. L., and J. W. Herbstreit (1964), Tropospheric propagation, (to be published in Vol. 20 of Advances in Electronics, Academic Press).

Rice, S. O. (Jan. 1945), Mathematical analysis of random noise, Bell. System Tech. J. 24, 46-156.

Rice, S. O. (1954), Diffraction of plane radio waves by a parabolic cylinder, Bell System Tech. J. 33, 417-504.

Rider, G. C. (1953), Some VHF experiments upon the diffraction effect of hills, The Marconi Rev. 16, No. 109, 96-106, 2nd quarter.

Rowden, R. A., L. F. Tagholm, and J. W. Stark (1958), A survey of tropospheric wave propagation measurements by the BBC, 1946-1957, Proc. IEE 105B, Suppl. 8, 84-90 and 122-126, Paper No. 2517R.

Ryde, J. W. (1946), The attenuation and radar echoes produced at centimetre wavelengths by various meteorological phenomena, Conference on meteorological factors in radio-wave propagation, Phys. Soc. (London) and Royal Meteorological Society, 169-188.

Ryde, J. W. and D. Ryde (1945), Attenuation of centimeter waves by rain, hail, fog, and clouds, General Electric Co., Wembley, England.

Saxton, J. A. (Sept. 1951), The propagation of metre radio waves beyond the normal horizon, Part 1, Proc. 1EE 98, Part III, No. 55, 360-369.

Saxton, J. A., and J. A. Lane (May 1955), VHF and UHF reception-effects of trees and other obstacles, Wireless World 61, 229-232.

Saxton, J. A., J. A. Lane, R. W. Meadows, and P. A. Matthews (Feb. 1964), Layer structure of the troposphere, Proc. 1EE 111, No. 2, 275-283.

Schelkunoff, S. A. and H. T. Friis (1952), Antennas, theory and practice, Wiley and Sons, New York City.

Schelling, J. C., C. R. Burrows, and E. B. Ferrell (Mar. 1933), Ultra-short wave propagation, Proc. IRE 21, No. 3, 427-463.

Schünemann, R. (Sept. 1957), Mechanism of ultra short wave propagation over great distances, Hochfreq. u. Electroak. 66, No. 2, 52-61.

Sherwood, E. M., and W. L. Ginzton (July 1955), Reflection coefficients of irregular terrain at 10 cm., Proc. IRE 43, No. 7, 877-878.

Shkarofsky, I. P. (Mar. 1958), Tropospheric scatter propagation, Res. Rpt. No. 7-200-1, RCA Victor Co., Ltd. Res. Labs., Montreal, Canada.

Siddiqui, M. M. (March-April 1962), Some problems connected with Rayleigh distributions, J. Res. NBS 66D (Radio Propagation), No. 2, pp. 167-174.

Silverman, R. A. (Apr. 1957), Fading of radio waves scattered by dielectric turbulence, J. Appl. Phys. 28, No. 4, 506-511. Also New York Univ. Inst. of Math. Sci., Electromagnetic Res. Division, Res. Rept. EM 101 (Jan. 1957).

Staras, H. (Oct. 1952), Scattering of electromagnetic energy in a randomly inhomogeneous atmosphere, J. Appl. Phys. 23, No. 10, 1152-1156.

Staras, H. (Oct. 1955), Forward scattering of radio waves by anisotropic turbulence, Proc. 1RE 43, No. 10, 1374-1380.

Staras, H. (April 1957), Antenna-to-medium coupling loss, 1RE Trans. Ant. Prop. AP-5, No. 2, 228-231.

Starkey, B. J., W. R. Turner, S. R. Badcoe, and G. F. Kitchen (Jan. 1958), The effects of atmospheric discontinuity layers up to and including the tropopause on beyond-the-horizon propagation phenomena, Proc. 1EE 105B, Suppl. 8, 97-105 and 122-126, Paper No. 2486R.

Stokes, G. G. (1922), Mathematical and physical papers, Vol. III, On the composition and resolution of streams of polarized light from different sources, (Cambridge University Press, London), 233-258.

Straiton, A. W., and C. W. Tolbert (May 1960), Anomalies in the absorption of radio waves by atmospheric gases, Proc. 1RE 48, No. 5, 898-903.

Sutton, O. G. (1955), Atmospheric turbulence (John Wiley and Co.).

Tao, K. (Jan. 1957), On the relationship between the scattering of radio waves and the statistical theory of turbulence, J. Radio Res. Lab. (Tokyo) 4, No. 15, 15-24.

T.A.S.O. (March 1959), Engineering aspects of television allocations, Report of the television allocations study organization.

Taylor, G. I. (1922), Diffusion by continuous movements, Proc. London Math. Soc. II 20, 196.

Thourel, L. (1960), The antennas, translated by H. de Laistre Banting (John Wiley and Sons, Inc., New York, N. Y.).

Tolbert, C. W., and A. W. Straiton (Apr. 1957), Experimental measurement of the absorption of millimeter radio waves over extended ranges, IRE Trans. Ant. Prop. AP-5, No. 2, 239-241.

Troitski, V. (May 1956), The propagation of ultra-short waves at great distances beyond the horizon, Radio Technika 11, No. 5, 3-20.

Troitski, V. N. (Jan. 1957a), About the influence of the form of the structure function of non-homogeneous dielectric permeability of air on long distance tropospheric propagation of ultra short waves, Radio Eng. 2, 34-37.

Troitski, V. N. (1957b), Fading of ultra-short waves in radio relay systems. Electrosviaz 10.

Ugai, S. (May-June 1961), Characteristics of fading due to ducts and quantitative estimation of fading, Rev. Elect. Comm. Lab., Japan 9, No. 5-6, 319-360.

Ugai, S., S. Aoyagi, and S. Nakahara (May 1963), Microwave transmission across a mountain by using diffraction gratings, Electronics and Communications in Japan 46, No. 5, 7-17.

Unwin, R. S. (Nov. 1953), Ultra-short-wave field-strength in a ground-based radio duct, Nature 172, No. 4384, 856-857.

Van Vleck, J. H. (Apr. 1947a), The absorption of microwaves by oxygen, Phys. Rev. 71, No. 7, 413-424.

Van Vleck, J. H. (Apr. 1947b), The absorption of microwaves by uncondensed water vapor, Phys. Rev. 71, No. 7, 425-433.

Van Vleck, J. H. (1951), Theory of absorption by uncondensed gases, Propagation of Short Radio Waves, (McGraw-Hill Book Co., New York, N. Y.), 646-664.

Villars, F., and V. F. Weisskopf (Oct. 1955), On the scattering of radio waves by turbulent fluctuations of the atmosphere, Proc. IRE 43, No. 10, 1232-1239.

Voge, J. (Mar. 1953), The troposphere and wave propagation (Summary of Proceedings of Commission II, 10th General Assembly URSI (1952),) L'Onde Electronique 33, No. 312, 136-150.

Voge, J. (1955), Radioelectricity and the troposphere, part I, theories of propagation to long distances by means of atmospheric turbulence, L'Onde Electrique 35, 565-581.

Voge, J. (Nov. 1956), Useful bandwidth in scatter transmission, Proc. IRE 44, No. 11, 1621-1622.

Voge, J. (Nov.-Dec. 1960), Theories of transhorizon tropospheric propagation, Ann. des Télécomm. 15, No. 11, 260-265.

Vogler, L. E. (July 1964), Calculation of groundwave attenuation in the far diffraction region, Radio Sci. J. Res. NBS/USNC-URSI 68D, No. 7, 819-826.

Vogler, L. E., and J. L. Noble (Sept. - Oct. 1963), Curves of ground proximity loss for dipole antennas (a digest), J. Res. NBS 67D (Radio Prop.), No. 5, 567-568.

Vvedenskii, B. A., and A. G. Arenberg (1957), Long distance tropospheric propagation of ultra-short waves, Radio Eng. 12, No. 1, 3-13; Radio Eng. 12, No. 2, 10-25.

Vvedenskii, B. A., and A. V. Sokolov (1957), Investigation of tropospheric propagation of meter, decimeter, and centimeter radio waves in the USSR, Radio Eng. and Elect. (USSR) 2, No. 11, 84-105.

Vysokovskii, D. M. (1957a), Calculation of multiple scattering in the diffusion propagation of ultra-short waves in the troposphere, Radio Eng. and Elect. (USSR) 2, No. 6, 183-187.

Vysokovskii, D. M. (1957b), Geometrical characteristics of the scattering of radio waves by turbulent inhomogeneities in the troposphere, Telecommunications (USSR) 9, 11-20.

Vysokovskii, D. M. (1958), Diffused propagation of ultra-short waves in the troposphere with high-directivity antennas, Telecommunications (USSR) 5, 488-497.

Wait, J. R. (1958), On the theory of propagation of electromagnetic waves along a curved surface, Can. J. Phys. 36, No. 1, 9-17.

Wait, J. R. (1959), Electromagnetic radiation from cylindrical structures (Pergamon Press, New York, N. Y.).

Wait, J. R. (April 1959), Transmission of Power in Radio Propagation, Electronic and Radio Engineer, Vol. 36, Series No. 4, pp. 146-150.

Wait, J. R. (1962), Electromagnetic waves in stratified media, International Series of Monographs on Electromagnetic Waves 3, (Pergamon Press, New York, N. Y.).

Wait, J. R. (Nov. 1963), Oblique propagation of ground waves across a coastline, part I, J. Res. NBS 67D (Radio Prop.), No. 6, 617-624.

Wait, J. R., and A. M. Conda (Sept. - Oct. 1959), Diffraction of electromagnetic waves by smooth obstacles for grazing angles, J. Res. NBS 63D (Radio Prop.), No. 2, 181-197.

Wait, J. R., and C. M. Jackson (Nov. 1963), Oblique propagation of ground waves across a coastline, part II, J. Res. NBS 67D (Radio Prop.), No. 6, 625-630.

Wheelon, A. D. (June 1957), Relation of radio measurements to the spectrum of tropospheric dielectric fluctuations, J. Appl. Phys. 28, 684-693.

Wheelon, A. D. (Sept. - Oct. 1959), Radio-wave scattering by tropospheric irregularities, J. Res. NBS 63D (Radio Prop.), No. 2, 205-234; also, J. Atmos. and Terr. Phys. 15, Nos 3, 4, 185-205 (Oct. 1959).

Wilkerson, R. (1964), Multiple knife-edge diffraction, (private communication).

Williamson, D. A., V. L. Fuller, A. G. Longley, and P. L. Rice (Mar. 1960), A summary of VHF and UHF tropospheric transmission loss data and their long-term variability, NBS Tech. Note 43.

12. LIST OF SYMBOLS AND ABBREVIATIONS

In the following list the English alphabet precedes the Greek alphabet, and lower-case letters precede upper-case letters. As a general rule, upper-case letters have been used for quantities expressed in decibels, for example p_t is transmitter power in watts, and P_t is transmitter power in decibels above one watt.

Sometimes a symbol may be used in quite different contexts, in which case it is listed for each separate context. Subscripts are used to modify the meaning of symbols. The order is:

1.	Symbol without a subscript.	h
2.	Symbol with a subscript, (letter subscripts in alphabetical order followed by number subscripts in numerical order).	h_r h_1
3.	Symbol as a special function.	$h(x)$
4.	Abbreviations.	ht.

Following each definition an equation number or section number is given to show the term in its proper context. Where applicable, reference is made to a figure.

Throughout the report, logarithms are to the base 10 unless otherwise noted.

a Effective earth's radius, allowing for average radio ray bending near the surface of the earth. (4.4) figure 4.2.

a_e An equivalent earth's radius which is the harmonic mean of the radii a_t and a_r, (7.10).

a_e The "effective absorbing area" of an antenna, (2.24).

a_{en} The effective absorbing area for the nth discrete plane wave incident on an antenna from a single source, (II.34).

a_{e1}, a_{e2} The effective absorbing area of the receiving antenna for each of two waves, (II.86).

a_p The fraction of energy absorbed along a ray path, or scattered out of it, (II.26).

a_{pm}, a_{pn} The fraction of energy, a_p above, for the mth and n^{th} multipath components from a single source, where m and n take on integral values from 1 to N, (II.39).

a_r The radius of a circular arc that is tangent to the receiving antenna horizon ray at the horizon, and that merges smoothly with the corresponding arc through the transmitting antenna horizon, (8.9) figure 8.7.

a_s Effective earth's radius factor corresponding to D_s, (8.15).

a_s Radiowave scattering cross-section of a single scatterer or group of scatterers, (IV.13).

12-1

a_t Radius of a circular arc that is tangent to the transmitting horizon ray at the horizon, and that merges smoothly with the corresponding arc through the receiving antenna horizon, (8.9) figure 8.7.

a_v Radiowave scattering cross-section per unit volume, (IV.14).

a_{vo} Radiowave scattering cross-section from refractivity turbulence, (IV.21).

a_{v1}, a_{v2}, a_{v3} Radiowave scattering cross-sections per unit volume for large, medium, and small layers, (IV.15) to (IV.17).

a_x The axial ratio of the polarization ellipse of a plane wave, (II.15).

a_{xn}, a_{x1}, a_{x2} Axial ratios of the polarization ellipse of the nth, first, and second plane wave from a single source, (II.35) and (II.85).

a_{xr} The axial ratio of the polarization ellipse associated with the receiving pattern, (II.17).

a_{xrn}, a_{xr1}, a_{xr2} Axial ratios of the polarization ellipse associated with the receiving pattern for the nth, first, and second plane wave from a single source, (II.35) and (II.82).

a_o The actual earth's radius, usually taken to be 6370 kilometers, (4.4).

a_1 Radius of the circular arc that is tangent to the transmitting antenna horizon ray at the horizon, and that passes through a point h_{te} kilometers below the transmitting antenna, (8.8) figure 8.7.

a_2 Radius of the circular arc that is tangent to the receiving antenna horizon ray at the horizon, and that passes through a point h_{re} kilometers below the receiving antenna, (8.8) figure 8.7.

a_1, a_2 Positive or negative amplitudes of real and imaginary components of a complex vector: $\underline{\vec{a}} = \vec{a}_1 + i\vec{a}_2$, $\underline{\vec{a}}^2 = a_1^2 + a_2^2$, (II.52).

$\vec{a}$, $\hat{a}$ The real vector $\vec{a} = a\hat{a}$, where $\hat{a}$ is a unit vector.

$\vec{a}_1$, $\vec{a}_2$ Real vectors defining real and imaginary components of a complex vector: $\underline{\vec{a}} = \vec{a}_1 + i\vec{a}_2$, (II.45).

$\underline{\vec{a}}$ A complex vector: $\underline{\vec{a}} = \vec{a}_1 + i\vec{a}_2$, (II.45).

$\underline{\vec{a}}_0$ A complex vector defined in terms of the unit vector system $\hat{x}_0$, $\hat{x}_1$, $\hat{x}_2$, (II.62).

$a_e(-\hat{r})$ The effective absorbing area of a receiving antenna in the direction $(-\hat{r})$, (2.22) and (2.24).

A   An antenna terminal, figure 6.3.

A   Attenuation relative to free space, expressed in decibels, defined as the basic transmission loss relative to that in free space, (2.35). See A_t.

A_a The long-term median attenuation of radio waves due to atmospheric absorption by oxygen and water vapor, section 3.

A_{ar}, A_{at} For transhorizon paths, $A_a = A_{at} + A_{ar}$, the sum of the absorption from the transmitter to the crossover of horizon rays and the absorption from the crossover of horizon rays to the receiver, section 3.

A_c Total absorption attenuation within a cloud, (3.13).

A_m The hourly median attenuation relative to free space, annex I.

A_r Total absorption due to rainfall over a given path, (3.7).

A_t Attenuation relative to free space, defined as basic propagation loss relative to that in free space, (2.47). See A.

A_w Rate of attenuation through woods in full leaf, (5.18).

A_0 Diffraction attenuation relative to free space at an angular distance $\theta = 0$ over a smooth earth, section 9.2.

A_1, A_2 Antenna terminals, figure 6.1.

$A(v, 0)$ Attenuation relative to free space as a function of the parameter v, (7.2) figure 7.1.

$A(v, \rho)$ Diffraction attenuation relative to free space for an isolated perfectly conducting rounded obstacle, (7.7), figure 7.3.

$A(0, \rho)$ The diffraction loss for $\theta = 0$ over an obstacle of radius r, (7.7) figure 7.4.

$A(v_j)$ Attenuation relative to free space for each of several rays as a function of the parameter v_j, where $j = 1, 2, 3, 4$, (III.34).

$A_m(p)$ The time availability of hourly median values A_m. Figures I:21-I:26 show $A_m(p)$ plotted against the straight-line distance, r, for values of p ranging from 0.01 to 99.99 percent.

b   The dimensions of an atmospheric layer or feuillet in any direction perpendicular to $\hat{\kappa}$, (IV.9).

b   Effective bandwidth of a receiver in cycles per second, (V.7).

b°   The parameter b, a function of ground constants, carrier frequency, and polarization, expressed in degrees, figure 8.2, and equations (III.40) and (III.41).

b_h The parameter b for horizontal polarization defined by (III.40).

b_v The parameter b for vertical polarization, (III.41).

B   Effective bandwidth, b, expressed in decibels above one cycle per second, (V.8).

B   An antenna terminal, figure 6.3.

B_s The parameter $B(K, b)$ corresponding to the effective earth's radius a_s, (8.15).

$B_{1, 2, t, r}$ Values of the parameter $B(K, b)$ that correspond to values of $K_{1, 2, t, r}$, (8.13).

B_0 Defined by (8.2) as the product of several factors, combined for convenience in considering diffraction.

B'   Any point along the great circle path from A to B, figure 6.3.

B(K, b°)   A parameter plotted in figure 8.3 as a function of K and b°, (8.2).

c   Free space velocity of radio waves, c = 299792.5 ± 0.3 km/sec.

c   A parameter showing the phase change $\pi - c$ associated with the complex plane wave reflection coefficient $R \exp[-i(\pi - c)]$ corresponding to reflection from an infinite smooth plane surface, (5.4) figures III.1 through III.8.

c_h, c_v Values of c for horizontal and vertical polarization, respectively, (III.13) and (III.14) figures III.1 through III.8.

c_p Polarization efficiency of the power transfer from transmitter to receiver, (IV.13).

c_2, c_3 The phase changes associated with the complex reflection coefficients R_{e2}, R_{e3}, (III.32).

C   Difference in longitude between A and B, (6.1) and (6.2).

Ci   Cosine integral, (III.51).

C_j Fresnel integral, (III.33), where j = 1, 2, 3, 4.

C_o A parameter which relates K to K(8497), (8.2).

C_{or}, C_{os}, C_{ot} Values of C_o corresponding to effective earth's radii a_r, a_s, and a_t, (8.13).

C_{o1}, C_{o2} Values of C_o corresponding to effective earth's radii a_1 and a_2, (8.13).

C'   Difference in the longitude of the points A and B', (6.6) to (6.9).

C(u), C(v)   Fresnel cosine integrals, (IV.8).

C_1(K, b°)   A parameter used in calculating diffraction attenuation, (8.1) figure 8.4.

C_1(K_1, b°), C_1(K_2, b°)   The parameter C_1(K, b°) corresponding to K_1 and K_2, also written C_1(K_1) and C_1(K_2), (8.11).

$\overline{C}_1$($K_{1, 2}$)   The weighted average of values of C_1(K_1, b) and C_1(K_2, b), (8.11).

Ci(r)   Cosine integral as a function of r, (III.51).

Ci(r_1), Ci(r_2)   Cosine integral as a function of r_1, r_2, (III.50).

CCIR   International Radio Consultative Committee.

CRPL   Central Radio Propagation Laboratory, National Bureau of Standards, U.S.A.

C.W.   Continuous wave.

d   Great circle propagation path distance, measured at sea level along the great circle path determined by two antenna locations, A_1 and A_2, figure 6.1.

d_c Clearing depth in meters, defined as the distance from the edge of woods to the lower antenna along a propagation path, (5.19).

d_e Effective propagation path distance, a function of d, f_{mc}, h_{te}, and h_{re}, section 10.1, (10.3).

d_{Lr} Great circle distance from the receiving antenna to its horizon, figure 6.1.

d_{Lt} Great circle distance from the transmitting antenna to its horizon, figure 6.1.

dq	A differential amplitude reflection coefficient for a tropospheric layer, (IV.5).
d_r	Distance used in calculating ground reflections in knife edge diffraction; d_r is defined by (III.29).
d_{sr}	Distance between the receiving antenna horizon and the crossover of horizon rays as measured at sea level, (6.20).
d_{st}	Distance between the transmitting antenna horizon and the crossover of horizon rays as measured at sea level, (6.20).
d'_{sr}, d'_{st}	If θ_{or} or θ_{ot} is negative, d'_{sr} or d'_{st} is computed and substituted for d_{sr} or d_{st} in reading figure 6.9, (6.23).
d_{so}	A factor used to normalize effective antenna heights in computing d_e, (10.2).
d_{s1}	The theoretical distance where diffraction and scatter fields are approximately equal over a smooth earth, (10.1).
d_o	The greatest distance for which the attenuation relative to free space is zero, (5.10).
d_1, d_2	Distance from the transmitting, or the receiving antenna, to the crossover of horizon rays, measured at sea level, figure 6.1.
d_1, d_2	Great circle distance from one antenna of a pair to the point of reflection of a reflected ray, figure 5.1.
$d_{11}, d_{12}, d_{21}, d_{22}$	Distances used in computing diffraction attenuation with ground reflections, (III.31) figure III.9.
db	Decibels = $10 \log_{10}$ (power ratio) or $20 \log_{10}$ (voltage ratio). In this report, all logarithms are to the base 10 unless otherwise stated.
dbu	Decibels above one microvolt per meter.
dbw	Decibels above one watt.
D	Divergence coefficient, a factor used to allow for the divergence of energy due to reflection from a convex surface, (5.2).
D	Diameter of a parabolic reflector in meters, (2.16).
D_s	Great circle distance between transmitting and receiving horizons, (6.17), figure 6.1.
D_{str}	A function of d_{st}, d_{sr} used in computing diffraction loss, (8.16), figure 8.8.
e_c	The positive or negative amplitude of the cross-polarized vector component $\vec{e}_c$ of a complex polarization vector $\underline{\vec{e}}$, sections 2.4 and II.2.
e_{cr}	The positive or negative amplitude of the cross-polarized vector component $\vec{e}_{cr}$ of a receiving antenna response pattern, (II.16).
e_i	The positive or negative amplitude of the real vector $\vec{e}_i$ associated with a complex plane wave $\sqrt{2}\,(\vec{e}_r + i\,\vec{e}_i)\exp(i\tau)$, where $\vec{e}_r$ and $\vec{e}_i$ are time-invariant and $\exp(i\tau)$ is a time phasor, (II.8b).

e_p The positive or negative amplitude of the principal polarization component $\vec{e}_p$ of a complex polarization vector $\vec{\underline{e}}$, sections 2.4 and II.2.

e_{pr} The positive or negative amplitude of the principal polarization component $\vec{e}_{pr}$ of a receiving antenna response pattern, (II.16).

e_r The positive or negative amplitude of the real vector component $\vec{e}_r$ associated with a complex plane wave $\sqrt{2}\,(\vec{e}_r + i\vec{e}_i)\,\exp(i\tau)$, where $\vec{e}_r$ and $\vec{e}_i$ are time-invariant and $\exp(i\tau)$ is a time phasor, (II.8a)

e_o Equivalent free space field strength, (II.5), (2.44).

e_I Equivalent inverse distance field strength, (2.45).

e_1, e_2 The positive or negative real amplitudes of real and imaginary components of the complex polarization vector $\vec{\underline{e}}$, (II.10).

e_θ, e_ϕ The positive amplitudes of real vectors $\vec{e}_\theta$ and $\vec{e}_\phi$ associated with the θ and ϕ components of a complex plane wave, (II.7) figure II.1.

$\vec{e}_c, \vec{e}_p$ Real vectors associated with cross and principal polarization components of a uniform elliptically polarized plane wave, annex II, section II.2.

$\hat{e}_c, \hat{e}_p$ Directions of cross and principal polarization, chosen so that their vector product $\hat{e}_p \times \hat{e}_c$ is a unit vector in the direction of propagation, (II.14).

$\vec{e}_{cr}, \vec{e}_{pr}$ Cross and principal polarization field components of a receiving antenna response pattern, (II.16).

$\hat{e}_{cr}, \hat{e}_{pr}$ Directions of cross and principal polarization components of a receiving antenna response pattern, (II.18), (II.20).

$\vec{e}_i$ The real vector associated with the imaginary component of the time-invariant part of a complex plane wave $\sqrt{2}\,(\vec{e}_r + i\vec{e}_i)\,\exp(i\tau)$, (II.8b).

$\vec{e}_r$ The real vector associated with the real component of the time-invariant part of a complex plane wave $\sqrt{2}\,(\vec{e}_r + i\vec{e}_i)\,\exp(i\tau)$, (II.8a).

$\vec{e}_1, \vec{e}_2$ Real vector components of a complex polarization vector $\vec{\underline{e}}$ which has been resolved into components which are orthogonal in both space and time, (II.10).

$\vec{e}_\theta, \vec{e}_\phi$ Real vectors associated with the θ and ϕ components of a complex plane wave $\sqrt{2}\,[\vec{e}_\theta\,\exp(i\tau_\theta) + \vec{e}_\phi\,\exp(i\tau_\phi)]\,\exp(i\tau)$, where only the phasor $\exp(i\tau)$ depends on time, (II.7) figure II.1

$\hat{e}_\theta$ A unit vector $\hat{e}_\phi \times \hat{r}$ perpendicular to $\hat{e}_\phi$ and $\hat{r}$, (II.3 b) figure II.1.

$\hat{e}_\phi$ A unit vector $(\hat{r} \times \hat{x}_o)/\sin\theta$ perpendicular to $\hat{r}$ and $\hat{x}_o$, (II.3a) figure II.1.

$\vec{\underline{e}}, \vec{\underline{e}}_r$ A bar is used under the symbol to indicate a complex vector: $\vec{\underline{e}} = \vec{e}_p + i\vec{e}_c$, $\vec{\underline{e}}_r = \vec{e}_{pr} + i\vec{e}_{cr}$, (2.19).

$\vec{\underline{e}}^*$ The complex conjugate of $\vec{\underline{e}}$: $\vec{\underline{e}}^* = \vec{e}_p - i\vec{e}_c$.

$|\vec{\underline{e}}|, |\vec{\underline{e}}_r|$ The magnitudes of the complex vectors $\vec{\underline{e}}$ and $\vec{\underline{e}}_r$, (II.22).

$|e_c|, |e_{cr}|, |e_p|, |e_{pr}|$ The magnitudes of the cross and principal polarization components $\vec{e}_c, \vec{e}_{cr}, \vec{e}_p$, and $\vec{e}_{pr}$, sections 2.4, II.2, II.3.

E	Field strength in dbu, (2.43).
E_o	The equivalent free space field strength in dbu, (2.44).
E_I	The equivalent inverse distance field, (2.45).
E. R. P.	Effective radiated power, E. R. P. $= P_t + G_{pt}(\hat{r}_1) - 2.15$ dbw.
E_{1kw}	Field strength in dbu per kilowatt effective radiated power, see section 2.
f	Radio wave frequency in megahertz (megacycles per second).
f_j	Diffraction loss for each of several distinct rays over an isolated obstacle, where $j = 1, 2, 3, 4$, (III.32-III.35).
$f_{M Hz}$	Radio wave frequency in megahertz.
f_{op}	Operating noise factor of a receiving system, (V.7).
f_1, f_2, f_3, f_4	Diffraction loss for each of four distinct rays over an isolated obstacle, (III.32).
$f(r_1), f(r_2)$	Functions of the normalized antenna heights r_1 and r_2, (III.50).
$f(v_j)$	A function identically equal to f_j for $v = v_j$, (III.33) figure III.10.
$f(\theta_h)$	A factor used to reduce estimates of variability for antenna beams elevated above the horizon plane, (III.64) figure III.22. See θ_h and θ_b.
$f(v)$	A function used in computing path antenna gain, defined by (9.13) figure 9.7.
F_o	The correction term F_o allows for the reduction of scattering efficiency at great heights in the atmosphere, (9.1) and (9.7).
F_{oi}	Scattering efficiency correction term for the ith lobe of an antenna pattern, (III.63).
F_{op}	Operating noise factor of a receiving system expressed in decibels, (V.8).
$F(x_1), F(x_2)$	Functions used in computing diffraction attenuation, (8.1) and figures 8.5 and 8.6.
$F(\theta d)$	The attenuation function used in calculating median basic transmission loss for scatter paths, (9.1) figures 9.1, and III.11 to III.14.
$F(\theta_{ei} d)$	This function is the same as $F(\theta d)$ with the effective angular distance θ_{ei} substituted for the angular distance, θ, annex III, (III.57).
FM	Frequency modulation.
g	Grade of service. A specified grade of service guarantees a corresponding degree of fidelity of the information delivered to the receiver output, annex V, section V.5.
g	Maximum free space directive gain, or directivity, the ratio of the available mean power flux density and e_o^2/η_o for a loss-free antenna, section 2.3, annex II.
g_b	A high gain antenna radiates g_b watts per unit area in every direction not accounted for by the main beam or by one of the side lobes of an antenna, annex III, section III.6.
g_{bt}	The directive gain g_b for a transmitting antenna, annex III, section III.6.

g_c The cross-polarization component of the directive gain, (II.24).

g_{cr} The cross-polarization component of the directive gain of a receiver, (II.19).

g_p Principal polarization directive gain, (II.24).

g_{pr}, g_{pt} Principal polarization directive gains for the receiving and transmitting antennas, respectively, (II.26).

g_r, g_t Maximum free space directive gains for the receiving and transmitting antennas respectively, section 2.3.

g_{rn}, g_{tn} The directive gains g_r and g_t for the nth of a series of plane waves, (II.33) and (II.34).

g_{r_1}, g_{r_2} Directive gain factors defined for each antenna in the direction of the point of ground reflection, (5.1).

g_o The maximum value of the operating gain of a receiving system, (V.7).

g_o The directive gain for one antenna in the direction of the other, section 5.1.

g_{o1}, g_{o2} The directive gain of the transmitting and receiving antennas, each in the direction of the other, assuming matched antenna polarizations, (5.1).

g_θ, g_ϕ Directive gains associated with the field components $\vec{e}_\theta$, $\vec{e}_\phi$, (II.14).

$g(f)$ A frequency correction factor shown in figure III.30, (III.66).

$g(p, f)$ A frequency factor used to adjust predicted long-term variability to allow for frequency-related effects, (10.6) figure 10.3.

$g(10, f)$, $g(90, f)$ The frequency factor $g(p, f)$ used to adjust $Y_o(10)$ and $Y_o(90)$ predicted values, (10.6) figure 10.3.

$g(\hat{r})$ Directive gain in the direction $\hat{r}$, (II.56).

$g(-\hat{r})$ Directive gain in the direction $(-\hat{r})$, annex II.

$g_c(\hat{r})$, $g_p(\hat{r})$ Cross polarization and principal polarization directive gains in the direction $\hat{r}$, (II.61).

$g_r(-\hat{r})$ Free space directive gain of the receiving antenna in the direction $(-\hat{r})$, (2.32).

$g_r(\hat{r}_1)$, $g_r(\hat{r}_2)$ Directive gains associated with direct and ground-reflected rays, respectively, (II.84).

$g_t(\hat{r})$ Free space directive gain of the transmitting antenna in the direction $\hat{r}$, see also $g'_t(\hat{r})$, section 2.3.

g'_t Power gain of a transmitting antenna when the power input to the antenna terminals is p'_t watts, section 2.3.

$g'_t(\hat{r})$ Power gain of a transmitting antenna in the direction $\hat{r}$, see subsection 2.3.

gm   Grams.

g/m   Grams per meter.

G   The maximum free space directive gain relative to an isotropic radiator, (2.14).

G_b Decibel equivalent of g_b, $G_b = 10 \log g_b$, annex III section III.6.

G_{bt} Decibel equivalent of g_b for a transmitting antenna, annex III section III.6.

G_{ms} The hourly median operating signal gain of a receiving system, (V.8).

G_p Path antenna gain, the change in transmission loss or propagation loss if hypothetical loss-free isotropic antennas with no orientation, polarization, or multipath coupling loss were used at the same locations at the actual antennas, (2.29).

G_{pf} Path antenna gain in free space, (2.32).

G_{pm} Long-term median value of G_p, (2.36).

G_{pp} Path antenna power gain, (2.29).

G_r, G_t Free space gains of the receiving and transmitting antenna, respectively, in decibels relative to an isotropic radiator, (2.37).

G_{ri}, G_{ti} Gains of the ith lobe of receiving and transmitting antennas, respectively, (III.57).

G_o Maximum value, expressed in decibels, of the operating gain of the receiving system for C.W. frequencies in the receiver pass band, (V.21).

$G(\overline{h})$ Residual height gain function, figure 7.1.

$G(\overline{h}_{1,\,2})$ The function $G(\overline{h})$ for the transmitting or receiving antenna.

$G(\overline{h}_1)$, $G(h_2)$ The function $G(\overline{h})$ for the transmitting and receiving antennas, respectively, (7.5).

$G(\hat{r})$ Directive gain of an antenna in the direction $\hat{r}$. The maximum value of $G(\hat{r})$ is G, section 2.3.

$G_r(\hat{r})$, $G_r(-\hat{r})$ Directive gain, in decibels, of a receiving antenna in the directions $\hat{r}$ and $(-\hat{r})$, (2.32).

$G_r(\hat{r}_{1,\,2})$ $\equiv 10 \log g_r(\hat{r}_{1,\,2})$.

$G_r'(\hat{r})$ Power gain, in decibels, of a receiving antenna, (2.13).

$G_t(\hat{r})$ Directive gain, in decibels, of a transmitting antenna, (2.13).

$G_t'(\hat{r})$ Power gain, in decibels, of a transmitting antenna, $G_t'(\hat{r}) = G_t(\hat{r}) - L_{et}$, (2.13).

$G(x_o)$ A function used in computing diffraction attenuation, (8.1) figures 8.5 and 8.6.

GHz Radio frequency in gigacycles per second.

h Height above the surface of the ground as used in (3.10), (3.12).

h Height referred to sea level.

h_e Height for elevated beams that is equivalent to h_o for horizon rays, (III.63).

h_i Equidistant heights of terrain above sea level, (5.15), (6.10).

h_{Lr} Height of the receiver horizon obstacle above sea level, (6.15).

h_{Lt} Height of the transmitter horizon obstacle above sea level, (6.15).

h_o Height of the intersection of horizon rays above a straight line between the antennas, determined using an effective earth's radius, a, (9.3b) and figure 6.1.

h_r, h_t Height of the receiving or transmitting antenna above ground, assuming a smooth earth. A smooth earth is assumed in the curves of figures 1.5 and I.7 to I.26.

h_r, h_t The height h_r or h_t is defined as the height of the receiving or transmitting antenna above the average height of the central 80% of the terrain between the antenna and its horizon, or above ground, whichever gives the larger value, (6.11).

h_{re}, h_{te} Effective height of the receiving or transmitting antenna above ground. For h_r, h_t less than one kilometer $h_{re} = h_r$, $h_{te} = h_t$. For higher antennas a correction Δh is used, (6.12).

h_{rm}, h_{tm} Height of a knife edge above a reflecting plane on the receiver or transmitter side of the knife edge, (III.37).

h_{rs}, h_{ts} Height of the receiving antenna or transmitting antenna above sea level, figure 6.1, used in (6.11), (6.15).

h_s Elevation of the surface of the ground above mean sea level, (4.3).

h_{ti} The heights above sea level of evenly spaced terrain elevations between the transmitter and its horizon, (6.11).

h_{t0} The height above sea level of the ground below the transmitting antenna, (6.11).

h_{t30} The height of the horizon obstacle $h_{t30} = h_{Lt}$, (6.11).

h_1 Height of the crossover of horizon rays above a straight line between the transmitter and receiver horizon obstacles, (9.7) figure 6.1.

h_1, h_2 Heights of antenna terminals 1 and 2 above the surface of the earth, figure 5.1.

h'_1, h'_2 Heights of antenna terminals 1 and 2 above a plane tangent to a smooth earth at the bounce point of a reflected ray, (5.8).

$\overline{h}$ Average height above sea level, (5.15).

$\overline{h}_t$ Average height of the transmitting antenna above the central 80% of terrain between the transmitter and its horizon, (6.11).

$\overline{h}_1$, $\overline{h}_2$ Normalized heights of the transmitting and receiving antennas, (7.6).

$h(r)$ A function of r shown in figures III.20 and III.21.

$h(r_1)$, $h(r_2)$ A function of r_1 or r_2 defined by (III.50) and shown on figures III.20 and III.21.

$h(x)$ A straight line fitted by least squares to equidistant heights above sea level, (5.15).

$h(0)$, $h(d)$ Height above sea level of a smooth curve fitted to terrain visible to both antennas, and extrapolated to the transmitter at $h(0)$ and the receiver at $h(d)$. (5.17).

$h_i(x_i)$ A series of equidistant heights above sea level of terrain visible to both antennas, section 5.1.

H_o The frequency gain function, discussed in section 9.2.

H_{oi} The frequency gain function for the ith beam intersection in a scattering plane, (III.57).

$H_o(r_1)$, $H_o(r_2)$ The frequency gain function, H_o, as a function of r_1 and r_2, respectively, (9.5).

$H_o(\eta_s < 1)$, $H_o(\eta_s = 1)$ Value of the frequency gain function, H_o, where the parameter η_s is less than or equal to one, respectively, (9.6).

$H_o(\eta_s = 0)$ The frequency gain function when $\eta_s = 0$ which corresponds to the assumption of a constant atmospheric refractive index, figure 9.5.

Hz   Abbreviation for hertz $\equiv$ cycle per second.

i $i = \sqrt{-1}$, (2.19) annex II.

I_m Current in r.m.s. amperes where $m = 0, 1, 2$.

I_0, I_1, I_2 Current in r.m.s. amperes corresponding to three elementary dipoles in three mutually perpendicular directions, (II.46).

j   Represents a series of subscripts 1, 2, 3, 4, as used in equations (III.27) to (III.35).

k   Propagation constant, $k = 2\pi / \lambda$, (II.1).

k   Boltzmann's constant, $k = 1.38054 \times 10^{-23}$ joules per degree, (V.7).

$k T_o b$ Johnson's noise power that would be available in the bandwidth b cycles per second at a reference absolute temperature $T_o = 288.37$ degrees Kelvin, (V.7).

km   Abbreviation for kilometer.

kw   Abbreviation for kilowatt.

K   A frequency-dependent coefficient, (3.8).

K   A parameter used in computing diffraction attenuation, K is a function of the effective earth's radius, carrier frequency, ground constants, and polarization, figure 8.1 and annex III.4.

K   The decibel ratio of the root-sum-square of Rayleigh components of a received signal relative to a constant or power-fading component, annex V, section V.2 and figure V.1.

K_h The diffraction parameter K for horizontal polarization, annex III.4.

K_o An arbitrary constant in the systems equation, (V.22).

K_u The ratio K for an unwanted signal, annex V.

K_v The diffraction parameter K for vertical polarization, annex III.4.

K_1 A frequency and temperature-dependent attenuation coefficient for absorption within a cloud, (3.13) and table 3.1.

K_1, K_2, K_r, K_s, K_t Values of the diffraction parameter K for corresponding earth's radii a_1, a_2, a_r, a_s, a_t, (8.8) to (8.13).

K(a), K(8497)   The diffraction parameter K for an effective earth's radius a, and for $a = 8497$ km.

$K(f_{G Hz})$ A frequency-dependent coefficient used in computing the rate of absorption by rain, (3.9a) and figure 3.8.

$K(N_s)$ A function of the surface refractivity, N_s, used in computing F(0d), (III.46).

$K_0(N_s)$, $K_1(N_s)$, $K_2(N_s)$ Functions of the surface refractivity, N_s, used in computing $F(\theta d)$, (III.48).

ℓ Used as a subscript to indicate a load, for example, $z_{\ell\nu}$, represents the impedance of a load at a radio frequency ν, (2.4).

ℓ A range of eddy sizes or layers; the radio wave scattered forward is most affected by a particular range of "eddy sizes," ℓ, or by layers of an average thickness $\ell/2$, that are visible to both antennas, (IV.1).

ℓ_{er} The effective loss factor for a receiving antenna, or the reciprocal of the power receiving efficiency, (2.3).

$\ell_{er\nu}$ The effective loss factor for a receiving antenna at a frequency ν hertz, defined as the ratio $p_{a\nu}/p'_{a\nu}$, (2.9)

ℓ_{et} The effective loss factor for a transmitting antenna, or the reciprocal of its power radiation efficiency, (2.3).

$\ell_{et\nu}$ The effective loss factor for a transmitting antenna at a radio frequency hertz, (2.10).

$\ell_{m\nu}$ A mismatch loss factor defined by (2.7).

ℓ_o Scale of turbulence, (IV.19).

L Transmission loss expressed in decibels, (2.2).

L_b Basic transmission loss, (2.28) and (2.29).

L_{bd} Basic transmission loss for a diffraction path, (7.3), (7.4).

L_{bf} Basic transmission loss in free space, (2.31).

L_{bm} Hourly median basic transmission loss.

L_{bsr} Reference value of long-term median basic transmission loss due to forward scatter, (9.1).

L_c Calculated value of transmission loss.

L_{cp} Polarization coupling loss, (2.25).

L_{cr} Reference value of hourly median transmission loss when diffraction and scatter losses are combined, (9.14).

L_{dr} Reference value of hourly median transmission loss due to diffraction, (9.14).

L_{er} Effective loss factor for a receiving antenna, expressed in decibels, (2.11).

$L_{er\nu}$ The effective loss factor, L_{er}, at a radio frequency ν hertz, (2.11).

L_{et}, $L_{et\nu}$ The effective loss factor for a transmitting antenna, expressed in decibels, (2.3) and (2.11).

L_f An "equivalent free-space transmission loss," (2.34).

L_{fr}, L_{ft} The decibel ratio of the resistance component of antenna input impedance to the free space antenna radiation resistance for the receiving and transmitting antennas, respectively, (2.39).

L_{gi} Loss in antenna gain for the ith scattering subvolume, (III.57).

L_{gp} Loss ln path antenna gain, defined as the difference between basic transmission loss L_b and path loss L_o, or as the difference between the sum of the maximum gains of the transmitting and receiving antennas and the path antenna gain: $L_{gp} = L_b - L_o = G_t + G_r - G_p$ db, (2.37).

L_l Transmission loss associated with the lth power contribution, (III. 55) and (III. 57).

L_{lr} Transmission line and matching network losses at the receiver.

L_{lt} Transmission line and matching network losses at the transmitter, (V. 20).

L_m Hourly median transmission loss, (V. 20).

L_{mo} The transmission loss exceeded (100-p) percent of the time with a probability Q, (V. 43).

L_o Path loss, defined as transmission loss minus the sum of the maximum free space gains of the antennas: $L_o = L - G_t - G_r$, (2.27).

L_p Propagation loss, (2.41).

L_{pb} Basic propagation loss, (2.42).

L_{rr} The ratio of the actual radiation resistance of the receiving antenna to its radiation resistance in free space, (2.40).

L_{rt} The ratio of the actual radiation resistance of the transmitting antenna to its radiation resistance ln free space, (2.40).

L_s The system loss expressed in decibels, defined by (2.1). System loss includes ground and dielectric losses and antenna circuit losses.

L_{sr} Reference value of median forward scatter transmission loss, used with L_{dr} to obtain the reference value L_{cr}, (9.14).

L_{um} Median transmission loss of an unwanted signal, annex V. 4.

$L_1, L_2 \ldots L_n \ldots L_N$ A series of hourly median values of transmission loss arranged in order from the smallest to the largest value, annex III, subsection 7. 2.

$L(p)$ Transmission loss exceeded (100-p) percent of the time, (III. 68).

$L(50)$ The long-term median value of transmission loss, section 10. 3.

$L(0.01), L(0.1), \ldots L(99.99)$ Transmission loss exceeded (100-p) percent of the time where $p = 0.01, 0.1, \ldots 99.99$, section 10.3.

$L_b(50)$ Long-term median value of basic transmission loss, section 10. 3.

$L_{bm}(p)$ Time availability of hourly median basic transmission loss, annex I, figures I. 7 to I. 17.

$L_{bm}(50)$ Long-term median value of L_b, (2.36).

$L_i(p)$ Instantaneous values of transmission loss not exceeded p percent of the time, (V. 5).

$L_i(0.1), L_i(0.9)$ Instantaneous values of transmission loss not exceeded 10 and 90 percent of the time, (V.4).

$L_m(p)$ Hourly median transmission loss not exceeded for p percent of all hours or exceeded for $(100-p)$ percent of all hours, (V.25).

$L_m(50)$ Long-term median transmission loss, (V.2).

$L_m(p, Q)$ Hourly median transmission loss not exceeded for p percent of the time with a probability Q.

$L_{mo}(g)$ Maximum allowable transmission loss for a grade g service, (V.27).

$L_n(p)$ Transmission loss not exceeded p percent of the time in a given climatic region, (10.5).

$L_n(50)$ Predicted median long-term transmission loss for a given climatic region, characterized by the subscript n, (10.4).

$L_{um}(p)$ Hourly median transmission loss of an unwanted signal not exceeded for p percent of all hours, (V.33).

$L_{um}(50)$ Long-term median transmission loss for an unwanted signal, (V.39).

Lim. Abbreviation for limit, as used for example on figure 8.4.

m A symbol used to designate the slope of a straight line, (5.15).

m A subscript used to identify service limited by noise, annex V.

m Average refractive index gradient, dn/dz, across a layer, (IV.5).

m_h, m_v Parameters used in computing the magnitudes R_h and R_v of the smooth plane earth reflection coefficient R, (III.10).

m_o Average refractive index gradient for the region in which a layer is imbedded, (IV.5).

min. Abbreviation for minimum.

mho. A unit of conductance, the reciprocal of resistance which is measured in ohms, annex III.1, figures III.1 to III.8.

mm. Abbreviation for millimeter.

mv/m Millivolts per meter.

M Liquid water content of a cloud measured in grams per cubic meter, (3.13).

M A term defined by (IV.7) used in the power reflection coefficient q^2, (IV.6).

M_o A term defined by (IV.22) used in defining a_{vo}, the scattering cross-section from refractivity turbulence.

MHz	Radio frequency in megahertz.
M.U.F.	Abbreviation of maximum usable frequency.
n	Refractive index of the atmosphere, section 4.
n	The ratio α_o/δ_t or β_o/δ_r used to compute $\hat{n}$, (9.12).
n_s	Atmospheric refractive index at the surface of the earth, (4.1).
n_1, n_2	Refractive indices of adjacent layers of homogeneous media, (IV.3).
$\hat{n}$	A parameter used in calculating path antenna gain, (9.12).
N	Atmospheric refractivity defined as $N = (n-1) \times 10^6$, section 4.
N_{ℓ}	The number of layers per unit volume of a scattering cross-section, (IV.15) to (IV.17).
N_o	Surface refractivity reduced to sea level, (4.3).
N_s	The value of N at the surface of the earth, (4.1).
N_v	The number of scattering subvolumes that make an appreciable contribution to the total available power, (IV.11).
p	Time availability, the percentage of time a given value of transmission loss is not exceeded, section 10.
P	A function of the dielectric constant and grazing angle used in computing the plane wave reflection coefficient, (III.8).
P_a	Radio frequency signal power that would be available from an equivalent loss-free receiving antenna, (2.2).
P_{ab}	The available power corresponding to propagation between hypothetical iso-tropic antennas, (II.40).
P_{ai}	Contribution to the total available power from the ith scattering subvolume, (III.55) and (IV.11).
P_a'	Radio frequency signal power available at the terminals of the receiving antenna, (2.1).
$P_{a\nu}$	Available power at the terminals of an equivalent loss-free receiving antenna at a radio frequency ν, (2.9).
$P_{a\nu}'$	Available power at the terminals of the actual receiving antenna at a radio frequency ν, (2.6).
P_i	"Instantaneous" radio frequency signal power available at the terminals of an equivalent loss-free antenna, defined as the average power for a single cycle of the radio frequency, annex V.
$P_{\ell r}$, $P_{\ell r \nu}$	Power delivered to the receiving antenna load, at a radio frequency ν, (2.5).

$p_{\ell t}$, $p_{\ell t \nu}$ Power delivered by the transmitter to the transmission line, (2.5).

p_m The median wanted signal power available at the receiver, annex V.

p_{mn} Median value of the total noise power in watts, (V.7).

p_{mr} Operating sensitivity, the median wanted signal power, p_m, required for satisfactory service in the presence of noise, annex V.

p_o Fixed value of transmitter power output, expressed in watts, (V.26).

p_o Power, in watts, radiated from a wanted station, (V.34).

p_t Total power radiated from the transmitting antenna in a given band of radio frequencies, (2.2).

$p_{t\nu}$ Total power radiated at a frequency ν, (2.10).

p'_t Radio frequency power input to the terminals of the transmitting antenna, (2.1).

$p'_{t\nu}$ Total power delivered to the transmitting antenna at a frequency ν, (2.10).

p_u Power radiated from an unwanted station, (V.34).

p_{ui} Instantaneous power of an unwanted signal available to a receiving system, annex V.

p_v Available power per unit scattering volume, (IV.11).

p_{vi} Available power per unit scattering volume for the ith scattering subvolume, (IV.12)

p_{um} Median unwanted signal power, annex V.

$p_i(q)$ Value of "instantaneous" available power exceeded for $100\,q$ percent of a short period, (V.6). See p_i.

$p_{mr}(g)$ The value of p_{mr} required to provide service of grade g, annex V.

$\hat{p}$ Unit complex polarization vector for the incident wave, (II.21).

$\hat{p}_n$ Unit complex polarization vector for the nth incident plane wave, (II.35).

$\hat{p}_r$ Unit complex polarization vector associated with a receiving pattern, (II.18).

$\hat{p}_{rn}$ The complex polarization vector $\hat{p}_r$ associated with a receiving pattern and the nth incident wave, (II.35).

$\hat{p}_{r_1}$, $\hat{p}_{r_2}$ The complex receiving antenna polarization vectors $\hat{p}_r$ for each of two ray paths between transmitter and receiver, (II.83).

$\hat{p}(\hat{r})$, $\hat{p}_r(-\hat{r})$ Unit complex polarization vectors for the transmitter, $\hat{p}$, in the direction (r) and for the receiver, $\hat{p}_r$, in the direction $(-\hat{r})$, (2.18).

$\left| \hat{p} \cdot \hat{p}_r \right|^2$ Polarization efficiency for transfer of energy in free space at a single radio frequency, (2.22) and (II.29).

P The north or south pole in figure 6.3.

P_a The available power from a loss-free receiving antenna which is otherwise equivalent to the actual receiving antenna, (2.2).

P'_a The radio frequency signal power available at the terminals of the receiving antenna, (2.1).

P_{ab} Available power at the terminals of a hypothetical loss-free isotropic receiving antenna, assuming no orientation, polarization, or multipath coupling loss between transmitting and receiving antennas, (2.28).

P_i $P_i = 10 \log p_i$, the instantaneous power of a wanted radio signal expressed in decibels, (V.1).

P_{lr} Power, in dbw, delivered to the receiving antenna load, (2.5).

P_{lr} Power, in dbw, delivered by the transmitter to the transmission line, (2.5).

P_m The component of P_i which is not affected by the usually rapid phase interference fading, most often identified as the short-term median of the available power P_i, (V.1).

P_{mn} The hourly median value in dbw of the total noise power delivered to a receiver output: $P_{mn} = 10 \log p_{mn}$, (V.8).

P_{mr} Operating sensitivity, assuming a specified type of fading wanted signal and a specified type of noise, annex V.

P_o A fixed transmitter output power, expressed in dbw, (V.26).

P_o Total power radiated from a wanted station, expressed in dbw, (V.34).

P_t The total power radiated from the transmitting antenna in dbw: $P_t = 10 \log p_t$, (2.2).

P'_t Radio frequency power input to the terminals of the transmitting antenna, in dbw, (2.1).

P_u Power radiated from an unwanted station, (V.33).

P_{um} The median unwanted signal power available at a receiving antenna from an unwanted station radiating p_u watts, annex V.

$P_i(p)$ Percentage of time p that a given value of instantaneous power is exceeded, annex V.

$P_i(q)$ The percentage, $100\,q$, of a short period of time or the probability q that P_i will exceed $P_i(q)$ is known if the phase interference fading distribution of P_i relative to the short-term median value P_m is known, annex V.

P_{lt} Transmitter output power which will provide at least a grade g service for p percent of the time, (V.25).

$P_m(p)$ The hourly median wanted signal power P_m exceeded for p percent of all hours, annex V.

$P_m(50)$ The long-term median of all hourly median values P_m, usually identified also as the long-term median of P_i, (V.2).

$P_{mo}(p)$ Observed values of $P_m(p)$.

$P_{mr}(g)$ The operating sensitivity of a receiving system, defined as the minimum value of P_m which will provide a required grade of service g, in the presence of noise alone, (V.9).

$P_{um}(p)$ The hourly median power P_{um} expected to be available at least p percent of the time, annex V.

$P_{um}(50)$ The hourly median power P_{um} expected to be available at least 50 percent of the time, annex V.

q 100 q is the percentage of a short period of time or q is the probability that p_i will exceed $p_i(q)$ for a given median value p_m, which is the same as the probability that Y_i will exceed $Y_i(q)$, annex V.

q A parameter used in calculating a plane wave reflection coefficient, (III. 7) to (III. 14).

q The ratio $q = r_2/s\, r_1$ used to compute ΔH_o, (9.5).

q The power reflection coefficient, q^2, for a tropospheric layer is approximated by (IV. 6).

q_o The plane wave Fresnel reflection coefficient for an infinitely extended plane boundary, (IV. 3).

Q Service probability, discussed in subsection V. 8.

$Q(p)$ Service probability corresponding to the time availability p, annex V.

$Q(z_{mo})$ Service probability expressed as a function of the standard normal deviate z_{mo}, (V. 44).

r The length in free space of the direct ray path between antennas, figure 5. 1.

r Radius of curvature, (7.9).

r Resistance of an antenna, section 2.

r Magnitude of the vector $\vec{r} = r\,\hat{r}$ in the direction $\hat{r}(\theta, \phi)$, and a coordinate of the polar coordinate system r, θ, ϕ, annex II.

r_{eo} Effective distance for absorption by oxygen in the atmosphere, (3. 4) figures 3. 2 to 3. 4.

r_{er} Effective rain-bearing distance, (3. 11) and (3. 12) figures 3. 10 to 3. 13.

r_{ew} Effective distance for absorption by water vapor in the atmosphere, (3. 4). figures 3. 2 to 3. 4.

r_{fr}, r_{ft} Antenna radiation resistance in free space for the receiving and transmitting antennas, respectively, (2. 38).

$r_{\ell\nu}$ Resistance of a load, (2. 4).

r_m Ratio between the hourly median wanted signal power and the hourly median operating noise power, annex V.

r_{mr} A specified value of r_m which must be exceeded for at least a specified percentage of time to provide satisfactory service in the absence of unwanted signals other than noise, annex V.

r_o Length of a direct ray between antennas over an effective earth of radius a, figure 5.1.

r_r, r_t Antenna radiation resistance of the receiving and transmitting antennas, respectively, (2.38).

r_r', r_t' Resistance component of antenna input impedance for the receiving and transmitting antennas, respectively, (2.38).

r_u Ratio between the hourly median wanted signal power and the hourly median unwanted signal power available at the receiver, annex V, page V-1.

r_{ur} A specified value of r_u which must be exceeded for at least a specified percentage of time to provide satisfactory service in the presence of a single unwanted signal, annex V.

r_v Resistance of an equivalent loss-free antenna, (2.4).

r_v' Resistance of an actual antenna in its actual environment, (2.4).

r_1, r_2 Parameters used in computing the frequency gain function H_o, and defined by (9.4).

r_1, r_2 Distances whose sum is the path length of a reflected ray, figure 5.1.

r_{11}, r_{12}, r_{21}, r_{22} Distances to and from the bounce point of reflected rays, (III.28) figure III.9.

r_{1i}, r_{2i} Straight line distances from transmitting and receiving antennas to a point on the ground a distance x_i from the transmitting antenna, figure 6.4.

$\vec{r}$ The vector distance between two antennas, $\vec{r} = r\hat{r}$, (II.47).

$\hat{r}$ A unit vector directed away from an antenna, annex II, subsection II.1.

$\hat{r}_1$, $\hat{r}_2$ Direction of the most important propagation path from the transmitter to the receiver, or from the receiver to the transmitter.

$\hat{r}$, $\hat{e}_\theta$, $\hat{e}_\phi$ A cartesian unit vector coordinate system, annex II.

$r_{mr}(g)$ The minimum acceptable signal to noise ratio which will provide service of a given grade g in the absence of unwanted signals other than noise, annex V.

$r_{ur}(g)$ The protection ratio, r_{ur}, required to provide a specified grade of service, g, annex V section V.4.

r.m.s.   Abbreviation of root-mean-square.

R   Location of the receiving antenna, figure 5.1.

R   The magnitude of the theoretical coefficient $R \exp[-i(\pi - c)]$ for reflection of a plane wave from a smooth plane surface of a given conductivity and dielectric constant, (5.1).

R_e An "effective" ground reflection coefficient, (5.1).

R_h Plane earth reflection coefficient R for horizontal polarization, (III.12) and figures III.1 to III.8.

R_m $R_m = 10 \log r_m$ decibels, the median wanted signal to median noise ratio available at the receiver output, (V.9).

R_{mr} The decibel equivalent of r_{mr}, $R_{mr} = 10 \log r_{mr}$, annex V.

R_r Rainfall rate in millimeters per hour, (3.10).

R_{rs} Surface rainfall rate, (3.10).

R_u $R_u = 10 \log r_u$, the ratio between the hourly median wanted signal power and the hourly median unwanted signal power available at the receiving antenna terminals, (V.15).

R_{ui} The ratio between the instantaneous wanted signal power and the instantaneous unwanted signal power at the receiving antenna terminals, (V.10).

R_{ur} The decibel equivalent of r_{ur}, $R_{ur} = 10 \log r_{ur}$.

R_v Plane earth plane wave reflection coefficient R for vertical polarization, (III.12) figures III.1 to III.8.

$\vec{R}, \vec{R}_o$ Vector distances from transmitter and receiver, respectively, to a point $\vec{R}_o$.

$\hat{R}, \hat{R}_o$ Unit vectors from the centers of radiation of the receiving and transmitting antennas, respectively, (IV.1)

$\vec{R}_{oi}$ A point from which power is coherently scattered or reflected, (IV.11).

$\overline{R}_r$ Cumulative distribution of instantaneous path average rainfall rates, figure 3.14.

$R(0.5)$ A function of $L_{dr} - L_{cr}$, (9.14) figure 9.16.

$R_m(50)$ The value of R_m exceeded at least 50 percent of the time, (V.29).

$R_m(p)$ The value of R_m exceeded at least p percent of the time, (V.24).

$R_{mr}(g)$ The minimum value of R_m that will provide a desired grade of service in the presence of noise alone, (V.9).

$R_u(p)$ A specified value of R_u exceeded at least p percent of the time, (V.36).

$R_u(50)$ A specified value of R_u exceeded at least 50 percent of the time, (V.36).

$R_{ur}(g)$ Median wanted signal to median unwanted signal ratio required to provide a grade g service, annex V section 4.

$R_{ur}(g, p)$ The required ratio R_{ur} to provide service of grade g for at least p percent of the time, (V.35).

$R_{uro}(g)$ The required value of R_u for non-fading wanted and unwanted signals, (V.14).

s Path asymmetry factor, $s = \alpha_o / \beta_o$, (6.19).

s	Total mean power flux density, (II.25).
s_c	Mean power flux density associated with cross-polarization components, (II.23).
s_e	The fraction of the total flux density that contributes to the available power, (II.43a).
s_e	Path asymmetry factor for beams elevated above the horizon, $s_e = \alpha_e / \beta_e$, (III.64).
s_ℓ	Mean power flux density associated with left-handed polarization, (II.28).
s_o	Free space field strength in watts per square kilometer, (2.43).
s_p	Mean power flux density associated with principal polarization components, (II.23).
s_r	Mean power flux density associated with right-handed polarization, (II.28).
$<s_e>$	The statistical "expected value" of s_e, (II.43b).
$s(\vec{r})$	Total mean power flux density at the receiving antenna, (2.23).
$s_c(\vec{r}), s_p(\vec{r})$	Mean power flux densities associated with the cross and principal polarization components of $\underline{\vec{e}}$ in the direction $\vec{r}$, (II.23).
S_j	Fresnel integral, (III.33).
$S(u), S(v)$	Fresnel sine integrals, (IV.8).
$Si(r)$	Sine integral as a function of r, (III.51).
t	Time at the transmitter, in seconds, (II.1).
T	Location of transmitting antenna, figure 5.1.
T_o	Reference absolute temperature, $T_o = 288.37$ degrees Kelvin.
$T(r)$	Temperature in the troposphere in degrees Kelvin.
$T_s(°K)$	Effective sky noise temperature in degrees Kelvin.
T.A.S.O.	Abbreviation of Television Allocations Study Organization.
u	A subscript used to indicate signal from an unwanted or interfering station, annex V.
u	A parameter defined by (IV.9).
$U(v\rho)$	A parameter used in computing diffraction over a rounded obstacle, (III.26) and figure 7.5.
U H F	Abbreviation of ultra high frequency.
v	A parameter used in computing diffraction over an isolated obstacle, (7.1).
v	A parameter defined by (IV.9).
v_i	The ith scattering subvolume, (IV.11).
v_j	The parameter v for each of j paths over an isolated obstacle, (III.27).
v_n	Complex open-circuit r.m.s. signal voltage for coherently phased multipath components, (II.32).
v_ν	The open-circuit r.m.s. voltage for an equivalent loss-free antenna at a frequency ν, (2.8).
v'_ν	The actual open-circuit r.m.s. voltage at the antenna terminals at a frequency ν, (2.5).

$V(50, d_e)$ A parameter used with the calculated long-term reference value, L_{cr}, to predict median long-term transmission loss, figure 10.1 equations (10.4) and (III.67).

$V_n(50, d_e)$ The parameter $V(50, d_e)$ for a given climatic region characterized by the subscript n, (10.4) figure 10.1.

VHF   Abbreviation of very high frequency.

w   Half the width of a first Fresnel zone, (IV.7).

x   A specified value, the discussion preceding (2.14).

x   A variable designating distance from an antenna, figure 6.4.

x_a, x_b Points at which a first Fresnel ellipse cuts the great circle plane, III.18 to III.23.

$x_{\ell v}, x'_v, x_v$ Reactance of a load, an actual lossy antenna, and an equivalent loss-free antenna, respectively, (2.4).

x_i The ith distance from the transmitter along a great circle path, figure 6.4.

$\hat{x}_m$ One of three mutually perpendicular directions, $m = 0, 1, 2$, annex II.

x_0, x_1, x_2 Parameters used to compute diffraction loss, (8.2) figures 8.5 and 8.6.

x_0, x_{20} Points chosen to exclude terrain adjacent to either antenna which is not visible to the other in computing a curve fit, (5.15).

$\hat{x}_0, \hat{x}_1, \hat{x}_2$ Axes of a cartesian unit vector coordinate system, (II.2) figure II.1.

$\bar{x}$ The average of distances x_0 and x_{20}, (5.15b).

X   Initial bearing from antenna terminal A, measured from true north, figure 6.3.

y_i Terrain elevations, modified to account for the curvature of the earth, (6.10).

$y(x)$ Modified terrain elevation, $y(x) = h(x) - x^2/(2a)$, (5.16).

Y   Initial bearing from antenna terminal B, measured from true north, figure 6.3.

Y   A symbol used to describe the characteristics of long-term fading, (V.1) and (V.3).

Y_i The phase-interference fading of a received signal, (V.1) and (V.3).

Y_u Long-term fading component of unwanted signal fading, (V.16).

Y_{ui} The phase interference component of the fading of an unwanted signal, (V.10).

Y'   Bearing from any point B' along the great circle path AB, figure 6.3.

$Y(p)$ Long-term variability of L_m or of P_m in terms of hourly medians, (10.6) and (V.4).

$Y_i(q)$ Phase interference fading evaluated for the particular phase interference fading characteristic of a wanted signal exceeded p percent of the time, where $p = 100 q$, (V.5).

$Y_i(q, K)$ Cumulative distribution function for the phase interference fading of a wanted signal, (V. 12).

$Y_i(q, K_u)$ Cumulative distribution function for the phase interference fading of an unwanted signal, (V. 12).

$Y_m(p)$ Variability of hourly median transmission loss, (V. 29).

$Y_n(p)$ Variability of the operating noise factor, $Y_n(p) \equiv F_{op}(p) - F_{op}(50)$, (V. 32).

$Y_n(100 - p)$ Value of $Y_n(p)$ exceeded $(100 - p)$ percent of the hours or not exceeded p percent of the hours, (V. 31).

$Y_o(p)$ Basic estimate of variability in a continental temperate climate, figure 10. 2.

$Y_o(p, d_e)$ Basic estimate of variability as a function of effective distance, (10. 6) figure 10. 2.

$Y_R(p)$ Variability of the ratio of wanted to unwanted signal, (V. 38).

$Y_u(p)$ Variability of an unwanted signal, (V. 39).

$Y_u(100 - p)$ Value of $Y_u(p)$ exceeded $(100 - p)$ percent of the time, (V. 38).

z Thickness of a tropospheric layer, (IV. 6).

$z_{\ell v}$ Impedance of a load, (2. 4).

z_{mo} A standard normal deviate, (V. 43).

z_o The thickness of a tropospheric layer, (IV. 6).

z_{op} A standard normal deviate, (V. 50).

z_{uc} A standard normal deviate corresponding to the total variance $\sigma^2_{uc}(p)$ of an estimate of the service criterion, (V. 53).

z_v Impedance of an equivalent loss-free antenna, (2. 4).

z'_v Impedance of an actual lossy antenna, (2. 4).

$z'_v{}^*$ The conjugate of z'_v, following (2. 5).

Z Great circle path length between antenna terminals A and B, figure 6. 3.

Z The difference between the two random variables Y and Y_u, (V. 16).

Z_i The difference between the phase interference fading components Y_i and Y_{ui}, (V. 11).

Z' Great circle path distance between an antenna and an arbitrary point B', figure 6. 3.

$Z_a(p)$ Approximate cumulative distribution function for the random variable $Z \equiv Y - Y_u$, (V. 17).

$Z_a(50)$ The median value of $Z_a(p)$, by definition equal to zero.

$Z_i(q, \infty, \infty)$ The cumulative distribution function for the special case where Y_i is Rayleigh distributed, (V. 13).

$Z_{ia}(q, \infty, \infty)$ The approximate value of $Z_i(q, \infty, \infty)$ see (V. 12) and Table V.2.

$Z_{ia}(q, K, K_u)$ Approximate cumulative distribution function of the random variable Z_i, (V. 12).

α	The parameter α is defined in equation (3.9b) and plotted as a function of frequency on figure 3.9.
α_e, β_e	The angles between the "bottoms" of transmitting or receiving antenna beams or side lobes and a line joining the antennas, (III.61).
α_{ei}, β_{ei}	Angles α_e and β_e for the ith lobe of an antenna pattern.
α_{eo}, β_{eo}	When beams are elevated sufficiently that there is no bending of the ray due to atmospheric refraction $\alpha_e = \alpha_{eo}$, $\beta_e = \beta_{eo}$, (III.60); when ray bending must be considered α_e and β_e are computed using (III.61).
α_o, β_o	The angles α_{oo}, β_{oo} modified by the corrections $\Delta\alpha_o$, $\Delta\beta_o$, (6.19).
α_{oj}, β_{oj}	The angles α_o, β_o made by each of j rays, over an isolated obstacle, (III.36).
α_{oo}, β_{oo}	The angles between a transmitter or receiver horizon ray and a line drawn between the antenna locations on an earth of effective radius, a, (6.18) figure 6.1.
α_{o1}, α_{o2}, β_{o1}, β_{o2}	The angles α_o and β_o for each of four rays over an isolated obstacle, (III.36).
$\alpha(f_{GHz})$	The function α in (3.9b) as a function of frequency in GHz, figure 3.9.
γ_{oo}	Differential absorption in decibels per kilometer for oxygen under standard conditions of temperature and pressure, (3.4).
γ_r	Rate of absorption by rain, (3.8).
γ_{rs}	Surface value of the rate of absorption by rain, (3.11).
γ_{wo}	Differential absorption in decibels per kilometer for water vapor under standard conditions of temperature and pressure and for a surface value of absolute humidity of 10g/cc, (3.4).
$\gamma(r)$	Differential atmospheric absorption in db/km for a path length r, (3.1).
$\gamma_r(r)$	Differ ntial rain absorption along a path r, (3.7).
$\gamma_o(h)$, $\gamma_w(h)$	Differential absorption in db/km for oxygen and water vapor, respectively, as a function of height, h, (3.3).
$\Gamma(r)$	Absorption coefficient as a function of path distance r, (3.2) and (3.6).
δ	A parameter used in computing the first Fresnel zone in a reflecting plane, (III.18).
δ	The effective half-power semi-beamwidth of an antenna, (2.15) and annex III.
δ_e	The effective half-power semi-beamwidth of an antenna that is elevated or directed out of the great circle plane, annex III.6.
δ_o	The semi-beamwidth of an equivalent beam pattern with a square cross-section, $\delta_o = \delta\sqrt{\pi/4}$, annex III.6.
δ_r, δ_t	The effective half-power semi-beamwidth for the receiving and transmitting antennas, respectively, (9.11) and (9.12).
δ_{rwo}, δ_{two}	Azimuthal equivalent semi-beamwidths with square cross-section, (III.58) figure III.23.
δ_{rzo}, δ_{tzo}	Vertical angle equivalent semi-beamwidths with square cross-section, (III.58) figure III.23.

δ_w Azimuthal semi-beamwidth, (2.15).

δ_{wo} Azimuthal equivalent semi-beamwidth with square cross-section, annex III.6.

δ_z Vertical angle semi-beamwidth, (2.15).

δ_{zo} Vertical angle equivalent semi-beamwidth, annex III.6.

$\Delta\alpha_o, \Delta\beta_o$ Correction terms applied to compute α_o, β_o (6.19) figure 6.9.

Δ_c Depression of field strength below smooth earth values, (5.19).

Δh A correction term used to compute the effective height for high antennas, (6.12) figure 6.7.

Δ_j The jth value of Δr, where $\Delta r = r_1 + r_2 - r_o$, (III.27) and (III.29).

Δn The deviation of refractive index from its expected value, (IV.20).

Δr The path length difference between a direct ray, r_o, and a reflected ray, $\Delta r = r_1 + r_2 - r_o$, (5.4), (5.9) and (7.1).

$\Delta_{x_1}, \Delta_{x_2}$ Auxiliary functions used to check the magnitude of error in the graphical determination of diffraction attenuation, (8.5) figures 8.5 and 8.6.

ΔH_o A correction term applied to the frequency gain function, H_o, (9.5) and figure 9.4.

ΔN The refractivity gradient from the surface value, N_s, to the value of N at a height of one kilometer above the surface, (4.2).

$\Delta_1, \Delta_2, \Delta_3, \Delta_4$ Ray path differences between a direct ray and a ray path over a single isolated obstacle with ground reflections, (III.28) figure (III.9).

$\Delta_{1r}, \Delta_{2r}, \Delta_{3r}, \Delta_{4r}$ Ray path difference between straight and ground reflected rays on either side of an isolated obstacle, (III.31, (III.37) figure (III.31).

$\Delta\alpha_o(N_s), \Delta\beta_o(N_s)$ The correction terms $\Delta\alpha_o$, $\Delta\beta_o$ for values of N_s other than 301, (6.21) figure 6.10.

$\Delta\alpha_o(301), \Delta\beta_o(301)$ The correction terms $\Delta\alpha_o$, $\Delta\beta_o$ for $N_s = 301$, (6.21) read from figure 6.9.

$\Delta h(h_r, N_s), \Delta h(h_t, N_s)$ The correction Δh as a function of N_s and of receiver and transmitter heights h_r and h_t, (6.12) figure 6.7.

$<\Delta n>$ The expected value of refractive index, (IV.20).

$<(\Delta n)^2>$ The variance of fluctuations in refractive index, (IV.19).

ϵ Ratio of the dielectric constant of the earth's surface to the dielectric constant of air, figures 8.1 and 8.2, annex III.4.

ϵ A small increment as defined by (II.64) and used in (II.65), (II.72) to (II.75).

$\epsilon_{r1}, \epsilon_{t1}$ Angle between the axis of the main beam and the axis of the first side lobe of an antenna pattern, figure III.22.

ϵ_{tw1}, ϵ_{tw2} Azimuth angles of the first and second lobes of a transmitting antenna relative to the main beam axis, figure III.23.

ϵ_{tz1}, ϵ_{tz2} Elevation angles of the first and second lobes of a transmitting antenna relative to the main beam axis, figure III.23.

ζ The angle that a scattering plane makes with the great circle plane, (III.60), (III.61), and figure III.22.

η_s A function of h_o and N_s used in computing F_o and H_o, (9.3) and figure 9.2.

η_{se} A function of h_e and N_s used in computing F_{oi} and H_{oi} for scattering from antenna beams directed above the horizon or away from the great circle plane, (III.64).

η_o Characteristic impedance of free space, $\eta_o = 4\pi c.10^{-7} \cong 120\pi$ ohms, (II.5).

θ The angular distance, θ, is the angle between radio horizon rays in the great circle plane defined by the antenna locations, (6.19).

θ A polar coordinate, (II.56).

θ_b Angle of elevation of the lower half power point of an antenna beam above the horizontal, (III.62). See θ_h and $f(\theta_h)$.

θ_{br}, θ_{bt} Values of θ_b for the receiving and transmitting antennas, respectively, (III.61).

θ_{bri}, θ_{bti} Values of θ_b for the ith beam intersection, (III.59).

θ_e The angle between radio rays elevated above the horizon and/or away from the great circle plane, (III.64).

θ_{ei} The angle θ_e at the ith intersection of radio rays elevated above the horizon and/or away from the great circle plane, (III.57).

θ_{er}, θ_{et} Horizon elevation angles at the receiver and transmitter, respectively, (6.15).

θ_{e1}, θ_{e2}, ... θ_{en} The angle θ_e for the first, second, ... n^{th} intersection of radio rays, figure III.22.

θ_h Angle of elevation of a direct ray relative to the horizontal at the lower antenna, (5.12). See θ_b and $f(\theta_h)$.

θ_{hr}, θ_{ht} Angle of elevation of a knife edge relative to the horizontal at the receiving or transmitting antenna, (III.38).

θ_j Angle between direct and/or reflected ray over a knife-edge, where $j = 1, 2, 3, 4$ as shown in figure III.9.

θ_{jr} Angles defined in (III.29), where $j = 1, 2, 3, 4$, which are added to θ to determine θ_j,

$$\theta_j = \theta + \theta_{jr}.$$

θ_{1r}, θ_{2r}, θ_{3r}, θ_{4r} Values of θ_{jr} for $j = 1, 2, 3, 4$, (III.29).

θ_o Angle of elevation above the horizontal, figures 3.2 to 3.4.

θ_{oo} — Angle between radio horizon rays, assuming straight rays above an earth of effective radius, a, figure 6.1.

θ_{or}, θ_{ot} — The angular elevation of a horizon ray at the receiver or transmitter horizon, (6.16), figure 6.1.

θ_1, θ_2, θ_3, θ_4 — The angle between rays from the transmitting and receiving antennas over an isolated obstacle with ground reflections, figure III.9.

$\hat{\kappa}$ — A wave number direction defined by (IV.1).

λ — Free space radio wave length, used for example in (2.16).

μ — The ratio δ_r / δ_t used in (9.12) and figure 9.8.

ν — A parameter that is half the value of η_s, used in computing loss in antenna gain, (9.11), (9.12) and figure 9.7.

ν — Radio frequency in hertz, (2.4) to (2.12).

ν_ℓ, ν_m — Limits of integration (2.11) and (2.12) chosen to include essentially all of the wanted signal modulation side bands.

π — A constant, $\pi \cong 3.14159264$.

ρ — Correlation coefficient between two random variables.

ρ — Index of curvature for the crest curvature of a rounded obstacle in the great circle path direction, (7.8).

ρ_{ij} — The correlation between variations due to sources i and j, (10.8).

ρ_{1a} — The correlation between variations Y and Y_a, (10.9).

ρ_{1r} — The correlation between variations Y and Y_r, (10.9).

$\rho_{\ell u}$ — The normalized correlation or covariance between path-to-path variations of $P_m(50)$ and $P_{um}(50)$, (V.45).

ρ_{tn} — The long-term correlation between P_m and F_{op}, (V.27).

ρ_{tu} — The long-term correlation between P_m and P_{um}, (V.34).

σ — Surface conductivity in mhos per meter, figures 8.1 and 8.2, annex III.4.

$\sigma_c(p)$ — The standard deviation corresponding to the variance $\sigma_c^2(p)$.

$\sigma_c^2(p)$ — The path-to-path variance of observed from predicted p-percentiles of transmission loss for a large number of randomly different paths with a given set of values for all parameters used in the prediction process, (V.36) figure V.4.

$\sigma_c^2(50)$ — The path-to-path variance of the difference between observed and predicted long-term median values of transmission loss. The corresponding standard deviation is $\sigma_c(50)$, annex V.6.

σ_h — The root-mean-square deviation of great circle path terrain elevations relative to a smooth curve fitted to the terrain, (5.1).

$\sigma_{op}^2(p)$ — Total variance of any estimate of the service criterion for service limited only by external noise, (V.43). The corresponding standard deviation is $\sigma_{op}(p)$.

$\sigma_{uc}^2(p)$ — Total variance of any estimate of the service criterion for service limited only by interference from a single unwanted source, (V.45). The corresponding standard deviation is $\sigma_{uc}(p)$.

σ_{ur}^2 Variance of the estimate $R_{ur}(p, g)$, (V. 45).

Σ A symbol to represent the summation of terms, as in (5. 15) where $\sum_{i=0}^{20} h_i$ means the sum of all values of h_i from $i = 0$ to $i = 20$.

τ The amount a radio ray bends in the atmosphere, (III. 62).

τ Delayed time of the phasor, $\exp(i\tau)$, where $\tau = k(ct-r)$ is the time of reception at free-space radio-wave velocities, c is the free space velocity of radio-waves, t is the time at the radio source, and r is the length of the radio ray, (II. 1).

τ_a Time element defined by (II. 70) as $\tau_a = 10\pi \cos\theta$.

τ_{a1}, τ_{a2} The time element τ_a corresponding to direct and ground-reflected waves at the receiving antenna, (II. 79).

τ_i A time-independent phase which is a function of $\vec{r}$, (II. 9), (II. 31).

τ_{in} The time-independent phase for the nth component of an incident wave, annex II. 6.

τ_{i1}, τ_{i2} The time-independent phase for two components of an incident wave, (II. 85).

τ_m Initial phase of the current supported by one of m elementary dipoles, where $m = 0, 1, 2$, (II. 46).

τ_0, τ_1, τ_2 Initial phases of the currents supported by three elementary dipoles, (II. 46).

τ_p Time-independent phase which is a function of the ray path, including allowances for path length differences and diffraction or reflection phase shifts, (II. 31).

τ_{pn}, τ_{p1}, τ_{p2} The phase function τ_p for the nth, first, and second plane wave incident on an antenna from a single source, (II. 32) and (II. 85).

τ_r Antenna phase response for the receiving antenna, (II. 16).

τ_{rn}, τ_{r1}, τ_{r2} The antenna phase response, τ_r, for the nth, first, and second plane wave incident on the receiving antenna, (II. 32) and (II. 81).

τ_t Antenna phase response for a transmitting antenna, (II. 16).

τ_{tn}, τ_{t1}, τ_{t2} The antenna phase response τ_t for the nth, first, and second plane wave, (II. 32) and (II. 85).

τ_θ, τ_ϕ Phases associated with the electrical field components $\vec{e}_\theta$, $\vec{e}_\phi$, (II. 7).

$\tau(\theta_b, d, N_s)$ Bending of a radio ray that takes off at an initial angle θ_b and travels d kilometers through an atmosphere characterized by a surface refractivity N_s, (III. 61).

ϕ One of the polar coordinates, r, θ, ϕ, (II. 56) and figure II. 1.

$\phi(v, 0)$ Component of phase lag due to diffraction over an idealized knife edge, (7. 13) figure 7. 1, and (III. 30).

$\phi(v\rho)$ Component of phase lag due to diffraction over an isolated perfectly-conducting rounded obstacle, (7. 13) figure 7. 5 and (III. 30).

$\phi(0, \rho)$ The component of the phase lag of the diffracted field over an isolated perfectly-conducting rounded obstacle for $v = 0$, (7. 13) figure 7. 4 and (III. 30).

Φ_A, Φ_B Latitudes of antenna terminals A and B, (6.1) to (6.9) figure 6.3.

$\Phi_{B'}$ Latitude of an arbitrary point along the great circle path from A to B, (6.7).

Φ_j The phase lag of the diffracted field for the jth ray over an isolated perfectly-conducting rounded obstacle (III.30a), where $j = 1, 2, 3, 4$.

$\Phi(v, \rho)$ The total phase lag of the diffracted field over an isolated rounded obstacle with reflections from terrain, (7.13).

$\Phi(v, 0)$ The total phase lag of the diffracted field over an ideal knife edge with ground reflections, (7.13).

$\Phi_j(v, \rho)$ The phase lag of the diffracted ray over an isolated rounded obstacle for the jth ray, $\Phi_j(v, \rho) \equiv \Phi_j$, (III.30).

$\Phi_j(v, 0)$ The phase lag over an ideal knife edge for the jth ray, (III.30).

Φ_1, Φ_2, Φ_3, Φ_4 The phase lag $\Phi_j(v, \rho)$ for values of $j = 1, 2, 3, 4$, (III.32).

ψ The grazing angle of a ray reflected from a point on the surface of a smooth earth, (5.1) figure 5.1, or grazing angle at a feuillet, annex IV.

ψ_m Minimum grazing angle, section 5.1.

ψ_p The acute angle between principal polarization vectors $\vec{e}_p$ and $\vec{e}_{pr}$, (2.26).

ψ_{p1}, ψ_{p2} The acute angle, ψ_p, for each of two waves, (II.85).

ψ_r, ψ_t The angle between the plane of the lower half-power point of an antenna beam and the receiver or transmitter horizon plane, (III.60).

ψ_{ri}, ψ_{ti} The angle ψ_r or ψ_t for the ith lobe of an antenna pattern, (III.59).

ψ_1, ψ_2 Angle of reflection at the ground of a reflected ray that passes over a knife-edge, (III.36) figure III.9.

Ω The half-power beamwidth, $\Omega = 2\delta$, (9.10) and figure III.22.

Ω_r, Ω_t The half-power beamwidths of the receiving and transmitting antennas, respectively, (9.10).

Ω_{ro}, Ω_{r1}, Ω_{to}, Ω_{t1} Half-power beamwidths corresponding to $2\delta_o$, $2\delta_1$ for the receiving and transmitting antenna patterns, respectively, figure III.22.